(18) USAAMRDL (19) TR-77-37

(12)

(6) HEAVY LIFT HELICOPTER - ADVANCED TECHNOLOGY COMPONENT PROGRAM - HUB AND UPPER CONTROLS.

Boeing Vertol Company
P.O. Box 16858
Philadelphia, Pa. 19142

(11) Sep[redacted]977 (12) 249p.

(9) Final Report [redacted] Jul[redacted]71—Jul[redacted]975,

Approved for public release; distribution unlimited.

(15) Prepared for DAAJ01-71-C-0840

U. S. ARMY AVIATION RESEARCH AND DEVELOPMENT COMMAND
P.O. Box 209
St. Louis, Mo. 63166

APPLIED TECHNOLOGY LABORATORY
U. S. ARMY RESEARCH AND TECHNOLOGY LABORATORIES (AVRADCOM)
Fort Eustis, Va. 23604

403 682

APPLIED TECHNOLOGY LABORATORY POSITION STATEMENT

Due to the termination of the HLH program, reports summarizing the strides made in many of the supporting technology programs were never published. In an effort to make as much of this information available as possible, selected draft reports prepared under contract prior to termination have been edited and converted to the DOD format by the Applied Technology Laboratory. The reader will find many instances of poor legibility in drawings and charts which could not, due to the funding and manpower constraints, be redone. It is felt, however, that some benefit will be derived from their inclusion and that where essential details are missing, sufficient information exists to allow the direction of specific questions to the contractor and/or the U.S. Army.

Unclassified

SECURITY CLASSIFICATION OF THIS PAGE (When Data Entered)

REPORT DOCUMENTATION PAGE		READ INSTRUCTIONS BEFORE COMPLETING FORM
1. REPORT NUMBER USAAMRDL-TR-77-37	2. GOVT ACCESSION NO.	3. RECIPIENT'S CATALOG NUMBER
4. TITLE (and Subtitle) HEAVY LIFT HELICOPTER - ADVANCED TECHNOLOGY COMPONENT PROGRAM - HUB AND UPPER CONTROLS		5. TYPE OF REPORT & PERIOD COVERED Final Report - July 1971 - July 1975 6. PERFORMING ORG. REPORT NUMBER
7. AUTHOR(s)		8. CONTRACT OR GRANT NUMBER(s) DAAJ01-71-C-0840(P6A)
9. PERFORMING ORGANIZATION NAME AND ADDRESS Boeing Vertol Company P. O. Box 16858 Philadelphia, Pa. 19142		10. PROGRAM ELEMENT, PROJECT, TASK AREA & WORK UNIT NUMBERS
11. CONTROLLING OFFICE NAME AND ADDRESS U.S. Army Aviation R&D Command P. O. Box 209 St. Louis, Mo. 63166		12. REPORT DATE September 1977 13. NUMBER OF PAGES 181
14. MONITORING AGENCY NAME & ADDRESS(if different from Controlling Office) Applied Technology Laboratory, U.S. Army Research & Technology Laboratories (AVRADCOM) Fort Eustis, Va. 23604		15. SECURITY CLASS. (of this report) Unclassified 15a. DECLASSIFICATION/DOWNGRADING SCHEDULE

16. DISTRIBUTION STATEMENT (of this Report)

Approved for public release; distribution unlimited.

17. DISTRIBUTION STATEMENT (of the abstract entered in Block 20, if different from Report)

18. SUPPLEMENTARY NOTES

19. KEY WORDS (Continue on reverse side if necessary and identify by block number)

Rotor Hub and Controls	Frequency Selective Lag Damper
XCH-62 Prototype HLH	Safe-Life Fatigue Test
Elastomeric Bearing	Fail-Safe Fatigue Test
Shear Bearing	

20. ABSTRACT (Continue on reverse side if necessary and identify by block number)

The Heavy Lift Helicopter Advanced Technology Component (ATC) development program was conducted by the Boeing Vertol Company for the U.S. Army from July 1971 through July 1975. As a part of this program, an advanced rotor hub and upper controls system design was developed and demonstrated to be satisfactory for application to the XCH-62 Prototype HLH.

DD FORM 1 JAN 73 1473 EDITION OF 1 NOV 65 IS OBSOLETE

Unclassified

SECURITY CLASSIFICATION OF THIS PAGE (When Data Entered)

Block 20. Abstract - continued.

A fully articulated rotor configuration employing elastomeric bearings was selected for the ATC development. A preliminary design phase included configuration trade studies, material properties determination, and concept development tests. Full-scale components were fabricated and subjected to fatigue and endurance testing as part of a demonstration test program.

The ATC hub and upper control component development/demonstration activities included the flap/lag pitch elastomeric bearing, frequency selective lag damper, and shear bearing development efforts; manufacturing techniques development; fretting inhibitor evaluation; safe-life, fail-safe, and endurance testing of major hub and upper control components; whirl tower tests; and integrated rotor-drive system tests.

During 147 hours of rotor-drive system tests, there were no mission affecting malfunctions of the hub and upper control components, and the demonstrated MTBF was approximately two-thirds that of the mature aircraft objective. With a normal reliability growth program, the HLH reliability objectives would be achieved. Operating problems were identified during the DSTR program and design solutions defined which were demonstrated in subsequent testing. Incorporation of these and other design improvements identified during the ATC program were scheduled for incorporation in the Prototype XCH-62 aircraft components.

Both the ATC and Prototype programs were terminated on 1 August 1975 by action of the U. S. Congress prior to completion of the planned activities.

TABLE OF CONTENTS

LIST OF ILLUSTRATIONS

LIST OF TABLES

1.0 INTRODUCTION

OBJECTIVES

The primary objectives of the ATC Program were:

1. Demonstrate component technology to reduce development risk applicable to a 22.5-ton HLH at the lowest total HLH system cost.

2. Provide the Government with improved technology and reduced risk for program definition for large payload helicopters.

3. Advance level of industry expertise in HLH components.

APPROACH

The purpose of the ATC Program was to seek maximum reduction of technical and cost risk associated with the Engineering Development of an HLH system through the design, fabrication, demonstration and test of selected critical HLH components. Engineering Development or full-flight qualification of any component or concept was not the purpose of this program.

The critical components of the HLH were determined to be the rotor blades, hub and upper controls, drive system, flight control system and cargo handling system. The scope of the HLH ATC program was limited to these components, plus the interface analytical activities necessary for the ATC components to be considered suitable for subsequent integration with the complete aircraft.

The general arrangement of the HLH is shown in Figure 1.

HUB AND UPPER CONTROLS ATC PROGRAM

The Advanced Technology objectives for the hub and upper controls components were aimed at increasing flight safety and minimizing operating and support costs by providing fail-safe, simple, reliable, and lightweight hardware.

A fully articulated rotor configuration employing elastomeric bearings was selected for ATC development. The use of an elastomeric bearing at each blade to react radial blade forces and permit pitch, flap and lag motion eliminates the need for lubrication and provides a significant reduction in the number of parts. Because of parts reduction and lower maintenance man-hours, a significant reduction in operating and support costs should be realized.

All components were designed to fail-safe design criteria so that risk of catastrophic failure would be significantly reduced or eliminated.

MAJOR CHARACTERISTICS

ROTOR

DIAMETER (FT.)	92.0
TIP SPEED (F.P.S.)	750.0
DISC. LOADING (P.S.F.) AT DGW	8.9
BLADE AREA (8 AT 153 SQ. FT.)	1224.0
GEOMETRIC SOLIDITY RATIO	.09226
GEOMETRIC DISC. AREA (1 AT 6647.6 SQ. FT.)	13,299.0

PROPULSION

NUMBER OF ENGINES/TYPE	T701-AD-700(3) TURBOSHAFT
TRANSMISSION RATING (H.P.)	17,700
MAX. SINGLE ENGINE RATING	8,079
INTEGRAL FUEL CAPACITY (GAL)	2,938
INTEGRAL FUEL CAPACITY (LB)	19,100

WEIGHT (LB)

DESIGN GROSS WEIGHT, [illegible]	8,000
DESIGN PAYLOAD	[illegible]
DESIGN MISSION FUEL	[illegible]
FIXED USEFUL LOAD (INCLUDES 5 MAN CREW)	[illegible]
EMPTY WEIGHT	[illegible]
MAX. ALTERNATE GROSS WEIGHT	48,000
MISSION GROSS WEIGHT	[illegible]

GROUND ANGLES DEGREES

TURNOVER	[illegible]	360° @ 95,000 LBS
(WT. EMPTY)		
TIP BACK	[illegible]	360° FROM HOVER IGE @ [illegible]
(WT. EMPTY)		

CONTROL MOVEMENTS

COLLECTIVE PITCH	[illegible]	-1.0° TO +16.0°
DIFFERENTIAL COLLECTIVE PITCH	[illegible]	-3.5°
PROGRAMMED LONGITUDINAL CYCLIC PITCH	3.5° TO 7.0°	-3.0° TO +10.0°
SIDE ARM CONTROL CYCLIC PITCH	±3.5°	±3.0°
DIFFERENTIAL LATERAL CYCLIC PITCH	[illegible]	[illegible]
LATERAL CYCLIC PITCH	[illegible]	[illegible]

LANDING GEAR

NOSE - WHEEL / TIRE SIZE	[illegible]	[illegible]
MAIN - WHEEL / TIRE SIZE	[illegible]	[illegible]

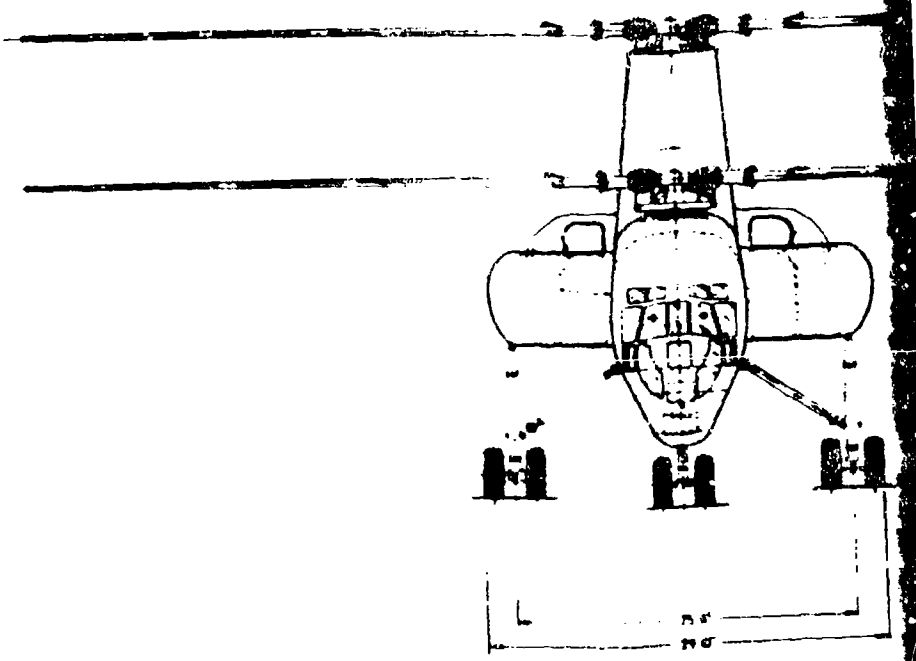

Figure 1. GENERAL ARRANGEMENT MODEL 301 HLH

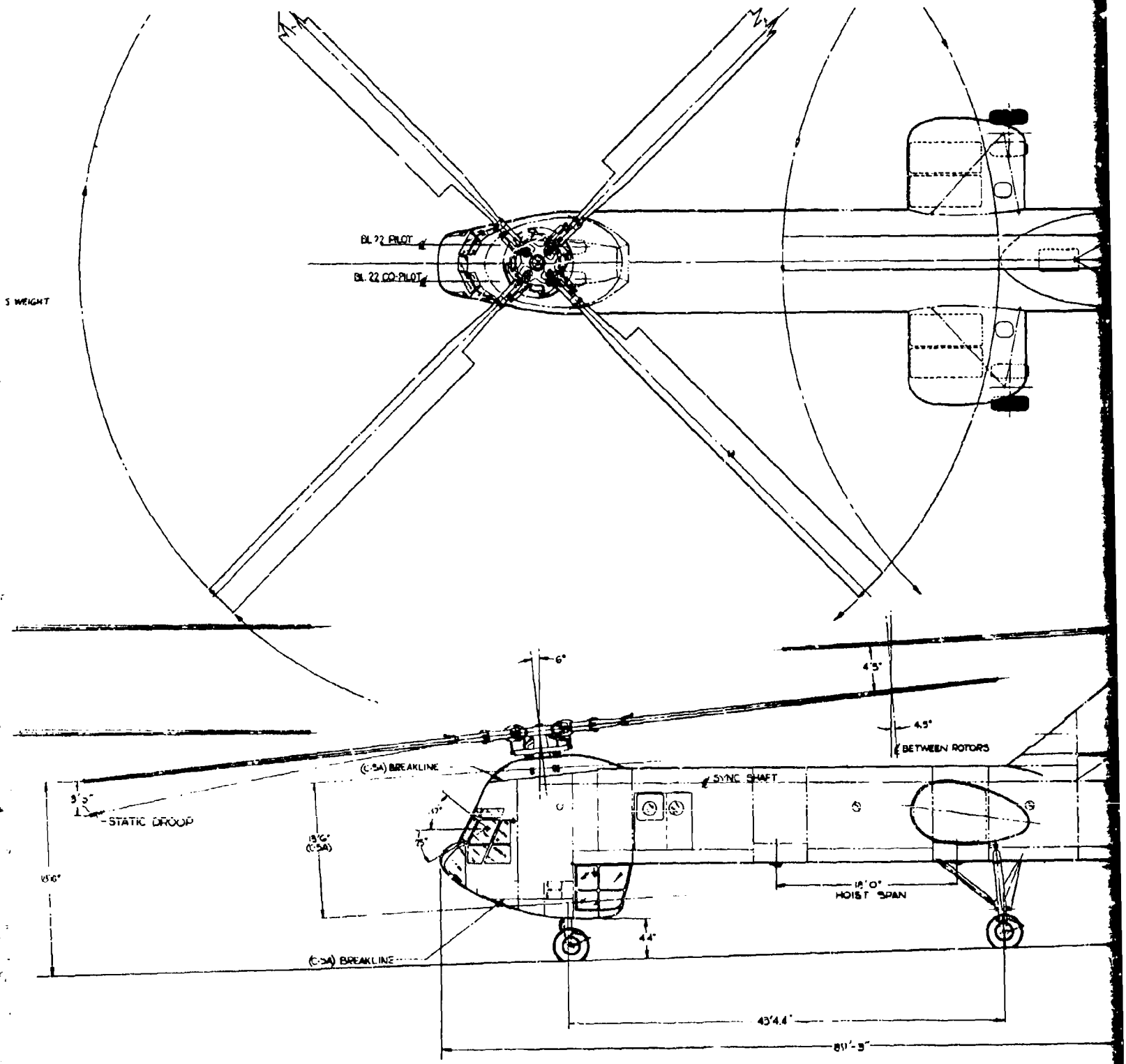

S WEIGHT

BEST AVAILABLE COPY

BEST AVAILABLE COPY

2

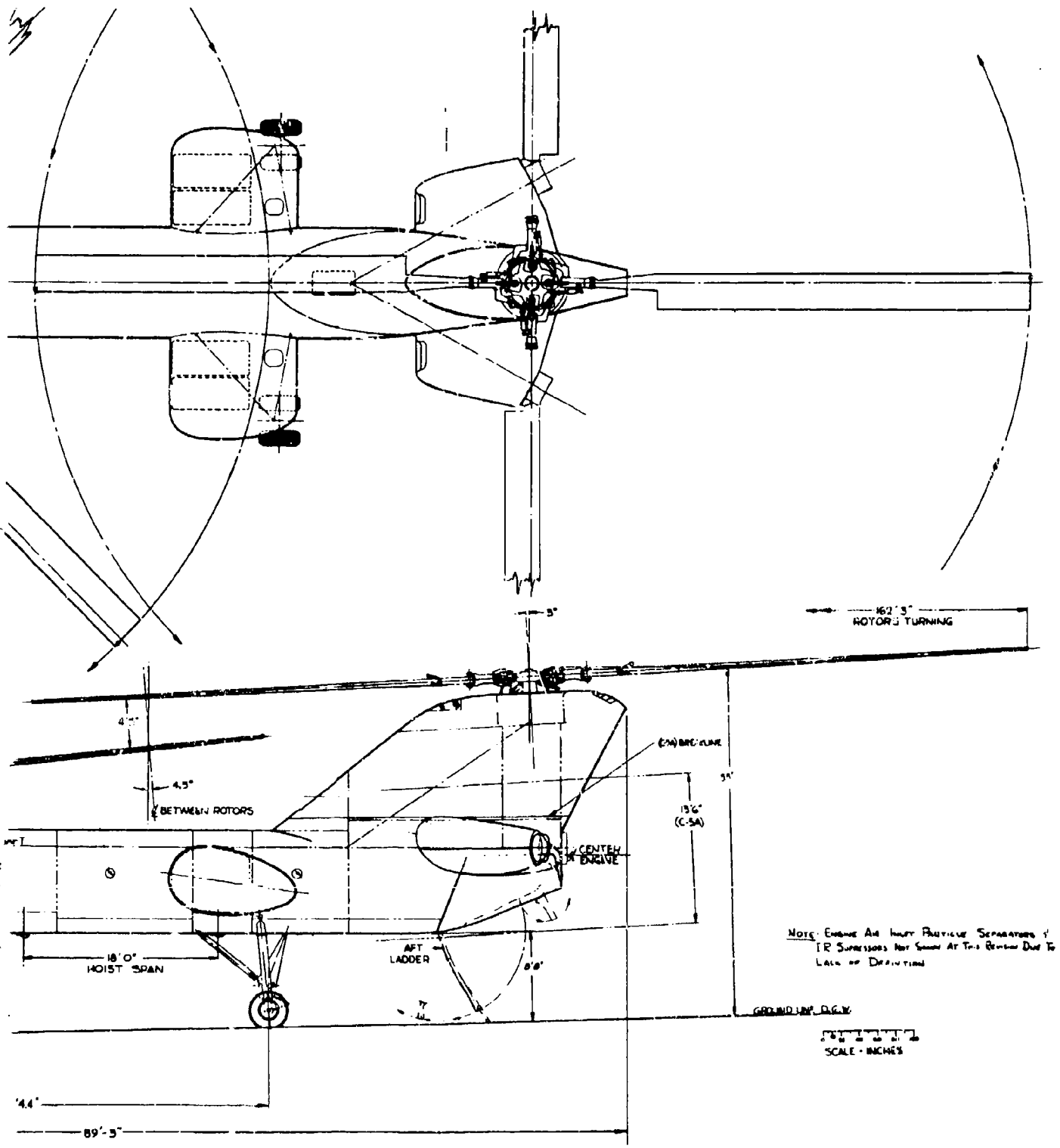

NOTE: ENGINE AIR INLET PARTICLE SEPARATORS & IR SUPPRESSORS NOT SHOWN AT THIS REVIEW DUE TO LACK OF DEFINITION

2.0 DESIGN DEVELOPMENT

2.1 OBJECTIVES

Table 1 shows the objectives and tasks initially established for the hub and upper controls ATC program. The objectives were later transferred into design requirements in the Prime Item Description Document (PIDD) for the HLH as summarized below.

Mission reliability. At the time of initial operational capability, the aircraft shall have at least a 97% probability of performing a 2-hour mission once flight for the mission commences. Mission reliability shall be based on "failures" which the crew cannot remedy while in flight or during a 15-minute ground turnaround using the onboard tools and equipment.

Operational availability. The aircraft shall have an operational availability or ready rate of 80% or greater when the average wartime utilization rate is 50 flight hours per month.

Mean time between removal(s) of major dynamic components. The mean time between removals (MTBR) objective for each major dynamic component shall be 2000 operation hours at time of Initial Operational Capability.

TBO (time between overhaul(s)). No repairable components shall require scheduled removal for overhaul. Removal or replacement will be "on-condition".

Fail-safety. The rotor hub and upper controls shall be designed to be fail-safe through the use of multiple load paths and/or low failure progressional rates and/or failure warning systems. Failure warning means shall be designed into the individual critical components and shall include but not be limited to the following:

- Dual load paths externally inspectable
- Pressure-sensitive gages
- Incipient failure warning by changes in vibration level
- Incorporation of bearing condition indicating systems to detect incipient bearing deterioration.

TABLE 1. ROTOR HUB AND CONTROLS - ATC PROJECT OBJECTIVES/TASKS

OBJECTIVE	CURRENT SYSTEM PROBLEM	BOEING CONCEPTS	ATC PROJECT TASKS
Improved Safety and Survivability	• Material Failure • Manufacturing Maintenance Errors • Combat Environment • Service Damage	• Redundancy, Failsafe Design. Failure Warning System • Design techniques to increase ballistic survivability • Design techniques to reduce probability of maintenance errors • Improved NDT methods	• Development of failsafe ballistic resistant components Multiple Load Path Hollow: Bleeding or Pressurized Failure Mode Determination • Diagnostic techniques for incipient failure warning Vibration Level Swashplate Signature
Improved Maintainability and Reliability	• Mechanical Complexity • Lubrication System Complexity	• Spherical Elastomeric Bearing Eliminates Lubrication Completely. Reduces number of hub components by 2/3.	• Advanced Elastomeric Bearing Technology Development of reduced size/light-weight elastomeric bearing. Evaluation of environmental effects. Evaluation of compression set. Development of incipient failure warning systems. Evaluation of bearing life. • Diagnostic Technique Development Swashplate Bearing Lag Damper • Development of Improved Control System and Lag Damper Bearings
	• Rotor Hinge and Swashplate Bearing TBO	• Elastomeric Hinge Bearing Replaceable "On-Condition" • Swashplate Bearing Diagnostics permits replacement "On Condition"	
	• Inadequate Field Procedure for checking Lag Damper	• "On-Board" Diagnostic Capability	
	• Control System and Lag Damper Bearing Life	• Improve Life by: Environmental Protection Materials Bonding Improvement	
Reduced Weight	• Large Lag Damper Forces Result in Heavy Components • Inefficient Ratio of: Finished Component Weight / Forging Weight	• Frequency Selective Lag Damper gives Lower Loads • Diffusion Bonding E2 Welding or a combination of both to improve weight/cost effectiveness	• Development of Frequency Selective Lag Damper. • Manufacturing Technology Development - Boeing and Forging Suppliers • Material Technology Development

2.2 TRADE STUDIES

Configuration trade studies were conducted for several of the areas of the hub and upper controls. The studies considered weight, cost, and maintainability as the primary factors with other factors peculiar to the item, such as the necessity for special tools. The trade studies are contained in Reference 1 and each of the trade studies is summarized below.

2.2.1 Rotor Hub Fail Safe Design

Three basic hub configurations were evaluated:

One-piece Offset Hub (Figure 2)
One-piece Strap Hub (Figure 3)
Two-piece Offset Hub (Figure 4)

Six fail-safe and one safe-life hub designs were derived in this study from the three basic configurations. The single safe-life (nonfailure) design, one piece offset hub was studied only to determine the weight penalty for fail-safety of the six safe-life designs. The type of warning system to detect the first failure was not considered in this study as it would be the same for any design.

Safe-life calculations assumed the following failures:

Design 2 - One-piece Offset Hub (Figure 2)

Either lead or lag side beam completely severed or severence of one cap flange across the damper opening in the lag side beam.

Designs 3 and 4 - One-piece Strap Hub (Figure 3)

Either lead or lag side beam completely severed or severence of one cap flange across the damper opening on the lead side beam. However, the glass strap on failed beam assumed to be intact and capable of sharing CF load.

Designs 5 through 7 - Two-piece Offset Hub (Figure 4)

One of the four side arms to the crossbeam is completely severed.

The minimum weight was achieved by the safe-life (no failure) one-piece offset hub. However this design was not considered as it could not sustain a failure. This design did show that a weight penalty of 200 pounds or more is incurred by a "fail-safe" design.

The minimum weight "fail-safe" design was the two-piece offset hub. The two-piece hub was the basis for the final design.

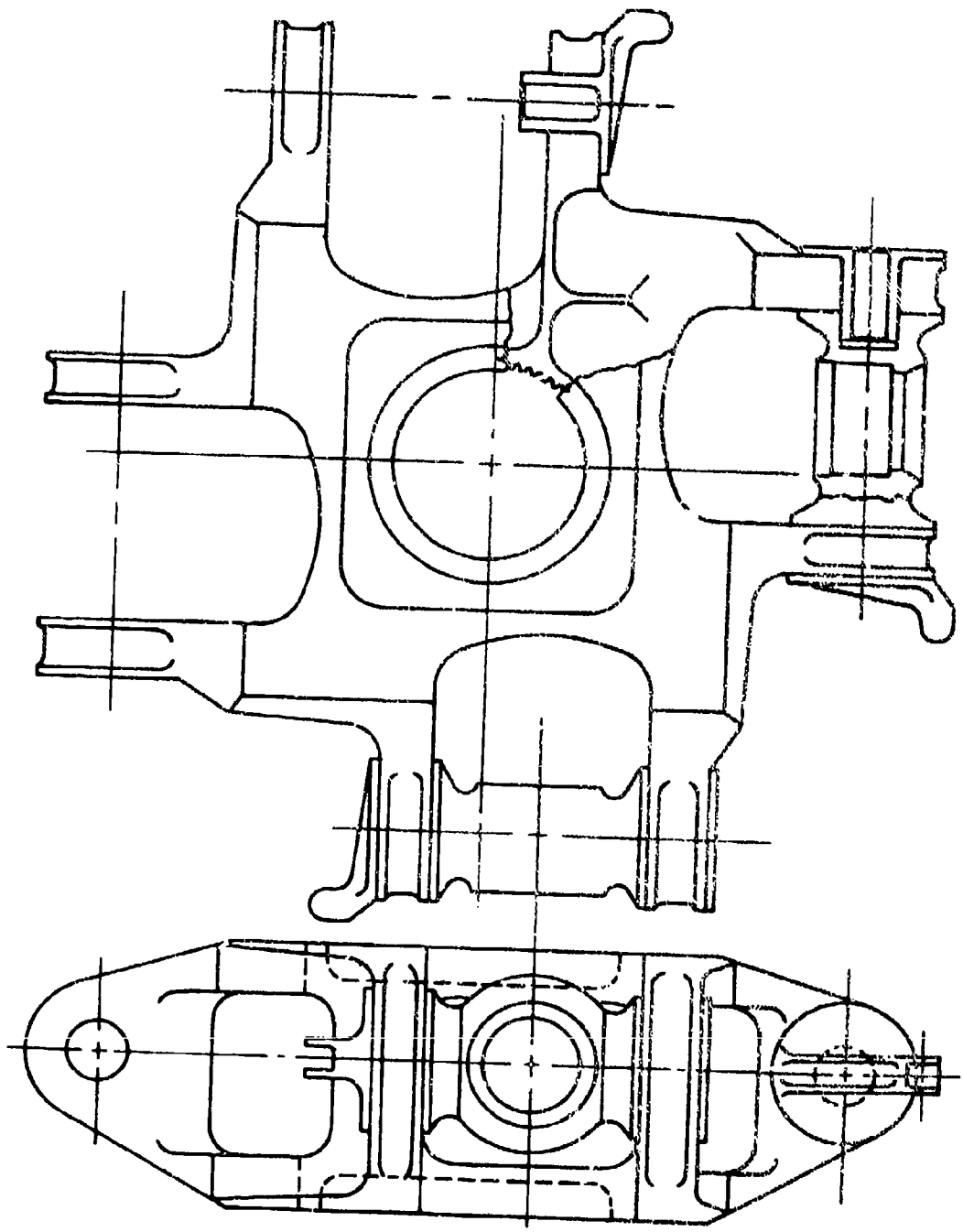

FIGURE 2. ONE-PIECE, FAIL-SAFE OFFSET HUB

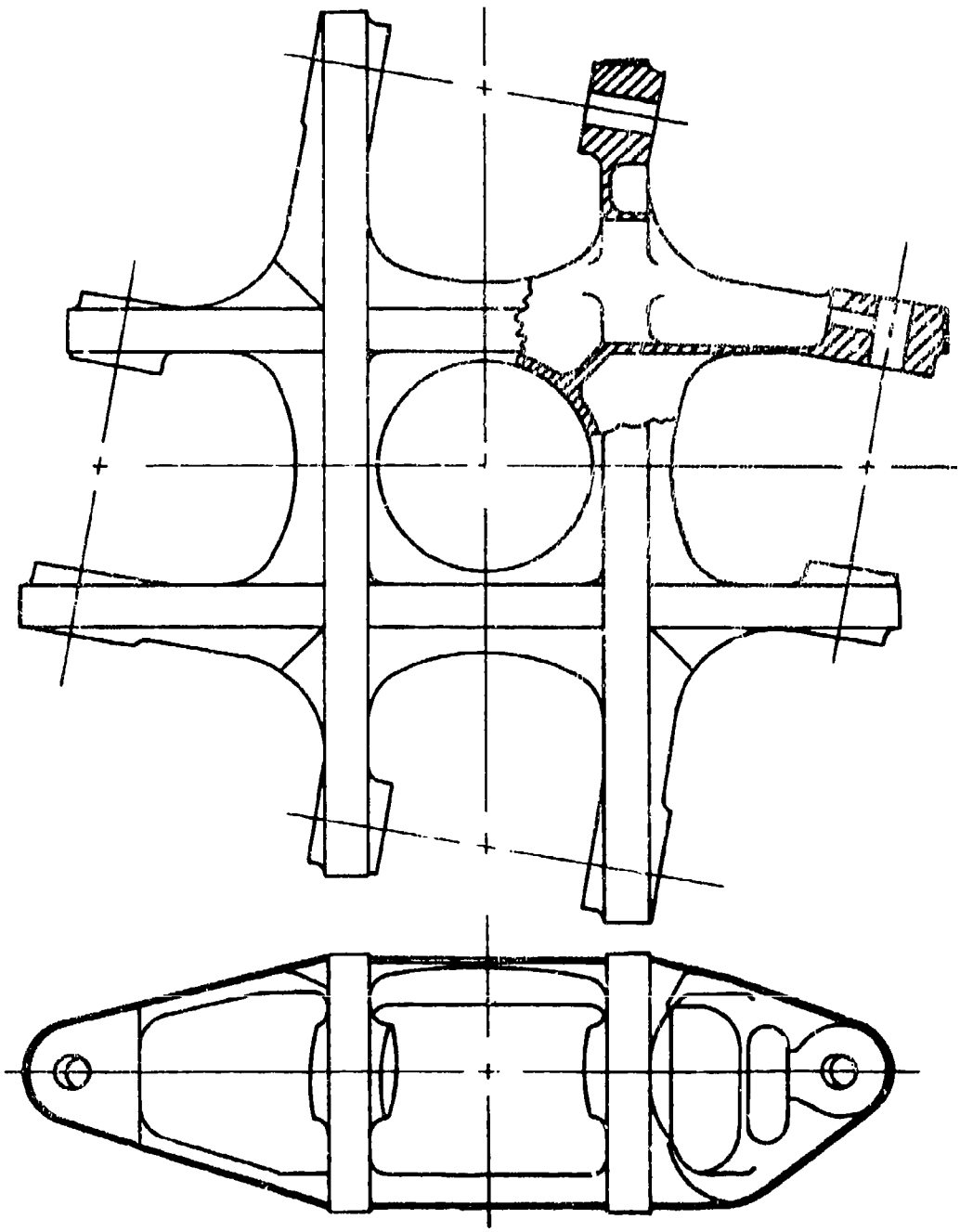

FIGURE 3. ONE-PIECE, FAIL-SAFE STRAP HUB

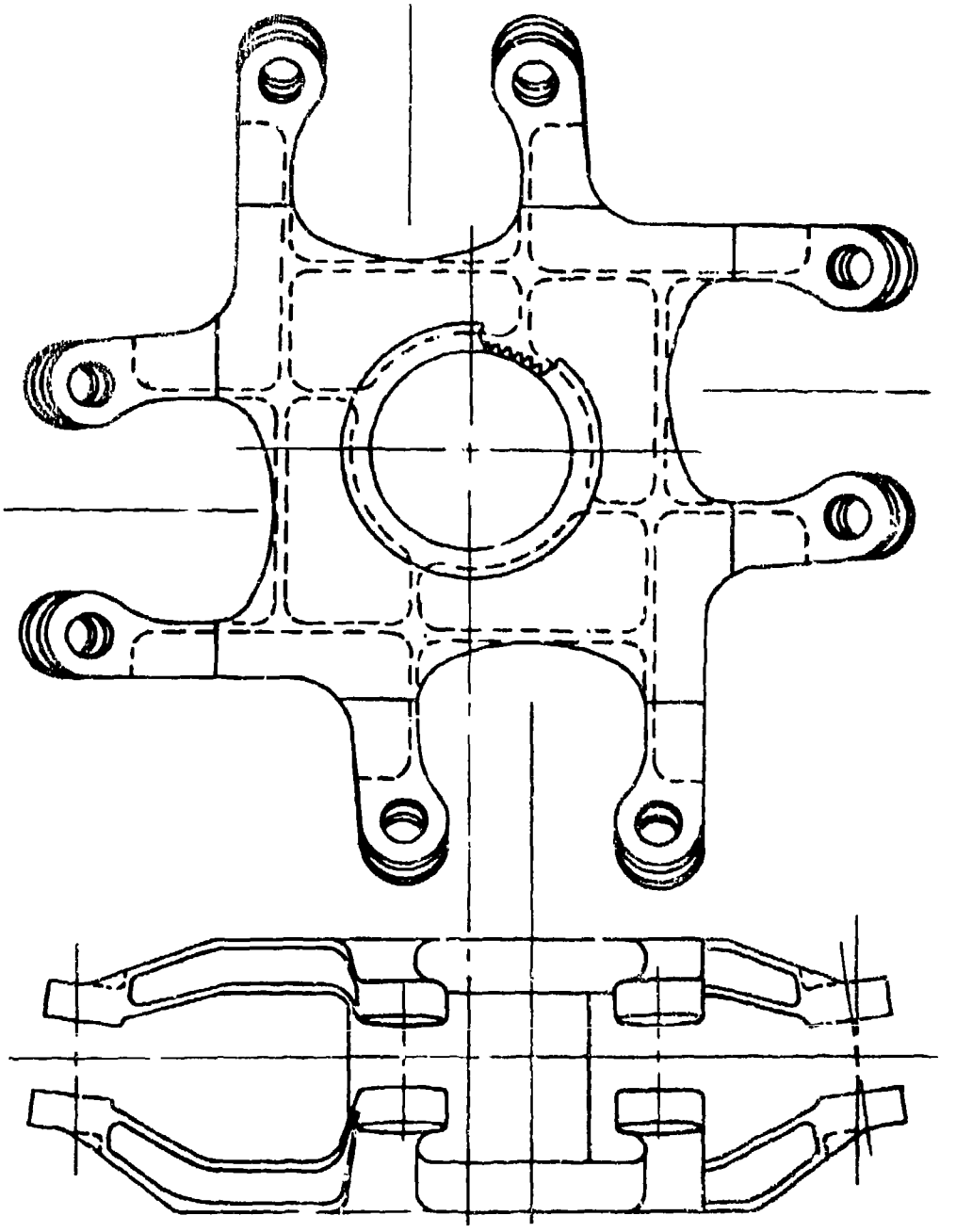

FIGURE 4. TWO-PIECE, FAIL-SAFE OFFSET HUB

The upper and lower hub halves for each configuration are identical and symmetrical about the horizontal centerline so that either half may be used in the upper or lower position on either the forward or aft rotor head.

2.2.2 Rotor Hub/Crossbeam Attachment

Three rotor hub crossbeam attachment configurations (Figure 5 were reviewed. Configuration A uses bolts in tension. Configuration B uses vertical pins. Configuration C uses horizontal pins.

Each of the attachment configurations was evaluated for weight, complexity, accessibility, and design characteristics. Configuration C, the horizontal pin connection, was selected as the recommended design approach for the HLH ATC rotor hub/crossbeam attachment method because this configuration provided:

- Lightest weight
- Lowest torque requirement
- Use of standard tools for installation
- Good accessibility
- Fewest parts
- No shimming required

2.2.3 Rotor Hub/Rotor Shaft Attachment

Fourteen configurations were studied. The features included torque path through bolts or splines and thrust load through bolts or a single nut, and combinations of these. The three principal configurations are shown in Figure 6 and described as follows:

Configuration II - Lower hub flange bolted to transmission shaft with large diameter bolts.

Torque and thrust carried by the bolts.

Configuration III - Three-inch spline (centered on lower hub flange) and thrust nut.

The spline transmits hub torque and the thrust nut transmits the lift load.

Configuration IIIA - Two 3-inch splines (centered on top and bottom hub flange) and thrust nut.

Configuration IIIA provides better load path distribution and better access to thrust nut and preloaded bolts. It was selected from consideration of all evaluation parameters, and was the basis for the final design.

2.2.4 Teflon Lined Spherical Bearing Vs. Elastomeric Bearings for Pitch Links and Hub/Blade Shear

This study considered the choice of a centering type, non-lubricated bearing capable of reacting vertical shear forces due to pitch link load and blade inertia while at the same time providing freedom of motion for blade flap/droop, lead/lag, and pitch, and freedom for blade radial motion under deflections due to centrifugal force.

The candidates were:

Elastomeric Bearing - A bearing consisting of alternate metal and elastomer laminates molded into a single spherical part. (See Figure 7 for proposed design.)

Teflon-Lined Spherical Bearing - A bearing consisting of a spherical stainless steel ball around which is swaged a stainless steel outer race lined with a woven Teflon fabric. Flap/droop and lead/lag motions to take place at the spherical interface of ball and Teflon liner. Similar lining of the bore of the ball with Teflon fabric in the fashion of a journal bearing to permit pitch motion and unrestrained radial movement of the blade. (See Figure 8 for proposed design.)

The Teflon-lined spherical bearing was selected for use as the HLH/ATC shear bearing. The Teflon-lined bearing is smaller, lighter in weight, and less expensive to develop than the elastomeric bearing while providing all the advantages of the elastomeric bearing.

2.2.5 Loop

A trade study was conducted of various designs of the loop structure, which transmits the blade centrifugal loads from the pitch housing to the elastomeric bearing as shown in Figure 18.

The study investigated the 13 pitch housing loop configurations, and the 7 bearing attachment configurations shown in Figure 9. The configurations were judged for weight, fail-safety, structural adequacy, and manufacturing difficulty.

Each configuration is discussed briefly below and summarized in Table 2.

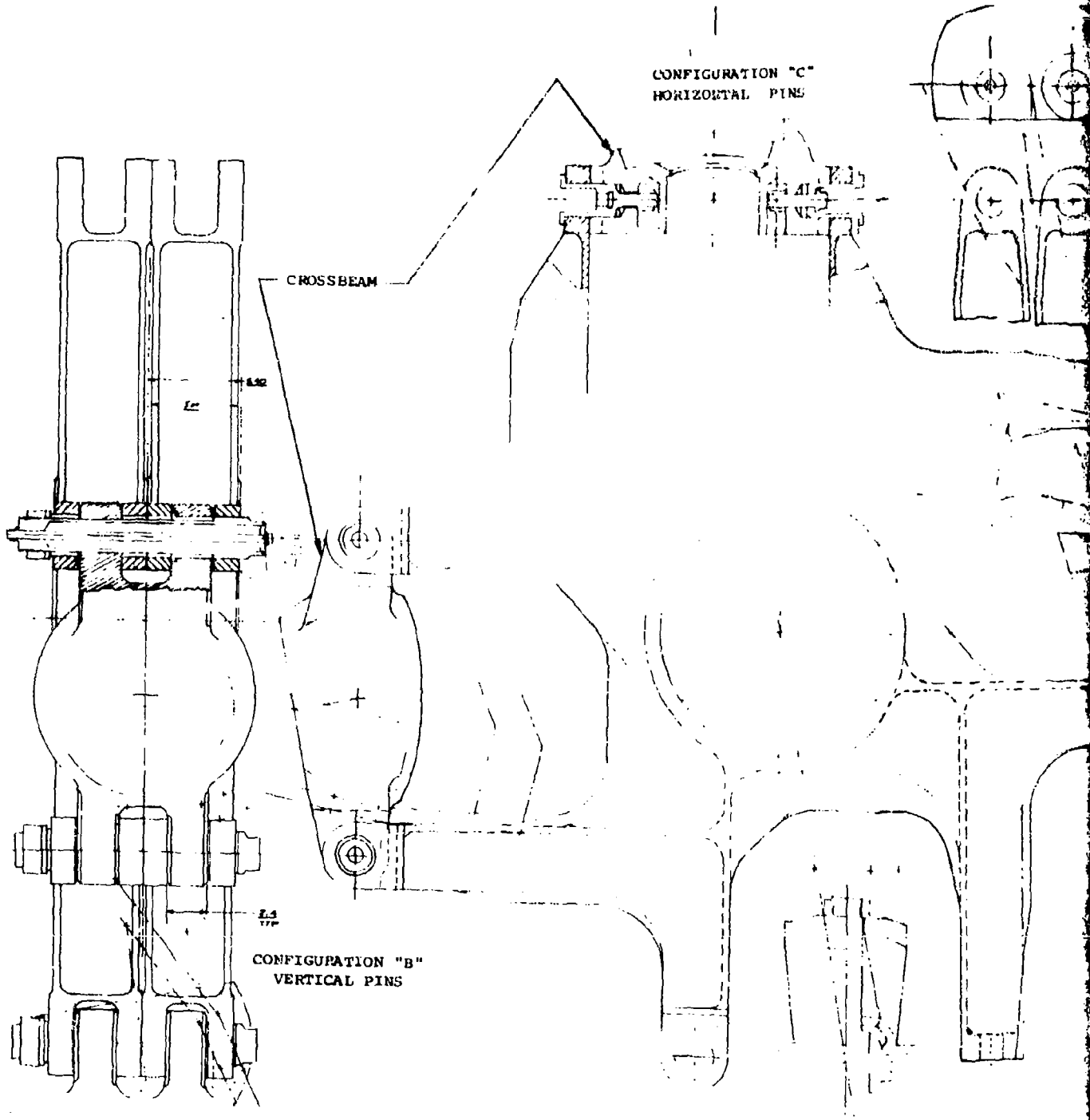

FIGURE 5. ROTOR HUB/CROSSBEAM ATTACHMENTS

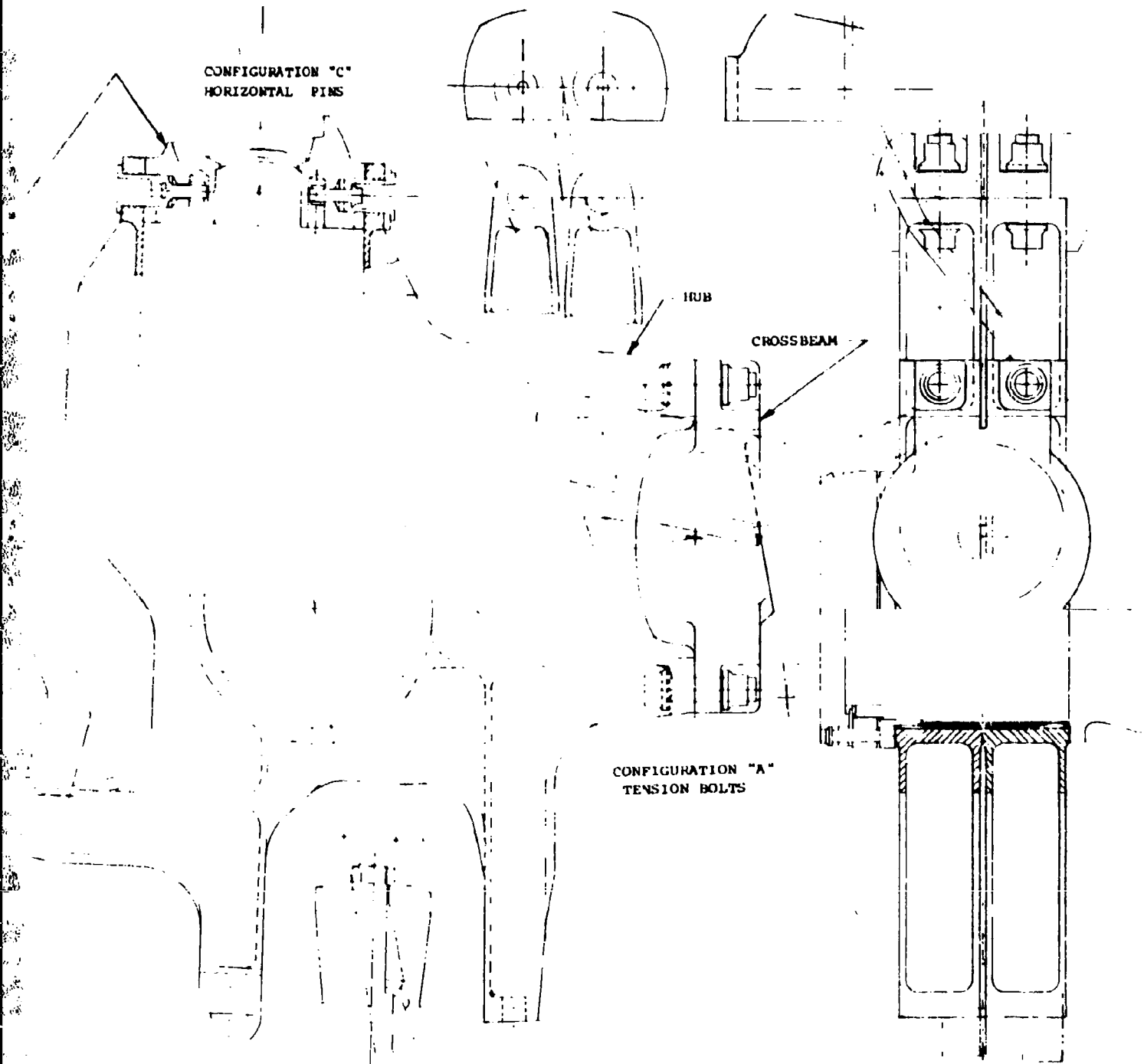

M ATTACHMENTS

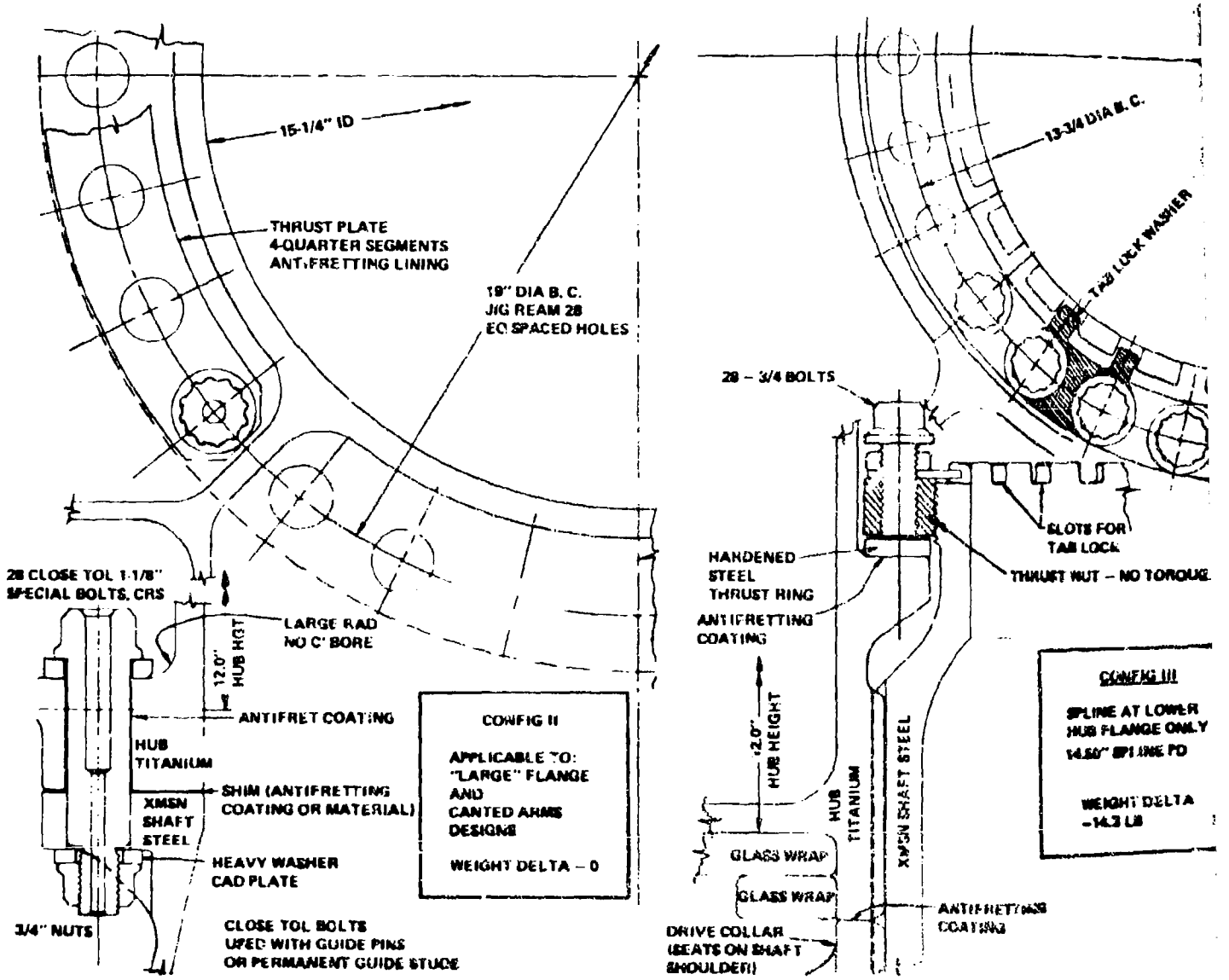

FIGURE 6. ROTOR HUB/SHAFT ATTACHMENTS

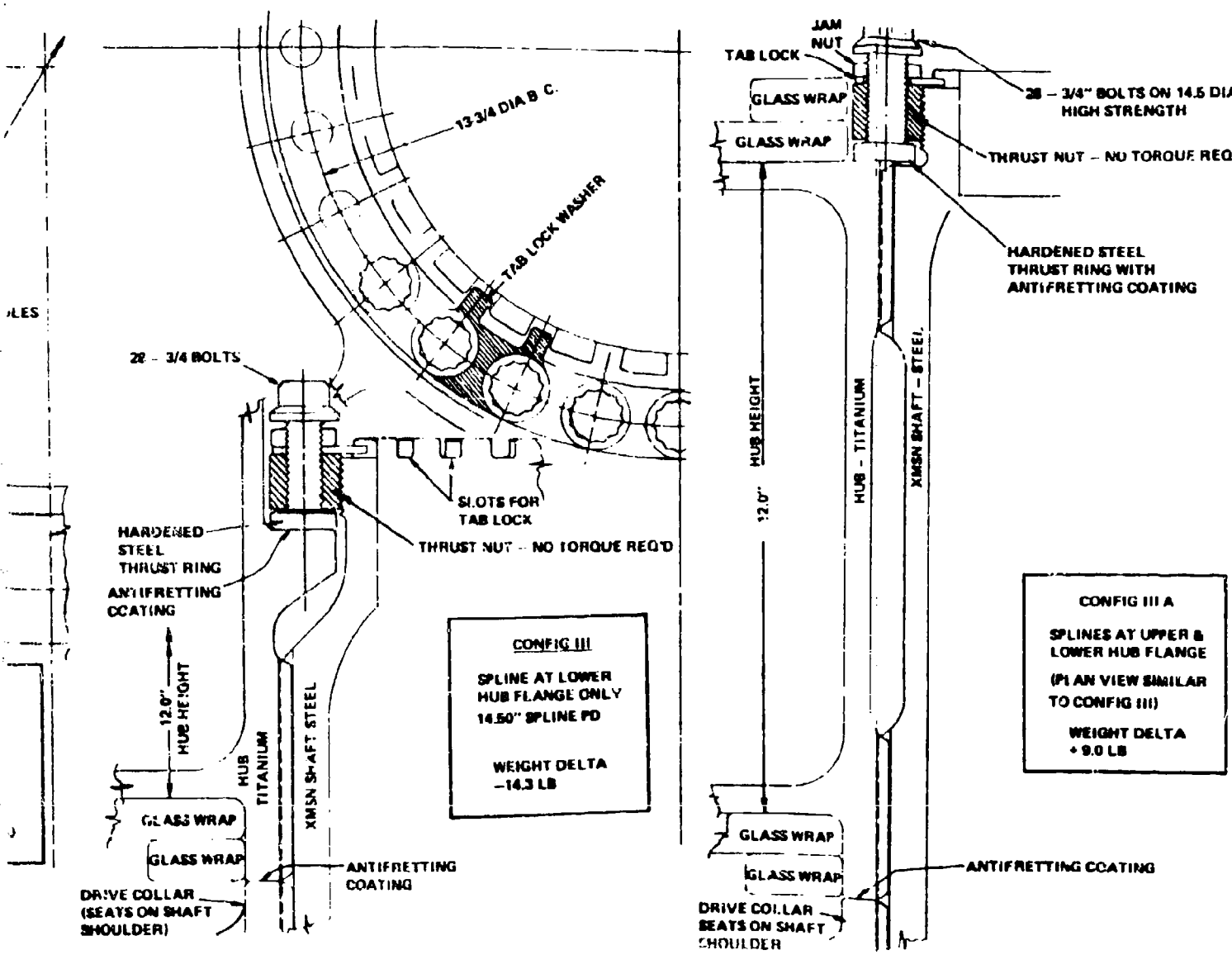
13.3/4 DIA B. C.
TAB LOCK WASHER
28 – 3/4 BOLTS
SLOTS FOR TAB LOCK
THRUST NUT – NO TORQUE REQ'D
HARDENED STEEL THRUST RING
ANTIFRETTING COATING
12.0" HUB HEIGHT
HUB TITANIUM
XMSN SHAFT STEEL
GLASS WRAP
GLASS WRAP
ANTIFRETTING COATING
DRIVE COLLAR (SEATS ON SHAFT SHOULDER)
CONFIG III
SPLINE AT LOWER HUB FLANGE ONLY
14.50" SPLINE PD
WEIGHT DELTA –14.3 LB
JAM NUT
TAB LOCK
GLASS WRAP
GLASS WRAP
28 – 3/4" BOLTS ON 14.5 DIA B. C. HIGH STRENGTH
THRUST NUT – NO TORQUE REQ'D
HARDENED STEEL THRUST RING WITH ANTIFRETTING COATING
HUB HEIGHT
12.0"
HUB – TITANIUM
XMSN SHAFT – STEEL
GLASS WRAP
GLASS WRAP
ANTIFRETTING COATING
DRIVE COLLAR SEATS ON SHAFT SHOULDER
CONFIG III A
SPLINES AT UPPER & LOWER HUB FLANGE
(PLAN VIEW SIMILAR TO CONFIG III)
WEIGHT DELTA +9.0 LB

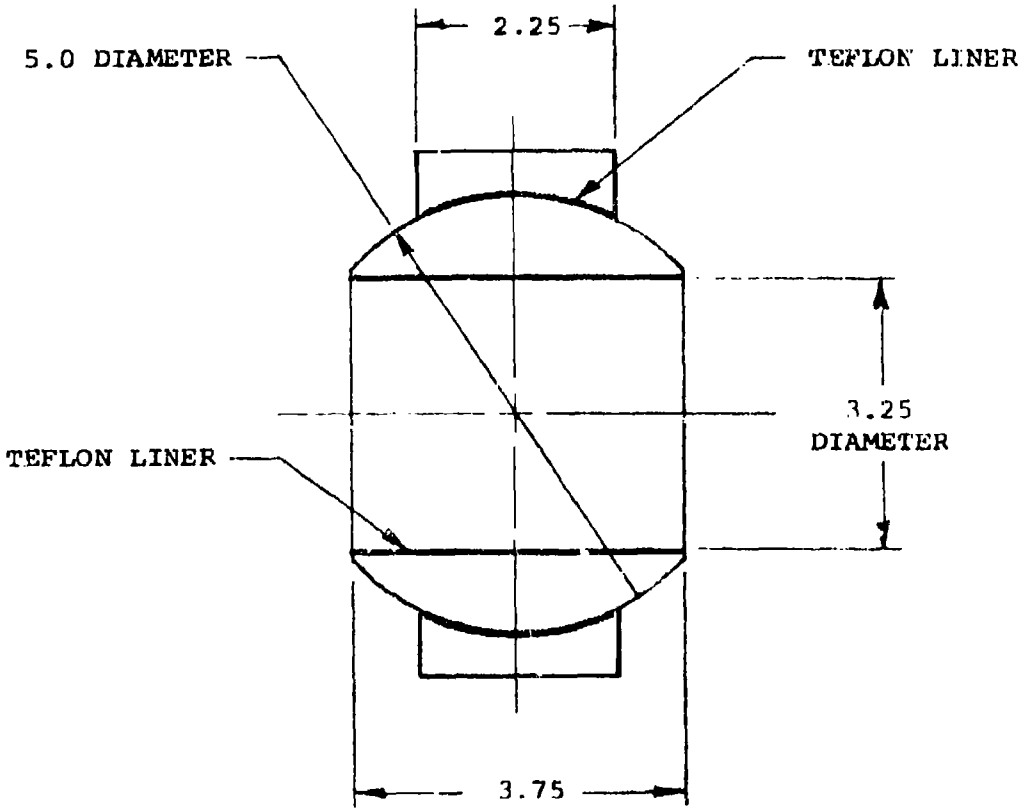

FIGURE 7. PROPOSED DESIGN OF TEFLON-LINED SPHERICAL BEARING

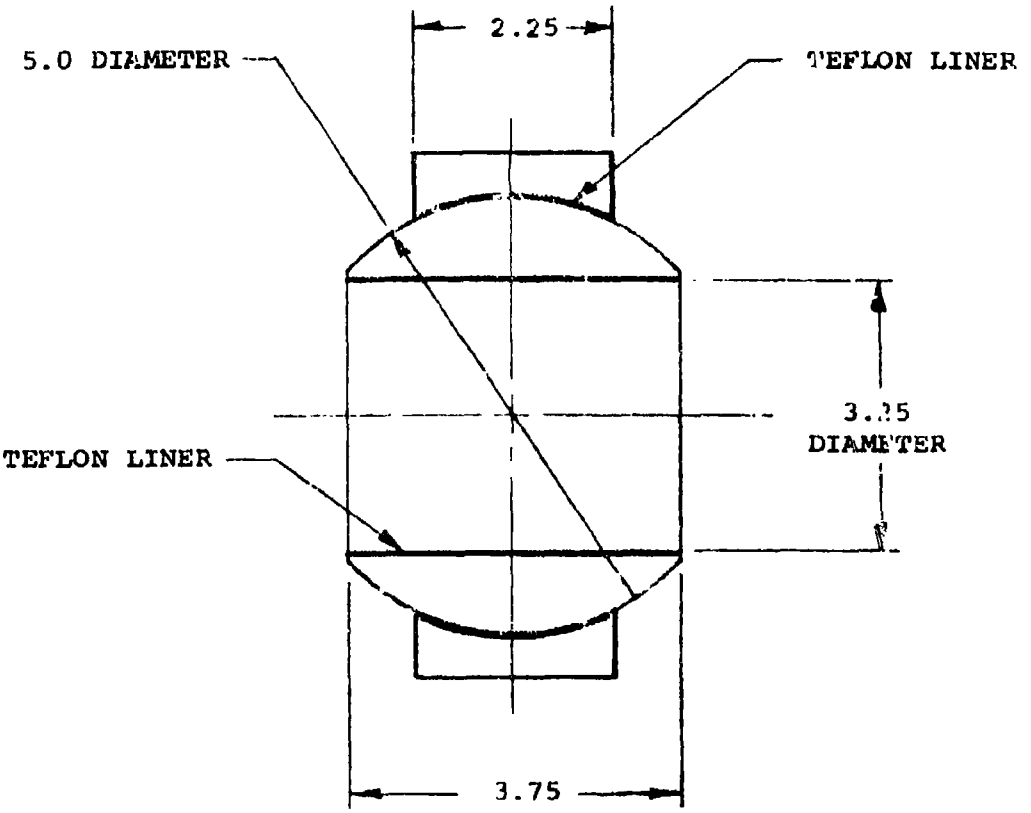

FIGURE 7. PROPOSED DESIGN OF TEFLON-LINED SPHERICAL BEARING

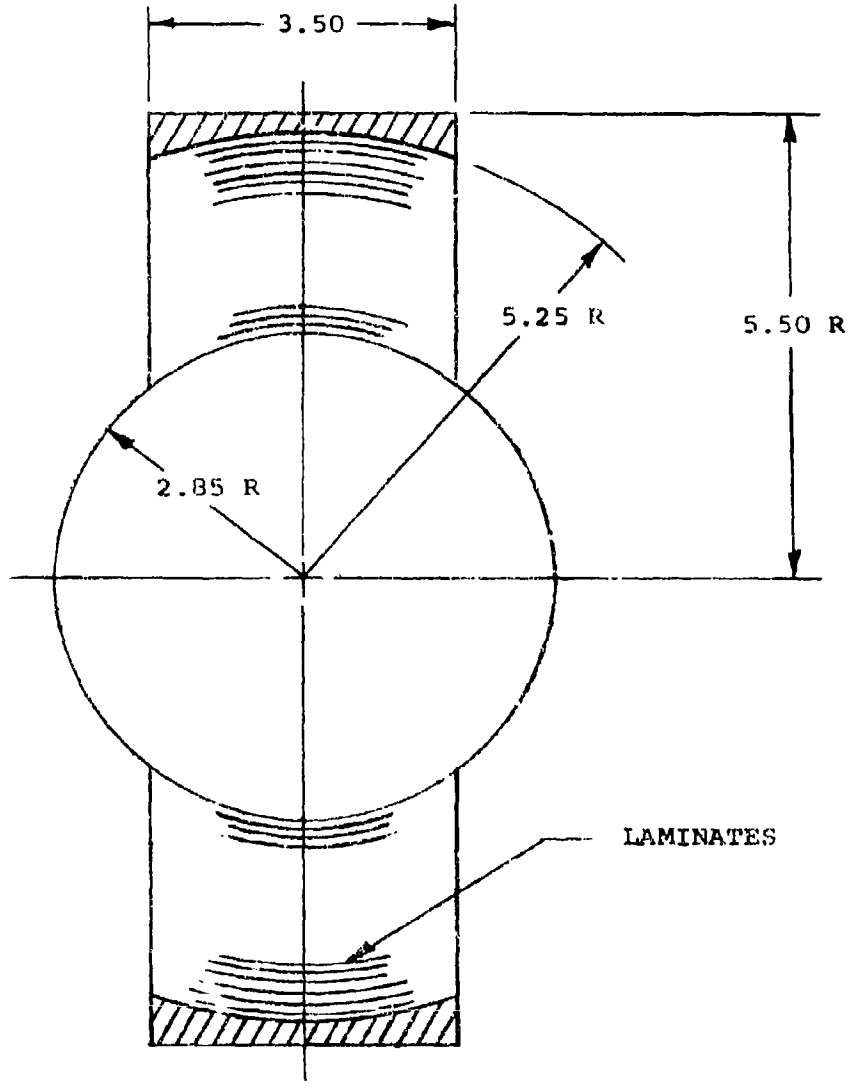

FIGURE 8. PROPOSED DESIGN OF ELASTOMERIC BEARING

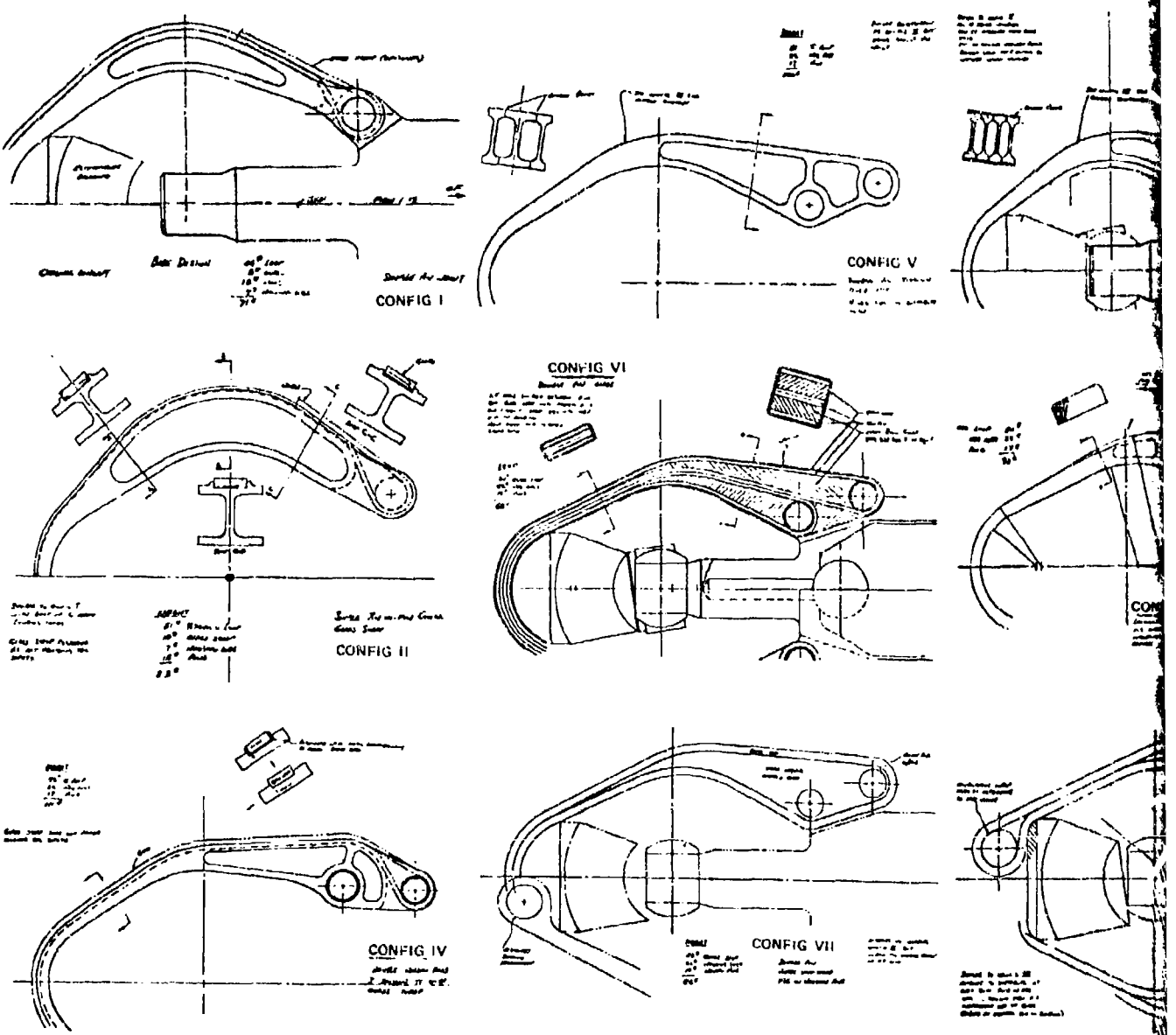

FIGURE 9. LOOP CONFIGURATIONS AND BEARING ATTACHMENTS
(Sheet 1 of 2)

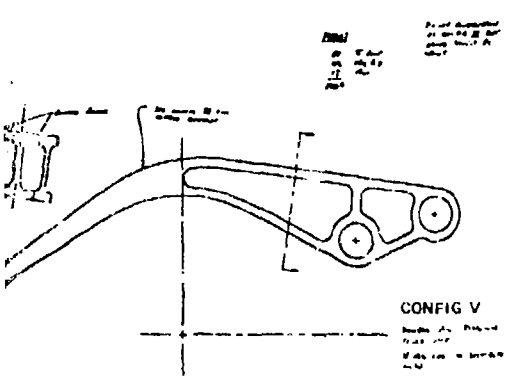

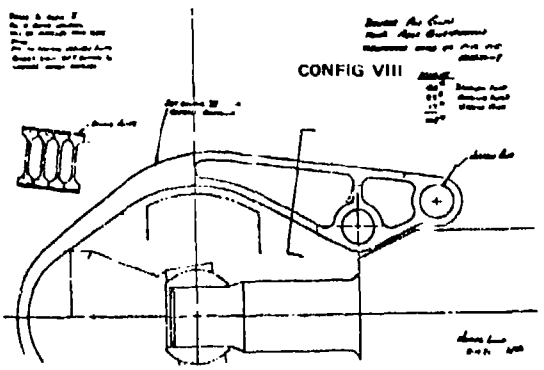

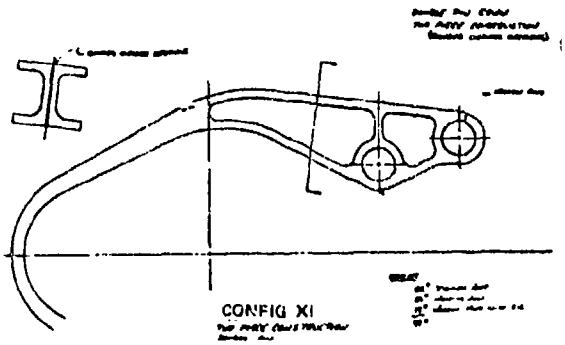

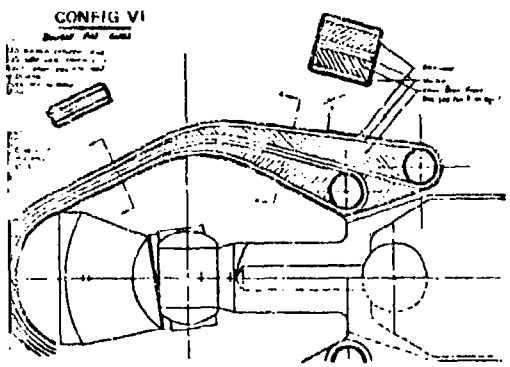

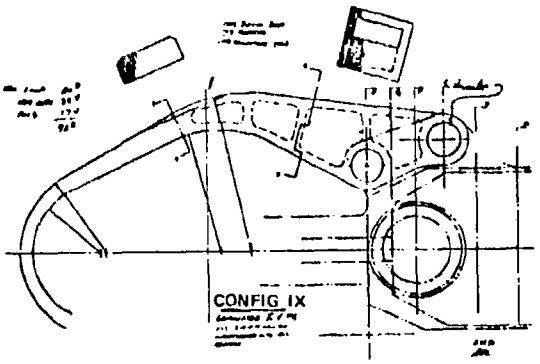

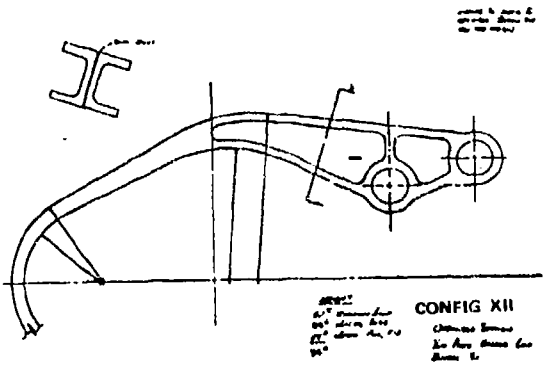

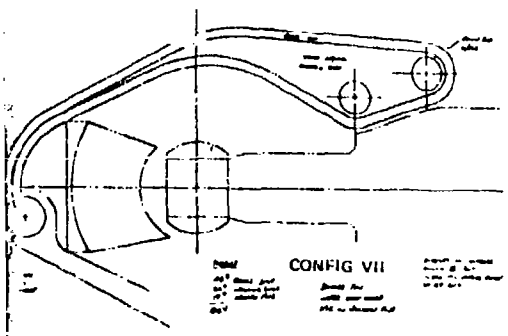

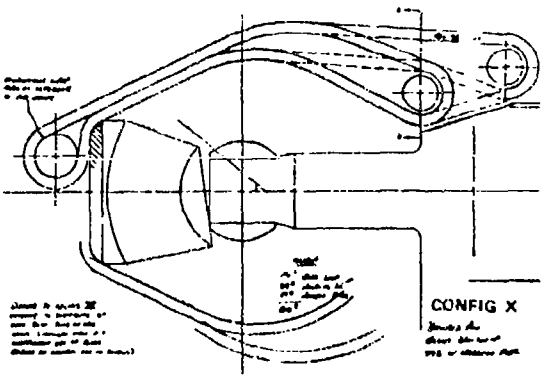

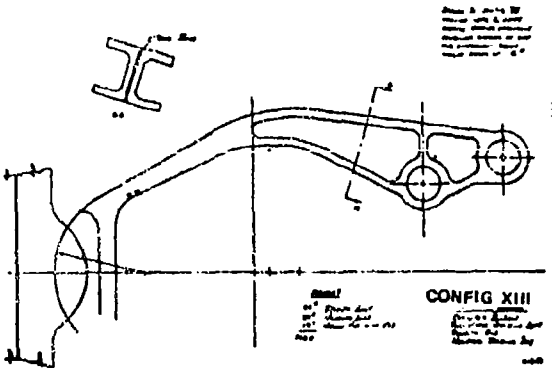

EARING ATTACHMENTS

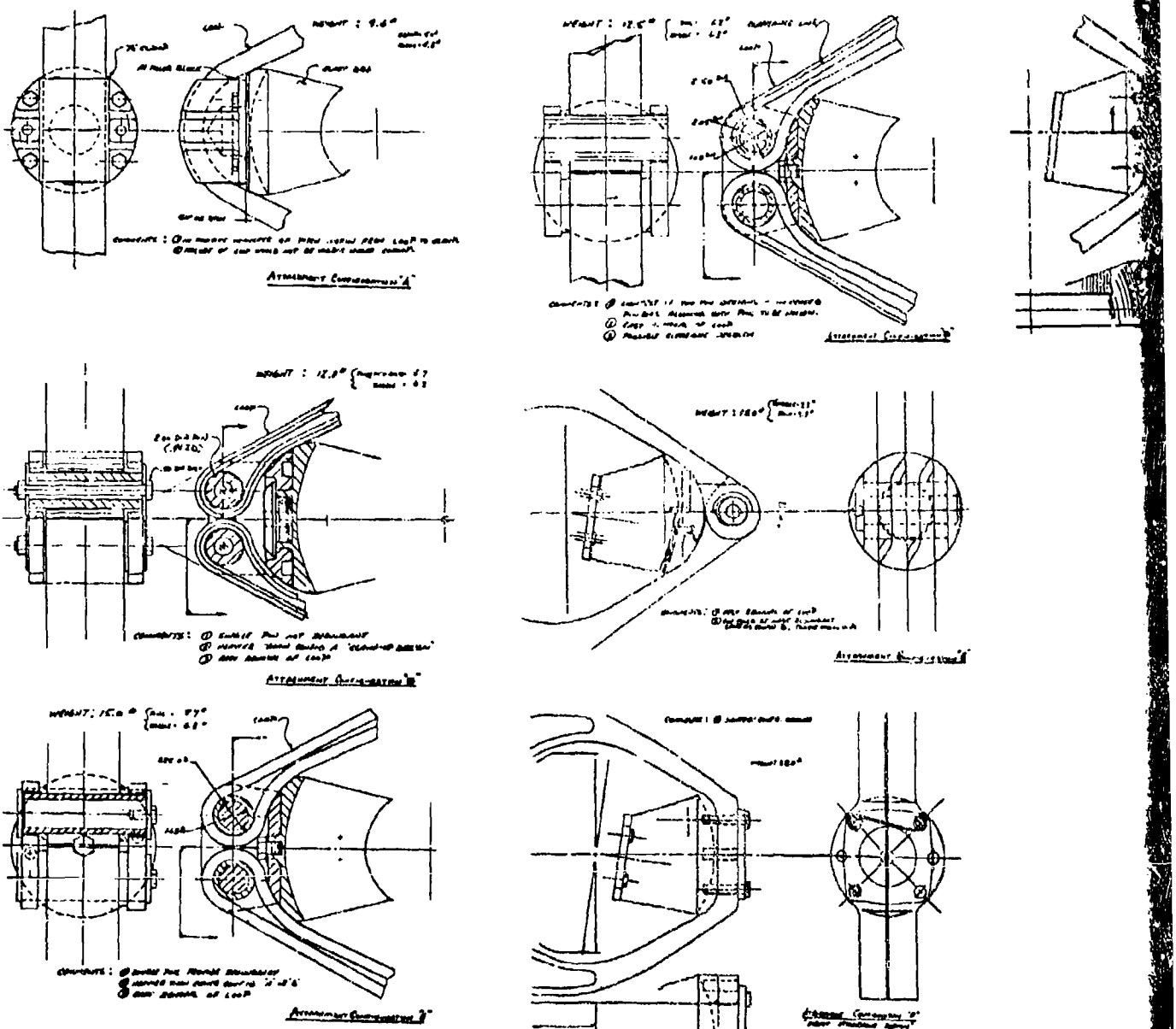

FIGURE 9. LOOP CONFIGURATIONS AND BEARING ATTACHMENTS
(Sheet 2 of 2)

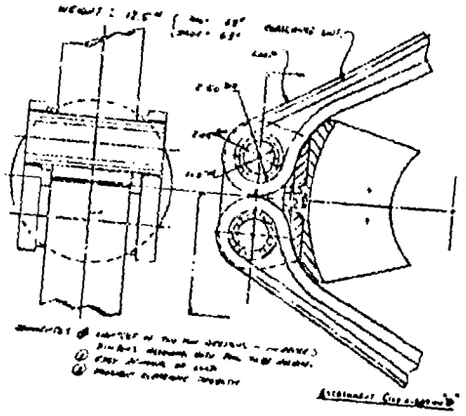

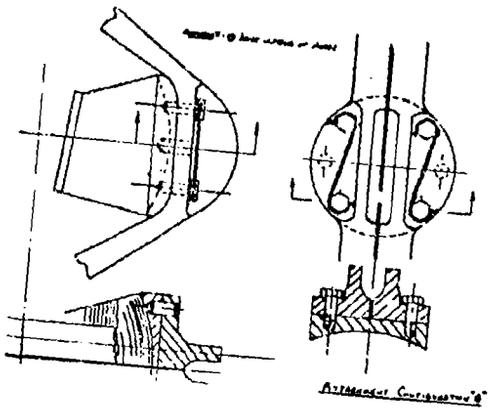

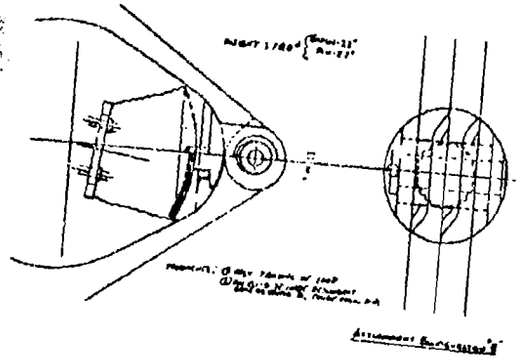

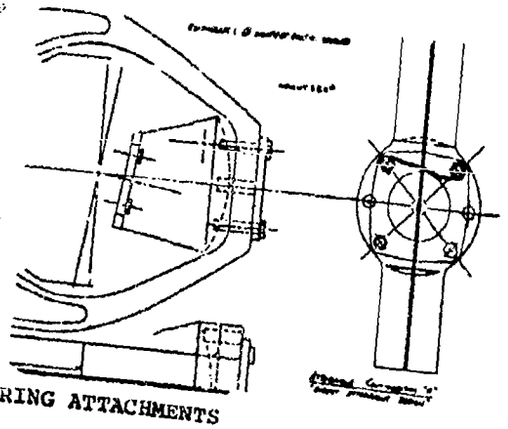

RING ATTACHMENTS

TABLE 2. LOOP DESIGN SUMMARY

CONFIGURATION	HOUSING JOINT	MATERIAL	SECTION DESCRIPTION	WEIGHT LOOP	WEIGHT TOTAL	REMARKS
I.	Single pin-in-pin redundant design FIS.	Titanium Forging With Glass Strap Alt.	One piece I section.	44#	71#	Original concept. No FIS. (2)
II.		Titanium Forging With Glass Strap Alt.	One piece I section similar to Configuration I strengthened.	51#	83#	Glass strap does not provide fail safety. No FIS.
III.		Titanium Forging	Three piece I section of Configuration II contour, four hag. lugs.	52#	77#	Redundancy and FIS in cavities. Increased pitch motion causes hub interference with contours. (Configurations I, II, III.)
IV.	Double pins hollow with FIS.	Titanium Forging With Glass Strap Alt.	One piece I section, glass strap in metal channel bonded to Ti section.	72#	111#	Glass strap does not provide fail safety.
V.		Titanium Forging	Three I sections bonded together at flanges forming FIS cavities (Configuration III)	61#	Note1 100# (1)	No glass, FIS in cavities. Four housing lugs reduce pin size.
VI.		Fiberglass Uni. X ply. Epoxy resin.	Box section of Uni fiberglass & resin filler, outside wrapped with X ply..	27#	66#	Shear loads too great for resin filler. Uni-wrap near neutral axis inefficient. Layup problems.
VII.		Fiberglass Uni Chopped Glass Filler	Box section of Uni fiberglass wrap, chopped glass filler.	45#	84#	Attempt to improve VI. Inboard pin not sharing CF load.
VIII.		Titanium Plate Stock	Four identical I sections bonded at flanges, covered with bonded titanium cap strip, top and bottom. (Configuration V)	68#	Note1 107# (1)	Same as V. Better configuration, for extended life in failed condition, than V. No forging required.
IX.		Sheet Titanium/Fiberglass Laminate	Box section with ribs and webs, stamped Ti sheet, 40 laminates	54#	93#	FIS in cavities. Better fail safety than Configuration VIII. Better stress allowables. Required development program. Needs saddle mount for bearing.
X.		Fiberglass Uni Chopped Glass Filler	Box section, Uni fiberglass outside, chopped glass filler.	41#	80#	Attempt to improve VII by distributing CF load over both pins. Weak in bending. Layup problems.
XI.		Titanium Forging		58#	97#	Similar to V in concept. No FIS cavities.
XII.			I section formed by bonding two channel sections back--to-back.	55#	94#	Similar to XI but with computer optimized section.
XIII.				61#	100#	Similar to XII but with modified nose for bearing attachment Configuration G.

NOTE (1) Configurations V and VIII weights, when recalculated using the optimized sections, should be approximately equal to Configuration XII.

(2) FIS - Failure Indicator System

Configurations I and II - One-piece, single pin loop/housing attachment

These one-piece, forged titanium loop designs (with a fiberglass strap option) were light in weight and structurally sound, but did not meet the fail-safe criteria.

Configuration III - Three-piece, single pin loop-housing attachment

Similar in shape to Configuration II, this three-piece bonded construction design provided fail-safety through redundancy. Cavities between the sections would be used to contain a dye or for a pressure system as a failure-indicating device. At that time, however, blade control motions were increased, and Configurations I, II and III exceeded this new clearance envelope.

Configuration IV - One-piece, double pin loop/housing attachment with glass strap

This design, a one-piece forged titanium loop with a fiberglass strap reinforced with a metal shear strip, was the heaviest of all configurations. The two-pin attachment configuration, working as a cantilever beam, fits the clearance envelope and is structurally sound, but the fiberglass strap will not meet the fail-safety criteria.

Configurations V and VIII - Multiple-piece, double pin, loop/housing attachment

These three-and four-piece designs, similar to Configuration III, were found to be heavy and difficult to manufacture.

Configurations VI, VII, X - Fiberglass, double pin loop/housing attachment

These three configurations were an attempt to design a composite loop using fiberglass uni and cross ply with chopped glass and resin filler. These designs could not be made structurally adequate within the limited space available.

Configuration IX - Laminated, double pin loop/housing attachment

This design uses approximately 40 titanium sheets bonded with fiberglass plies to form a strong, stiff, and efficient (in bending and torsion) section of a box shape The cavities are pressure chambers for a failure indication system. This design was judged complex and difficult to fabricate.

Configurations XI, XII, XIII - Two-piece, bonded, double pin loop/housing attachment

Similar to Configuration V, these designs use two forged titanium channel sections bonded to form an I section. Fabrication simplicity and some weight savings were achieved. Configuration XII is a minor modification to Configuration XI, reducing the weight by 25 pounds per aircraft. Configuration XIII is a modification of the bearing attachment area, permitting use of the Configuration C, Direct Attachment Method (see Configurations F and G below). This combination results in less overall weight, and was judged to have the best chance of success.

Configuration A - Clamp design bearing attachment

This configuration clamps the housing loop against a filler block on the elastomeric bearing plate. Since the system depends upon friction alone to maintain orientation, there is no positive transfer of pitch motion from loop to clamp. Also, any loop failure originating under the clamp would not be visible for inspection.

Configurations B, C, D and E - Pin-type attachments

These configurations provide positive transfer of pitch motion from the loop to the bearing. Replacement of the bearing is accessibility to the elastomeric bearing, and simplified assembly are the advantages of these designs, but they incurred a weight penalty.

Configurations F and G - Direct attachment

These configurations require a wider, and, therefore, heavier housing loop configuration to permit the use of attachment bolts. However, the weight of the combined loop and attachment, Configuration XIII bolted to Configuration G, is less; therefore, this combination was selected.

Configuration XIII, the two-piece bonded titanium loop, in conjunction with the direct bearing attachment, Configuration G, was chosen. The rationale was:

- Simplicity of Fabrication
- Best Weight Compromise
- Best Load Path

As the design was further defined, it was found that a three-element loop with the elements separated by an anti-fretting layer of the Teflon fabric was structurally more efficient than the two-piece bonded loop when evaluated against the fail-safe criteria.

A single failure of the two-piece loop resulted in a doubling of the load on the remaining structure and considerable eccentricity in load application.

The three-piece design, shown in Figures 17, 18, and 20, has the central element of approximately double the thickness of the two outer elements. Failure of an outer element results in much less eccentricity of load than with the two-piece design, and the increase in load on the remaining structure is only a third. If the central element fails, the load is doubled on the two outer elements but there is no eccentricity of load so the design is again more efficient than the two-piece.

2.2.6 Swashplate and Upper Controls

This study included:

Materials and construction of the swashplate
Swashplate centering device
Single and dual clevis lugs

The combinations of swashplate material and construction included two bearing diameters.

BEARING DIAMETER	42"		59"	
CONSTRUCTION	WELDED	TWO-PIECE BOLTED	WELDED	TWO-PIECE BOLTED
MATERIAL	TITANIUM	ALUMINUM	TITANIUM	ALUMINUM

The centering devices considered were the ball/slider of the CH-47, and four-arm scissors. Dual clevis and single clevis configurations of fail-safe actuator and pitch link attachment lugs were studied. Although both configurations are approximately equal in load-carrying ability, the single clevis lug is recommended for the following reasons:

- Lighter weight
- Easier visual inspection to find failed lug
- Can provide holes through center or lugs from swashplate ring for pressure/vacuum failure monitoring

The two-piece bolt aluminum swashplate with centering scissors was chosen for further design.

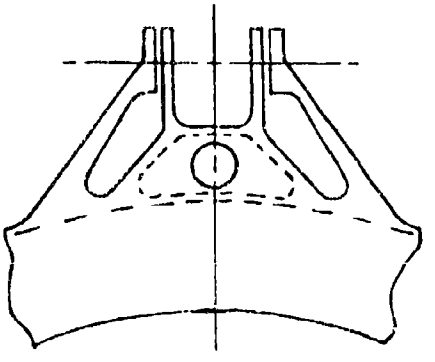

Dual Fail-Safe Clevis

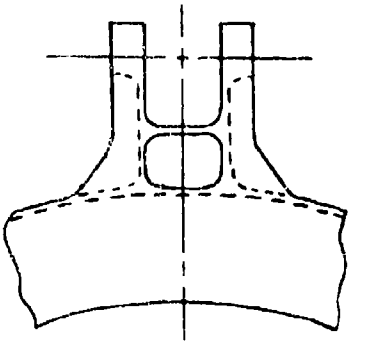

Single Fail-Safe Clevis

2.3 DESIGN DEVELOPMENT TESTS

Fatigue and endurance tests were conducted on representative specimens of hub and upper controls parts and features to acquire design data and to prove the concepts. Results of these tests are summarized below.

2.3.1 Titanium Hub Materials Test Summary

The titanium hub materials tests are reported in Reference 2.

Engineering material properties were developed for a 9 x 16 x 36-inch 6Al-4V titanium alloy billet finish forged in Alpha-Beta range and subsequently processed to the solution treated and over-aged (STOA) condition. These properties were obtained for application in the design of large fatigue critical forged titanium helicopter dynamic system components. Static strength, smooth and notched axial fatigue strength, fretted fatigue strength, fatigue crack propagation, and fracture toughness data were obtained. Fatigue strength data which indicate the influences of shotpeening and the use of coatings to inhibit fretting were also obtained.

The titanium alloy forging, procured to AMS4928, was sectioned into blanks for test specimens. Each fatigue and fracture specimen was coded to indicate its original location within the forging.

Both the forged billet and specimen blanks in the machined and nonmachined condition were subjected to ultrasonic, penetrating radiation, liquid penetrant, and blue etch anodize inspections. These inspections did not reveal any significant material or processing anomalies.

The structure of the titanium forging used for the fatigue and fracture specimens can be metallurgically characterized as large grained with sizes in the approximate range of 0.06 to 0.10 inch. The microstructure was comprised of elongated Alpha platelets in a transformed Beta matrix. To a much lesser extent, globular Alpha in a transformed Beta matrix was observed.

The elements of this test program were structured to provide inter-relating pieces of data often required in a particular sequence. Each of the tests and the more significant results are summarized below.

Fretting Inhibitor Evaluation Tests

The initial test involved the screening of 24 candidate material-surface, condition-coating combinations with the objective of identifying four systems with superior fretting inhibiting properties for use with titanium. The candidate systems were tested in a machine which produced oscillatory relative motion at the interface between the titanium and the coating or other specially process material surface. While undergoing this motion, the interface surfaces were maintained in contact through externally applied pressure. Coefficient of friction and wear measurements were determined at various lifetimes up to 50,000 cycles. Based on these results, the following four candidate coatings were identified for further use in fretting fatigue evaluation tests:

- Teflon-Dacron Type L1276 - A weave of Teflon and Dacron impregnated with phenolic resin.
- Sermetel 72 - An inorganically bonded coating of Teflon and molybdenum disulfide.
- Nylon 11 - A Corvel NCA77 fluidized bed coating
- Silver - An electroplated silver

The selection of the initial three systems above was based on their demonstration of low wear and coefficient of friction. The silverplate was selected on the basis of its wide use as a fretting inhibitor for titanium in many aerospace applications.

Shotpeening Process Evaluation Test

The influence of shotpeening on the fatigue strength of titanium was evaluated. Two candidate shotpeening processes, differing only in shotpeening intensity, were applied to three types of axially loaded fatigue specimens. Results of fatigue testing groups of smooth, notched, and fretting specimens indicated no clear superiority of one candidate process over the other. More significantly, additional testing indicated that shotpeening did not appreciably improve the fatigue strength of titanium over the range of conditions investigated in this program. Improvements in mean fatigue strength at 5×10^7 cycles with a stress ratio of 0.05 were approximately zero percent for smooth specimens, and five percent for fretted specimens. An improvement in notched specimen fatigue strength could not be clearly identified.

Mean Stress - Alternating Stress Relationship Fatigue Test

The presence of a steady tension stress was found to significantly influence the fatigue strength of the forged titanium material. Increasing the steady tension stress on smooth specimens from zero ksi to 25 and 50 ksi resulted in 65 and 70 percent reductions, respectively, in the average fatigue strength at 5×10^7 cycles. This same general trend was seen in the notched fatigue strength data. This data is summarized in the modified Goodman Diagram of Figure 10. Although insufficient testing was conducted to enable complete definition of similar diagrams for shotpeened material, trends similar to the non-shotpeened material would be expected.

Fretting Fatigue Test

The relative fatigue strength of titanium when subjected to fretting environments of various severity was investigated using pin-ended link specimens. Baseline data was collected on specimens having a steel bolt bearing directly on the titanium bore. Other groups of specimens utilized steel interference fit bushings with the outside bushing diameter coated with one of the four candidate fretting inhibitors identified previously. At 5×10^7 cycles and a stress ratio of 0.05, the mean fatigue strength of the specimens with coated bushings was greater than that of the specimens without bushings. Of those specimens with coated bushings, those with Sermetel 72 fell in the top of scatter indicating a mean fatigue strength at 5×10^7 cycles which was approximately 10 to 20 percent greater than that of the specimens with Nylon, Silver, or Teflon-Dacron coated bushings.

Detailed metallurgical examination disclosed some fretting on the bores of those specimens with Sermetel-coated and silver-plated bushings. On the Nylon-coated bushings, a localized buildup of the coating at the bushing edges indicated that some extrusion of the coating had occurred. All bushing coatings showed wear to some degree.

Fracture Toughness Test

The determination of fracture toughness proved to be highly sensitive to test techniques and material characteristics. Tests utilizing four-point bending specimens were conducted according to the requirements of ASTM Method E399-70T. The majority of tests did not yield valid measurements of plane

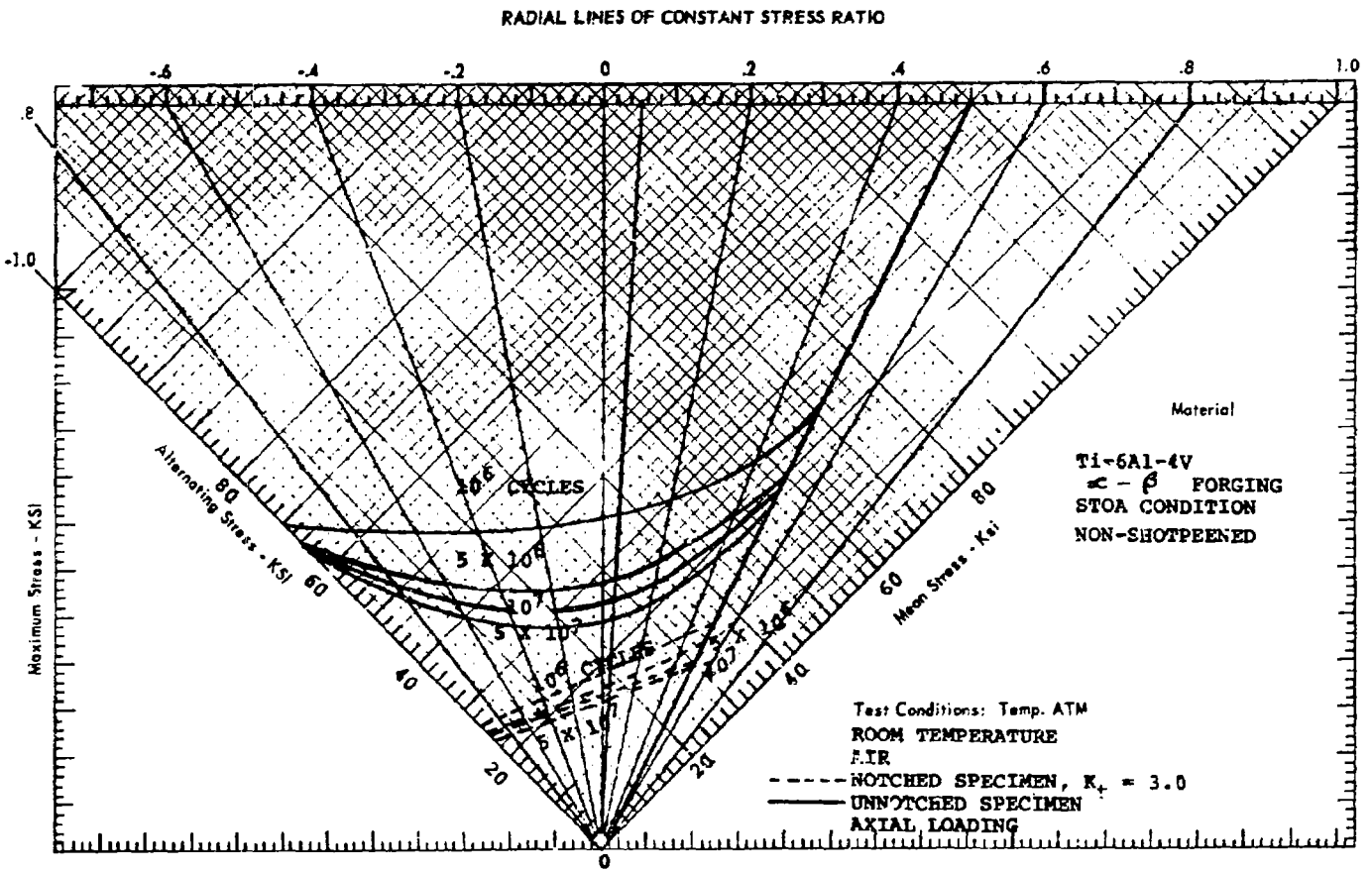

FIGURE 10. MODIFIED GOODMAN DIAGRAM

strain fracture toughness. The primary causes of invalid results were nonuniformity of crack front and fatigue precrack length in excess of the maximum permitted by the test method specification. From the valid tests, a plane strain fracture toughness, K_{Ic}, of approximately 100 ksi $\sqrt{\text{in.}}$ was determined at -65°F.

Fatigue Crack Propagation Test

Fatigue crack propagation tests were conducted to investigate the influences of stress ratio, environment, loading frequency, and grain direction on the fatigue crack growth rates of the titanium forging material. The expected trend in crack growth rates and stress ratio was seen. For a given value of the stress intensity range, ΔK, the fatigue crack growth rate increased with increasing values of the stress ratio, R. This trend was seen in the data for specimens tested in air and for specimens tested in a 3.5 percent salt solution. For comparable conditions, crack growth rates in the 3.5 percent salt solution ranged from approximately the same to three times the rates in air. No significant influences of loading frequency were seen over the range of 4 to 30 Hz which was investigated in this program. Similarly, longitudinal and transverse specimens yielded approximately the same crack growth rates for the conditions evaluated. The majority of specimens exhibited considerable crack branching. The primary cracks in a few specimens grew in such a manner as to propagate almost parallel rather than perpendicular to the loading. This phenomenon has tentatively been attributed to the properties of the large grain structure.

During the course of the program, it became evident that optimum mechanical properties, especially high-cycle fatigue strength in the presence of steady tensile stress, could not be consistently achieved or regulated in large titanium forgings without controls in addition to those of AMS 4928. This conclusion was based primarily on the experiences and emerging practices of the industry, but was reinforced by the mean stress/alternating stress (Goodman diagram) data obtained in this program.

While the majority of data and trends obtained in this test program are felt to be representative of large titanium forgings, there are instances where potential exists for

achieving more favorable properties by closer control of the forging process. Specifically, the trend of the alternating stress/mean stress diagram is felt to be controlled by the amount of work and associated macrostructre and microstructure of the forging. Obviously, a forging material which exhibits a small, rather than large, decrease in fatigue strength with increasing tensile steady stress would be advantageous for use in helicopter rotor components.

Since these components are generally sized for a condition of fatigue loading in association with a steady tensile load, the resulting component weights are highly dependent on how the fatigue strength of the material varies as a function of steady tensile stress. In order to realize and maintain consistently favorable mechanical properties for fatigue critical helicopter dynamic system components, a specification for premium quality titanium forgings was prepared. This specification, Reference 3, covers the material and process requirements for triple melt premium 6Al-4V titanium alloy forgings and establishes the control requirements for the various processors involved in forging manufacture.

2.3.2 Fail-Safe Pitch Link and Attachment Tests

The Fail-safe Pitch Link and Attachment tests are reported in Reference 4.

2.3.2.1 Pitch Link

The fail-safety requirement of the Model 301 pitch link, Figure 11, is met by the provision of dual load paths (a primary and a secondary) each comprising upper and lower rod ends connected by left- and right-hand threads to a turnbuckle. The primary path is the outer and has forked rod ends which enclose those of the secondary load path. The rod ends of the latter have a clearance fit with respect to the outer race of the spherical bearings and thus remain unloaded until a failure of the primary permits the outer race to make contact with the lug of the secondary rod ends which then carries the load.

The primary and secondary load paths are each designed on the same basis as safe-life parts with fatigue life requirements of 3600 and 100 hours, respectively, referred to the mission profile.

The objectives of the test were

- Determination of the loads required to fail the primary load path.
- Confirmation of the ability of the secondary load path to pick up the load on failure of the primary.
- Determination of the loads required to fail the secondary load path.
- Determination of the modes of failure.
- Identification of which of the two load paths is primary. (This identification is predetermined by the design.)

In flight, friction in the ball joints results in the application of end moments to the link. Bending moments are also induced by column effects when the link is loaded in compression, so that the turnbuckle tends to be critical under this type of loading; whereas the rod ends are sensitive to tensile mean loads. It was, therefore, necessary to investigate the

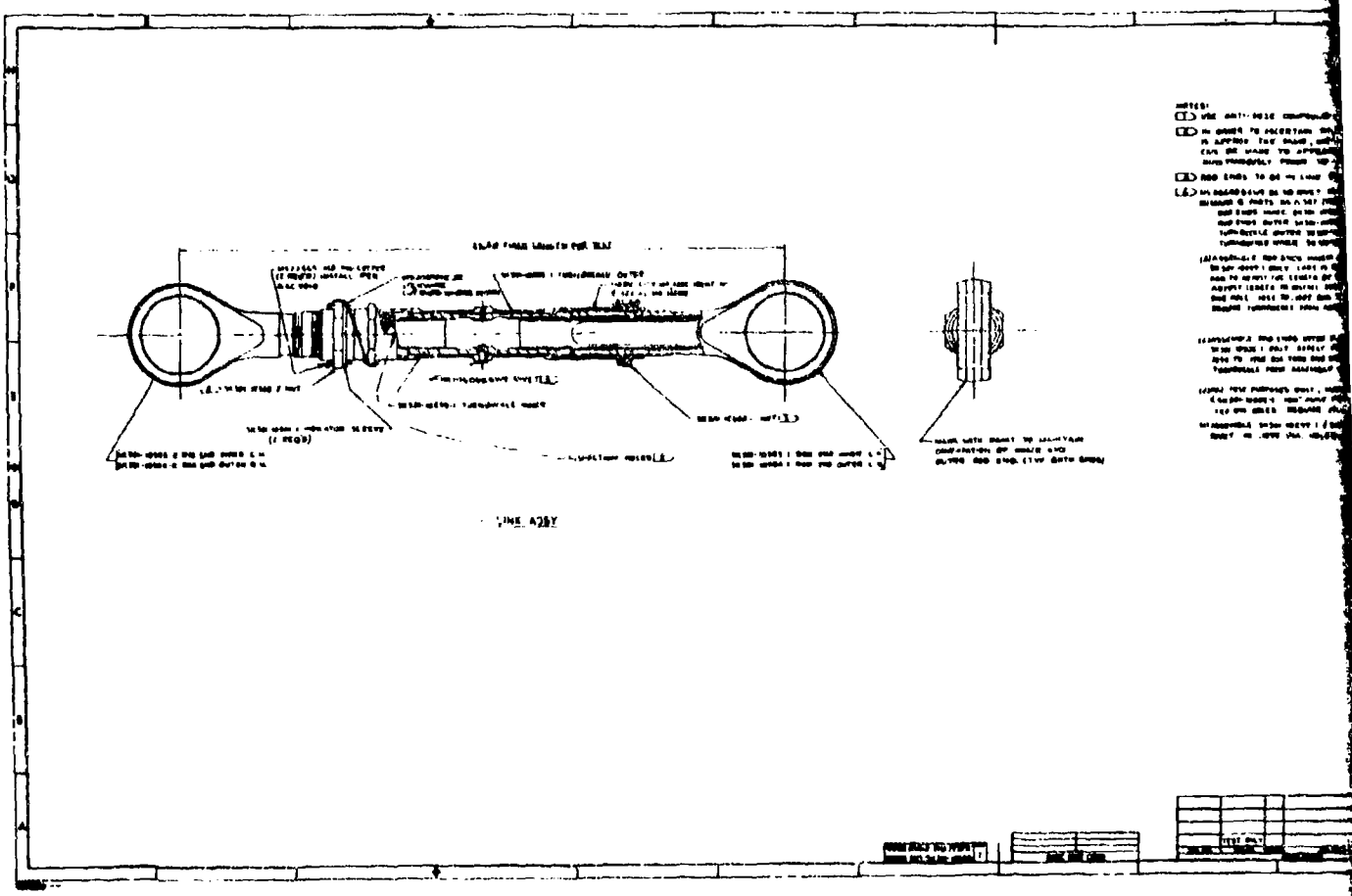

FIGURE 11. FAIL-SAFE PITCH-LINK TEST SPECIMEN

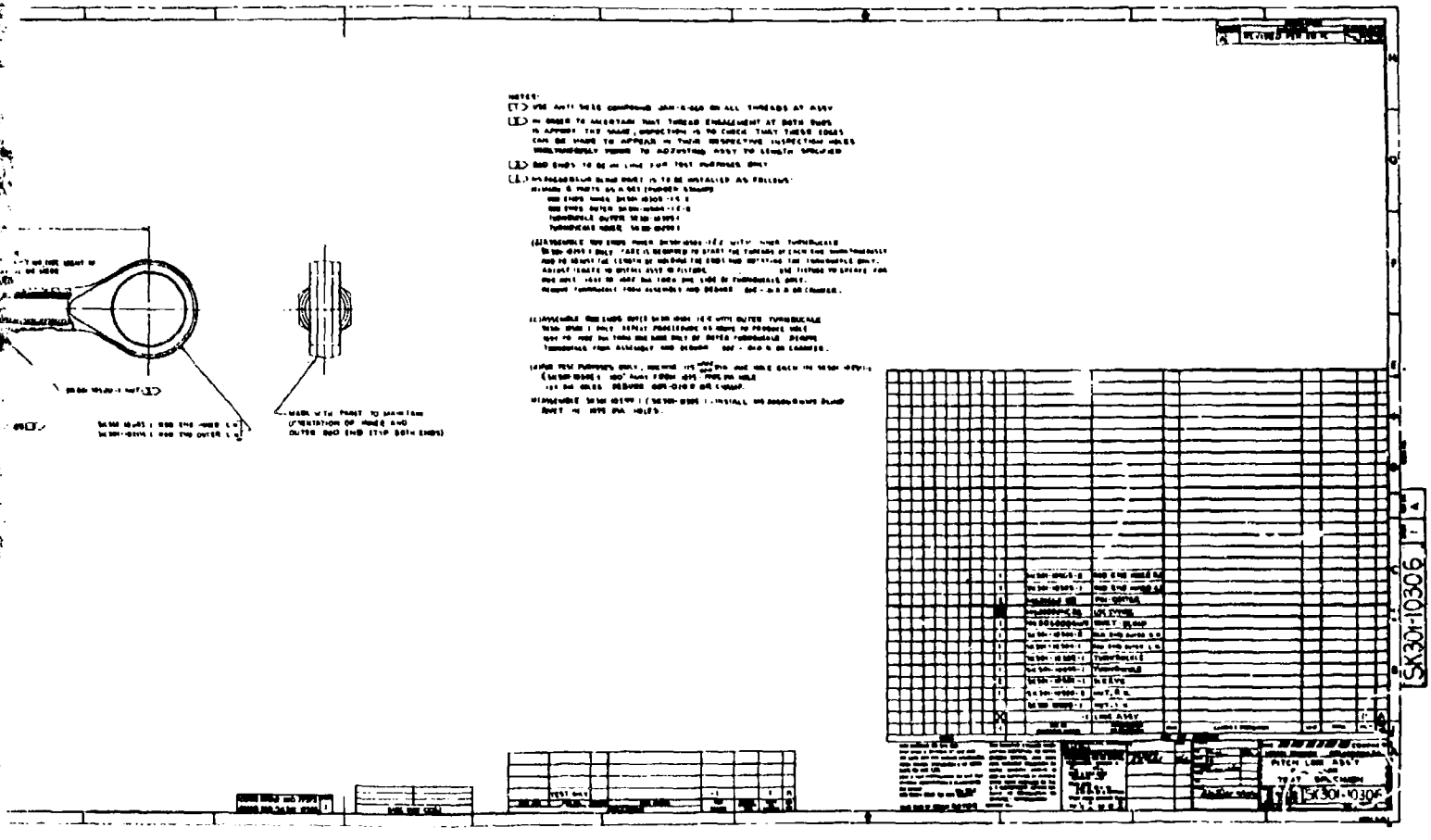

TEST SPECIMEN

effect of both a tensile and a compressive mean load. Two specimens were tested, the first with a tensile, and the second with a compressive mean load.

The specimens were instrumented and mounted in a heavy frame installed on a Weston-Boonshaft and Fuchs fatigue test machine. To represent the effects of the friction end moments, the specimens were set up with special fittings in the rod ends to apply the load with an offset of 0.3 inch from the central axis of the link.

Testing was conducted in a series of constant amplitude runs of approximately two million cycles, load being increased after each run-out until failure occurred. At this point, the load level was reduced and the process repeated until both load paths failed.

Specimen 1

This specimen was tested with a tensile mean load (Load Ratio, min/max = -0.5). The first crack developed in the ring portion of the primary rod end. To accelerate the test, the ring was cut through near the crack and the procedure repeated until both rings of the primary rod end had completely failed. As failure of the primary load path progressed, load was transferred to the secondary path which, in turn, failed in the threads connecting the rod end to the turnbuckle.

Specimen 2

The second specimen was tested to investigate the consequences of a primary turnbuckle failure, and testing was conducted at a load ratio of -2.0. The primary turnbuckle was notched on the outside surface opposite the run-out of the internal thread. When it was found that high-level alternating loads failed to cause a crack to propagate from the notch, the turnbuckle was cut through and testing continued until the secondary load path failed. The mode of failure, wear of the threads, was the same as that of the first specimen.

Because of the difference in load ratio, the endurance limits of the primary rod end and turnbuckle are based on test results of a single specimen. In the case of the secondary load path, the differences in load ratio merely changes the direction of mean load on the threads so that the two results may be combined to determine the mean strength. The table below compares the results with predictions of the endurance limits needed to achieve the required fatigue lives.

	Test Endurance Limit - Lb	Required Endurance Limit - Lb
Primary (M -3σ)		
Rod End (R = -0.5)	$\pm$ 5200	
(R = -2.0)	$\pm$ 8400	$\pm$ 6360
Turnbuckle	$\pm$ 5200	
Secondary M -1σ)	$\pm$ 4360	$\pm$ 4420

Since the failures were precipitated by fretting between the lug and the bearing outer race, the endurance limit can be improved without weight penalty by the incorporation of anti-fretting material at the affected interface. Also, a slight adjustment of secondary load path thread engagement will bring the strength of the secondary load path to the required level. It should be noted that the total test cycles applied between observation of the first crack in the rod end of specimen #1 and complete rod-end failure are equivalent to the cycle accumulation of over 700 flight hours at operating rpm.

The test proved conclusively that the dual-load-path concept will provide ample time for the detection of a pitch link failure.

2.3.2.2 Pitch Link to Swashplate Attachment

Fail-safety of the attachment of the pitch link to the rotating swashplate ring is achieved by designing the structural components on the assumption that a failure has occurred. The principal elements are the attachment clevis, which is an integral part of the aluminum alloy swashplate, and the bolt connecting the pitch link to the clevis at the rod end ball joint (Figure 12). Both the bolt and each lug of the clevis are designed to meet the 100-hour post-failure fatigue life requirement in the event of a failure of either the opposite lug or of the bolt, broken in such a location that the load can only be transmitted to one lug. During this 100-hour interval, it is expected that the first failure will be detected by visual inspection. Since the bolt is totally enclosed when assembled, it is made with a hollow shank containing a quantity of dye-penetrant fluid, the escape of which indicates the presence of a crack in the bolt.

The test objectives of this test were identical to those of the pitch link test. Since the attachment is not of dual-load-path design, it is appropriate to refer to "intact structure" and "structure with single failure" instead of "primary load path" and "secondary load path", respectively. (The objective of confirming the ability of the secondary load path to pick up the load is automatically met and the identification of the primary load path is irrelevant.)

The swashplate attachment was tested to investigate the pre- and post-failure capabilities of both the clevis and the bolt. It was, therefore, arranged that one specimen should represent a lug failure and the other a bolt failure.

Motion of the pitch link around the tilted swashplate causes angular oscillations which result in alternating loading in the direction of the bolt axis. To account for this, the specimens were loaded through a dummy pitch link having a 6° inclination to the vertical. They were mounted on the same rig as was used to test the pitch links and subjected to a similar loading procedure.

This testing is also reported in Reference 4.

Specimen 1

This specimen was tested at increasing load levels until cracks appeared in the lugs. These originated at the lug interfaces with the bushings and were first observed when they had extended beyond the bushing flanges. Testing was continued at reduced load levels to check that the rate of crack propagation was acceptably low and it was found that the lug carrying the lateral load had a considerably higher propagation rate than the other. When the laterally loaded lug was practically severed, it was cut through. The load was again reduced and the remaining lug tested until failure was virtually complete. The bolt did not fail.

Specimen 2

Testing of the second specimen was begun with the bolt notched in order to initiate a failure and to prove the effectiveness of the dye-penetrant method of failure indication. Following the same loading procedure as was adopted with the first specimen, testing continued until dye was seen to be leaking around the bolt washer, showing that the crack had reached the bore surface of the bolt. At this point, the bolt was cut through and the remainder of the test carried out with the load transmitted through the remaining part of the bolt to one lug. The test was concluded when the loaded lug failed. There was no other bolt failure.

Comparison of derived and required endurance limits as follows:

	Test Endurance Limit - Lb	Required Endurance Limit - Lb
Structure Intact (M -30°)		
Clevis	± 5,450	± 4,020
Bolt	± 8,590	± 6,480
Structure Failed (M -10°)		
Clevis	± 2,750	± 2,390
Bolt	± 4,590 *	± 4,530

* Bolt failures are based on run-outs.

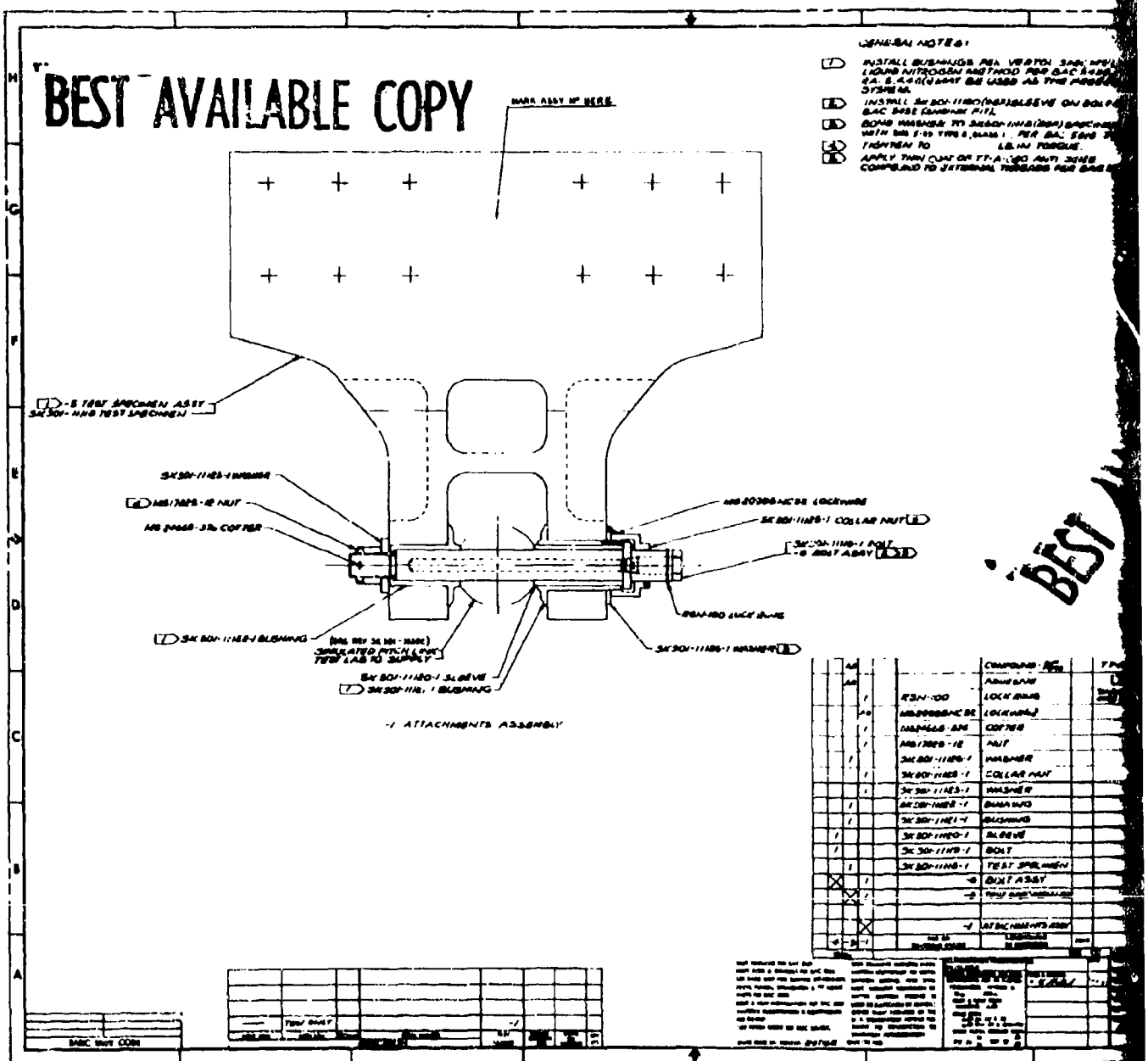

FIGURE 12. FAIL-SAFE EVALUATION SWASHPLATE ATTACHMENT

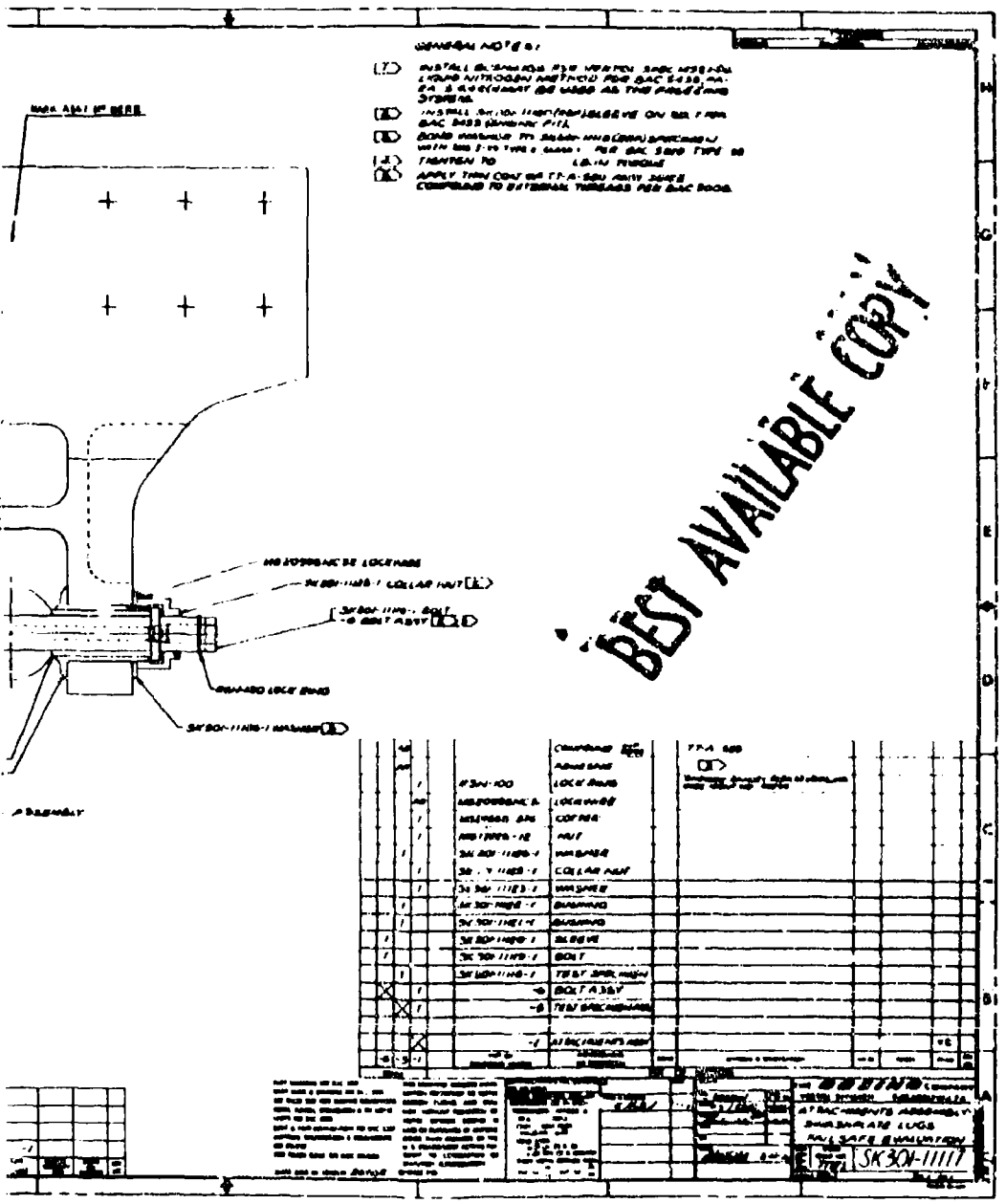

PLATE ATTACHMENT

It should be noted that the cycles applied to Specimen 1 in the crack propagation phase represent more than 700 flight hours at 156 rpm.

The tests indicate that a joint of this type, designed to meet the case of partial failure, can provide a safe interval within which failure detection is possible. It is also clear that the application of anti-fretting material to the clevis bushings and improving the fit will result in weight reduction in the final design.

2.3.3 Frequency Selective Lag Damper

One of the advanced technology concepts which was evaluated under this program is a frequency selective lag damper (FSD). The FSD concept increases the damping efficiency and reduces the damper force, thus permitting substantial rotor weight reduction.

The FSD concept development consisted of three phases:

a. Analysis and laboratory testing of a breadboard configuration using a modified CH-47C damper.

b. Design, fabrication and development testing of an HLH size FSD.

c. Rotor testing of the HLH frequency selective dampers on the Whirl Tower and Dynamic System Test Rig.

The function of the blade lag damper is to prevent a buildup of blade motion at the lag natural frequency (approximately ¼ per rev on the HLH). A tendency toward blade resonance may occur on the ground at takeoff (ground resonance) or at certain flight conditions.

Conventional hydraulic blade lag dampers are most effective for the ground resonance condition where the blade motion is predominantly at the lag natural frequency. During forward flight, the blade has a large one-per-rev velocity superimposed on the relatively low ¼-per-rev velocity as illustrated in Figure 13.

Since the damper forces in a conventional lag damper are proportional to the total blade velocity, the damper effectiveness is very low for this condition as will be shown.

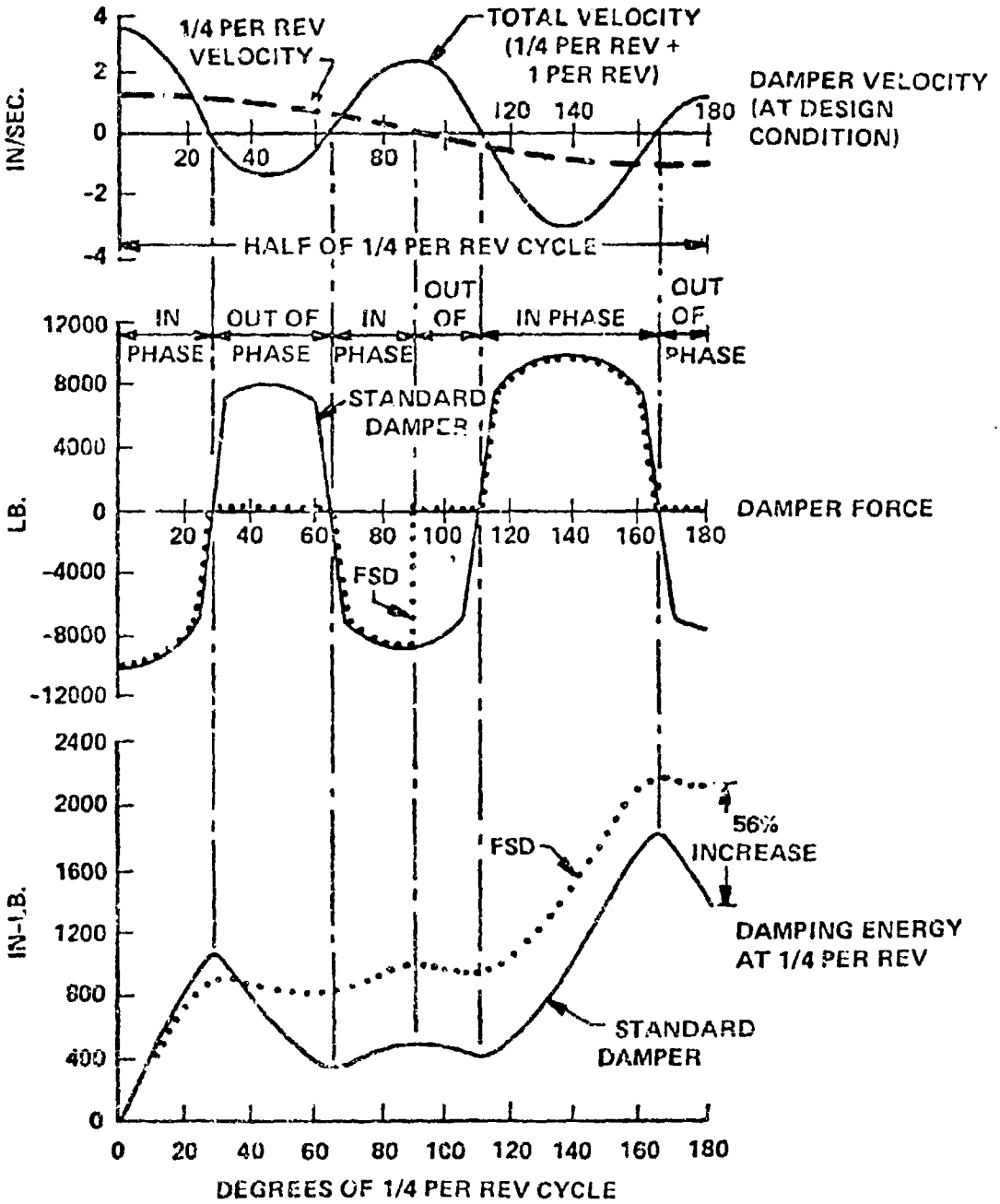

FIGURE 13. OPERATING CHARACTERISTICS OF IDEAL FSD WITH LAG FREQUENCY OF 1/4 PER REV

The damper force during forward flight (Figure 13) is out of phase with the ¼-per-rev component during part of each revolution (30° to 60°, 90° to 110°, etc.). During these portions of the lag cycle, energy is introduced into the rotor system at the lower frequency as indicated by the decline in the damping energy level shown in Figure 13. Thus the net energy available at ¼ per rev for control of aeromechanical instability is reduced.

The frequency selective damper (FSD) is intended to prevent degradation of damping available to oppose ¼-per-rev motion. This is achieved by preventing energy introduction into the rotor system at the ¼ per rev frequency by allowing the piston to displace without exerting a damping force whenever the ¼-per-rev velocity is out of phase with the total velocity. The FSD concept increases the damping efficiency of a standard damper in suppressing forward flight instabilities by 56%. Thus, an FSD needs 56% less capacity than a standard damper, permitting force output, damper weight, and size of the rotor hub components to be reduced.

A frequency selective damper is illustrated schematically in Figure 14. The damper cylinder, preload valve, check valves, and associated interconnecting fluid passages comprise a conventional preload type lag damper. The control valve, control cylinder, orifices and interconnecting fluid passages, and the control rod spring comprise the frequency selective elements.

Connection of the control valve to the damper is such that the flow bypasses the preload valve of the damper when the velocity of the damper piston and the control valve displacement are out of phase (one retracting and one extending). When the damper velocity and valve displacement are in phase, fluid is forced across the preload valve of the damper. Therefore, if the valve displacement is in phase with the ¼-per-rev velocity, the required selective loading and unloading of the damper previously discussed is obtained.

The frequency selective lag damper "breadboard" development bench testing is reported in Reference 5. The objective of this program was to demonstrate the frequency selective damper (FSD) concept. This included the specific objectives of:

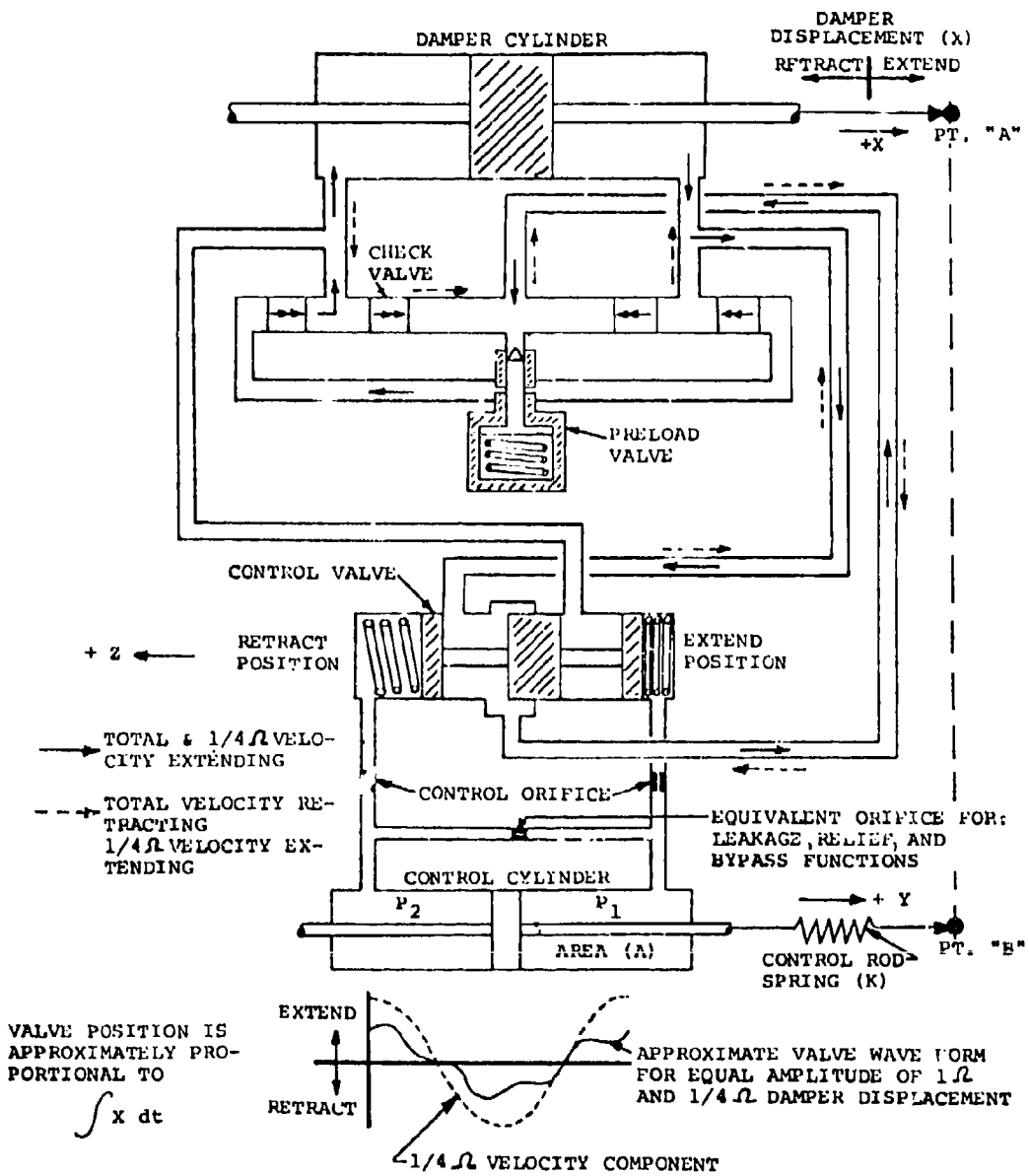

FIGURE 14. SCHEMATIC OF FREQUENCY-SELECTIVE DAMPER

a. Determination of performance in both the FSD (mixed frequency) and non-FSD (single frequency) modes

b. Investigation of sensitivity to system parameters

c. Correlation of analytical and test results

This test program was conducted on a laboratory model, consisting of a CH-47C lag damper (P/N 114 H 6800) with an externally mounted frequency selective control, to determine the performance and parameter sensitivity of a frequency selective (FSD) blade lag damper. Single frequency tests, and mixed frequency tests using a 1/3-per-rev subharmonic frequency, (1 per rev = 3.78 Hz) were conducted for both the FSD and non-FSD configurations.

The test program successfully demonstrated the frequency selective damper concept. Under mixed frequency conditions at a one-to-one input displacement ratio, the FSD produced a 100% increase in the 1/3-per-rev subharmonic energy dissipation for phase angles of 0° and 90°. At a phase angle of 180°, a 54% increase in the 1/3-per-rev energy dissipation was obtained. It was concluded, therefore, that the FSD offers a significant improvement in mixed frequency damper performance.

Overall, the analytical correlation was good to excellent once the basic (non-FSD) damper characteristics were matched. The poorest correlation for the FSD configuration was obtained for 180° phase. Based on an examination of the test waveforms, it was concluded that the FSD performance at 180° phase is highly sensitive to both the valve motion and the valve shaping (area vs. stroke relationship). This was confirmed by analytical results which showed a substantial variation in damper performance with minor variations in valve shaping.

As a result of this test program, it was recognized that in a prototype FSD design, a symmetric control cylinder piston (equal areas) and essentially equal control cylinder volumes was required.

2.3.4 Pitch Link Bearing Comparative Test

Teflon fabric dry lubricant bearings were successfully introduced in the helicopter rotor control system in the early 1960's. Performance of these bearings has continually been improved as design and manufacturing techniques were developed. The most recent dry lubricant bearing configuration used in the CH-47C pitch links, for example (Boeing Vertol P/N 114RS318-2) is giving two to three times the life of the bearing previously used.

The objectives of this test program were:

- Evaluate two dry lubricant control system bearing configurations under typical loads and motions and under environmental conditions against the performance of the baseline 114RS318-2 bearing configuration.
- Develop a condition indicator for dry lubricant bearings to aid in diagnosing bearing wear.

The test results are reported in Reference 6.

An important part of this program was the conduct of a bearing Quality Assurance examination. This examination included destructive and nondestructive examination of test bearings in an effort to find attributes that could be used as standards in the evaluation of future bearing procurement to assure consistant performance.

This testing was done on the CH-47 swashplate endurance test machine (Figure 15) as this makes possible testing with realistic loads and motions applied to the bearings; i.e., steady plus alternating bearing loads with cyclic misalignment. Pitch link bearing wear values obtained in previous testing with this test fixture correlated well with the wear data resulting from helicopter operation. This test was done concurrently with the Swashplate Bearing Condition Indicator, and the latter test is summarized in the following section of this report. All pitch link bearings were tested under conditions representative of the HLH's expected service and simulated the environment found to be typical for a helicopter rotor control system. The testing consisted of cyclic tension-compression tests, with the spherical ball nutating. Eight Teflon pitch link spherical bearings were tested simultaneously to determine the bearing wear and to establish life. The effects of temperature, sand, and salt were established. The 114RS318-2 present design CH-47C pitch link bearings were tested under identical conditions to the candidate alternate bearings. Two of these had the bearing wear indicator installed. This test determined the comparative life of the bearings both in a dry environment and also under a severely contaminated environment.

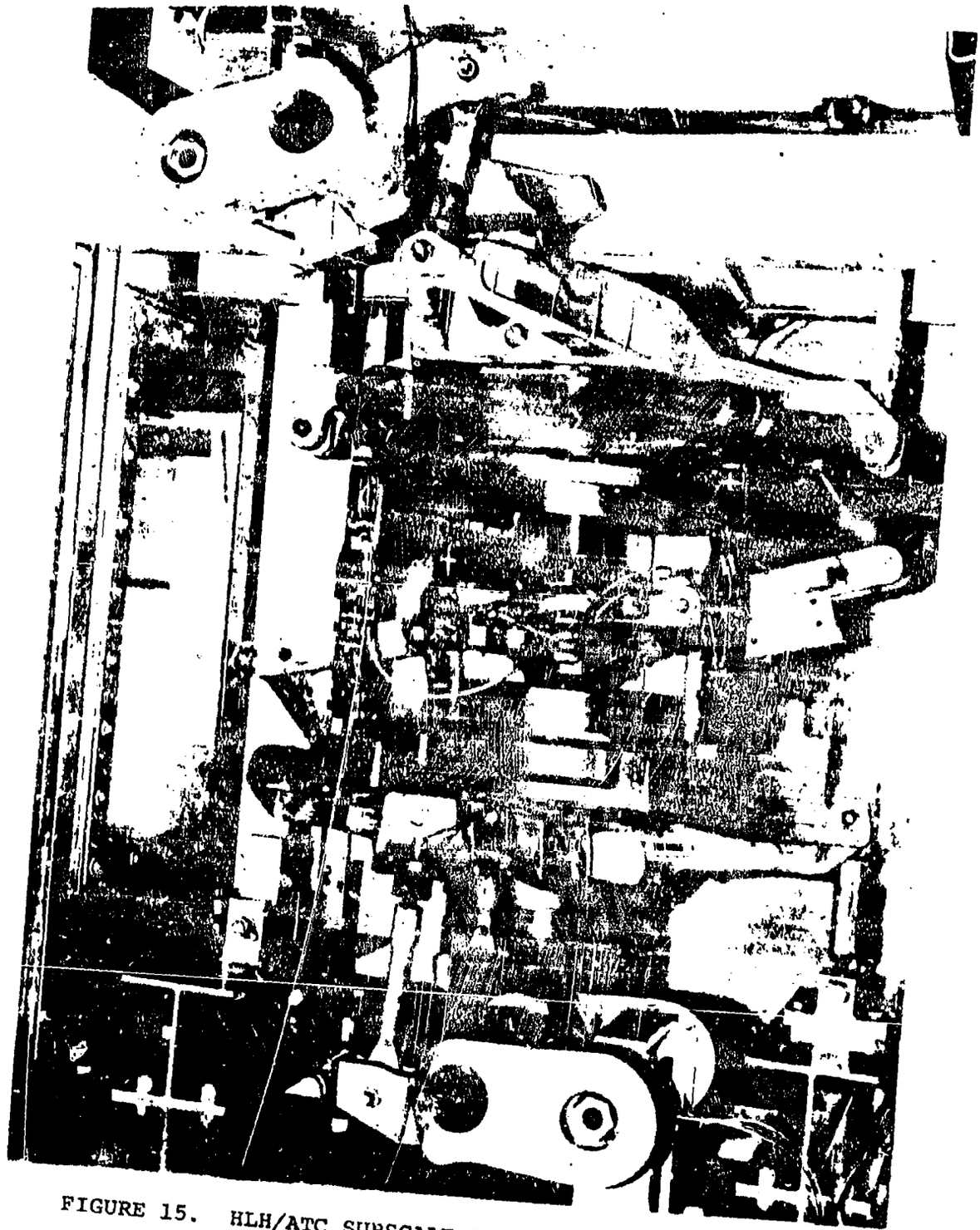

FIGURE 15. HLH/ATC SUBSCALE SWASHPLATE ENDURANCE TEST SPECIMEN INSTALLATION

The test bearing pressures, surface velocities and the pressure-velocity product (PV) correspond to those of the Model 301 helicopter as shown in Table 3 below.

TABLE 3. PITCH LINK BEARING COMPARATIVE TEST LOADS

% Test Time	HLH		Test Load, L, on CH-47 Pitch Links to Simulate HLH Pressure	Brg. Surface V Velocity ft/min	PV Product
	Max. Load, L,Lbs.	Max. Pressure, P, PSI			
95	3250	1000	275 ± 925	15	15,000
5	4290	1310	366 ± 1220	15	19,000

NOTE: $P = \frac{L}{D \times W}$

where L = maximum load, lbs.
D = bearing ball diameter, inches = 2.5 inches
W = bearing outer race width, inches = 1.3 inches

$V = S \times N$

where S = surface travel of HLH ball surface under load/cycle -.0965 feet
N = cycles/minute of oscillation = 156 cycles/min.

Eighteen different groups of bearings were tested, reflecting different manufacturers, processing variations and materials. These groups are described in Table 4. Wear values varied greatly from group to group.

The significant findings of this testing are:

1. The present production configuration of Teflon fabric bearing (P/N 114RS318-2) manufactured by the Astro Division, New Hampshire Ball Bearing Company gave the most consistantly good performance and gave an equivalent HLH life of 1150 hours to 0.007 inch wear (an index value of wear not necessarily related to the permissible pitch link wear of the HLH aircraft).

2. Processing problems appeared to be the most prevalent reason for poor performance of the majority of other bearing configurations.

3. The pitch link bearing wear indicating system was not effective in determining bearing condition.

TABLE 4. PITCH LINK BEARING SPECIMEN DESCRIPTION

GROUP	MANUFACTURER	SPECIMEN IDENTIFICATION	BALL MATERIAL	OUTER RACE MATERIAL	BEARING WEAR SURFACE	CAUSE OF FAILURE	COMMENTS
I	Transport Dynamics Inc. Division of Lear Siegler	114RS318-2 (09455) 76500 S/N's TD-X Series	440 C Stainless Steel	17-4 PH	"Fiberglide" Dacron/Teflon Weave Phenolic Resin	Manufacturer examined failed bearings. Claimed failure due to poor bonding of liner to outer race.	Bearings manufactured with improved conformity. Manufacturer made new swaging dies for this purpose.
II	Transport Dynamics Inc. Division of Lear Siegler	114RS318-2 (09455) 76500 S/N's T-X Series	440 C Stainless Steel	17-4 PH	"Fiberglide" Dacron/Teflon Weave Phenolic Resin	Unknown	Standard production configuration without the improved conformity.
III	Transport Dynamics Inc. Division of Lear Siegler	114RS318-2 (09455) 76904 S/N's X-A Series	440 C Stainless Steel	17-4 PH	"Fiberglide" Dacron/Teflon Weave Phenolic Resin	Unknown	Bearings the same as group I except curing operation changed to solve original failure problem. 0.009 in. crack wire installed between liner and outer race.
IV	Fafnir Bearing Company	B516ATTC56Z EXP 13895 F-X Series	440 C Stainless Steel	410 Stainless Steel	"Teflon" Proprietary Liner and adhesive System	Specimens F2, F3, F10 had excessively high friction torque causing running temps 350°F during first 5 min. of testing. Liner only good to 350°F. See Note.	High test rig temperature caused by these specimens assumed to be cause of Shafer specimen failures (Group VIII).
V	Fafnir Bearing Company	B516ATTE56 PS 695 FI-X Series	440 C Stainless Steel	410 Stainless Steel	"Teflon R" Proprietary Liner and Polyimide Adhesive	Unknown	Polyimide adhesive allows higher temperature operation under test.
VI	MRC Martin-Rockwell Corporation Division of TRW	SA-08-ST-1	"Filimide" Carbon Filament	440 C Stainless Steel	Carbon Ball on 440 C Steel Outer Race	First two specimens failed (S/N's 2 & 5) early (1 hr) because installation spec. torque of 600 in-lb was too large. Last two specs (torqued to 100 in-lb) failed because of bolt bore elongation.	Bearing has split outer race with a snap ring retainer. Eliminates swaging.

TABLE 4. Continued

GROUP	MANUFACTURER	SPECIMEN IDENTIFICATION	BALL MATERIAL	OUTER RACE MATERIAL	BEARING WEAR SURFACE	CAUSE OF FAILURE	COMMENTS
VII	New Hampshire Bearing Co. Astro Div.	P/N 114RS318-2 ATB8-6C MR-X Series	440 C Stainless Steel	17-4 PH	Unknown		Exhibit longest life to date.
VIII	Shafer - Division of Rex Chain Belt	YYA 346 SX Series	440 C Stainless Steel	17-4 PH	"Arelon" Unknown Composition	High temperature environment caused by Fafair specimens (Group IV). Liner good to 350°F.	Second set tested with good results.
IX	Shafer - Division of Rex Chain Belt	Not Identified MX Series	440 C Stainless Steel	Fiberglass	Fiberglass (Outer Race)		Specimens exhibit second longest life.
X	Kahr Bearing Division of Sargent Indus.	KMTD8-1 KX Series	440 C Stainless Steel	17-4 PH	"Karlon" Dacron Cloth Impregnated with Chopped Teflon Fiber & an Adhesive	Specimens failed because final liner cure (350°F for 8 hrs) had not been performed.	Two specimens to be cured by Boeing Vertol.
XI	Kahr Bearing Division of Sargent Indus.	KMTD8-1 X Series	Titanium (Ti-5Al-4V) with "tiodize" Surface	Titanium (Ti-6Al-4V)	Titanium Ball on Titanium Outer Race	Failure seem due to poor conformity and excessive amount of "tiodize" removed from ball when being finished. "Scotch-brite" used instead of #400 stainless steel wool.	Second set of specimens reworked to reduce installed misalignment torque.
XII	New Hampshire Bearing Co.	NH 1298 MR-8 and MR-9	440 C Stainless Steel	17-4 PH	Unknown		

NOTE: Additional specimens P5, P7, P11, P13 and P14 had outer race cold worked by vendor to reduce running torque.

TABLE 4. Continued

Group	MANUFACTURER	SPECIMEN IDENTIFICATION	BALL MATERIAL	OUTER RACE MATERIAL	BEARING WEAR SURFACE	CAUSE OF FAILURE	COMMENTS
XIII	Transport Dynamics Inc. Division of Lear Siegler	114RS318-2 S/N's X-C Series	440C Stainless Steel	17-4 PH	"Fiberglide" Dacron/Teflon Weave Phenolic Resin	Unknown	Same as Group III Except Bearings were cleaned without caustics
XIV	Valley-Todeco	VTB01634 S/N's VT-X Series	Stellite	440C (Nitrided & Honed)	Ball on Outer Race	Excessive installed Misalignment Torque	See Group XIII. Bearing has Separable ball Bearings to be reworked to reduce installed torque
XV	Valley-Todeco	VTB01634 S/N's VT-X Series	Stellite	440C (Nitrided & Honed)	Ball on Outer Race		See Group XIII. Bearings reworked to keep installed torque below 50 in-lbs.
XVI	MRC Marlin-Rockwell Corporation Division of TRW	SA-06-RR-2	"Filimide" Carbon Filament	440C Stainless Steel	Carbon Ball on 440C Steel Outer Race		See Group VI. Bearings reworked to incorporate bushing to reject mounting bolt torque
XVII	Fafair	S/N's FRC - X	440C Stainless Steel With Chrome Oxide Coating	17-4 PH	Dacron/Teflon Weave		
XVIII	Fafnir	S/N's FRC - X	440C Stainless Steel with Tungsten Carbide	17-4 PH	Dacron/Teflon Weave		

This device, which worked on the electrical conductivity principle, was later found to be ineffective because of a break in the electrical path introduced in manufacture. Further development of this principle is required to prove or disprove the practicality of this approach.

The salt environment in which the bearings operated was the concentration specified in MIL-STD-810. That method of testing is accelerated for corrosion testing. It was not possible to correlate the test environment to real oceanic atmospheric conditions. The sand and dust test attempted to provide more realistic conditions. The concentration of sand and dust was within an order of magnitude greater than observed conditions at the rotor hub location on the helicopter. Operation in the sand and dust environment with one exception showed negligible increase in wear, indicating that no unusual operational maintenance problems should be expected because of this environment.

2.3.5 Swashplate Bearing Condition Indicator

One of the ATC tasks was the evaluation of methods of diagnosing swashplate bearing conditions. The ability to detect swashplate bearing failures at early stages of defect progression is desirable from a reliability viewpoint and to help prevent catastrophic failures. Since the swashplate bearing performance is critical to flight safety, better methods are desirable for detecting incipient failure of this bearing. This program task evaluated the following:

- Acoustical Pickup
- Vibration Sensors Accelerometers and Shock Pulse
- Temperature Sensors

This test is reported in Reference 6.

The acoustic emission technique utilizes the phenomenon that most materials emit sound waves during deformation and that these sound waves provide information on the deformation characteristics of the material and, in addition, provide a warning of impending failure.

A sensitive piezo-electric transducer is used to detect the low-level sound waves that occur as a result of the acoustic emission phenomenon. The sound waves are of very short duration and of a variable amplitude; i.e., the waves have the predominant characteristics of a variable amplitude impulse, time function.

Data (events per unit of sample time) was sampled at regular intervals and plotted against test time with an increase in the number of events per unit of sample time indicative of bearing damage.

Vibration Sensors

Accelerometers - Three accelerometers for detecting vibration levels were installed on the swashplate assembly. The transducers were arranged so that the vibration levels normal, radial and tangential to the bearings could be determined. The vibration levels (peak g's) were indicated on a panel meter and periodically monitored for evidence of swashplate bearing deterioration.

SKF MEPA-10A Shock Pulse Meter - The SKF shock pulse meter is a diagnostic instrument for use in determining and defining the condition of rolling element bearings while installed in their operating environments. With the aid of the shock pulse meter, the shock emission envelope of the bearing is constructed by

measurement of rate of emission of shock pulses versus level of the emitted shock. The change in shock level in relation to time of operation provides an indication of bearing surface damage. The rate profile of shock emission gives a measure of extent of damage and may be used to determine the propagation of the damaged area. Typically, three general types of curves are generated.

- Existence of foreign matter in the lubricant is diagnosed from a plot of having high rates of very small shock levels.

- A dry bearing or rolling element damage may be indicated by a curve shape with very low rates of very high shock levels.

- A curve shape which starts to fill out having a significant rate of shock is indicative of bearing damage. The spread in shock level with rate illustrates that there is a spread of shock emission level with the way each individual rolling element encounters the damage or wear product.

Piezo-electric crystal transducers were installed on the swashplate assembly to detect the shock signal. The signal was then processed by a signal conditioning electronic package with a data readout meter. For optimum performance, the transducers should be in a direct line to the bearing. This was not possible to accommodate on the available swashplate.

Temperature Sensors

Thermocouples were installed at two locations on each bearing row of the swashplate bearing. Temperatures were continually monitored.

Test Summary

The bearing failure detection device was evaluated on a back-to-back swashplate test rig shown in Figure 15. This test evaluated two CH-47C swashplate bearings simultaneously. Total test time for the rig was 3000 hours. Two new bearings were tested for 1000 hours each for baseline information on the failure detection systems and to determine if any degradation could be observed. No sign of deterioration was visible after the initial 1000 hours. The bearing from the lower swashplate assembly was mechanically etched in an attempt to generate a bearing failure and reinstalled for continued test. A bearing which had been in helicopter service for approximately 700 hours was installed in the upper swashplate assembly. This service bearing had evidence of corrosion pitting on the raceway and ball surfaces when installed. After the salt spray

test (2200 hours total test time), the swashplates were again disassembled for inspection. The inspection showed that the swashplate bearing from the upper assembly had a spalled area approximately 3 inches long on the rotating ring (Figure 16). There was no apparent damage on the lower swashplate assembly bearing. Inspection at the conclusion of the test program showed that the size and severity of the spalled area of the upper swashplate bearing had not changed noticeably and the lower swashplate bearing still had not failed. Both swashplate assemblies had been regreased at the end of the 1000-hour and 2200-hour inspections. The failing condition of the upper bearing provided a test for the indicators.

Test Results

The general trend of the acoustic emission data is such as to indicate increasing damage with time. It cannot be shown, however, that the information is entirely the result of swashplate bearing damage. The data shows one period in which the emission from the vicinity of the lower bearing reduced greatly. This is inconsistent with normal rolling element bearing performance which does not show an appreciable improvement with age.

During two test periods, the acoustical emission signals were detected at high rates and appear to correlate to the pitch link bearing condition. One period occurred at approximately 2200 hours of testing after a salt spray environment had resulted in extreme wear of all pitch link bearings. The second period occurred at 2500 hours of test when experimental pitch link bearings were installed which had metal-to-metal bearing surfaces as opposed to the conventional Teflon fabric lining.

The detection devices relying on a shock or vibration signal were also ineffective in isolating swashplate bearing deterioration. These signals sensed information from the total test system, the two swashplate assemblies, the connecting pitch links, drive linkages and the test rig drive system components. The signal from the spalled area of the upper bearing could not be isolated from the many other shock and vibration signals originating from the test system. This was due in part to the physical location of the transducers which were not in the optimum location for monitoring bearing information only; the shock pulse transducers particularly are known to be highly directional in their signal sensing capability. Deterioration also appeared to be masked by the magnitude of the signals originating from the pitch link bearings.

As a rolling element bearing fails, it would be expected that a pattern develop in shock information to describe the mechanism of the behavior of the damage. In the case of grease lubricated

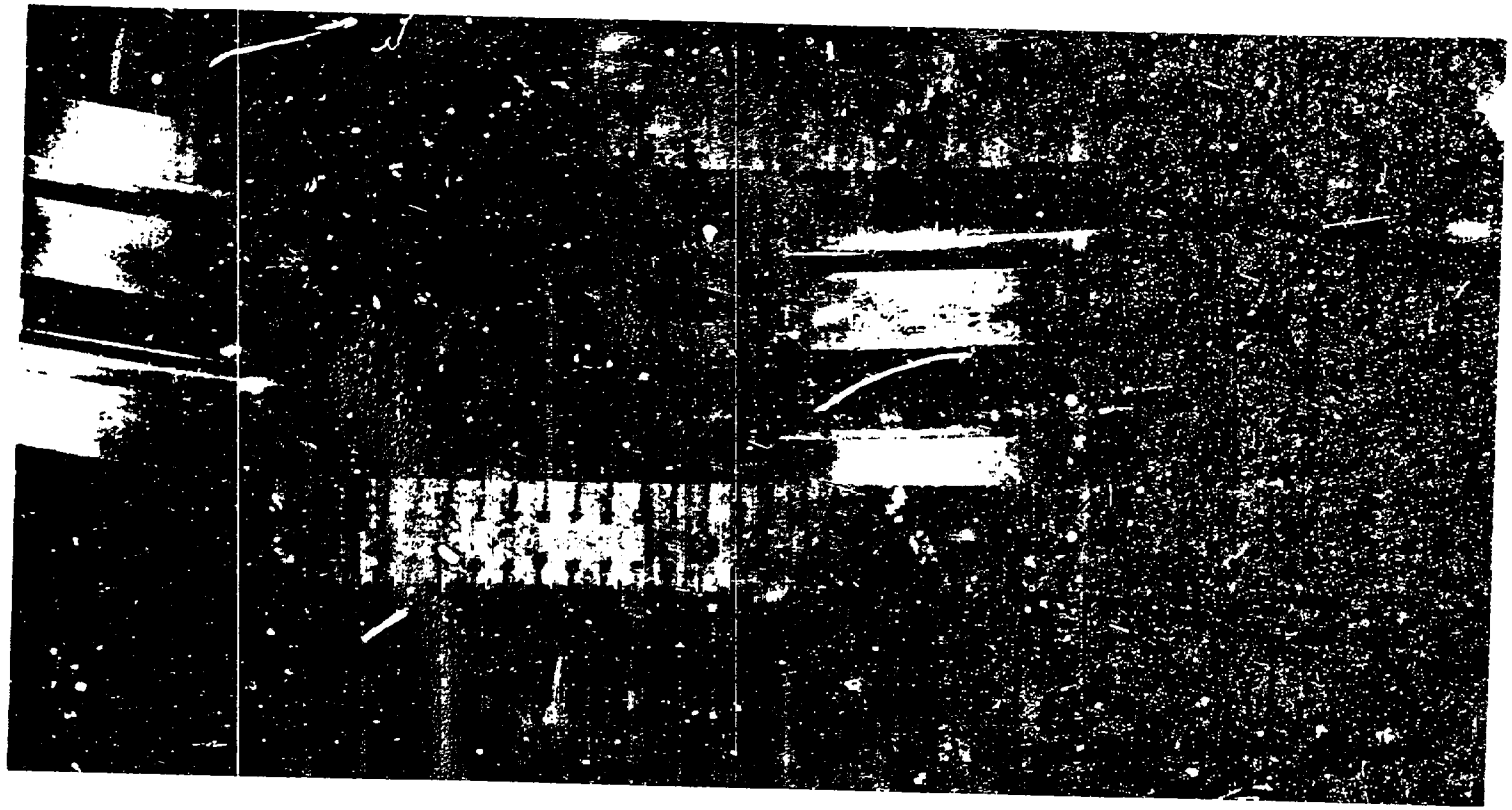

FIGURE 16. UPPER SWASHPLATE ASSEMBLY BEARING AFTER 2,200 HOURS OF TESTING

bearings, it might be expected that a high shock value would decrease as the edges of the damage are polished by the rolling elements. One might also expect the rate of change of the shock amplitudes to be relatively small. The signals recorded indicate a high rate of change of shock amplitude values which would be more indicative of pitch link bearing wear than swashplate bearing deterioration. The 1000-hour swashplate bearing inspection did not indicate any bearing deterioration that would cause rapid changes in shock amplitudes. During this same time span, however, there were many pitch link bearing replacements which could result in changes in shock amplitudes. Similar signals were recorded during the 2200-to 2500-hour time frame. The predominant contribution to shock amplitude changes was probably pitch link bearing wear and not change in the swashplate bearing condition.

Thermocouple measurements were taken and temperature histories were recorded during 2800 hours of the test program. During the final 200 hours, the sand and dust environment caused the temperature sensing circuit to fail with the result that there is no reliable temperature indication for this portion of the test program.

Temperature records show no positive indication of a swashplate bearing failure. Variations in operating temperature appeared to coincide with the following test events.

1. Operating temperature rises of 10 to 30 degrees occurred after each bearing relubrication. (1000 and 2200 hours). The temperature then returned to the previous operating level.

2. Temperature drops of fifty degrees occurred during the salt spray testing, possibly due to the improved cooling by the moist atmosphere.

3. Temperature increases of 10 to 20 degrees occurred during the elevated temperature (125°F) testing.

None of the bearing condition monitoring devices were able to detect deterioration of the upper swashplate bearing with any assurance.

2.4 SYSTEM DESCRIPTION

The HLH rotor hub and upper controls design that evolved from the trade studies and design development test was the basis for hardware for component and system testing.

The Heavy Lift Helicopter has a four bladed fully articulated rotor head assembly as shown in Figure 17. A sketch of the assembly is shown in Figure 18. The rotor blade attaches to the titanium pitch housing via two titanium pins. The pitch housing transfers radial loads to a spherical elastomeric bearing through a titanium loop assembly. An integral (pitch) arm on the pitch housing provides a reaction point for rotor blade pitching moments. Another integral portion of the pitch housing, the shear shaft permits the reaction of loads normal to the blade axis, through a spherical Teflon fabric shear bearing.

The elastomeric bearing is designed to react all radial blade forces and permit pitch, flap and lag motions. The bearing consists of bonded concentric spherical laminations of rubber and steel. The end fittings are titanium. The bearing is mounted so that rotor blade centrifugal force results in compression of the elastomer while pitch, flap and lag motions produce shear deflections.

A titanium crossbeam transfers loads from the elastomeric and shear bearings into the hub assembly. Two titanium plates form the central hub assembly. These plates are splined to the rotor shaft and both they and the crossbeams are interchangeable between the forward and aft rotors.

A lag damper is attached to the hub, and a fitting at the blade root end. In addition to its required damping function, the damper provides stops for lead and lag motion. Flap and drag stops at low rotor speeds are provided by a centrifugally operated, spring loaded wheel, which slides on the pitch housing shear shaft and contacts pads on the crossbeam. In flight, the shear shaft itself would contact these pads.

The function of the upper controls is to convert the displacement of the pilot's controls to the required degree of cyclic and collective pitch change of the rotor blades. (See Figure 19). A conventional swashplate arrangement is employed and is raised, lowered or tilted by three hydraulic actuators, the extension of which is determined by the fly-by-wire system controlled by the pilot. The actuators, mounted on the transmission cover, are attached to the stationary (inner) ring of the swashplate around which the rotating (outer) ring revolves on a double row angular contact ball bearing. Connected to the outer rim of the rotating ring are the lower ends of four

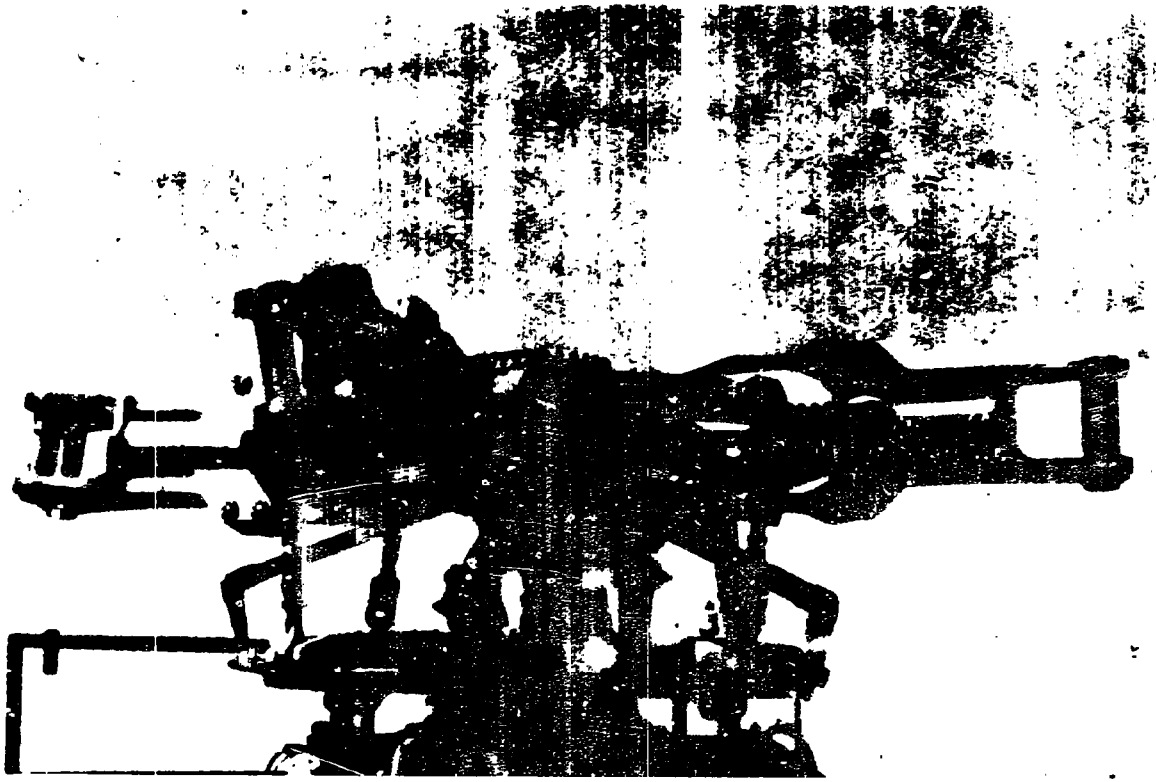

FIGURE 17. HLH ROTOR AND UPPER CONTROLS ON DSTR

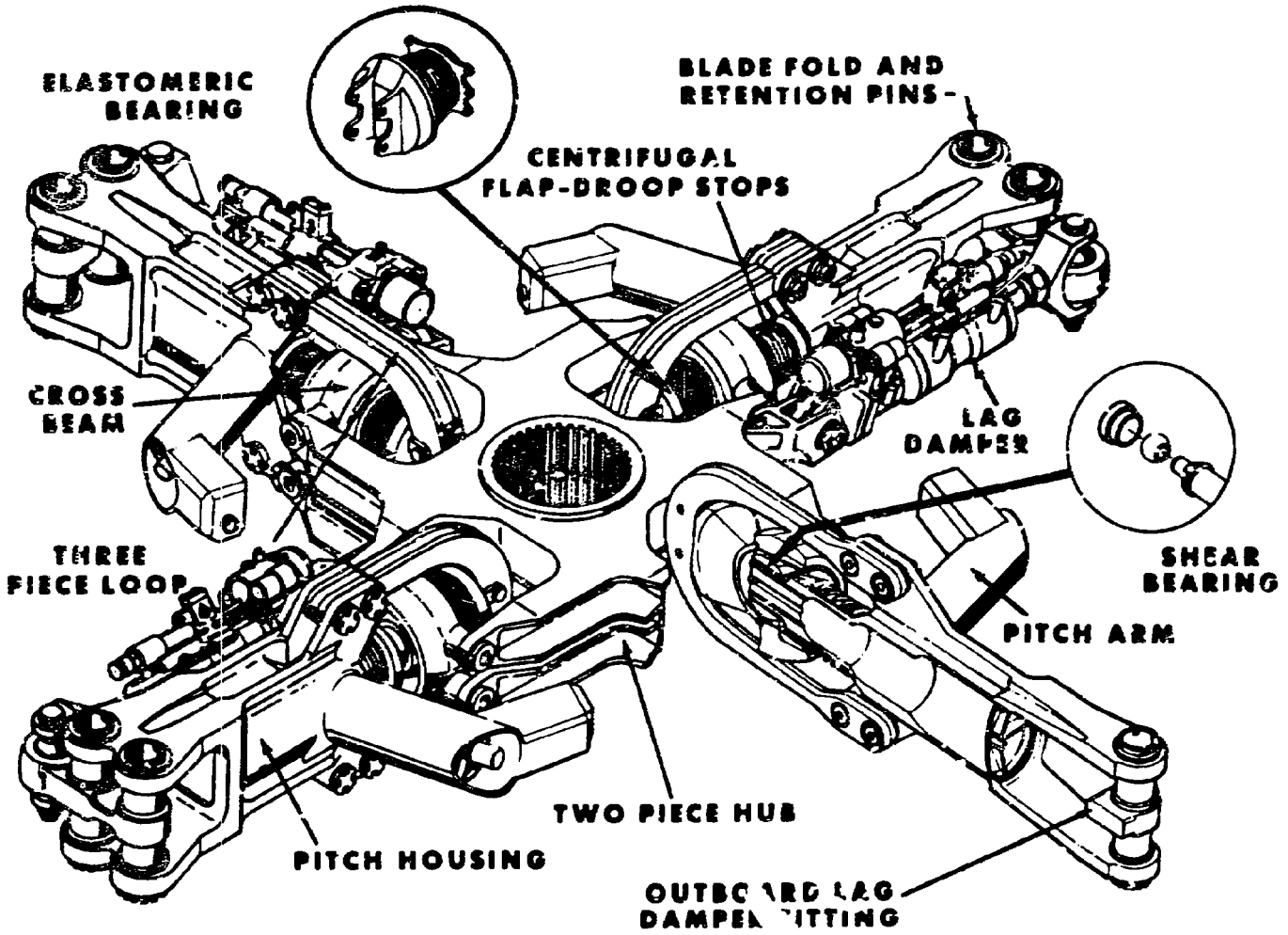

FIGURE 18. HLH MAJOR HUB COMPONENTS

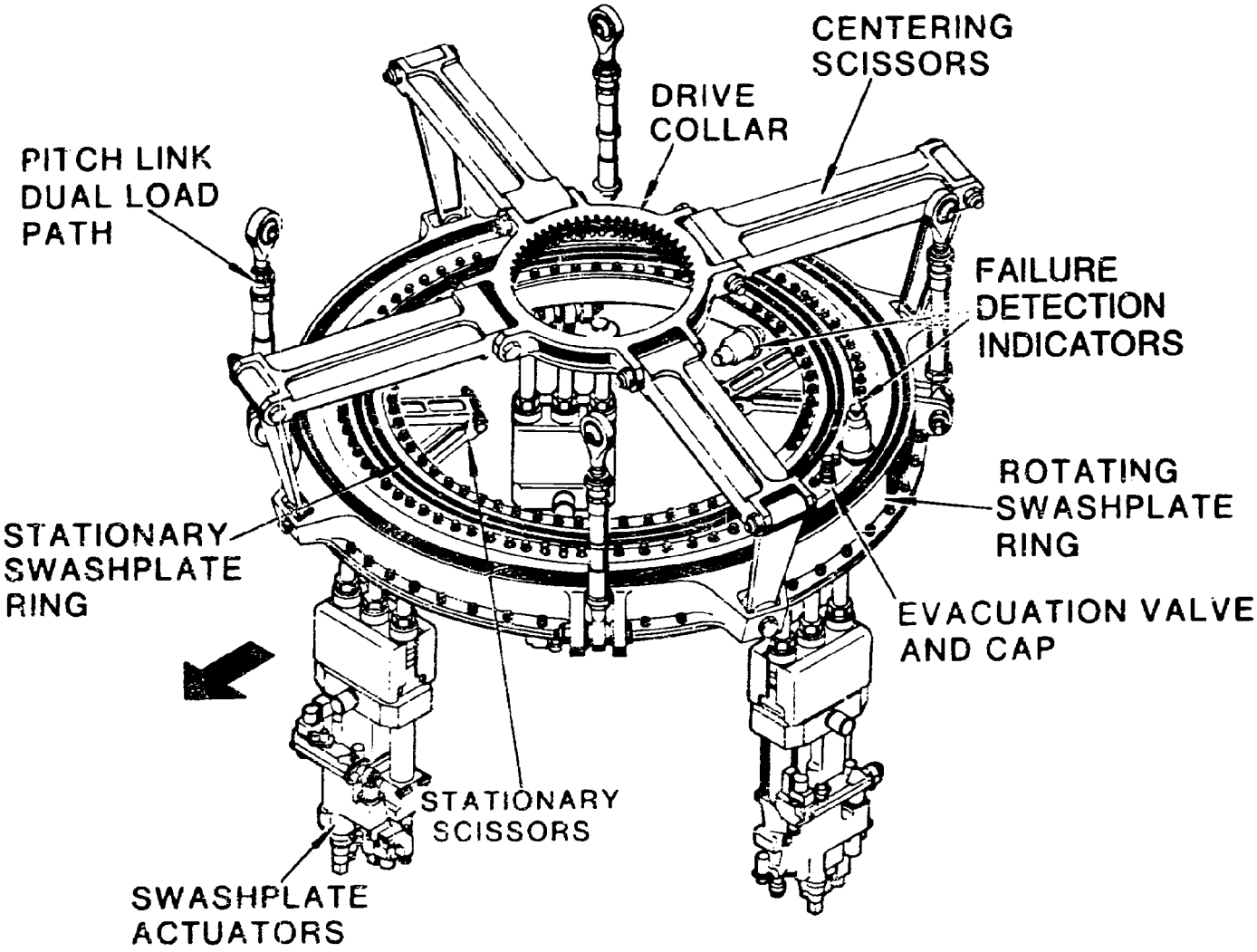

FIGURE 19. HLH UPPER CONTROLS

equally spaced pitch links whose upper ends are attached to the four rotor blade pitch arms. Vertical movement of the swashplate results in equal pitch changes on all blades, and tilt of the swashplate produces an approximately sinusoidal variation of pitch angle as the blade performs a revolution about the rotor center.

The swashplate rotating ring is driven at rotor speed by a drive scissors mechanism consisting of four scissors linkages, arranged at right angles, with their upper ends hinged to the drive collar and their lower ends connected by ball joints to lugs on the outer periphery of the swashplate rotating ring. Internal splines on the drive collar mate with those on the rotor shaft. The axes of the hinge pins connecting the upper drive to the collar and the lower arm to the upper are parallel. The linkage can thus take load only in a circumferential direction and offers no resistance to vertical or tilting motion of the swashplate. Three such linkages spaced around the swashplate are sufficient to prevent in-plane movement. The addition of the fourth arm in a cruciform arrangement provides a redundant system which can tolerate the loss of one arm.

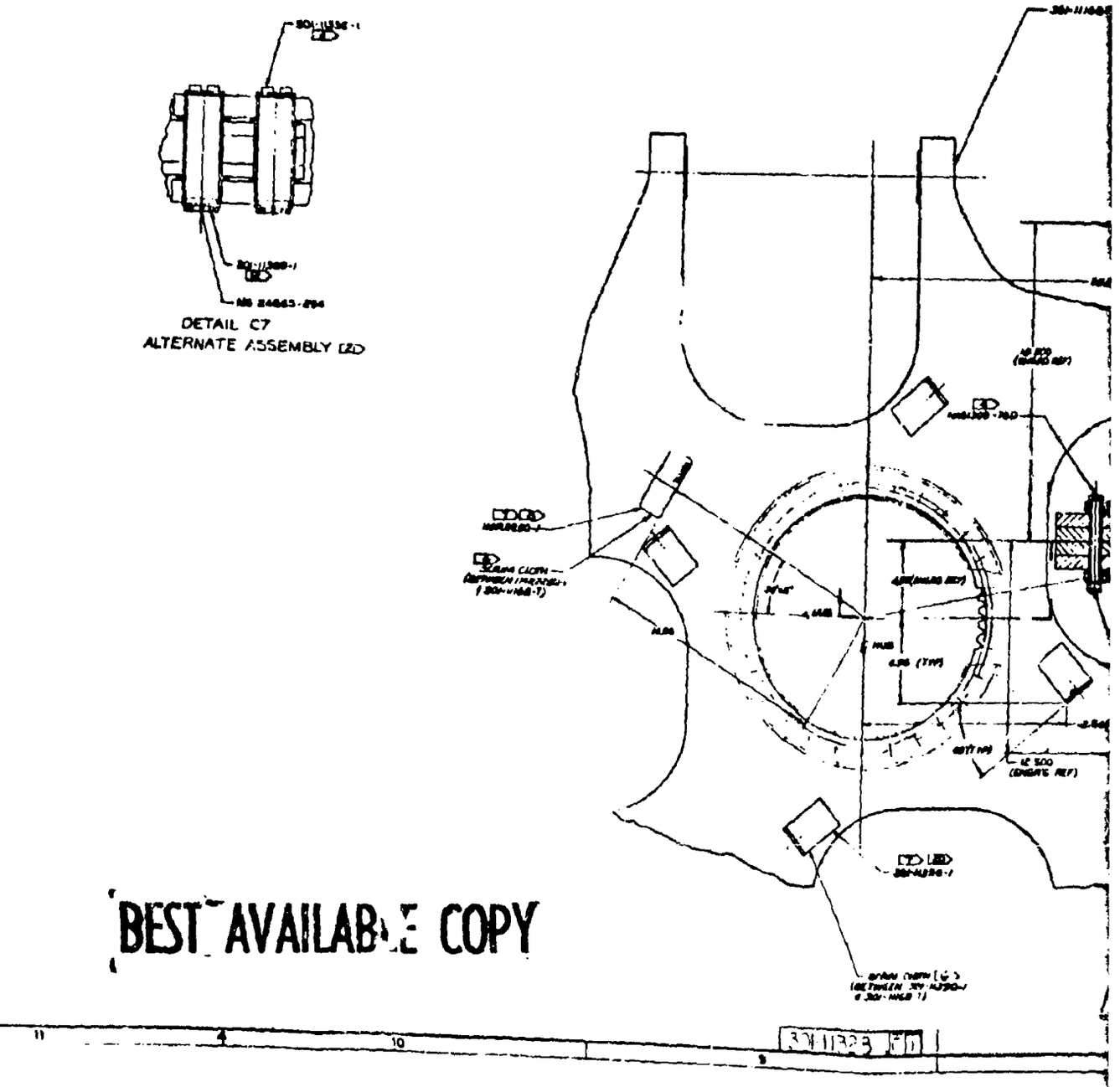

FIGURE 20. HLH/ATC ROTARY-WING-HEAD ASSEMBLY (Sheet 1 of 2)

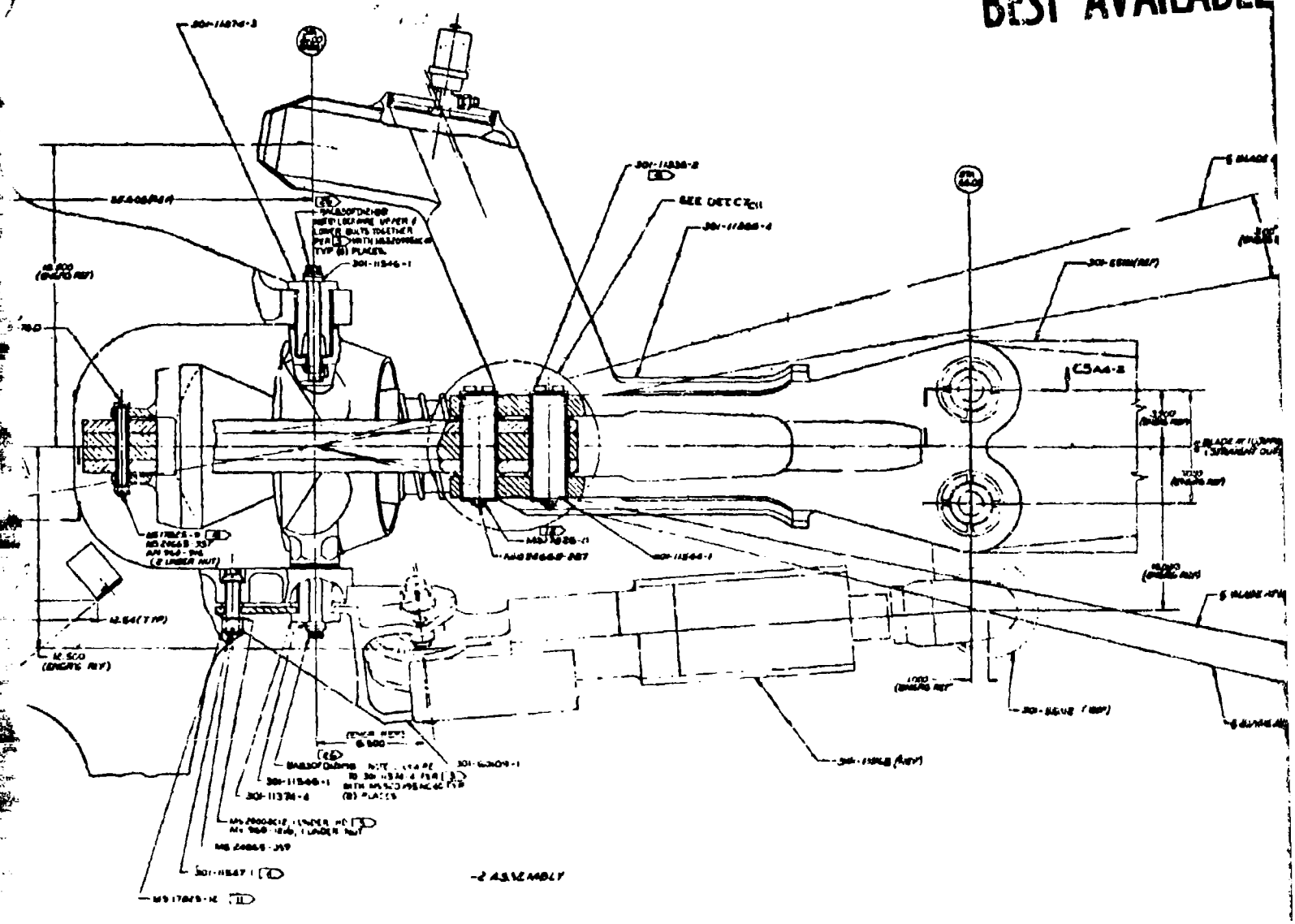

LE COPY

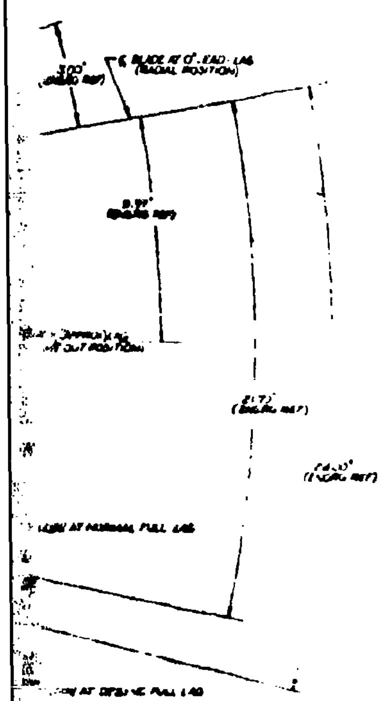

1. THIS IS A CRITICAL PARTS ASSEMBLY SUBJECT TO THE CONTROL SPECIFIED IN BOEING PROCESS SPEC. MS 14 00
2. INSTALL LOCKWIRE PER BAC 5 O18 DOUBLE TWIST METHOD
3. THESE PARTS TO BE INSTALLED WITH ANTI SEIZE COMPOUND TT-A-580 (WEARING SURFACES) CAUTION: KEEP ANTI-SEIZE COMPOUND OFF ALL THREADS
4. INSTALL WASHERS WITH CHAMFER ON I D AGAINST BOLT HEAD.
5. SCRIM CLOTH STYLE #1562 SOURCE: BURLINGTON GLASS FABRIC CO. NEW YORK, NY
6. PREPARE SURFACE PER BAC 5 [illegible] TYPE II CLASS 2
7. BOND IDENTIFICATION PLATE [illegible] TO HUB USING EC [illegible] ADHESIVE WITH ONE LAYER OF SCRIM CLOTH
8. TORQUE BOLT TO [illegible] IN-LBS
9. TORQUE NUT TO 480-600 IN-LBS
10. TORQUE NUT TO 2500-2800 IN LBS
11. TORQUE BOLT TO [illegible] 200 IN LBS
12. TORQUE 301-11378-1 BOLT TO 3800-4600 IN LBS. YELLOW INDICATOR IN BOLT HEAD WILL TURN BLACK WHEN PROPERLY TORQUED
13. TORQUE 301-11376-1 BOLT PER [illegible] PRIOR TO PERFORMING [illegible]
14. HUB CONSISTS OF MATCHED SET (2 PLATES) ASSEMBLED WITH HUB INDICES ALIGNED AND EXTERIOR FACES TOP & BOTTOM IN PROPER ORDER.
15. INSTALL PART BY SHRINK FIT METHOD PER BAC 5436 PARA 8.2.5 USING LIQUID NITROGEN FREEZING SYSTEM. DO NOT COAT WITH ANY CORROSION INHIBITORS
16. CAUTION: ALL CRES WASHERS ARE TO BE USED WHERE DESIGNATED. ANY SUBSTITUTION OF STEEL/CADMIUM PLATED WASHERS FOR CRES WASHERS IS STRICTLY PROHIBITED
17. CAUTION: DO NOT USE CADMIUM PLATED TOOLS, JIGS OR FIXTURES WHERE ACTUAL CONTACT OF MATING SURFACES WITH ANY TITANIUM PARTS IS ENCOUNTERED.
18. POSITION 301-11354-1 FIRMLY AGAINST INBOARD MATING SURFACE (BACK FACE) BEFORE APPLYING TORQUE PER [illegible]
19. BOND BRACKET 301-11390 TO HUB PER BAC 5010 TYPE 36, SPECIAL METHOD II
20. 301-11358-1 AND 301-11389-1 TOGETHER SUBSTITUTE FOR 301-11316-2, 301-11344-1, MS17826-8
21. THE ASSOCIATED SPRING CORPORATION, WALLACE BARNES DIV, BRISTOL, CONN 06010
22. BOND 301-60111-2, -3, -4, 09-6 SHIM TO PITCH HOUSING PER BAC 5010 TYPE 96, SPECIAL METHOD II
23. SELECT SHIM FROM PARTS LISTED THAT WILL COMPRESS ELASTOMERIC BEARING 301-11563-1 .035-.045 FROM FREE STATE WHEN ASSEMBLED AS SHOWN
24. 301-11168-10 SUBSTITUTE FOR 301-11168-7
25. TORQUE BOLT 3800-4500 IN-LBS

PARTS LIST CONTINUED

Qty	Qty	Part No.	Name
	10	301-11375-1	BOLT
	8	301-11374-2	SHEAR PIN
	8	301-11374-1	SHEAR PIN
	4	301-11391-1	[illegible] DAMPER FITTING
	8	301-11394-1	C/F RING STOP PAD
	4	301-11806-1	PITCH HOUSING ASSY
	4	301-11284-1	LOOP ASSY
	4	301-11280-	CROSSBEAM ASSY
	1	301-11168-1	HUB PLATE ASSY
[illegible]	[illegible]	EC 2216	ADHESIVE
1	1	SCRIM CLOTH	[illegible]
4	4	301-11390-1	BRACKET
[illegible]	[illegible]	AN960-416	WASHER
[illegible]	[illegible]	AN960-516	WASHER
[illegible]	[illegible]	[illegible]	WASHER
[illegible]	[illegible]	NAS1587-5C	WASHER
[illegible]	[illegible]	[illegible]	BOLT
[illegible]	[illegible]	[illegible]	COTTERPIN
[illegible]	[illegible]	[illegible]	COTTERPIN
[illegible]	[illegible]	[illegible]	LOCKWIRE
[illegible]	[illegible]	[illegible]	WASHER
[illegible]	[illegible]	[illegible]	LOCKNUT
[illegible]	[illegible]	[illegible]	LOCKNUT
[illegible]	[illegible]	[illegible]	[illegible]
[illegible]	[illegible]	[illegible]	BOLT
[illegible]	[illegible]	[illegible]	COTTERPIN
[illegible]	[illegible]	[illegible]	COTTERPIN
1	1	[illegible] 2230-1	[illegible] PLATE
[illegible]	[illegible]	301-11399-1	[illegible] NUT
[illegible]	[illegible]	[illegible]	[illegible]
[illegible]	[illegible]	[illegible]	BOLT
[illegible]	[illegible]	[illegible]	WASHER
[illegible]	[illegible]	[illegible]	WASHER
[illegible]	[illegible]	[illegible]	BOLT
[illegible]		[illegible]	BOLT
[illegible]		[illegible]	SHEAR PIN
[illegible]		[illegible]	SHEAR PIN
4		[illegible]	[illegible]
4	[illegible]	[illegible]	[illegible]
[illegible]	[illegible]	[illegible]	[illegible]
[illegible]		[illegible]	C/F RING STOP [illegible]
[illegible]	[illegible]	[illegible]	[illegible]
[illegible]		[illegible]	[illegible]
4		[illegible]	LOOP ASSY
4		[illegible]	CROSSBEAM ASSY
1		[illegible]	HUB PLATE ASSY
1		[illegible]	HUB PLATE ASSY
		-2	HEAD ASSY
		-1	HEAD ASSY

[illegible]

BEST AVAILABLE COPY

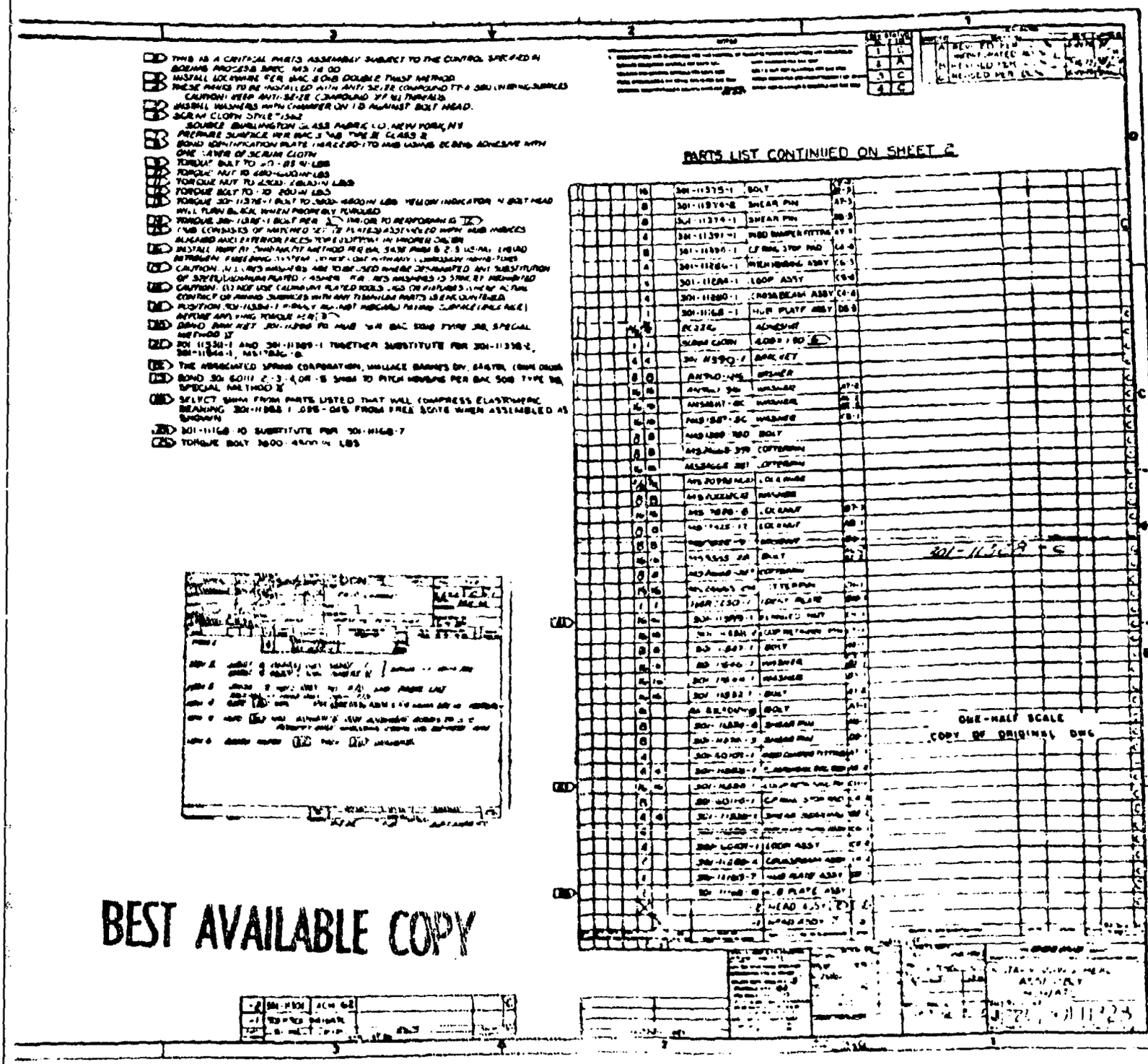

PARTS LIST CONTINUED ON SHEET 2

ONE-HALF SCALE
COPY OF ORIGINAL DWG

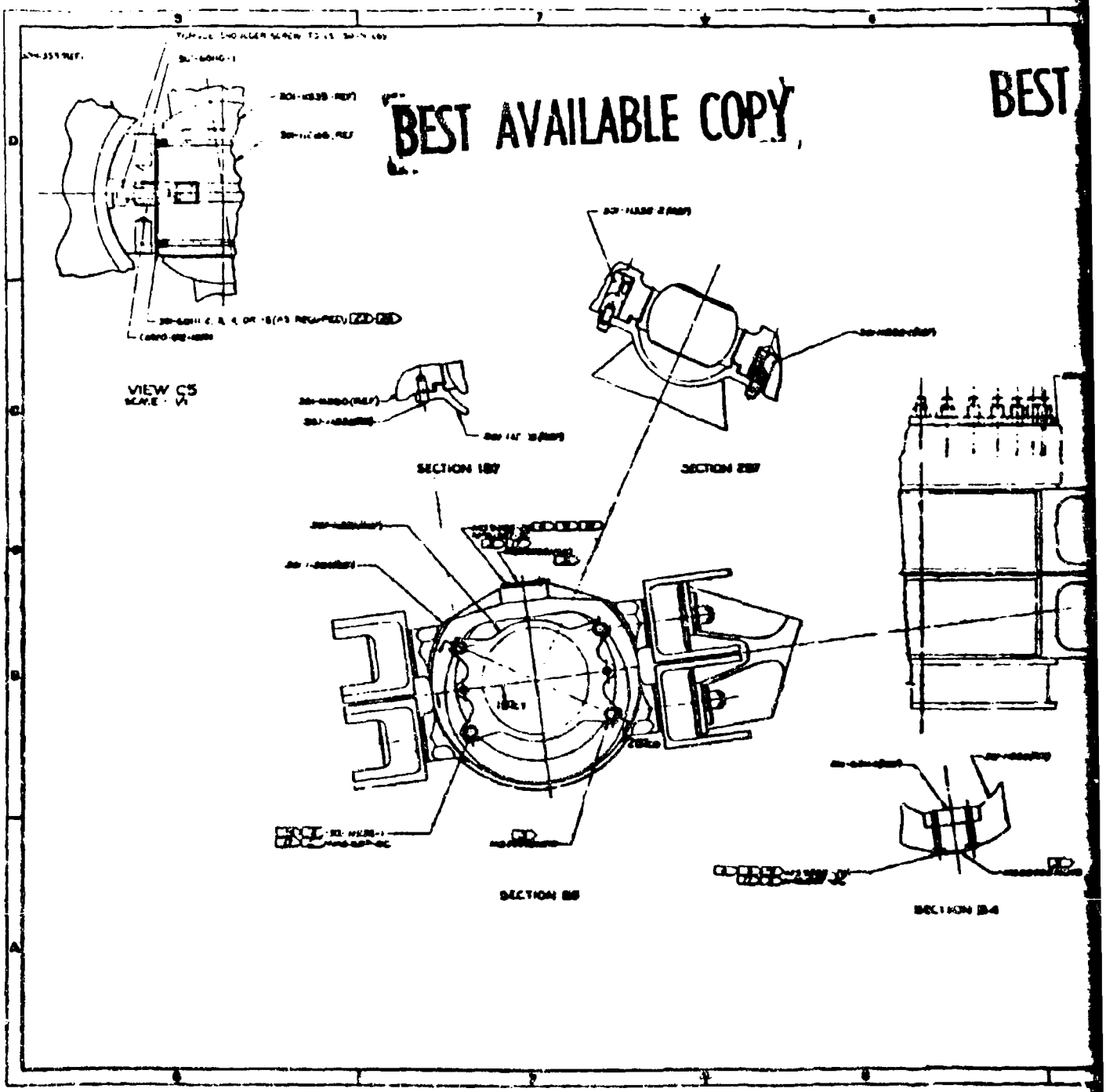

FIGURE 20. HLH/ATC ROTARY-WING-HEAD ASSEMBLY (Sheet 2 of 2)

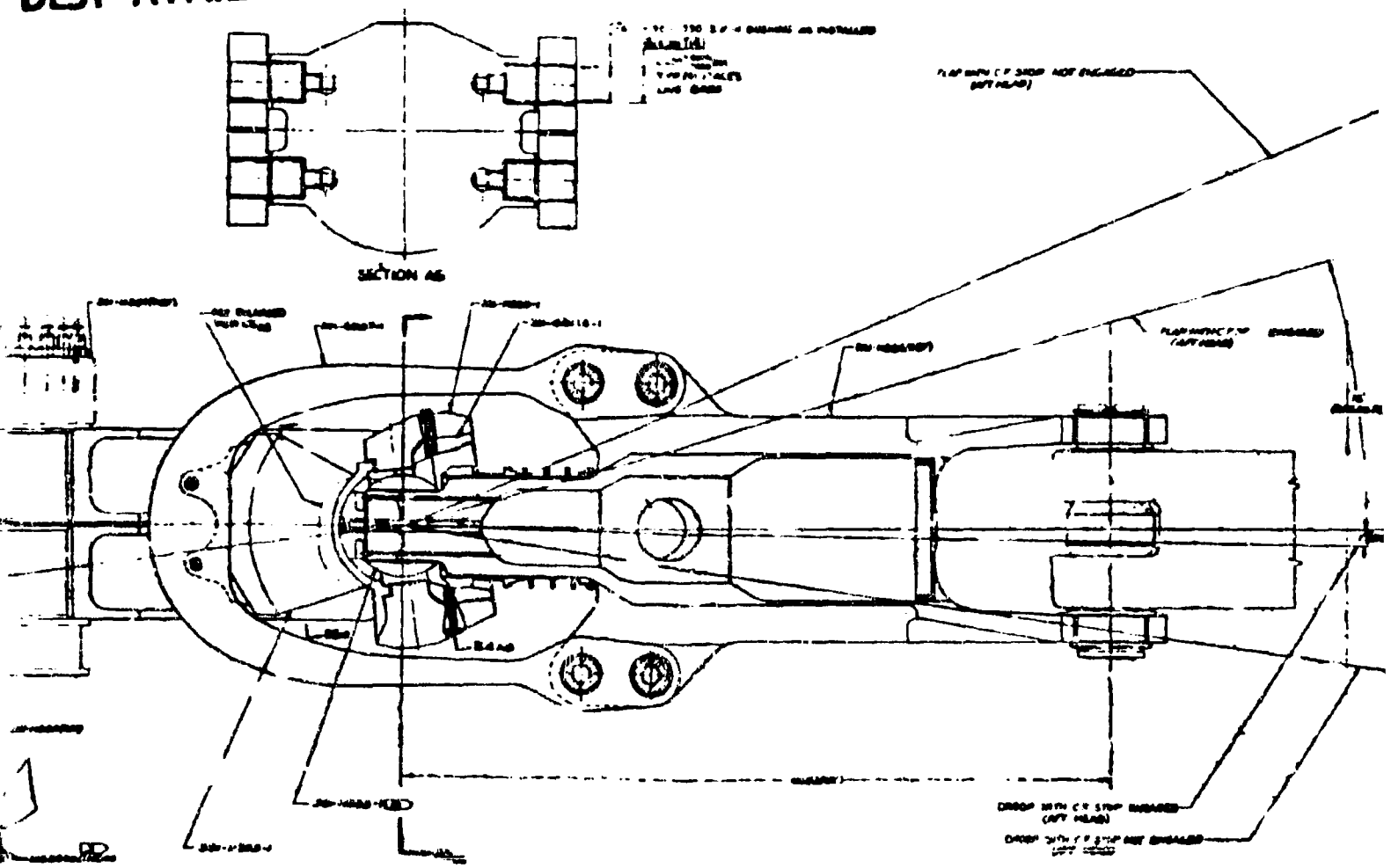

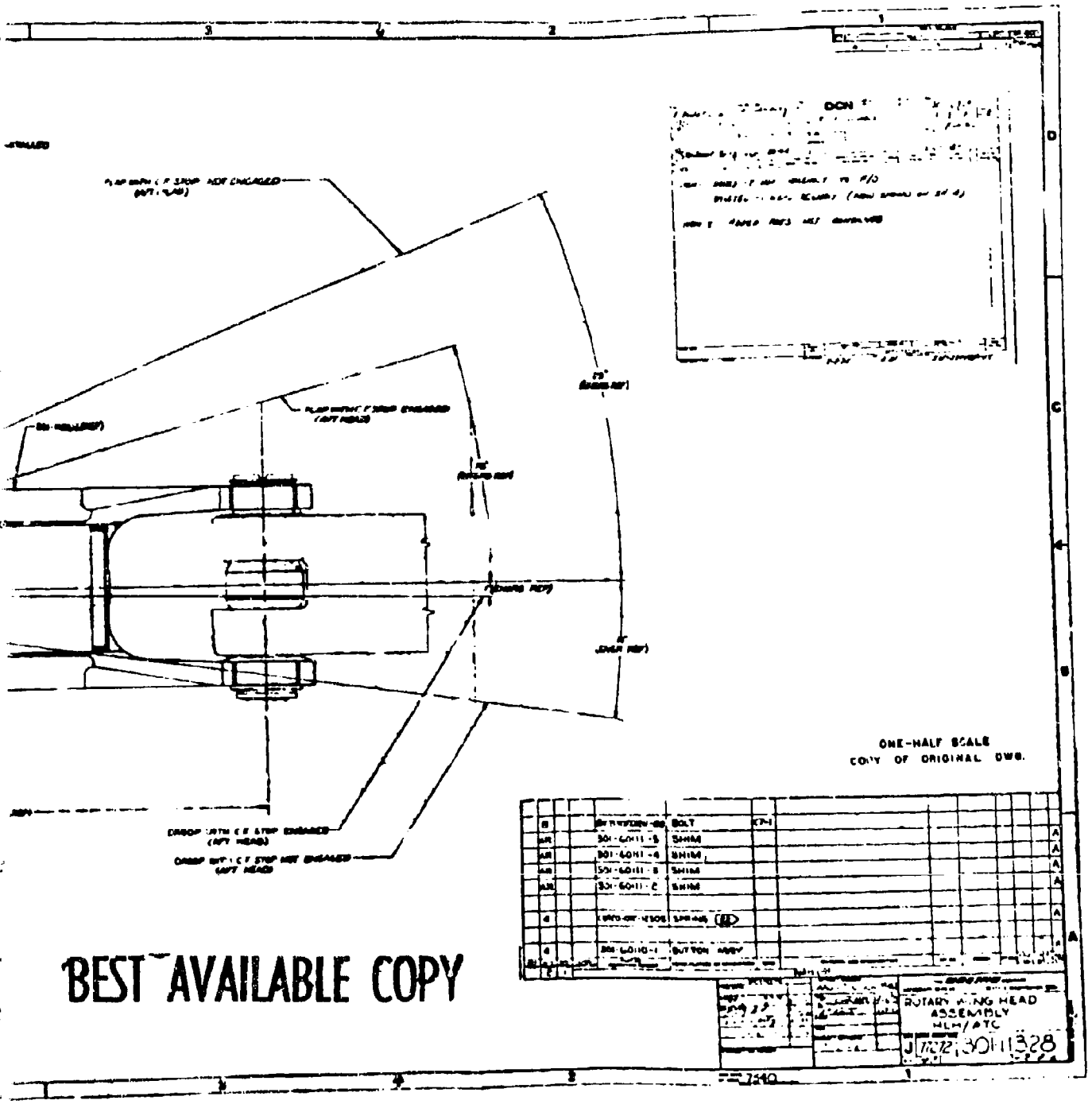

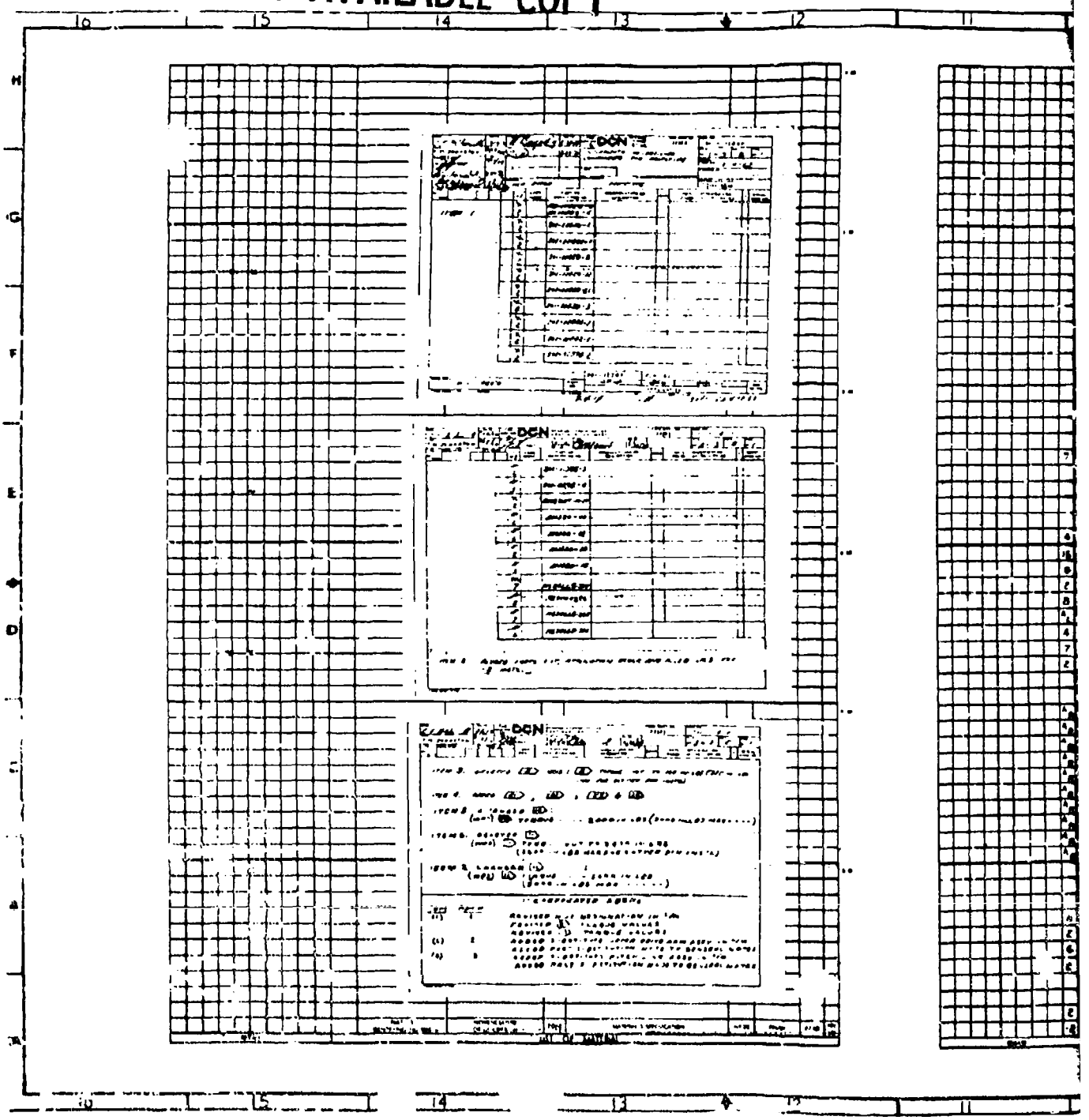

FIGURE 21. ROTARY-WING-HEAD CONTROLS AFT INSTALLATION
(Sheet 1 of 2)

NOTES:

1. DURING ASSEMBLY AND STORAGE, ALL EXPOSED TEFLON SURFACES ARE TO BE PROTECTED FROM DAMAGE AND DIRT, GRIT, PAINT, OR ANY MEDIA WHICH COULD CAUSE ABRASION.
2. THESE PARTS ARE TO BE COMPLETELY DRY AND FREE FROM PAINT.
3. USE AN960-616L AND/OR AN960-616 WASHERS AS REQUIRED TO ALIGN COTTER PIN HOLE IN BOLT AND SLOT IN NUT.
4. USE AN960-1016L AND/OR AN960-1016 WASHERS AS REQUIRED TO ALIGN COTTER PIN HOLE IN BOLT AND SLOT IN NUT.
4. USE AN960-1216L AND/OR AN960-1216 WASHERS AS REQUIRED TO ALIGN COTTER PIN HOLE IN BOLT AND SLOT IN NUT.
5. USE AN960-1416L AND/OR AN960-1416 WASHERS AS REQUIRED TO ALIGN COTTER PIN HOLE IN BOLT AND SLOT IN NUT.
7. USE AN960-816L AND/OR AN960-816 WASHERS AS REQUIRED TO ALIGN COTTER PIN HOLE IN BOLT AND SLOT IN NUT.
8. [illegible]
9. TORQUE BOLT TO 300 IN-LBS. (400 IN-LBS MAX FOR COTTER PIN INSTL)
6. TORQUE NUT TO 300 IN-LBS (500 IN-LBS MAX FOR COTTER PIN INSTL)
11. [illegible]
12. TORQUE NUT TO 1000 IN-LBS (1500 IN-LBS MAX FOR COTTER PIN INSTL).
13. TORQUE NUT TO [illegible] IN-LBS (8000 IN-LBS MAX FOR COTTER PIN INSTL)
14. SPIROLOX - RAMSEY CORP, ST LOUIS, MO.
15. INSTALL LOCKWIRE PER BAC 5018 DOUBLE TWIST METHOD.
16. TORQUE SHOULDER BOLTS 75-200 IN-LBS.
17. USE AN960-1616L AND/OR AN960-1616 WASHERS AS REQD TO ALIGN COTTER PIN HOLE IN BOLT AND SLOT IN NUT.
18. TORQUE NUT TO 2200 IN-LBS (6000 IN-LBS MAX FOR COTTER PIN INSTL.)
19. 301-11412-1 SUBSTITUTE TO 301-11412-2 FOR HEMS/ATC PROGRAM ONLY.
20. 301-11408-1 SUBSTITUTE FOR 301-11408-5 FOR WHIRLTOWER AND OSTR TESTING ONLY.
21. TORQUE NUT TO 1600 IN-LBS. (2800 IN-LBS MAX FOR COTTER PIN INSTL.)
22. TORQUE NUT TO 80 IN-LBS. (150 IN-LBS MAX FOR COTTER PIN INSTL.)
23. TORQUE BOLT TO 300 IN-LBS (600 IN-LBS MAX FOR COTTER PIN INSTL.)
24. TORQUE NUT TO 800 IN-LBS. (1200 IN-LBS MAX FOR COTTER PIN INSTL.)

Qty	Part or Identifying No.	Nomenclature or Description	Notes	Code
	RSN100S	RETAINER	14	B
4	RSN100	RETAINER	14	
7	MS24665-377	COTTER PIN		B
10	-376			
6	374			
2	MS24665-304	COTTER PIN		B
6	MS20002C6	WASHER, CSK		B
	MS20995NC32	LOCKWIRE		
	MS17826-10	NUT		B
	MS17825-12	NUT		
2	MS17826-6	NUT		B
	AN960-616	WASHER		A
	AN960-616L	WASHER		A
	AN960-1416	WASHER		
	-816L			
	-1416			
	-1416L			
	-1216			
	-1216L			
	-1016			
	-1016L			
	[illegible]			
	AN960-616L	WASHER		
3	AN320-15	NUT		B
4	AN320-18	NUT		
2	-14			B
6	-12			B
6	AN320-10	NUT		B
4	AN320-12	NUT		B
2	BACB30LT10 [illegible]	BOLT		B

PARTS OR IDENTIFYING NO. | NOMENCLATURE OR DESCRIPTION | ITEM | MATERIAL & SPECIFICATION

LIST OF MATERIAL

301-11301	RCH-68	-2	143	B
301-11301	HEMS ATC	-1	142	

APPLICATION

CODE IDENT NO. 77272

DWG NO. 301 [illegible]

BASIC PART CODE

7540

BEST AVAILABLE COPY

BEST AVAILABLE COPY

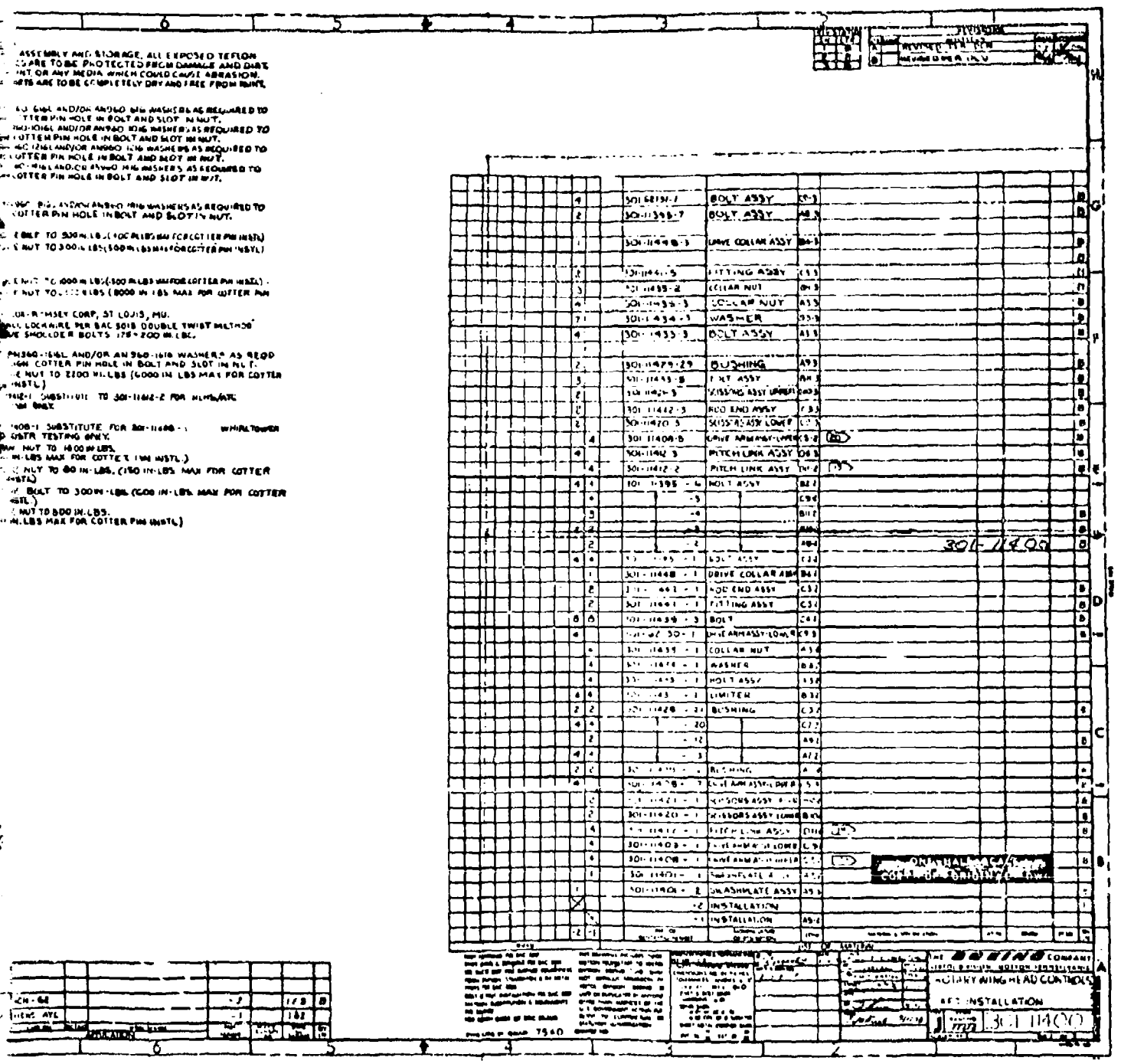

BEST AVAILABLE COPY

BEST AVAILABLE COPY

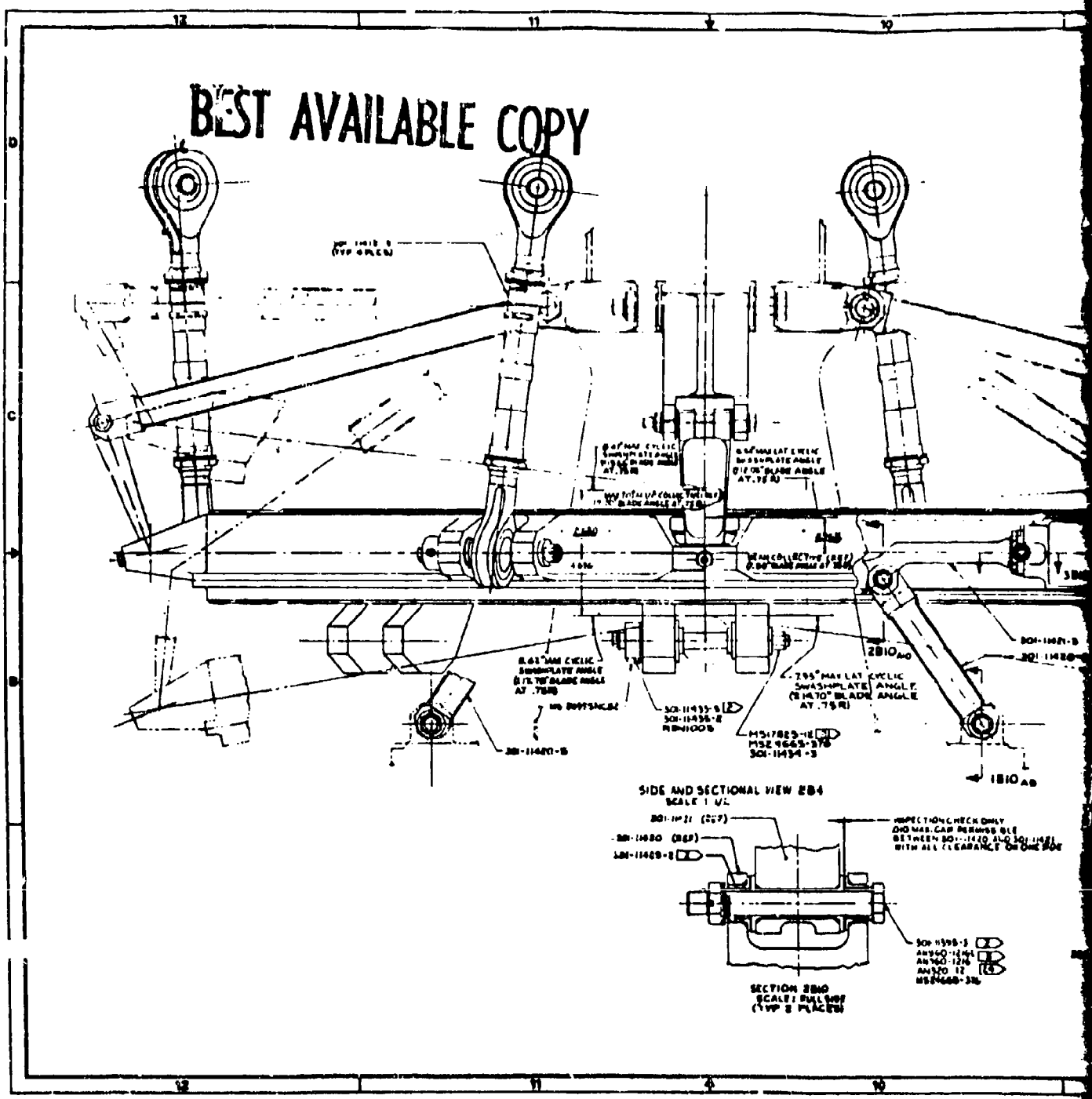

FIGURE 21. ROTARY-WING-HEAD CONTROLS AFT INSTALLATION
(Sheet 2 of 2)

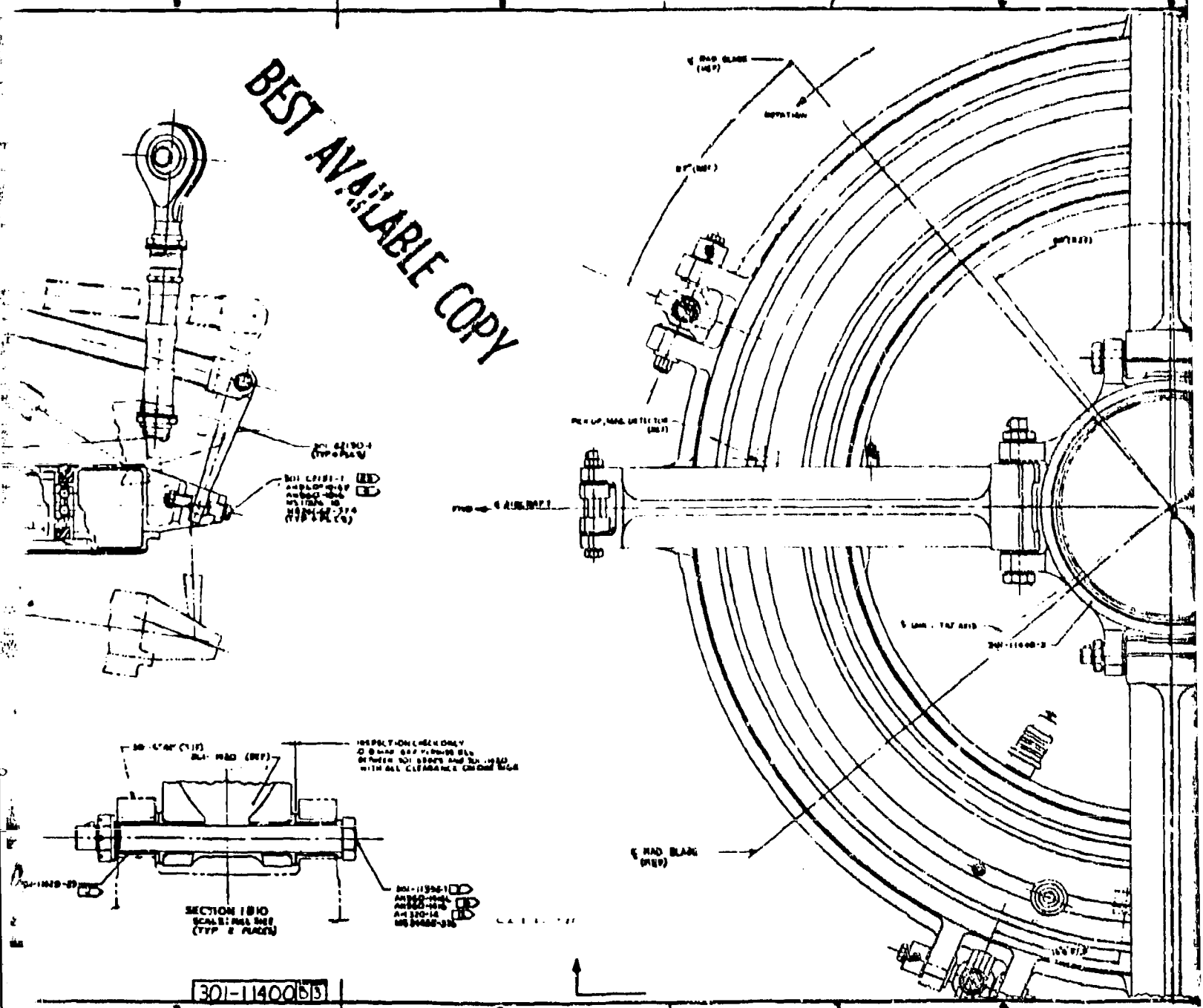

301-11400 [5]

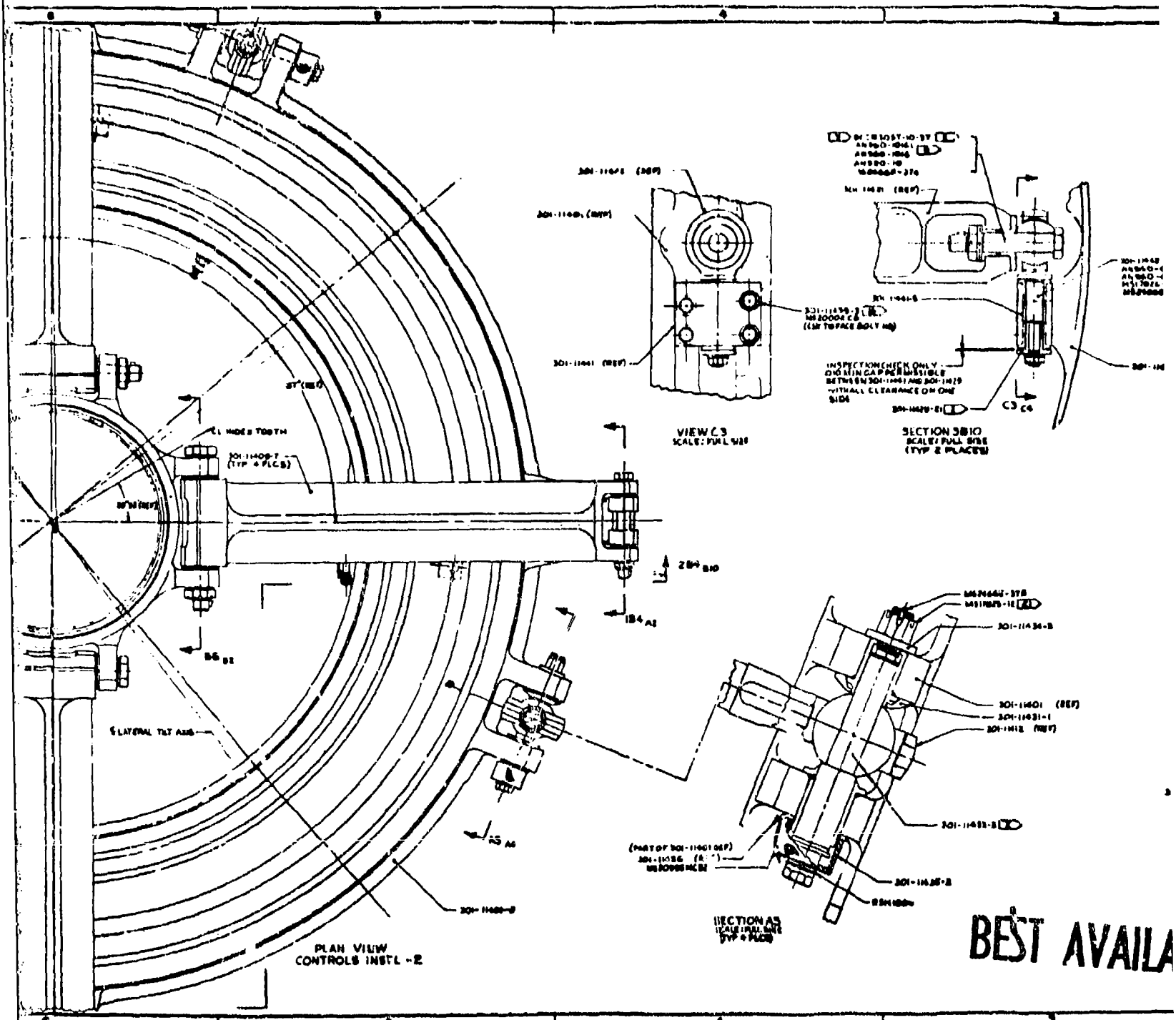

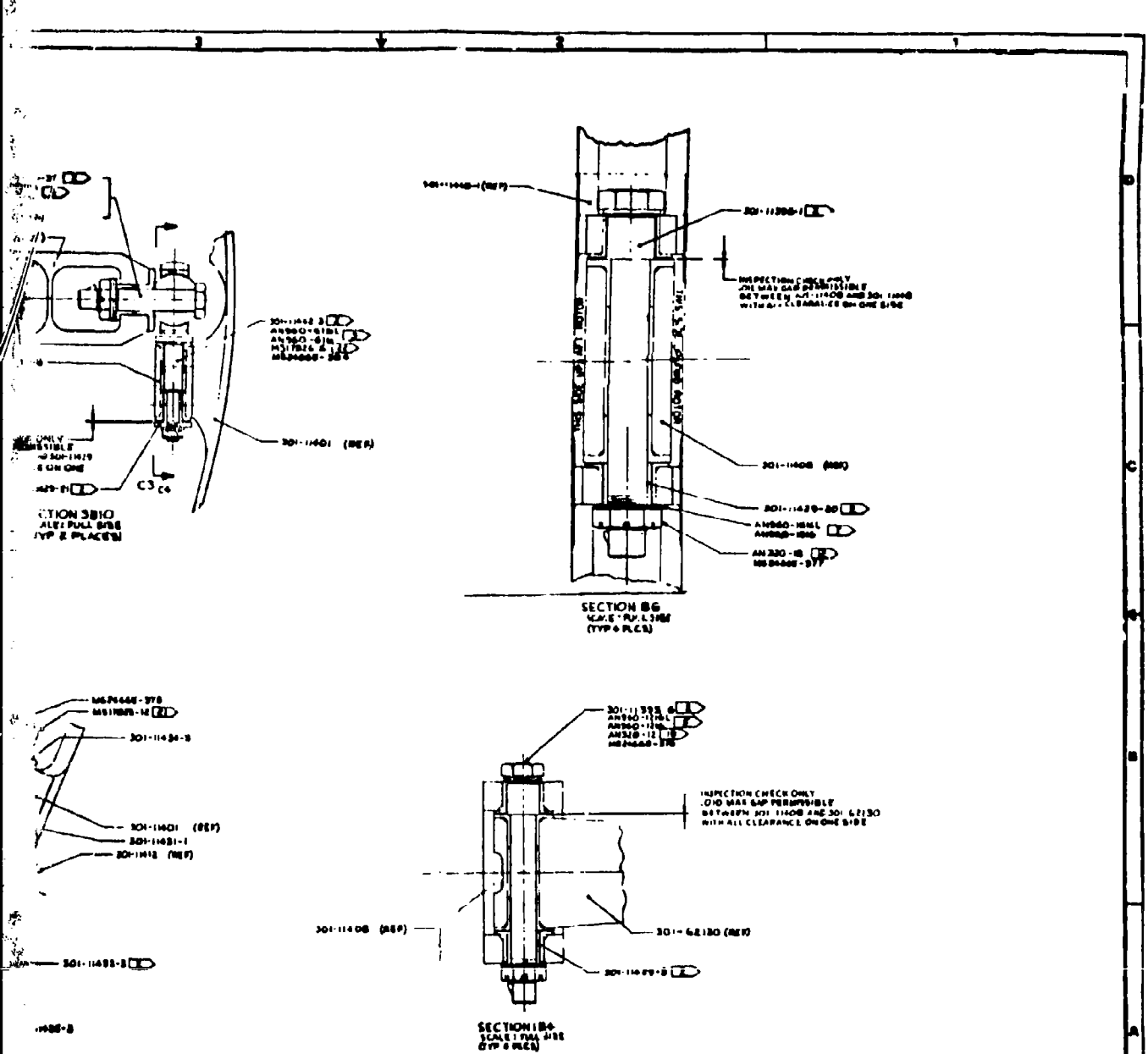

BEST AVAILABLE COPY

ROTARY WING HEAD CONTROLS

AFT INSTALLATION

J 77672 301-11400

4

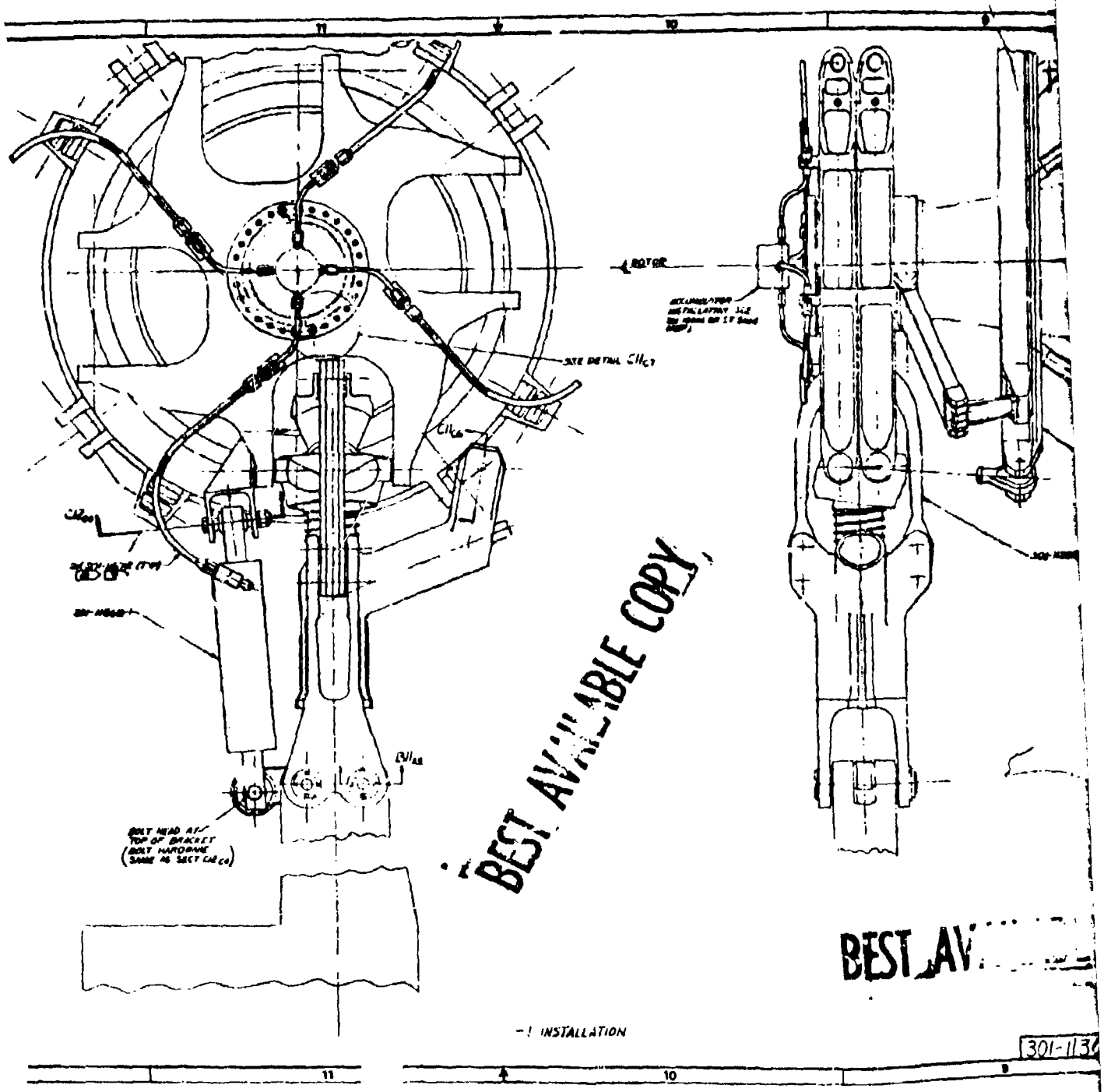

FIGURE 22. AFT ROTARY-WING-HEAD INSTALLATION (Sheet 1 of 2)

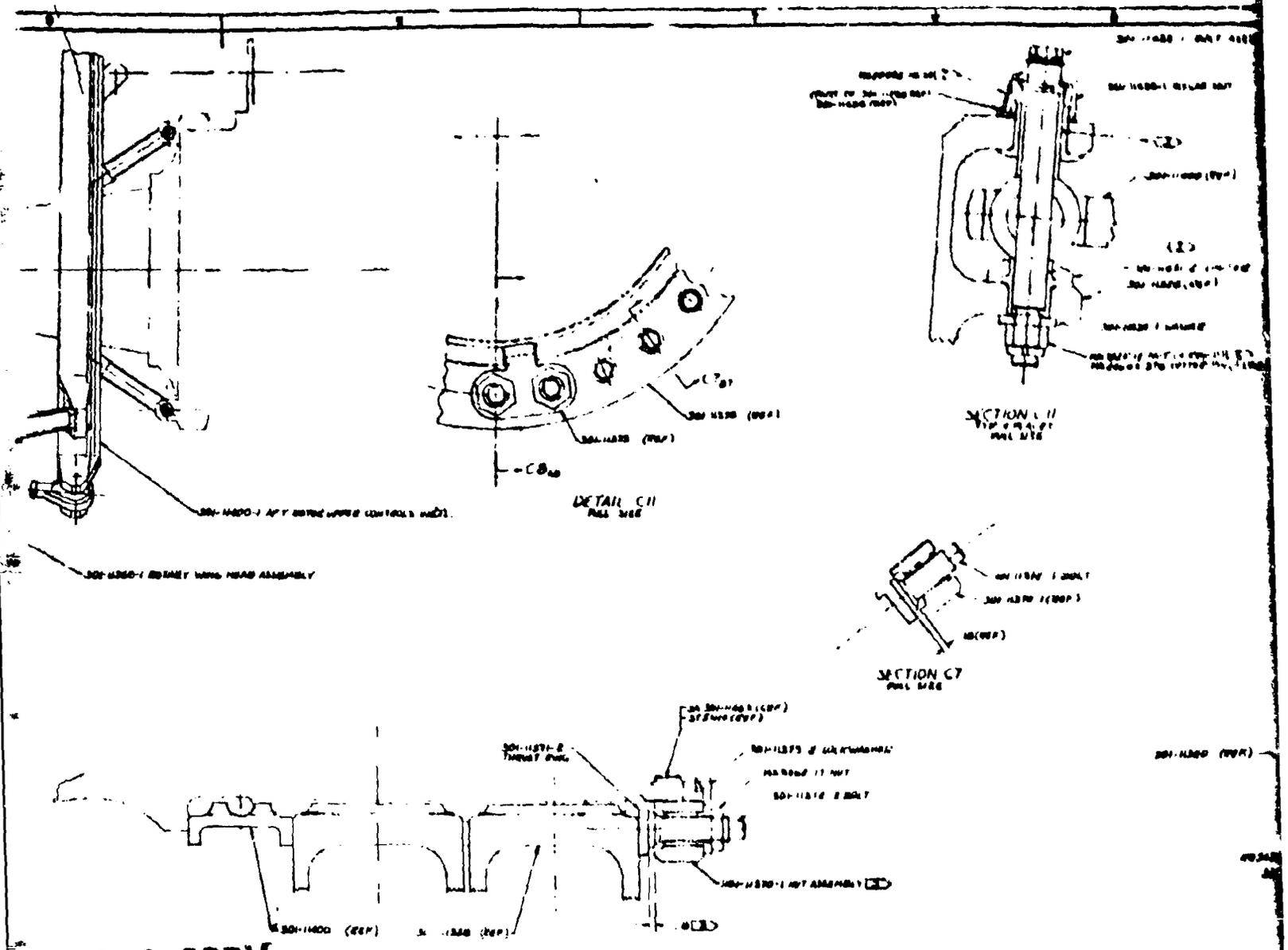

(TORQUE BOLT TO 1600 IN LBS)
(1800 IN LBS MAX FOR COTTER PIN HOLES)

[illegible]

INSTALL [illegible]

INSTALL [illegible]

CADMIUM PLATED TOOLS, JIGS OR FIXTURES SHALL NOT BE USED AT ANY TIME DURING MANUFACTURE OR ASSEMBLY OF THIS INSTALLATION

TORQUE NUT TO 480 - 650 FOOT POUNDS OR TO A MAXIMUM OF 1280 FOOT POUNDS TO ALIGN SLOT IN NUT WITH HOLE IN BOLT.

USE AN960-[illegible] AND/OR AN960 [illegible] WASHERS AS REQD TO ALIGN COTTER PIN HOLE IN BOLT AND SLOT IN NUT

PROCEDURE FOR INSTALLING HUB NUT:
A. INSTALL HUB NUT ON ROTOR SHAFT UNTIL NUT BOTTOMS ON UPPER SURFACE OF THRUST RING
B. INSTALL ALL 28 BOLTS (WITH LOCK NUTS & KEYS) INTO THE HUB NUT AS SHOWN ON FIELD OF DRAWING
C. BACK OFF HUB NUT UNTIL THE FIRST ALIGNMENT POSITION OF KEY AND ROTOR SHAFT SLOT IS OBTAINED
D. TURN ALL 28 BOLTS UNTIL CONTACT IS MADE BETWEEN BOLTS AND THRUST RING WHILE MAINTAINING POSITION OF HUB NUT.
E. TORQUE ALL 28 BOLTS PER THE FOLLOWING PROCEDURE:
1. IN THE NUMERICAL SEQUENCE INDICATED ON THE HUB NUT, TORQUE ALL BOLTS TO:
FIRST ROUND 25-40 FOOT POUNDS
SECOND ROUND 60-75 FOOT POUNDS
THIRD ROUND 125-140 FOOT POUNDS
F. TORQUE JAM NUTS TO 11-25 FOOT POUNDS

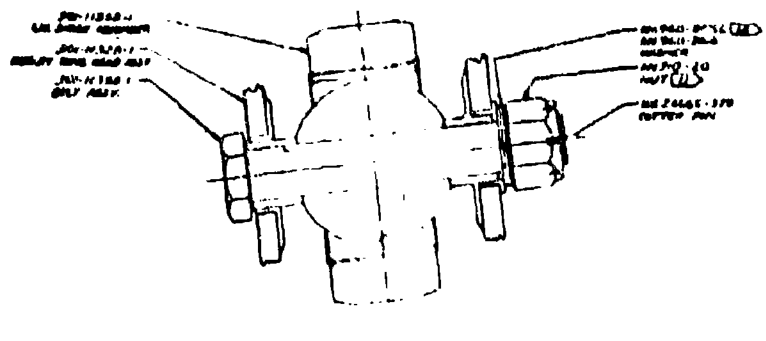

SECTION [illegible]
TYPICAL 4 PLACES
FULL SIZE

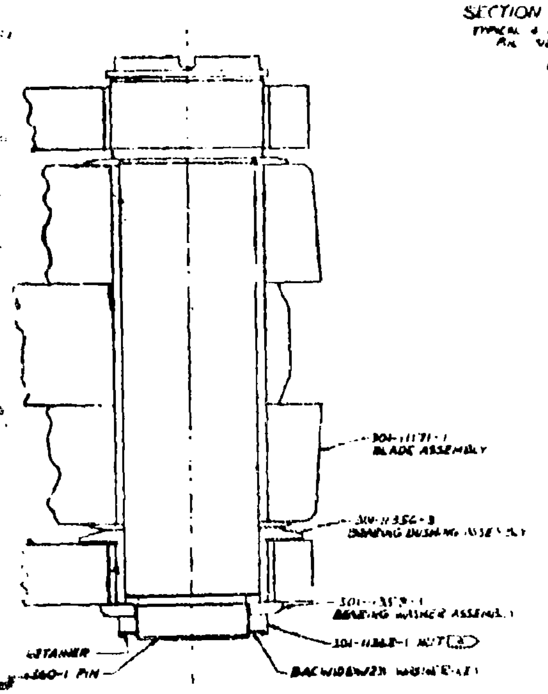

SECTION B-B
TYP 8 PLACES
FULL SIZE

SEE SH 2

BEST AVAILABLE COPY

-2	301-11800	KCH-62		1&2	B
-1	ST51114	HLH/ATC		1	
-1	[illegible]	HLH/ATC		1	

3

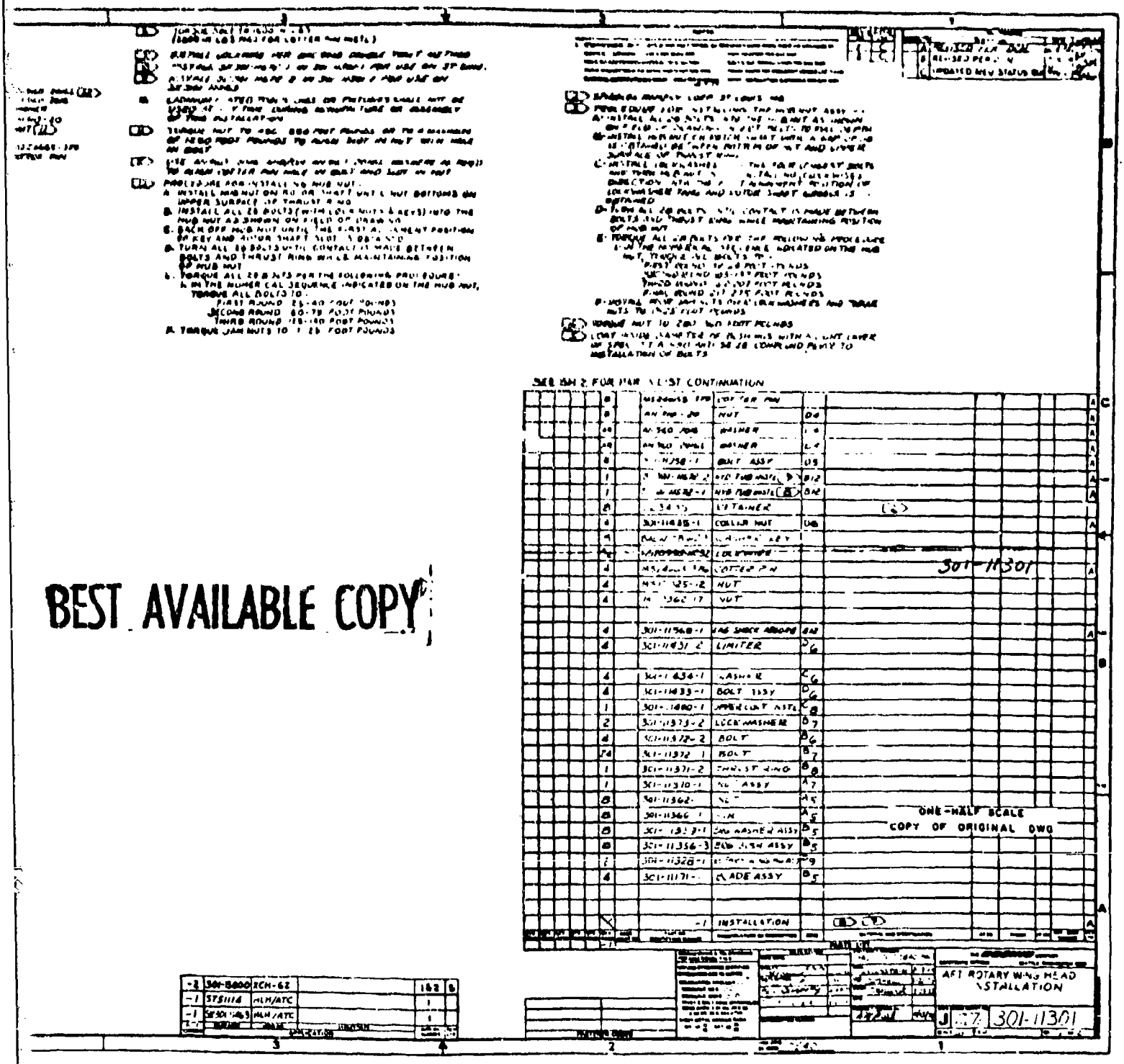

BEST AVAILABLE COPY

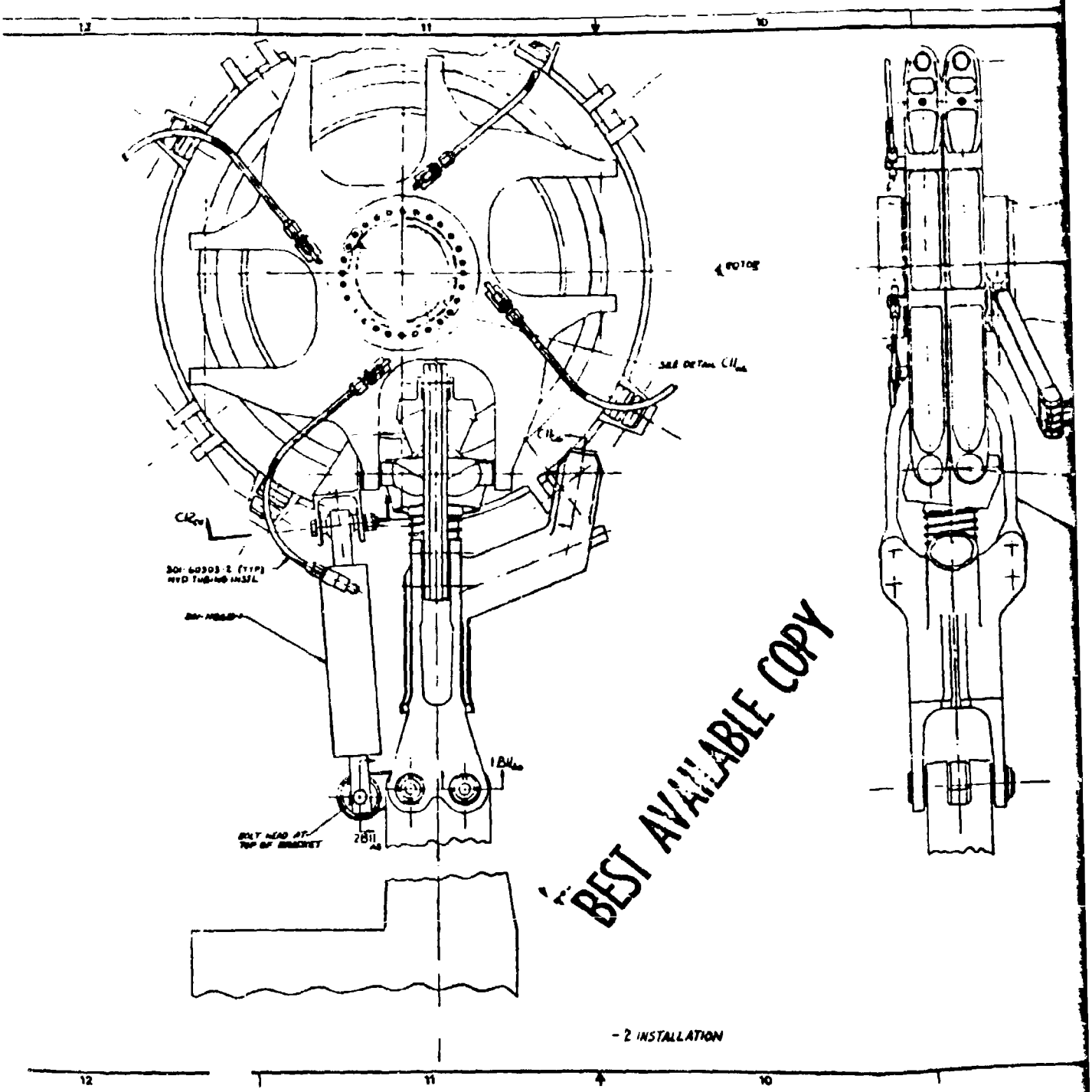

FIGURE 22. AFT ROTARY-WING-HEAD INSTALLATION (Sheet 2 of 2)

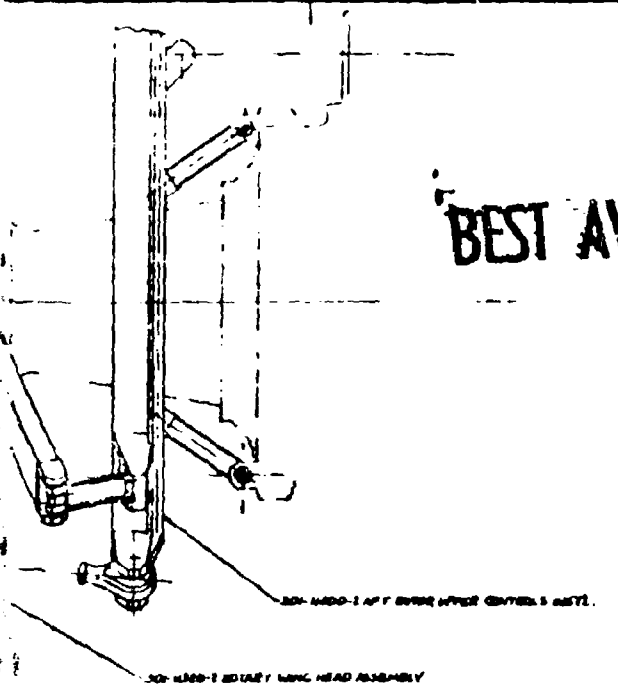

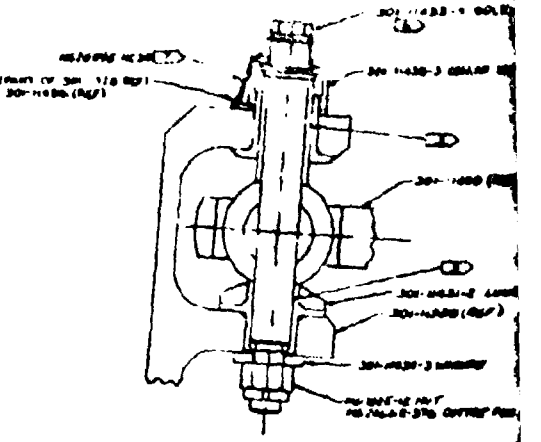

SECTION C11
TYP 4 PLACES
FULL SIZE

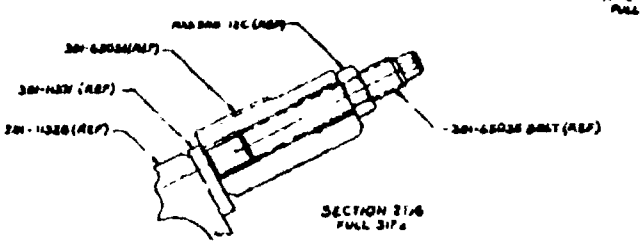

SECTION 31A
FULL SIZE

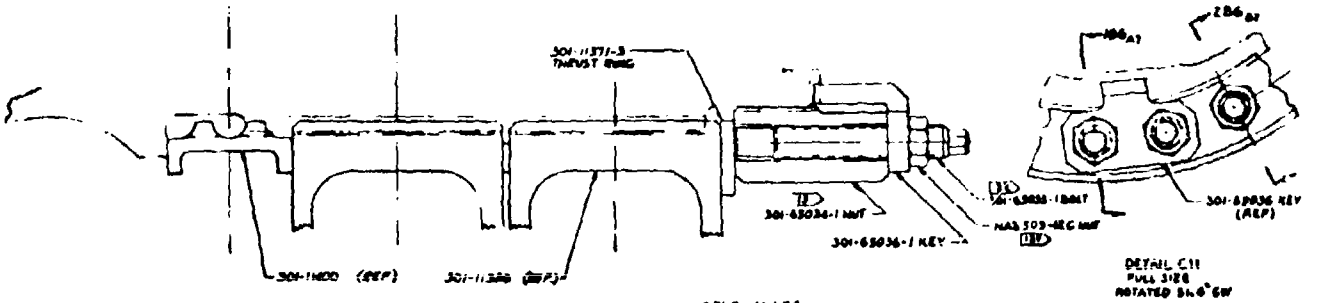

SECTION C8
FULL SIZE

SECTION 186
FULL SIZE

DETAIL C11
FULL SIZE
ROTATED 54.6° CW

2

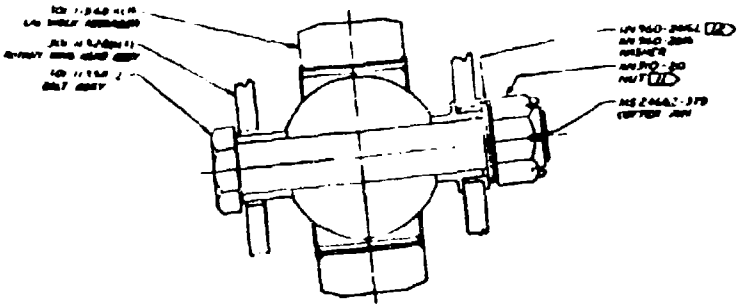

SECTION C12
TYPICAL 4 PLACES
FULL SIZE

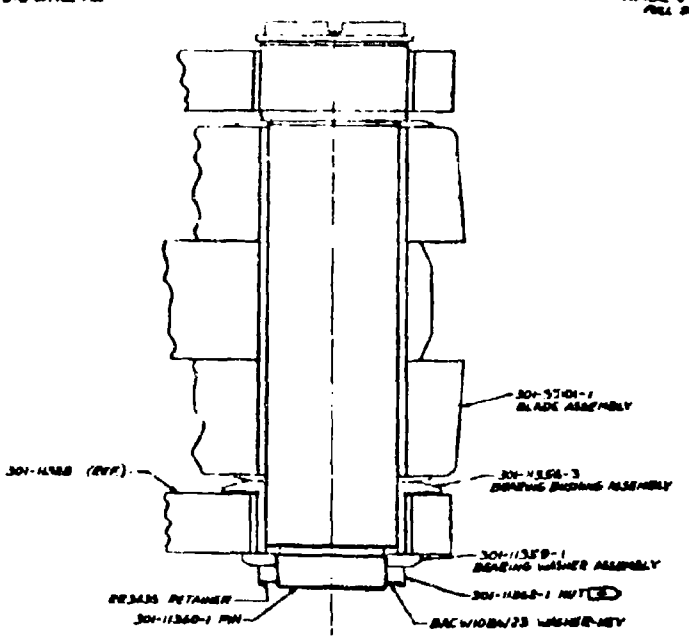

SECTION B11
TYP 18 PLACES
FULL SIZE

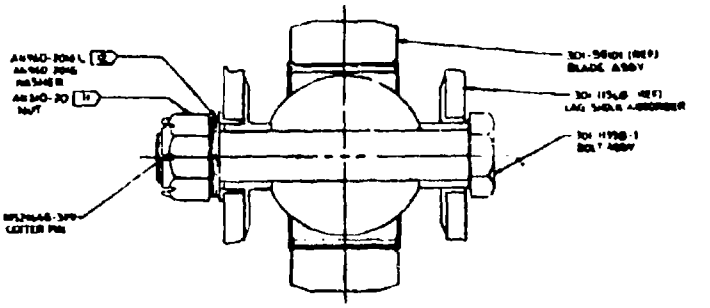

SECTION 2B11
(TYP 4 PLACES)
FULL SIZE

BEST AVAILABLE COPY

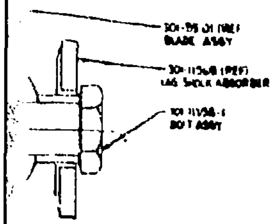

Qty	Part No.	Nomenclature	Zone
8	MS 24665-379	COTTER PIN	
8	AN 310-20	NUT	D4
AR	AN 960-416	WASHER	D4
AR	AN 960-416L	WASHER	D4
1	301-11358-1	BOLT ASSY	D5
4	[illegible]	[illegible] ASSY	
1	301-60??5-2	[illegible]	B/C
8	RR 3435	RETAINER	
4	301-11485-3	COLLAR NUT	D6
8	[illegible]	WASHER-KEY	
AR	MS 20995 NC32	LOCKWIRE	
4	MS 24665 [illegible]	COTTER PIN	
4	MS 17825-12	NUT	
28	NAS509-2C	NUT	
4	301-11568-1	LAG SHOCK ABSORB	B/C
4	301-11431-2	LIMITER	D6
4	301-11434-3	WASHER	C6
4	301-11433-1	BOLT ASSY	D6
1	301-11400-2	UPPER CONT INSTL	C8
2	301-45036-1	KEY	D7
28	301-65035-1	BOLT	B7
1	301-11371-3	THRUST RING	B8
1	301-65034-1	NUT	A7
8	301-11362-1	NUT	A5
8	301-1136?-1	PIN	A5
8	301-113?9-1	BRG WASHER ASSY	B5
8	301-11356-1	BRG BUSH ASSY	B5
1	301-11328-2	[illegible]	B9
4	[illegible]	BLADE ASSY	B5
	-1	INSTALLATION	

ONE-HALF SCALE
COPY OF ORIGINAL DWG

INSTALLATION

2540

4

3.0 DESIGN CRITERIA AND STRUCTURAL ANALYSIS

3.1 AIRCRAFT MISSION PROFILE (FLIGHT SPECTRUM)

The mission profile (Table 5) used in the analysis is the same as that described in Reference 7 except for the modifications described below:

1. The distribution of time spent in OEI flight, is transferred to full engine flight, since rotor blade and control loads are considered identical.

2. The expression of autorotative control reversals and landings as a number per 100 hours rather than a percent occurrence, and the addition of this time to time spent in steady autorotation.

3. The addition of turns expressed as a number per 100 hours. These represent the transient portion of the maneuver and are in addition to the turns represented as a percent occurrence. The latter is considered as representative of the steady-state portion of the turn.

3.2 STRUCTURAL DESIGN CRITERIA

- Gross Weight and Maximum Load Factors

ITEM	DESIGN GROSS WEIGHT	ALTERNATE DESIGN G.W.	MINIMUM FLYING WT.
Gross Wt.	118,000	148,000	63,063
Limit Man. Load Factor	+2.5/-.5G	+2.0/-.5G	+2.5/-.5G

- Center-of-Gravity Range

  Most Forward CG = 60 in. Fwd
  Most Aft CG = 40 in. Aft

TABLE 5. DYNAMIC COMPONENT DESIGN FATIGUE LOADING

Condition	Percent Time/Occurrences
Ground Conditions	1.0
Take Off	(400)
Steady Hovering	30.0
Turns Hovering	(2000)
Control Reversals/Hovering	(2000)
Sideward Flight	2.0
Rearward Flight	1.0
Landing Approach	(750)
Forward Level Flight:	
20% V_H	5.0
40% V_H	2.0
50% V_H	2.0
60% V_H	5.0
70% V_H	8.0
80% V_H	9.0
90% V_H	16.0
V_H	1.0
115% V_H	1.0
Takeoff Power Climb	3.0
Full Power Climb	4.0
Partial Power Descents	(500)
Right Turns	2.5
Left Turns	2.5
Control Reversals	(800)
Pull Ups	(250)
Power to Autorotation	(40)
Autorotation to Power	(40)
Autorotation - Steady	0.5
Autorotation - Left Turn	0.2
Autorotation - Right Turn	0.2
Autorotation - Control/Reversals	0.3
Autorotation - Landing	0.3

- Rotor Design Speeds

DESIGN RPM	POWER ON	POWER OFF
Minimum	155.7	140.1
Normal	155.7	---
Maximum	155.7	176.9
Limit	171.3	194.6

3.3 DESIGN CONDITIONS

(1) Fatigue - The loads used for fatigue analysis are described in detail in References 8 and 9.

(2) Maneuver - Limit condition is a 2.5G symmetrical pull-up with nose-up pitching.

G.W.: 118,000 lb.
C.G.: 60 in.fwd
A/S : 150 k.

(3) (a) Ground Flapping - 4.67G limit for the hub components. This condition is not critical for the controls because of the coincidence of lag and flap hinges.

(b) Blade Folding - The system shall withstand a 45-knot wind from any direction.

3.4 FATIGUE METHODOLOGY

Fatigue Allowables

The S-N curves and Goodman diagrams for steel and titanium in Figures 23 through 25 were used for the safe-life fatigue and fail-safe fatigue analysis.

Design Allowable Stresses

Material	Design CV	End. Limit Cycles	M - 3σ *		M - σ *	
			Non-Fretted	Fretted	Non-Fretted	Fretted
Steel	.12	10^7	±25000	±10000	±32000	±12800
Ti	.13	$5x10^7$	±20000	± 6000	±26000	± 7800
Al	.13	$5x10^7$	± 6000	± 2000	± 7930	± 2640

*Does not include K_t effects

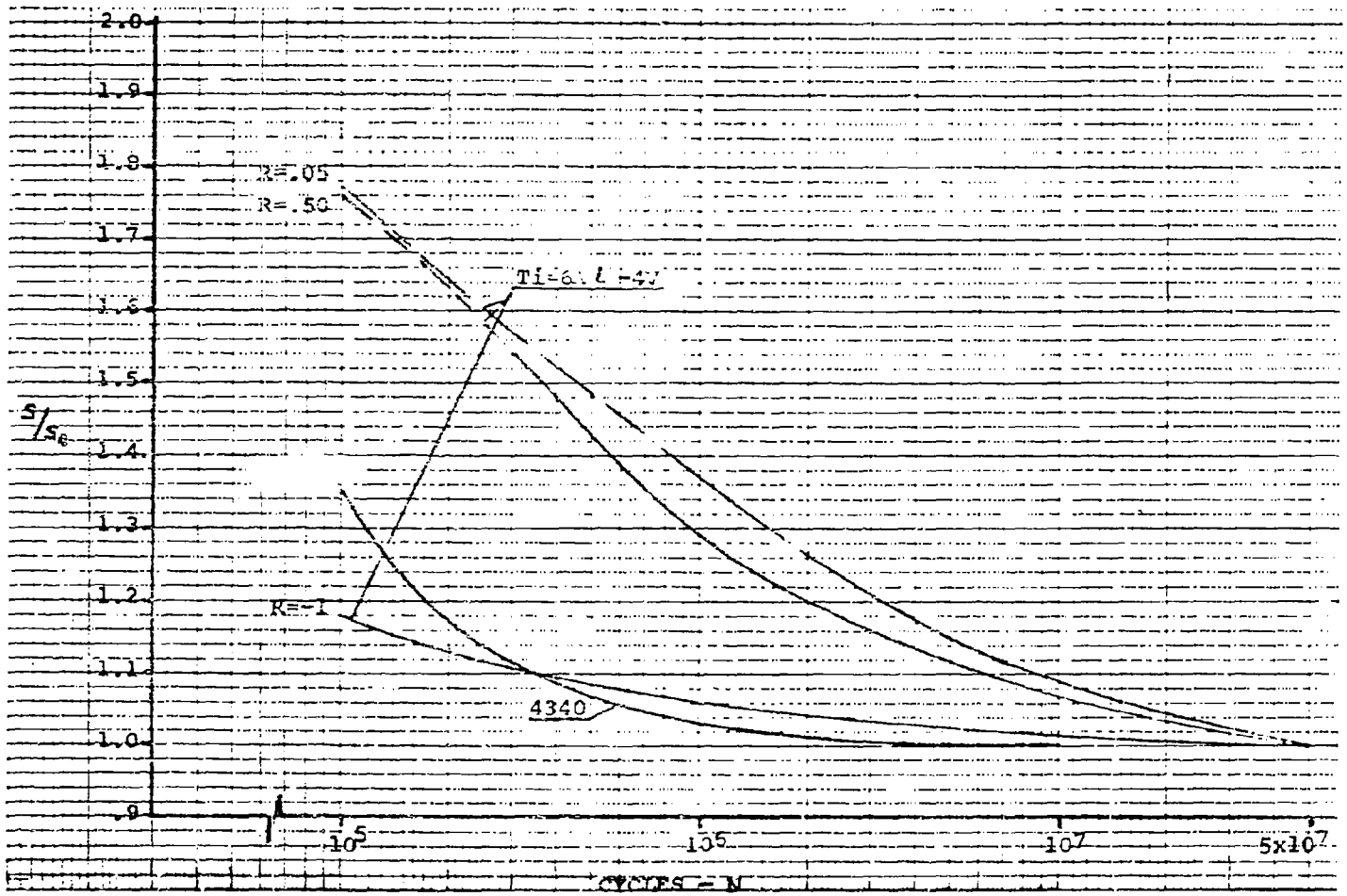

FIGURE 23. S-N CURVES FOR SMOOTH Ti-6Al-4V AND 4340 STEEL, 140 KSI UTS

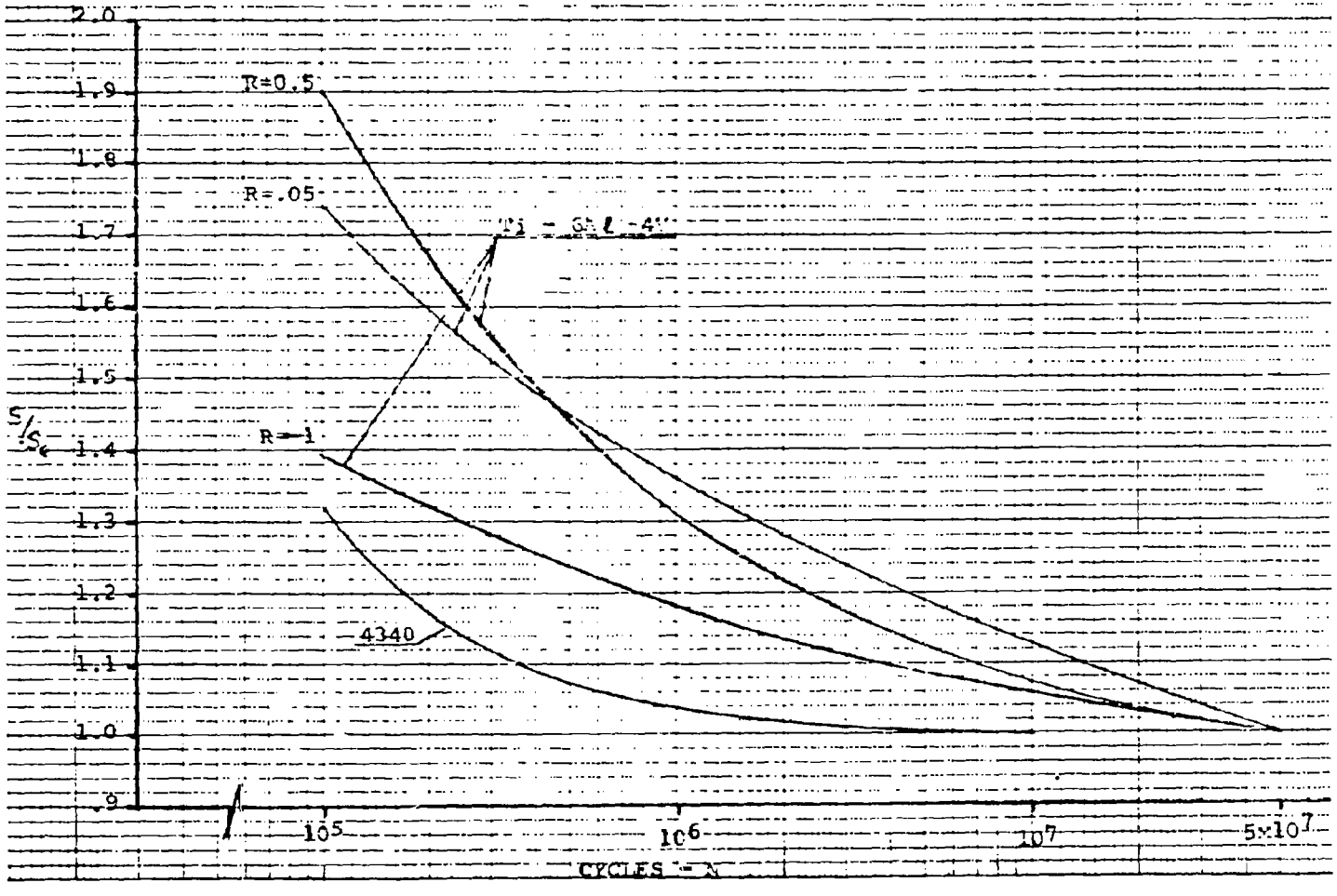

FIGURE 24. S-N CURVES FOR NOTCHED Ti-6Al-4V AND 4340 STEEL, 140 KSI UTS

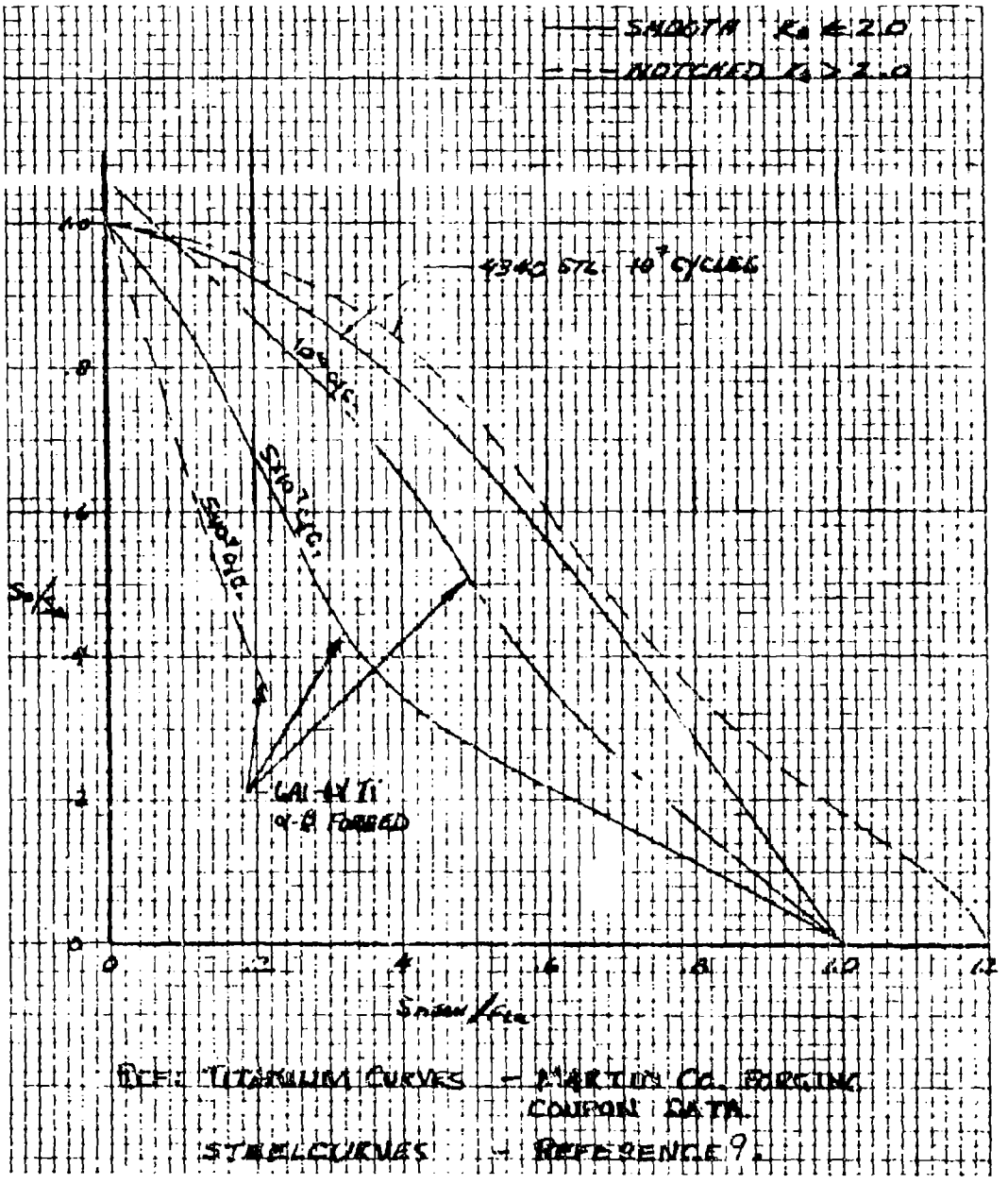

FIGURE 25. GOODMAN DIAGRAM FOR Ti-6Al-4V AND 434 STEEL

3.5 OTHER REQUIREMENTS

Safe-Life

Safe-life is a design philosophy applied to fatigue critical components in which a service life is established and the component is removed from service at or before this interval to preclude catastrophic failures. Fatigue design parameters are specified in Table 6.

Fail-safety

Fail-safety is a design philosophy applied to fatigue critical components in which features are incorporated into the design which will permit the timely detection of fatigue damage or operational deterioration. Flight-critical upper control components and most of the hub components are designed to be fail-safe.

The fail-safe requirements of AR-56 shall be satisfied by failure detection devices, inspection procedures and structural redundancy. See Table 6 for complete criteria.

Ambient Temperature

All components shall be designed for operation at ambient temperatures of -65°F to 160°F. Because of the extremely adverse effect of cold temperatures on the elastomeric bearing spring rates, it is assumed that a bearing warm-up procedure will be followed prior to starting the rotors. This warm-up procedure consists of cycling the collective pitch lever, from 3^{o} to 10^{o}, 30 times. Only a safe-life condition will be considered at -65°F.

Droop Stops

Blade flapping shall be limited by droop and flap stops. Failure of the stops shall not cause a catastrophic failure of the rotor system.

Fretting Protection

To take advantage of the significantly higher allowable fatigue stress for nonfretted (vs. fretted) structures (Reference Section 6.5), all areas of possible metal-to-metal contact, except some bolts and pins, are protected against fretting. The fretting protection originally used throughout the rotor system was a thin (.0005" thick), Teflon base dry film lubricant with the trade name, Sermetel 72. The coating is applied to the bushing outer diameters to protect the lugs. Bolts are not protected against fretting since the curing of Sermetal 72 requires a baking process which relieves compressive residual

TABLE 6. HLH CRITICAL STRUCTURES - SYSTEMS DESCRIPTION AND DESIGN PARAMETERS

CASE	FAIL-SAFE SYSTEM DESCRIPTION			DESIGN PARAMETERS FOR STRUCTURE				
	Failure Detection Device	Structural Redundancy	Ground Inspection	Ult. Factor of Safety on Limit Load: Before Initial Failure	Ult. Factor of Safety on Limit Load: After Initial Failure	Propagation Time from Detection of Initial Failure to Complete Failure (Flight Hours) [A]	Life Req'mt. and Design Fatigue Stress [B]: Before Initial Failure	Life Req'mt. and Design Fatigue Stress [B]: After Initial Failure
1	Onboard with Cockpit Display	Not Required	Not Required	1.5	1.0	Minimum of 10 Hours	MEAN -3 σ ENDURANCE LIMIT 3600-HOUR LIFE	Not Applicable
2	Onboard with No Cockpit Display	Not Required	Ground Inspection of Failure Warning Device at Specified Intervals	1.5	1.0	3 Times the Specified Ground Inspection Interval Min. 30 Hrs.		Not Applicable
3	None	Redundant Load Paths	Ground Inspection at Specified Intervals	1.5	1.0	Not Applicable		Mean -1 σ at 100-Hour Life
4	None	Redundant Load Paths	Retirement at 3600 Flight Hrs.	1.5	1.0	Not Applicable		M -2 σ 3600 Hrs.
5 [A]	None	None	Ground Inspection at Specified Intervals	1.5	1.0	Three Times the Specified Ground Inspection Interval		Not Applicable

[A] Initial failure is defined as the point when a crack is detectable by acceptable field inspection procedures, or a failure warning system. Complete failure is defined as the inability to carry design limit load. (75% TOS loads and mean crack rate data will be used for crack propagation.) With top of scatter flight loads.

[AAA] This system will not be used in component design. It may be required for in-service problems. Rotor Blades shall have a minimum of 200 hours operating life after failure detection with a confidence level of mean -2 σ.

stresses under the bold head and reduces its fatigue strength. Sermetal 72 was chosen as a result of fretted coupon testing reported in Reference 2. Subsequent full-scale component testing indicated that Sermetel was not a suitable fretting inhibitor for the pressures experienced in the HLH rotor head components. The section describing the rotor hub developments discusses other fretting inhibitors used. All critical stress locations with the exception of bolt surfaces are to be protected against fretting. A coating or liner will be used for this purpose.

3.6 LOADS AND ANALYSIS

Top-of-scatter loads have been used in design. For those components which would be identical on both rotors, the higher of forward or aft rotor loads, or the most conservative combination of both, was used. The derivation of fatigue design loads is shown in Appendix B of References 8 and 9.

3.6.1 Rotor Hub Loads and Analysis

The rotor hub was analyzed to determine fatigue life and ultimate strength using the loads in Figures 26, 27, 28, and 29. Figure 30 defines the loads used for the pitch housing stress analysis. The structural analysis is reported in Reference 8. Table 7 lists the minimum margins of safety from this analysis.

3.6.2 Control Loads and Analysis

All upper control loadings are based on pitch link loads, either directly, as in the case of the pitch links and swashplate, or as the result of some kinematic derivation, as for the drive scissors and actuator attachments on the stationary swashplate. The steady and alternating components are listed in Table 8.

In these derivations, where loading by all four pitch links is involved, it is necessary that suitably phased pitch link loads be applied. For this purpose, the pitch link waveform shown in Figure 31 has been selected for design. It is a computed waveform appropriate to high-speed level flight at 1.15 V_H with the rotor blade stalled. This form is used in all analyses with the mean and alternating values modified as required.

The structural analysis of the controls is reported in Reference 9. Table 9 lists the minimum margins of safety from this analysis.

GW: 46,000 LB
CG: 30 IN FWD
A/S: 150 K
LEVEL FLIGHT, 1g

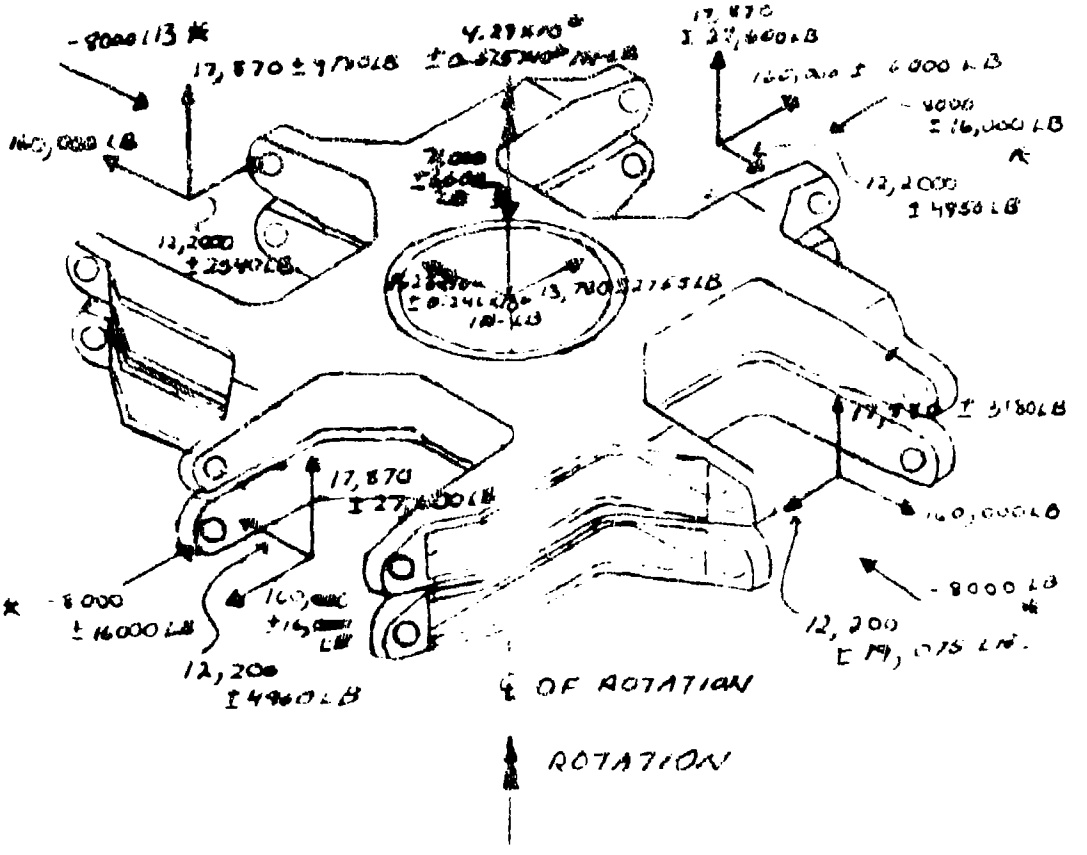

LOADS ARE SHOWN AS APPLIED TO CROSSBEAM AND REACTED BY THE ROTOR SHAFT.

* LAG DAMPER LOADS

FIGURE 26. HUB FATIGUE LOADS AT STATION 26, SAFE-LIFE, MEAN MINUS 3σ

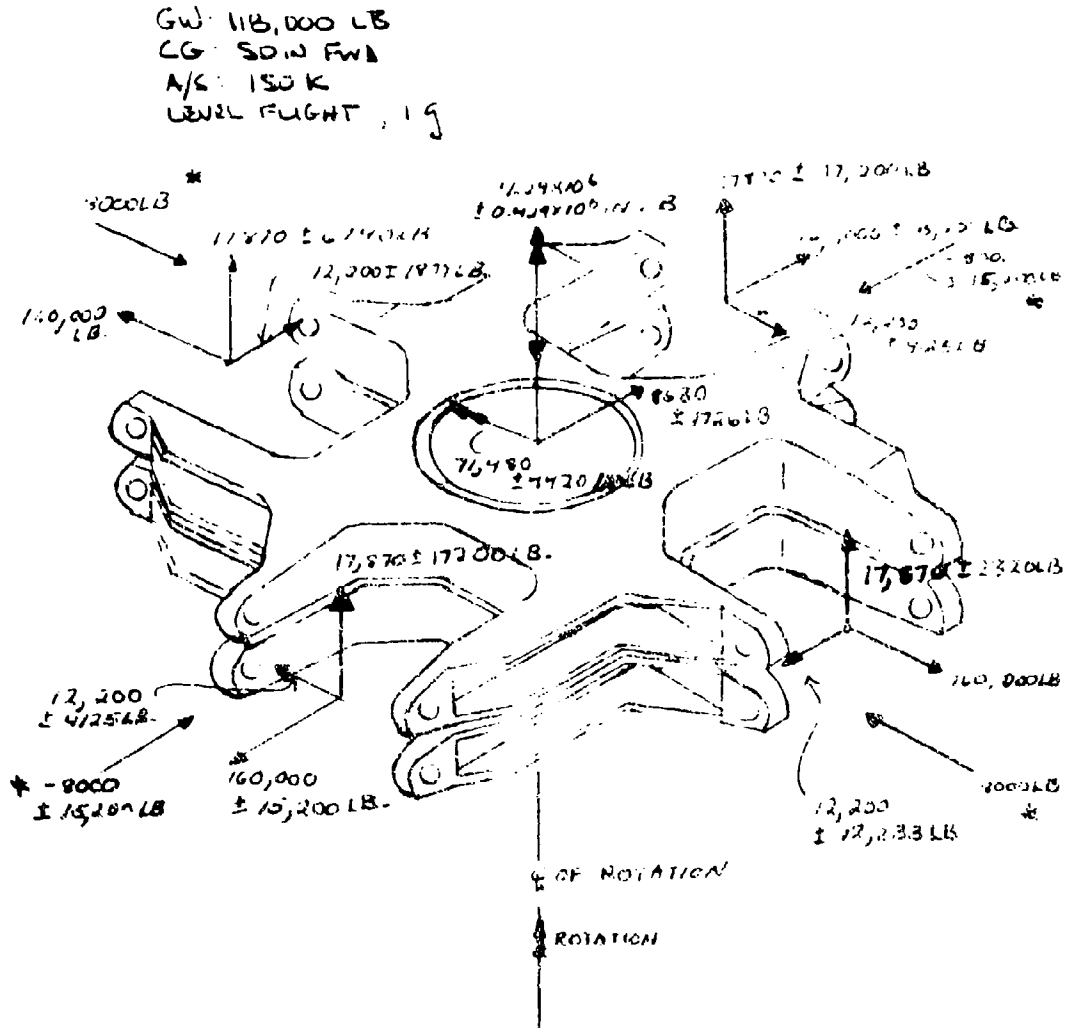

LOADS ARE SHOWN AS APPLIED TO CROSSBEAM AND REACTED BY THE ROTOR SHAFT.

* LAG DAMPER LOADS

FIGURE 27. HUB FATIGUE LOADS AT STATION 26, FAIL-SAFE, MEAN MINUS 3σ

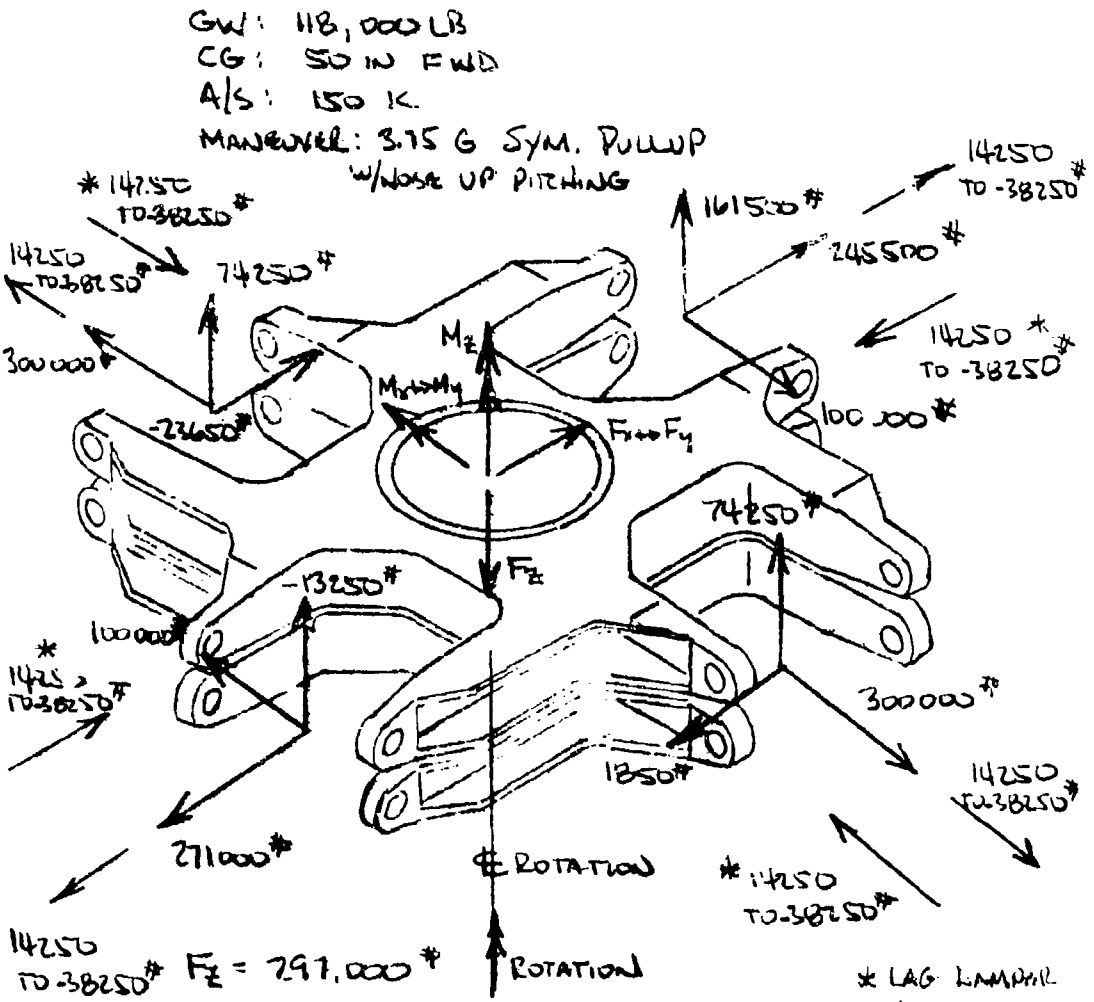

FIGURE 28. HUB ULTIMATE LOADS AT STATION 26, POWER ON

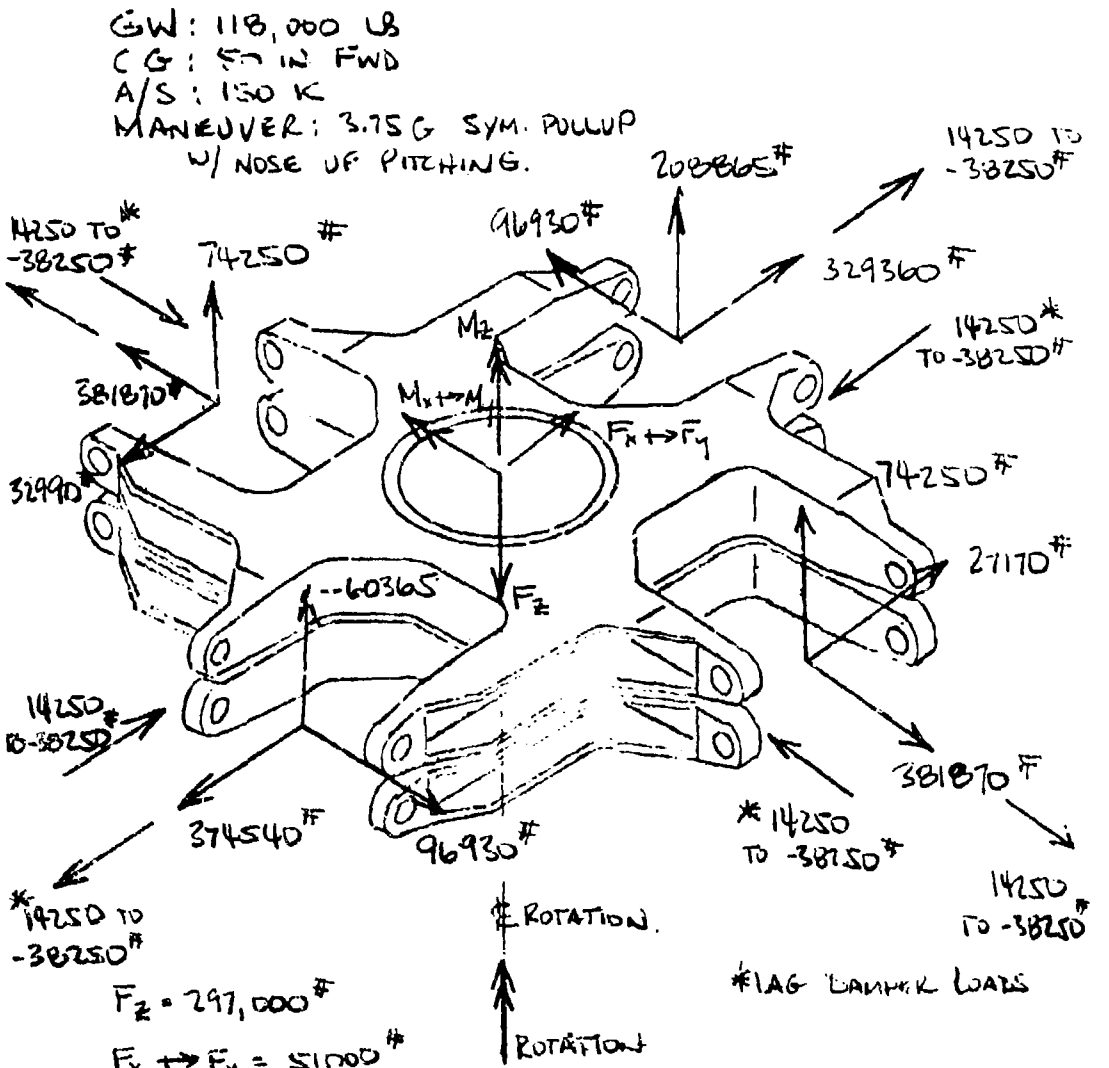

FIGURE 29. HUB ULTIMATE LOADS AT STATION 26, POWER OFF

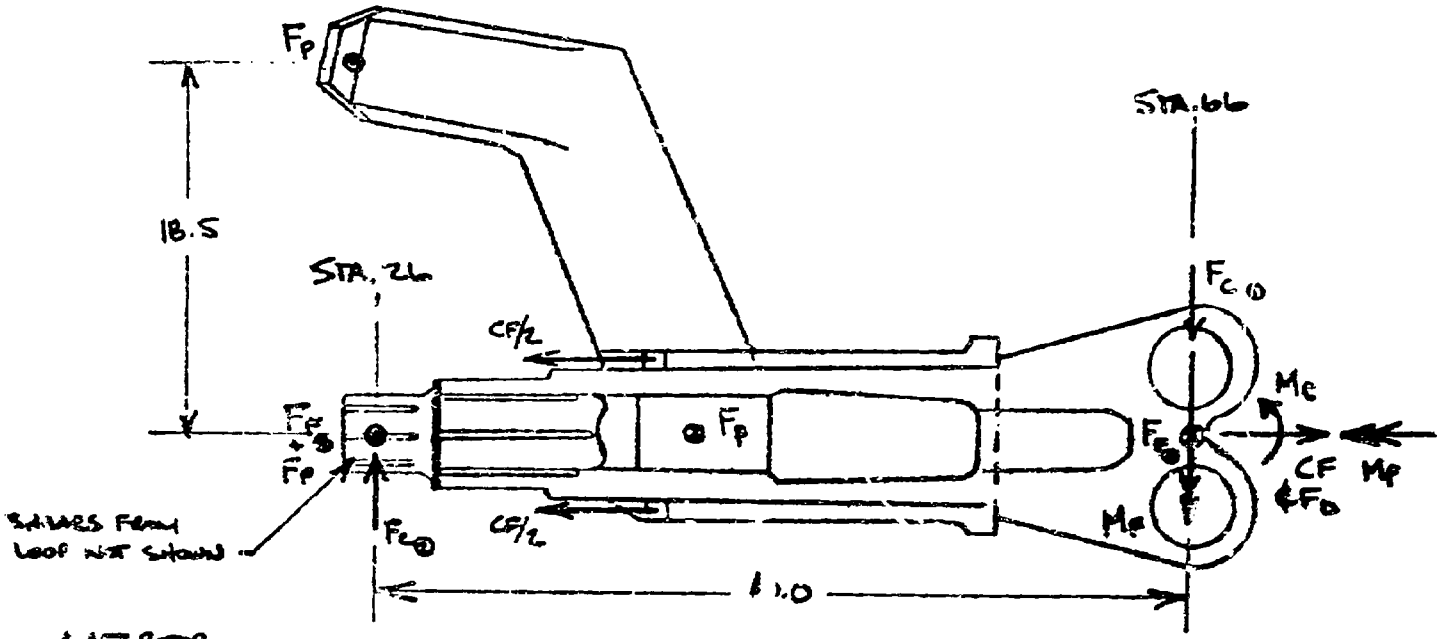

* AFT ROTOR

CONDITION	CF	FD	MF	Mc	Mp *	Fc	Fc	Fp *
SAFE LIFE FATIGUE	168000	-8000 ±16000	40000 ±100,000	50000 ±71000	71000 ±71000	400 ① 1600 ② ± 2500	340 ① 2160 ② ± 1850	4170 ±4170
FAIL SAFE FATIGUE	168000	-8000 ±15200	40000 ±65000	51000 ±46000	48400 ±43400	1000 ① 1600 ② ± 1625	1250 ① 2160 ② ± 1150	2620 ±2620
LIMIT	241,500	9500	240000	278,000	309,875	5012 ① 8018 ②	4675 ① 9225 ②	16750

FIGURE 30 BLADE LOADS AT STATION 66

TABLE 7. MINIMUM MARGINS OF SAFETY - HLH ROTOR HUB

COMPONENT	SAFE-LIFE				FAIL-SAFE			
	FATIGUE	PG.	ULTIMATE	PG.	FATIGUE	PG.	LIMIT	PG.
Hub (Lug)	1.5	36	2.03	37	0	39	1.10	51
Crossbeam	4.29	57	4.44	58	.03	60	.30	63
Pitch Housing (Blade Lugs)	.12	67						
(Pitch Link Lugs)							.72	109
(Loop Lugs)					.18	103		
(Shear Shaft)			.11	97				
Inbd Damper Bracket	.13	132	.64	136	N/A		N/A	
Outbd Damper Bracket	.56	146	.12	150	N/A		N/A	
Hub/Crossbeam Pins	.92	154	.22	155	.30	158	0	159
Hub Nut	.60	166	.32	167	N/A		N/A	
Blade Attach. Pins	0	175	.44	180	3.4	184	.02	188
Loop Attach. Pins	.45	193	.17	193	.05	197	.43	198

NOTE: MS=0 indicates a Safe-Life of 3600 hours or a Fail-safe Life of 100 hours.

PG = page number, Reference 8

TABLE 8. HLH/ATC PITCH LINK LOADS

118,000 LB. GROSS WEIGHT

Condition	% Occur.*	Forward Rotor	Aft Rotor
Ground Conditions	1.0	-410 ± 1,220	-330 ± 1,000
Takeoff	(400)	-530 ± 1,600	-430 ± 1,300
Steady Hovering	30.0	-530 ± 1,600	-430 ± 1,300
Turns Hovering	(2,000)	-610 ± 1,840	-500 ± 1,500
Hover Control Reversals	(2,000)	-610 ± 1,840	-500 ± 1,500
Sideward Flight	2.0	-1,100 ± 3,300	-900 ± 2,700
Rearward Flight	1.0	-1,100 ± 3,300	-900 ± 2,700
Landing Approach	(765)	-1,100 ± 3,300	-900 ± 2,700
Forward Flight			
20% V_H	5.0	-1,070 ± 3,200	-900 ± 2,650
40% V_H	2.0	-1,080 ± 3,230	-900 ± 2,700
50% V_H	2.0	-790 ± 2,370	-650 ± 1,950
60% V_H	5.0	-620 ± 1,850	-500 ± 1,500
70% V_H	8.0	-670 ± 2,000	-530 ± 1,600
80% V_H	9.0	-830 ± 2500	-660 ± 2,000
90% V_H	16.8	-1,070 ± 3,270	-860 ± 2600
V_H	1.0	-1,370 ± 4,100	-1,115 ± 3,350
115% V_H	1.0	-1,900 ± 5,700	-1,570 ± 4,700
Climb, T.O. Power	3.0	-610 ± 1,840	-500 ± 1,500
Climb, Full Power	4.0	-610 ± 1,840	-500 ± 1,500
Partial Power Descent	(500)	-820 ± 2,540	-660 ± 2,000
Turns	5.2	-1,570 ± 4,700	-1,290 ± 3860
	(1,000)	-6,120 ± 6,120	-5,000 ± 5000
Control Reversals	(815)	-6,120 ± 6,120	-5,000 ± 5,000
Pull Up	(270)	-8,200 ± 8,200	-6,700 ± 6,700
Power to Autorotation	(60)	-1,370 ± 4,100	-1,115 ± 3,350
Autorotation to Power	(60)	-4,900 ± 4,900	-4,000 ± 4,000
Steady Autorotation	1.1	-1020 ± 3,060	-830 ± 2,500
Autorotation Turns	0.4	-1,570 ± 4,700	-1,290 ± 3860
	(160)	-5,730 ± 5,730	-5,000 ± 5,000
Autorotation Control Rev.	(40)	-5,730 ± 5,730	-5,000 ± 5,000
Autorotation Landing	(40)	-3,300 ± 3,300	-2,700 ± 2,700
Autorotation Pull Up	(40)	-8,200 ± 8,200	-6700 ± 6,700
Ground-Air-Ground	(100)	-5,710 ± 5,710	-4,670 ± 4,670
Power Dive	2.5	-1,920 ± 5,750	-1,570 ± 4,700

*Bracketed numbers are occurrences per 100 flight hours.

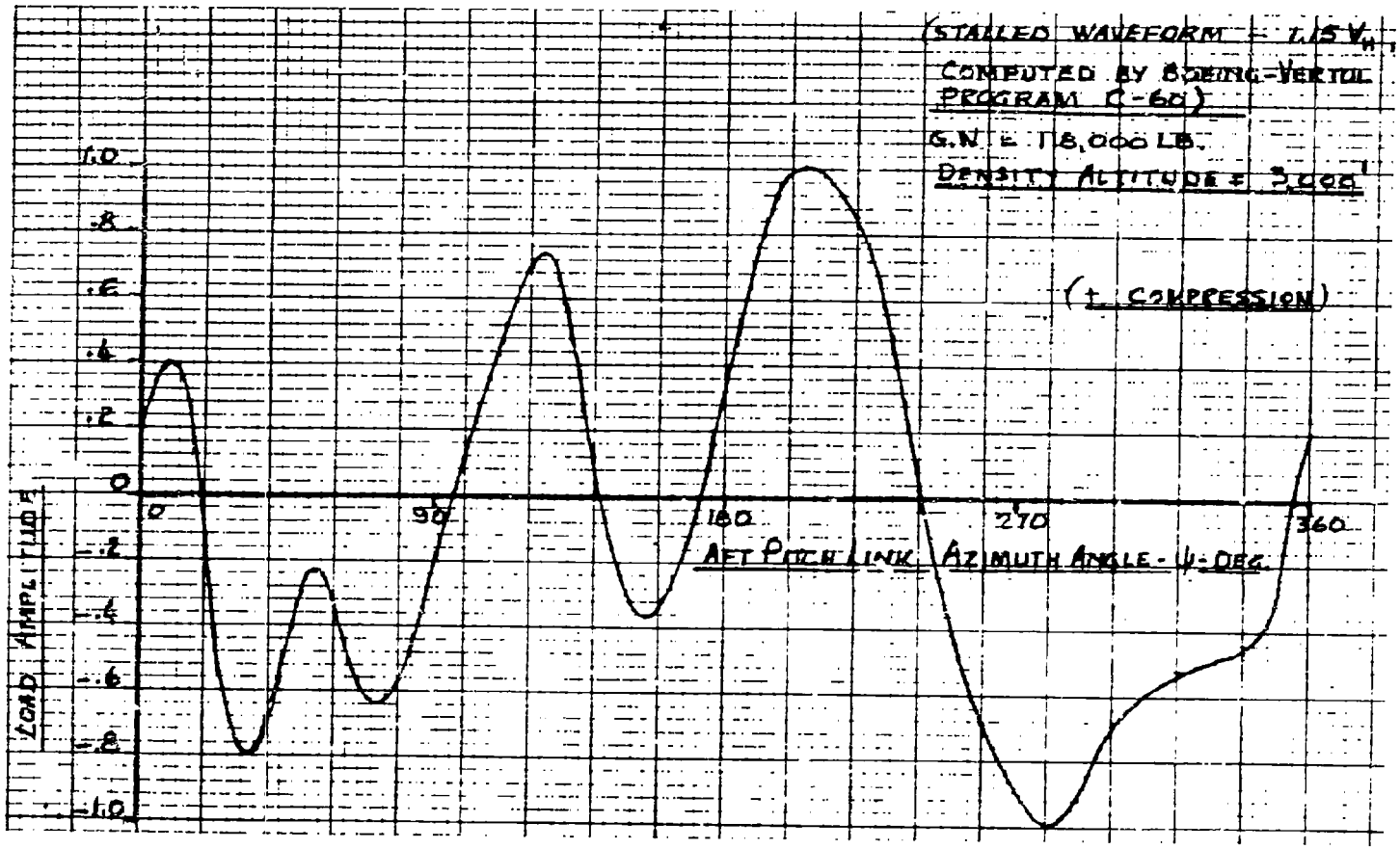

FIGURE 31. MODEL 301 PITCH LINK LOAD WAVEFORM

TABLE 9. MINIMUM MARGINS OF SAFETY - HLH UPPER CONTROLS

COMPONENT	MARGIN OF SAFETY							
	SAFE LIFE				FAIL-SAFE			
	Fatigue		Ultimate		Fatigue		Ultimate	
	M.S.	p.	M.S.	p.	M.S.	p.	M.S.	p.
Pitch Link	+ .07	87	+ .23	91	+ .01	107	0	113
Pitch Link Bolt	+ .22	88	+ .94	94	0	109	+ .07	113
Swashplate:								
Rotating Ring	+ .03	122	+ .14	149	+ .03	158	+ .02	165
Stationary Ring	+ .28	179	+1.52	181	+1.19	182	+1.38	188
Stationary Scissors:								
Bolt, Transmission Cover Attachment	+ .17	190	+ .09	210				
Lower Arm	+ .08	197	0	212				
Bolt, Lower-to-Upper Arm Attach.	+ .80	198	+ .35	216				
Upper Arm	0	201	+ .03	221				
Rod End, Swashplate Attachment	+ .02	206	+ .06	222				
Fitting, Swashplate Attachment	+ .14	208	+1.58	223				
Centering Scissors:								
Bolt, Drive Collar Attachment	+ .69	226	+ .63	241	+ .85	252	+ .53	257
Upper Arm	+ .37	231	+ .41	243	+ .27	254	+ .31	258
Bolt, Lower-to-Upper Arm Attachment	+ .92	234	+ .13	247	+1.16	254	+ .05	260
Lower Arm	+1.77	238	+1.32	248	+2.17	255	+1.14	260
Bolt, Swashplate Attachment	+1.3	240	+1.44	251	+1.33	256	+1.29	260
Drive Collar	+ .66	267	+ .09	269	+ .92	271	+ .16	272

p. = page number, Reference 9

4.0 COMPONENT DEVELOPMENT

The development of each hub and upper control component is discussed in this section; the configuration, the function, the construction, and the tests performed are considered. The assembly and installation drawings are shown in Figures 20, 21, and 22.

Certain features of several components are common and are described here, and they apply unless excepted in the description. For example, all titanium components are made from 6Al-4V titanium alloy in the solution-treated overaged condition. Parts were stress relieved after rough machining, and fatigue critical parts were shot peened after final machining. The Titanium Materials Tests showed that shot peening does not conclusively increase the fatigue strength. Shot peening is done to nullify surface damage occurring during machining that would initiate failures. All fastener holes, in both titanium and aluminum parts, that are assembly points were bushed with 17-4PH corrosion-resistant steel. Attachment hardware, where size permitted, was standard low alloy steel. Hardware contacting titanium parts were corrosion resistant steel to avoid cadmium plating in contact. Initially, all bushings were coated with Sermetel 72, an inorganically bonded fluorocarbon containing molybdenum disulfide, as a fretting inhibitor. Changes to the fretting inhibitor utilized are described in the following sections. Fasteners larger than standard hardware were fabricated from 15-5PH corrosion resistant steel. This alloy was chosen because of the lower occurrence of inclusions. Reference 10 presents the details of the fabrication of the hardware. Parts were fabricated for the complete demonstration rotor which was operated on the whirl tower and DSTR. Additional parts were fabricated for those items tested as components, and for spares.

4.1 HUB AND CROSSBEAM

The hub consists of two identical plates with four clevises each. The center body is splined to fit the rotor shaft. The outer end of each clevis is bored for pins which attach the crossbeam. The bushings in the hub clevises were machined to final inside diameter and the flanges machined to a specified dimension between the flanges. The titanium crossbeam configuration is a ring with four bosses which fit into the hub clevis. Bushings are installed in these bosses in a similar manner to those in the hub lugs. The diametral fit of the pins and the distance between flanges provide for interchangeability. The shear bearing is located in the inner diameter of the crossbeam ring and the elastomeric bearing is attached to the inboard face. The four shear pins connecting each crossbeam in

the clevis were retained by preload indicating bolts. These bolts had a small transparent cover on the head with a fluid inside the hollow shank. The appearance of the window changed when the specified tension was applied to the bolt.

The principal test of the hub and crossbeam was the fatigue test reported in Reference 11, which is summarized in Table 10. The first test revealed that Sermetel 72 was not an adequate fretting inhibitor. The second test specimen was fitted with separate sleeve bushings, and washers in place of the flanges. Some bushings were covered with a Teflon Dacron fabric, which has been used successfully; other bushings were covered with EP 15/FM1000, a Nylon epoxy adhesive on a Nylon carrier cloth. An aluminum bronze washer contacted each hub lug and crossbeam boss Between the pairs of bronze washers were a pair of corrosion resistant steel washers, with tungsten carbide on the sides that contacted each other. When loaded for the fatigue test, the loads in the various joints varied widely. It was concluded that the relative softness of the inhibitor materials was the reason, and they were abandoned.

The specimen was rebuilt with sleeve bushings of wrought aluminum bronze. A pair of washers at each joint were coated with plasma sprayed aluminum bronze with Ekonol on the side against the titanium, and tungsten carbide on the side against the other washer. Failure of the heads of the shear pins caused the pins to be redesigned from a semi-hollow head in which the securing bolt was recessed to a solid head. The bushing configuration reverted to a flanged design. Sermetel 72 was applied to the cylindrical part of the bushing because failures in the first test did not originate here. The underside of the flange was coated with aluminum bronze-Ekonol because it had performed well on the washers of the previous configuration. This configuration was subject to endurance testing (flight loads) and one bushing, was removed and examined. No damage to the titanium was seen, and the fatigue test was performed. It terminated with failure of two hub lugs. Failure due to fretting initiated at the edge of the cylindrical surface of the bushing and the undercut at the shoulder.

A third specimen was assembled with aluminum bronze-Ekonol on all surfaces of bushings which contacted titanium because this material performed the best of the inhibitor materials used thus far. The shear pin was also coated with this material because some distress had been seen on the pins at the shear line of the two bushings. This specimen underwent endurance loading examination of bushing contact surfaces and fatigue test. Failure in this test occurred in a crossbeam loss due to fretting which had occurred in a previous test.

TABLE 10. STRUCTURAL TEST SUMMARY
HLH HUB AND CROSSBEAM

TEST NO.	SPECIMEN NUMBER	LOADING	RESULTS	CONCLUSIONS
1	Hub #1 Crossbeam #1	Fatigue Endurance Limit	• Fatigue cracks in all crossbeam bosses and in lower lag hub lug. • Cracks originate from fretting under bushing flanges.	SAFE FATIGUE LIFE Demonstrated 2645-hour safe-life for Hub and Crossbeam Assembly. FAILSAFETY • Demonstrated limit load capability with one hub lug failed. • Demonstrated ten hours at V_H level flight load. FRETTING • Aluminum-Bronze-Ekonol coating eliminates fretting at flight loads.
		Failsafe	• Equivalent to 10.68 hours of V_H level flight load. • Load sustained without further propagation of fatigue crack on outboard side of hub	
		Limit	• Complete lug failure simulated by removal of lower lag pin. • Limit load sustained without further damage.	
2	Hub #2 Crossbeam #2	Fatigue	• Shear pin failure identified redesign requirement. • High fatigue loads cause excessive fretting. • Fatigue cracks caused separation of both lower hub lugs	
		Endurance Abreviated Flight Spectrum Loads	• Sermetol not effective fretting inhibitor. • AL-BR-Ek coating on O.D. of bushings and pin eliminated fretting.	
3	Hub #3 Crossbeam #3	Fatigue	• Fatigue cracks in lower lead crossbeam boss. • Origin - Fretting damage incurred during Test No. 2.	
		Endurance Abreviated Flight Spectrum Loads	• Bushings worn but no fretting with AL-BR-EK coating.	

Testing concluded that

- Fatigue testing of the 301-11168 hub and 301-11280-3 crossbeam substantiates a safe life of 2645 hours for the HLH. This is a conservative safe life because the failures were induced by fretting at the endurance limit fatigue test load levels which were substantially higher than flight loads.

- Aluminum bronze-Ekonol is the best fretting inhibitor for this hub and crossbeam configuration. This was demonstrated by an endurance test where 258 hours of flight load were applied to the specimen without deteriorating the fretting inhibitor.

- The ability to carry limit load with one lug failed has been demonstrated.

- The hub-crossbeam configuration is satisfactory for flight on the HLH prototype helicopter. The prototype crossbeam would have increased boss diameter, committed after the first test.

4.2 SHEAR BEARING

The shear bearing, secured in the crossbeam, locates the inboard end of the pitch housing and transmits loads perpendicular to the blade axis to the hub. The bearing permits motion about 3 axes; lead-lag and flap rotates the ball in the outer race: pitch rotation occurs in the cylindrical bore in the ball. The 440C corrosion resistant steel outer race was machined to finished size, then fractured into halves. The inside of this race is lined with Teflon-Dacron fabric. The ball, machined from the same steel alloy has a cylindrical bore which is also lined with the same fabric.

Endurance tests were conducted on three specimens,which is reported in Reference 12. . The bearing was subjected to steady plus alternating radial loads while being moved about 3 axes representative of its application in flight. The environments in which the bearing was tested include normal and elevated ambient temperatures and sand and dust. The loading is shown in Table 11 and the results in Table 12. Figure 32 shows a liner which has completed testing.

TABLE 11. LOAD AND MOTION SCHEDULE - SHEAR BEARING TEST

Load Lbs.	Misalignment		Rotation	Cyclic	%
	Flap/Droop	Lead/Lag	Pitch	Rate(RPM)	Time
4249 ± 4511	±5°	±1.5°	±11°	156	88.46
4854 ± 7607	±5°	±1.5°	±11°	156	11.536

TABLE 12. ROTOR HUB SHEAR BEARING SPECIMEN SUMMARY

Spec No.	Cumulative Hours Run	Test Hours	Test Condition	Wear In/Hr	Initial Wear-In Inches
3	0 to 301	301	Clear at 193 RPM Fan on 600 Ft/Sec	15.4×10^{-6}	.0068
	301 to 1205	904	Clear at 156 RPM		
	301 to 1205		Fan on 600 ft/sec	7.5×10^{-6}	
1	0 to 200	200	Sand & Dust at 156 RPM	13.7×10^{-6}	.0039
	200 to 427	227	Clear Fan on 600 Ft/Sec 156 RPM	4.21×10^{-6}	
	427 to 557	130	High Temp no Fan 156 RPM	12.7×10^{-6}	
2	0 to 402	402	Clear at 156 RPM Fan on 600 Ft/Sec	6.25×10^{-6}	.0058

The testing concluded that:

- Using average wear rates and initial wear-in, the HLH rotor hub shear bearing can be expected to exceed its required life of 1200 hours by a considerable margin.
- Initial wear-in is not related to initial tightness, measured by friction torque, based on only two relatively loose and one relatively tight bearings.
- Operation at elevated temperature will increase the wear rate.
- It is not necessary to protect the bearing from sand and dust.

FIGURE 32. SERIAL NO. 3 LINER WEAR AFTER 1,290 HOURS OF ENDURANCE TESTING

4.3 PITCH HOUSING

The titanium pitch housing secures the blade at its outboard end and transmits the blade centrifugal force to the loop through lugs near the inboard end. Blade shear loads are reacted at the shear bearing. An arm on the leading edge is connected to the swashplate for pitch control of the blade. The center body and pitch arm form a hollow chamber which is evacuated. Passages through the radial ribs and the inboard shaft are also connected to the evacuated center body. A crack into the evacuated volume will cause the pressure to rise. This condition is signaled by a visual indicator on the end of the pitch arm. Corrosion-resistant steel sleeves are interference fitted on the two inboard shaft diameters so that the droop stop ring and the shear bearing do not operate on the titanium.

Fatigue tests were conducted on two areas of the pitch housing: the blade attachment lugs and the pitch arm. These tests are reported in References 13 and 14, respectively. For the blade attachment lug test, the specimen was installed in the fatigue test fixture at an angle of 45° such that equal flap and chord moments could be applied with a single loading as shown in Figure 33. The load levels were as shown in Table 13 and three lugs were failed in the number of cycles shown.

A defect was deliberately introduced by an arc burn on the bottom trailing edge rib of the second specimen. After a total of 1.0×10^6 cycles had been applied, this arc burn did not induce a crack. Using a circular saw, a cut was then made through the arc burn to a depth of .25 inch. This was subsequently increased in size to .62 inch to activate the delta pressure crack detection system. This saw cut did not propagate until a total of 1.394×10^6 cycles. The specimen was then fatigued to the loads and cycles representing the flight spectrum. The specimen was then subjected to a static limit load of simulated centrifugal force and a bending moment.

The analysis of the test results for the blade attachment lugs indicate that they successfully demonstrate the safe life and fail-safe life requirements. The fail-safe criterion requires 3600 hours safe life and 100 hours of operation following an initial lug failure. Calculated lives for this joint are 4445 hours safe life and 116 hours in fail-safe operation. The fail-safety of the rib section was demonstrated in excess of 30 hours. In addition it was shown that a significant flaw, in the form of a saw cut, could be tolerated for relatively long periods with no crack initiation.

The same two pitch housing specimens were used for the pitch arm test. The loads were applied to the pitch link clevis with an instrumented link as shown in Figure 34 .

FIGURE 33. PITCH HOUSING FATIGUE TEST - BLADE LUGS

TABLE 13. FATIGUE SUMMARY - PITCH HOUSING - SPECIMEN NO. 1

TEST RUN REF. NO.	CF LOADS LBS	BENDING STEADY	MOMENT - IN.LB ± ALTERNATING	CYCLES x10^6	REMARKS
8	170,000	40,000	212,000	3.536	Load rate 5 CPS to .639x10^6 CY, 10 CPS to 3.536x10^6 CY. Failure of L.E. top lug. Failed lug cut off for the next test.
9	170,000	70,000	210,000	.7026	Load rate 5 CPS. Failure T.E. bottom lug. Crack extended .62 IN. from bushing.
9 cont'd	170,000	70,000	210,000	.0015	Test continued as in No.9 to complete fracture of T.E.bottom lug.
10	128,900	216,000*	210,000	.1785 to .2145	Load rate 5 CPS failure of L.E. bottom lug between .1785 x10^6 and .2145x10^6 cycles.

*T.E. bottom lug in compression,all others opposite

FIGURE 34. PITCH ARM FATIGUE TEST

The first specimen failed after 0.401 million cycles at the initial load level of +7600 ±7600 lbs. The calculated mean endurance limit is 5120 lbs and the (M-3σ) endurance limit is 3490 lbs, using a coefficient of variation of 12 percent. This results in a calculated safe life of 850 hours on the aft pitch arm. The failure occurred where the pitch link clevis intersected the unsupported pitch arm cylinder. No positive failure indication by the crack detection system was observed. The pitch housing was determined to be structurally deficient at the failure location and was redesigned for the prototype aircraft.

An initial photoelastic coating investigation was conducted on the second specimen pitch arm, prior to the modification, to determine the strain distribution and areas of strain concentration. Data was obtained at static load levels of ±7600 and ±15,200 lbs applied at the pitch arm lug. Isochromatic photographs were obtained at these load levels for documentation and subsequent reference. Strain gage rosettes were installed at the critical strain areas, to evaluate the minimum and maximum principal stresses, maximum shearing stress and the principal stress direction at each point. A corrosion resistant steel reinforcing sleeve was installed in the outer end of the pitch arm. This procedure was basically repeated on the modified pitch arm P/N SK301-11745, to assess any changes in the high strain areas. The strain gage rosettes were only used to evaluate the maximum and minimum principal strains.

The pitch arm was then subjected to sinusoidal load inputs according to the test conditions and loading sequence shown in Table 14. The loads were monitored as in the case of the first specimen. At the completion of the safe-life testing, a crack was induced at the base of the arm, at the location shown in Figure 35. The crack growth was measured with a scale using the dye penetrant method to permit visual inspection. After the completion of the crack growth testing, the limit load was applied.

The modified pitch arm completed 5 million cycles at the design endurance limit load without incident. This substantiated a safe life of greater than 3600 hours for the lug area and the base of the arm. The surface crack was 0.95 inch long at the surface at the indication of the vacuum detection system. The load spectrum tests (Table 14, runs 4 through 18), equivalent to 30 hours of flight, produced an additional 0.02 inch of crack growth, and the pitch arm sustained the limit load application without further crack growth. The required 30 hours of fail-safe operation had been demonstrated for the arm to barrel junction but the margin beyond this could not be reliably estimated. The test schedule permitted additional testing to be accomplished, and the following tests beyond the contract and test plan requirements were performed.

TABLE 14. HLH/ATC - PITCH ARM FATIGUE TEST RESULTS

SPEC NO.	RUN NO.	SIMULATED PITCH LINK LOAD - LBS	TEST FREQ Hz	TEST CYCLES	CRACK LENGTH IN.	REMARKS
1	1	+7600±7600	5	0.401×10^6	-	Failure at junction of pitch link attach & barrel sect. Figure 35
2	1	+7600±7600	5	5×10^6	-	Pitch arm modified per SK301-11745
	2	+8890±7280	6	168000	-	Crack propagation - slot cut in arm
	3	+6280±5160	6	2000	-	Intermediate crack propagation
	4	+2350±3520	6	123600	0.95	Loss of vacuum indication
	5	+2350±3520	12	4500		
	6	+ 650± 975	12	22500		
	7	+1350±2020	12	41500		
	8	+4000±1500	12	13500		
	9	+ 800±1200	12	27000		
	10	+1930±2900	12	9000		
	11	+ 650± 975	12	22500	0.95	
	12 thru 18	-	12	140500	0.97	Repeat of runs 5 thru 11
	19	+16750	-	-	0.97	Limit Load
	20	±5500±5000	12	20000	1.24	Increase crack growth
	21	±2350±3520	12	22900	1.34	Reduce crack growth
	22 thru 35	-	20	295000	1.40	Repeat of runs 5 thru 18
	36	+16750	-	-	1.40	Limit Load
2	37	+7030±7030	9	2×10^6	1.50	Prototype spare limited qual.

NOTE: [1] Positive load is tension in simulated pitch link

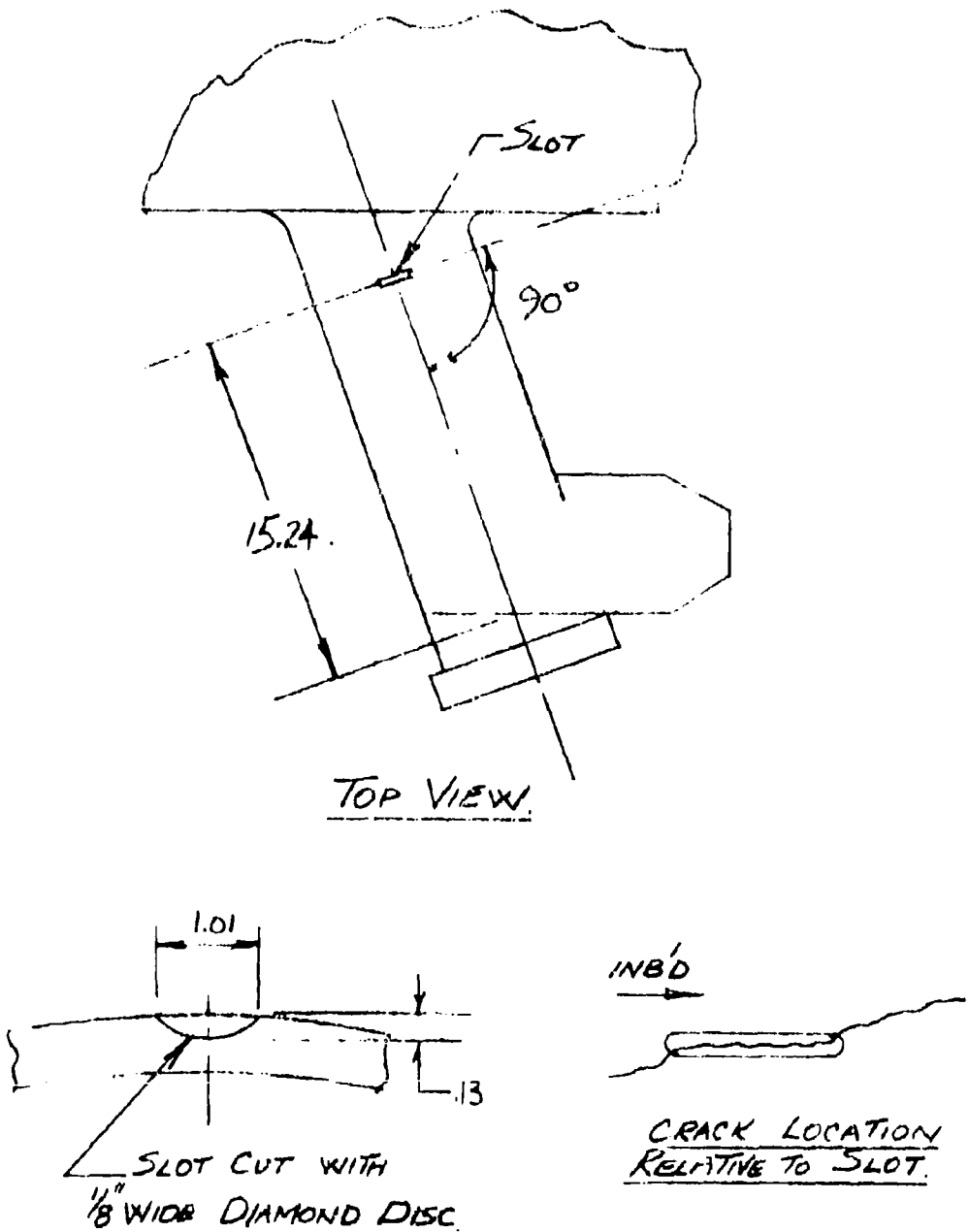

FIGURE 35. HLH/ATC PITCH ARM FATIGUE TEST - SLOT AND CRACK LOCATION

The pitch arm was loaded at +5500 ±5000 lbs for 20,000 cycles producing a crack growth to 1.24 inches. The pitch arm was then loaded at +2350 ±3520 lbs for 22,900 cyles with a crack growth to 1.34 inches. A repeat of the 30 hour equivalent load spectrum (Table 14), runs 22 through 35) produced an additional crack growth of 0.06 inch. After completion of the load spectrum, limit load was applied without incident. The final crack configuration is shown in Figure 35. This test demonstrates a safe-life capability of at least 60 hours, twice the requirement.

The fatigue test of the modified pitch arm assembly has shown that:

- The safe life of the pitch link lugs and the base of the pitch arm is greater than 3600 hours.
- The vacuum crack detection system is capable of indicating a failure, such that the required minimum of 30 hours of flight, after initial indication can be achieved.
- The safe life of the modified ATC configuration pitch housing, limited by the pitch link lug to arm area, is greater than 1000 hours.

4.4 LOOP

The loop transfers the blade centrifugal force from the pitch housing to the inboard end of the elastomeric bearing. The loop must also react the side loads and torsion due to deflecting the elastomeric bearing. The trade studies discussed in Section 2 concluded that a two-piece loop was optimum. For fail-safety consideration, the failure of one of the two loop halves would cause considerable bending moment in the loop when carrying the load on the remaining half. The final loop design is in three pieces where the center loop is twice the thickness of each of the outer loops. If the center loop failed, the remaining loading is symmetrical. If one of the outer loops fails, the remaining two accommodate the load with a small eccentricity. Teflon Dacron fabric is inserted between the individual loops and at the arch where the loop bears on the elastomeric bearing to prevent fretting. The arch of the loop is flat, to which Teflon Dacron fabric is bonded. The arch of the loop fits into the clevis of the elastomeric bearing for transmitting the centrifugal force.

Stress analysis reviewed after the loops were fabricated revealed a deficiency in the fatigue life. Additional loops were designed and fabricated with a slightly different contour from 6AL-4V titanium alloy in the Beta solution-treated overaged condition. In this heat treatment, the part is quenched

from a temperature over the Beta transus, rather than below. The original loops were utilized for the rotor whirl test and the initial DSTR operations. When the Beta heat treat loops were available, they were fitted into the DSTR rotor.

The fatigue analysis of the loops proved to be difficult because the reaction loads and moments from the elastomeric bearing were not available. Initial statement of elastomeric bearing spring rates were totally inadequate in view of the substantial hysteresis. The measurements of the elastomeric bearing were made statically, and the reactions can be expected to be different dynamically. The only load measurements of the bearing meaningful for loop analysis must come from the loop reacting the bearing loads because they are both highly dependent on deflections. For some insight into the effect on the loop, strain gages were applied to the loop during the elastomeric bearing static load tests. See Figure 45. A fatigue test was planned for the prototype loops. The test fixture would load the loop and bearing with equivalent rotor head parts duplicating the mounting stiffness, while stresses are measured with various deflections of the elastomeric bearing.

4.5 ELASTOMERIC BEARING

The elastomeric bearing development was carried out by Lord Kinematics, Erie, Pa. The principal items in the development were:

- Titanium shim feasibility
- 8 inch diameter bearing (LM-732-1)
- Preliminary design evaluation
- Static testing
- Endurance testing
- 10-inch-diameter bearing (LM-732-7)
- Static and low temperature dynamic testing
- Endurance testing, including environments

4.5.1 Titanium Shim Feasibility

The objectives of this study were:

- Select material
- Establish manufacturing methods, proce nd controls that can be scaled up for production
- Determine that parts produced conform irements

Three methods of forming shims from 6AL-4 ium alloy sheet were effected: cold forming to size, orming to size, and cold forming followed by hot siz.

The selected method was to cold form in a tool teel female die with a resilient punch, followed by sizing in stainless steel dies at 1,350°F for 10 to 15 minutes, depending on the size of the shim.

The sample parts conformed to dimensional contours and tolerances. Fluorescent penetrant inspection and scanning electron microscope examination confirmed absence of cracks or intergranular failure. The hydrogen content was at acceptable levels.

The study is fully reported in Reference 15.

4.5.2 Eight-Inch Bearing (LM-732-1)

The most significant design requirements for the elastomeric bearing are the operating schedule of motions with centrifugal load for 1500 hours endurance, and the static centrifugal capacity. The design specification, Reference 16 , Revision A, lists the operating schedule for the two rotors. The requirements were based on blade centrifugal force of 150,000 pounds. The test plan, Reference 17, Revision B, lists the test schedule for the forward rotor even though neither rotor is uniquely more severe in motion requirements.

Bearings were produced to the specification except that the first five bearings were made with steel end plates as an expedient resulting from a strike at the titanium forging vendor. While this was being carried out by Lord Kinematics, the increase in blade centrifugal force from 150,000 lbs to 170,000 lbs caused the predicted endurance life to decrease to an unacceptably low level. The development program was redirected to a 10-inch bearing. However,with 8-inch bearings available and the 10-inch bearing just begun, a certain amount of testing was performed to have foreknowledge of probable performance and to apply this to the 10-inch bearing. Endurance testing would also discover any problems in the test machine.

The preliminary design evaluation is reported in Reference 18. The objectives were:

- To determine the static spring rate characteristics of the LM-732-1 in the axial, torsional, radial and cocking (lead-lag or flap) directions
- To verify the capability of the LM-732-1 to support limit and ultimate axial loading
- To perform an experimental stress analysis with strain gages on the shims. No analysis was made of the end plates since the end plate configuration has been changed.
- To verify the suitability of the LM-732-1 bearing for pre-endurance and endurance testing.

Data available includes -

- Load-deflection curves for axial and side (radial) loading and for torsional and cocking rotation with and without axial loading.
- Measured stresses at the edges of 3 shims for axial loading and rotation about the lead-lag axis.

The first static test was performed by Lord Kinematics at Pittsburgh Testing Laboratory. The small end plate (outboard) was cocked 10° relative to the applied load. The axial load deflection curve was linear up to 235,000 pounds, then increasing to the maximum load sustained of 276,000 pounds, where the bearing became unstable. Figure 36 shows the bearing with increased axial deflection, sustaining approximately 170,000 pounds. Note the lateral displacement of the upper and lower loading blocks. An increased axial deflection resulted in a decreasing load until a loud noise occurred with a sharp drop off in load. Partial debonding occurred in the bearing. The bearing was subsequently loaded without cocking of the small end plate up to 200,000 pounds. Failure to sustain the limit load for the higher centrifugal force confirms the need for the 10-inch bearing.

A loading fixture was fabricated to simulate the end conditions of the bearing attachments. The steel simulated loop had the flatwise EI value equal to the titanium loop. The initial test conducted at Swarthmore College resulted in a maximum load of 190,000 pounds at 11°, and 132,000 pounds when repeated. Attempts to further load the bearing resulted in the central shims slipping, laterally, relatively large distances from the center line of the bearing. The first occurrence stretches the elastomer to some permanent set so that the column subsequently becomes unstable at lower loads. This test is reported in Reference 19.

With the 8-inch bearing loaded by representative rotor head parts, showing such poor correlation to predicted capacity, the ability of the 10-inch bearing, being designed by the same methods, to meet requirements was in serious doubt. One item postulated to be responsible was the test fixture. A vertical pin extending from the lower grip fitting of the test machine extending loosely into a hole in the upper frame was to keep the two parts in line by the horizontal shear force acting normal to the pin. See Figure 37. The pin was found to be bent. Vertical misalignment of the two parts induced a moment into the bearing which was a bias in the unstable direction. The test fixture was modified by a more sturdy pin acting in slotted brackets (shown in Figure 44). This configuration of the test fixture was used for all subsequent tests.

Even with the modified fixture, the 8-inch bearing could not meet the static load requirements. More significantly, the bearing performance did not verify the analytical design method. There was doubt that the 10-inch bearing would meet the static requirements. Three additional 8-inch bearings were prepared to explore what might be done to assure that the 10-inch bearing would meet its static requirements:

170,000 LB AT .84-INCH DEFLECTION

FIGURE 36. 8-INCH ELASTOMERIC BEARING DEFLECTION TEST

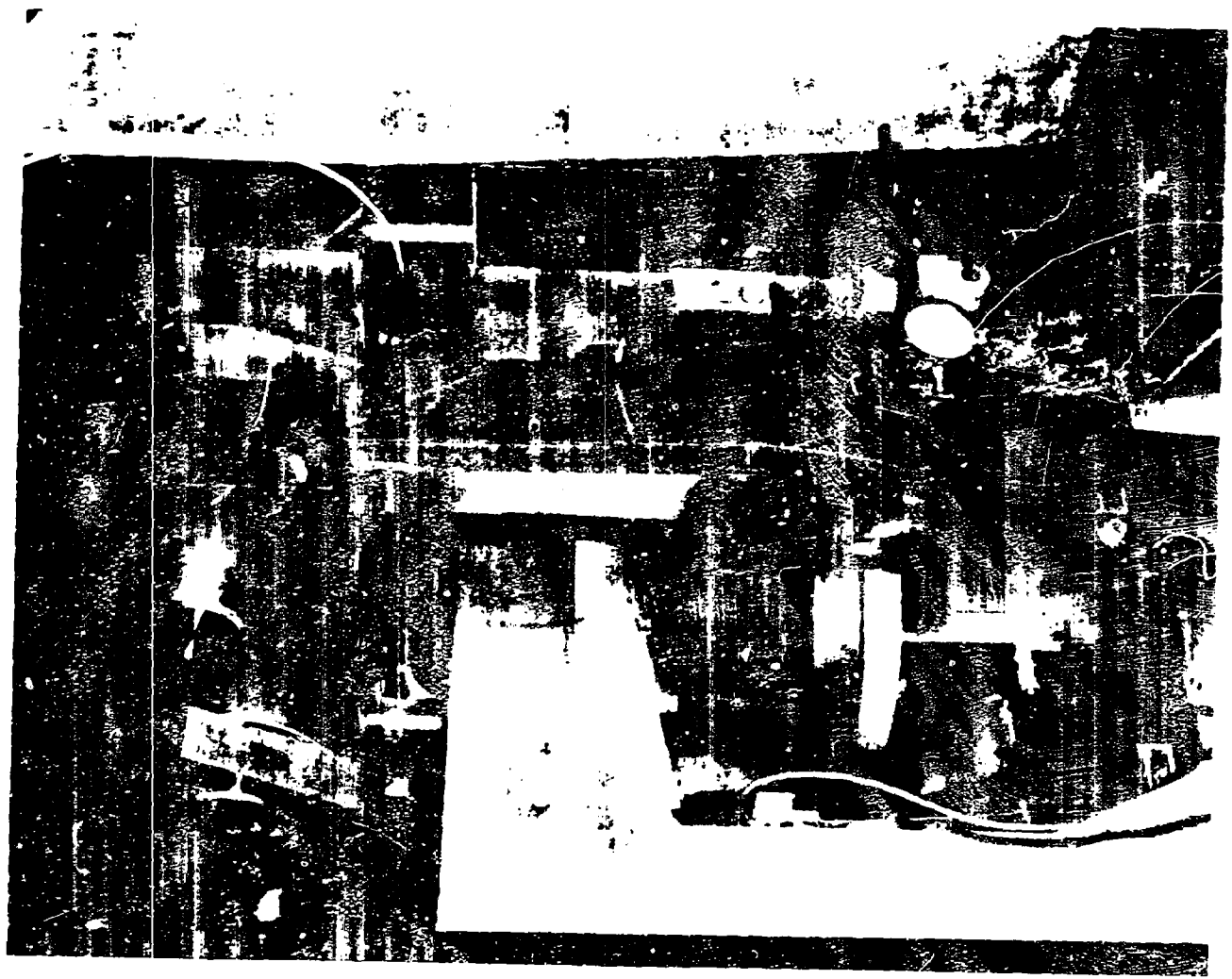

FIGURE 37. 8-INCH ELASTOMERIC BEARING STATIC TEST AT 11° COCKED ANGLE

1. One bearing was made with stainless steel shims rather than titanium, because the stiffness (Young's modulus) of the shim is a factor in bearing characteristics.

2. One of the bearings with titanium shims was cut apart at the small end plate, and the cone angle (or contour) of the shim/elastomer laminates was machined to the cone angle of the 10-inch bearing. The small end plate was bonded in place. This modified bearing approximated a 0.8-inch scale model of the 10-inch bearing.

3. A bearing with stainless steel shims was similarly modified as in item 2 above.

Results of the static tests of the 8-inch bearing are shown in Table 15. As a result of this testing, the 10-inch bearing was to have stainless steel shims, and confidence that the 10-inch bearing would meet static requirements was increased.

TABLE 15. STATIC TEST OF ELASTOMERIC BEARINGS

Bearing	Limit Load (Pounds x 10^3) Cocking Angle with Loop	
	0 Degrees	11 Degrees
8-inch titanium shims	230*	180
8-inch stainless steel shims	250*	210
cut-down titanium shims	237*	151*
cut-down stainless-steel shims	255** 272***	150 170**

Previous test history:
* tested beyond maximum load, considerable deformation
** tested to load limit, slight deformation
*** retested with 11 degree cocking angle

Endurance testing was performed on five 8-inch-bearings for a total of 150[illegible] hours. The Test Plan and Test Report are listed as References 17 and 19, respectively. The test machine is shown in Figure 38.

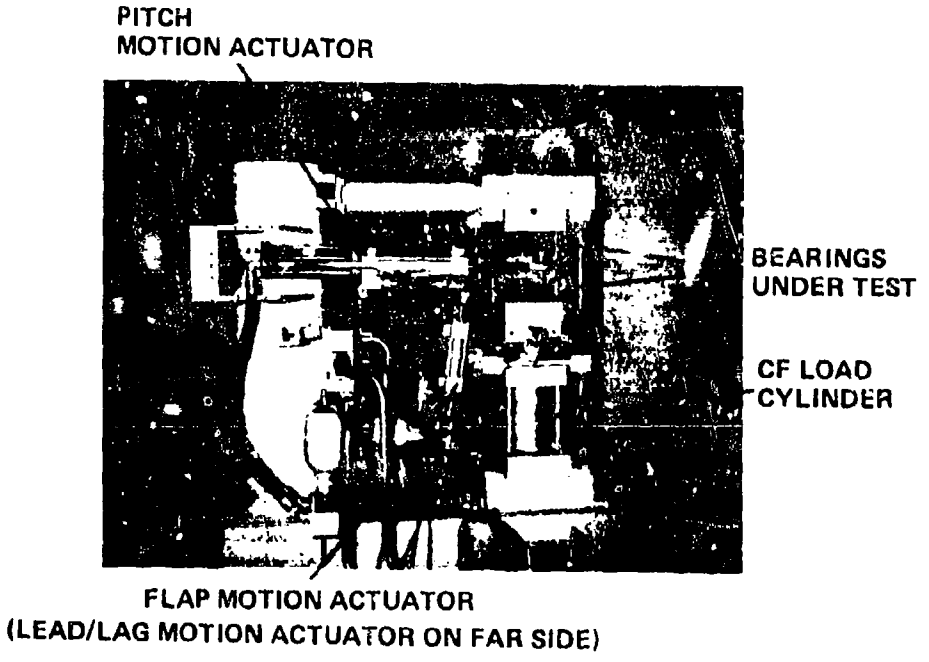

FIGURE 38. ELASTOMERIC BEARING ENDURANCE TEST MACHINE

The objectives of the test program were:

- To assess the endurance capability of the LM-732-1 bearing under laboratory test stand simulation of typical aircraft motion conditions and C.F. load of 150,000 lbs.
- To establish the environmental resistance of the spherical elastomeric bearing to typical exposures of Stoddard solvent, hydraulic fluid and JP4 fuel. Early fatigue test results led to the deletion of this objective.
- To check for fatigue sensitive process flaws in LM-732-1 bearing which may indicate a need for process changes in the manufacture of the LM-732-7 bearing.
- To check out and gain experience with the endurance test machine prior to the critical schedule testing of the LM-732-7 bearing.
- The additional objective of evaluating the fatigue life of a LM-732-1 bearing with stainless steel shims compared to the original LM-732-1 with titanium shims was added to the program as a result of early test results.

Significant events during the test are noted on the chronological chart below:

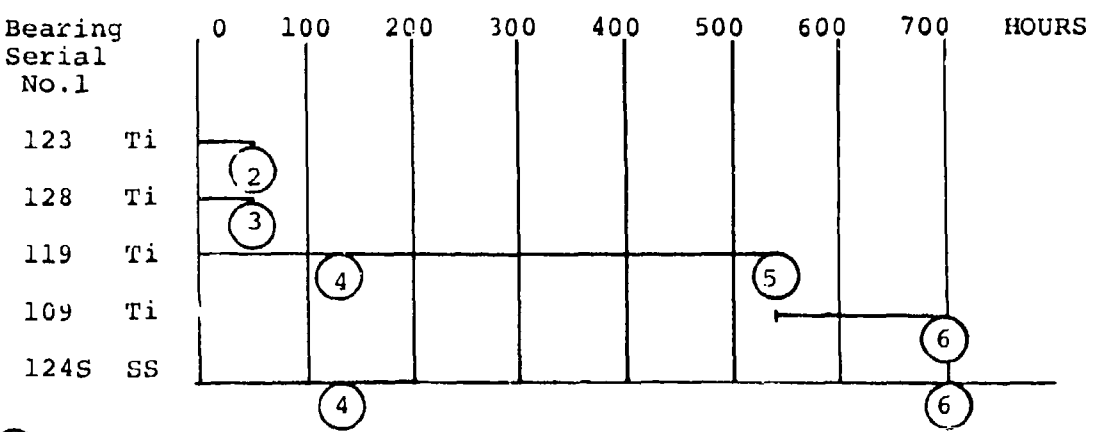

(1) Shim material indicated thus: Ti-Titanium, SS- stainless steel

(2) Testing terminated at 52 hours because of substantial abrading of elastomer between shims

(3) Testing terminated at 52 hours because of substantial abrading of elastomer between shims, and permanent set (axial bowing) of laminates

(4) Centrifugal force reduced at 128 hours to 121,000 pounds to be representative of the average compressive stress on the 10-inch bearing

(5) Testing terminated at 532 hours because of gross abrading and squeeze out (extrusion) of elastomer. New bearing installed.

(6) Testing terminated at 700 hours to start tests on 10-inch bearings.

Data available include:

- Individual bearing torsional load deflection curves at various input amplitudes and frequencies
- Torsional load deflection curves of a test sample pair subjected to axial loads
- Axial load deflection curves of individual samples
- Change in magnitude of key dimensions
- External appearance of individual samples subjected to varied loading (photographs)

Conclusions to the development testing of the 8-inch bearing are:

- The endurance testing indicated that the fatigue life and stability characteristics are interrelated.
- Quality of the bond affects the endurance performance of the bearing as evidenced by the early breakdown of the elastomer in the first two bearings. Failure analysis indicated that the poor bond, verified by pull test, was a result of the low heat transfer of titanium affecting the cure of the bond as compared to that of stainless steel commonly used.
- Stainless steel shims provide greater endurance life than do titanium shims. This fact reinforced the decision to use stainless steel shims in the 10-inch bearing.
- Endurance life is strongly affected by the compressive stress in the elastomer.

- Visual appearance changes provide ample advanced warning of approaching failure. The spring rate and dimensional data accumulated is not considered sufficient to formulate significant conclusions.

4.5.3 Ten-Inch Bearing

Revision B of the Development Specification, Reference 16, listed the higher blade centrifugal force loads. The 10-inch bearing with titanium shims was originally designated LM-732-6 by Lord Kinematics. When stainless steel shims were committed, the bearing was designated LM-732-7. The bearing is shown in Figure 39.

The Preliminary Design analysis is reported in Reference 20. The objectives were:

- To determine the static spring rate characteristics of the LM-732-7 in the axial, torsional, radial and cocking (lead-lag or flap) directions

- To verify the capability of the LM-732-7 to support limit and ultimate axial loading

- To perform an experimental stress analysis utilizing brittle lacquer coating and strain gages

- To verify the suitability of the LM-732-7 bearing for pre-endurance and endurance testing.

Data avaliable include:

- Load-deflection curves for axial and side (radial) loading, and for torsional and cocking rotation with and without axial loading.

- Measured stresses at the edges of 3 shims and several locations on the end plates for axial loading and rotation about the lead-lag and pitch axis.

The preliminary design evaluation shows -

- Spring rates should not be quoted simply as pounds per inch or inch-pounds per degree assuming a liner relationship. Figures 42 and 43 show that because of considerable hysteresis, the force at any deflection can vary over a wide range, depending upon how the bearing got to that deflection. For axial deflection, Figure 40, a secant spring rate from no load to a load such as normal RPM centrifugal force is necessary for determining blade radial position from test to normal RPM. A tangent spring rate is necessary to determine changes in blade position due to changes in radial load, as caused by the blade damper in the case of the HLH. For small

FIGURE 39. 10-INCH ELASTOMERIC BEARING

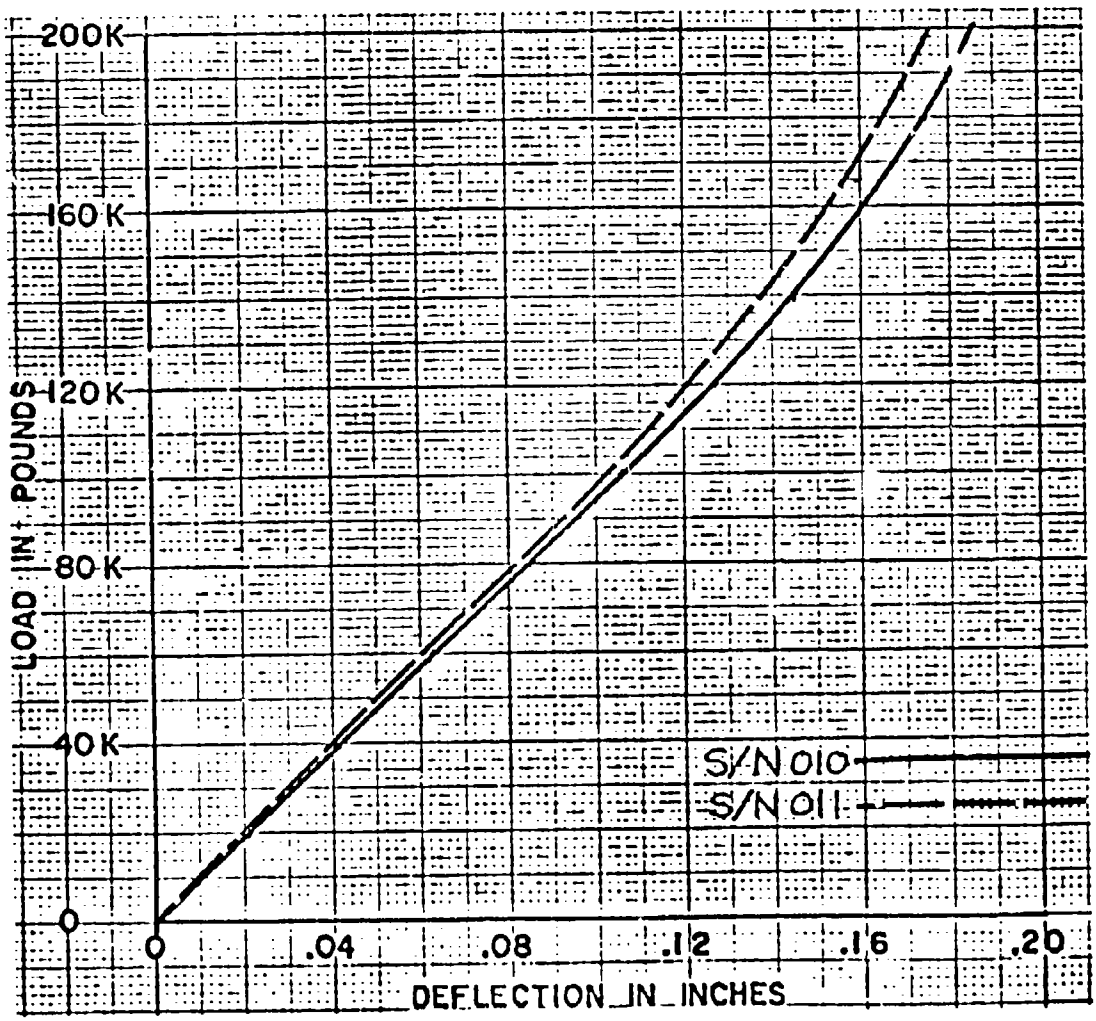

FIGURE 40. AXIAL LOAD-DEFLECTION CURVE

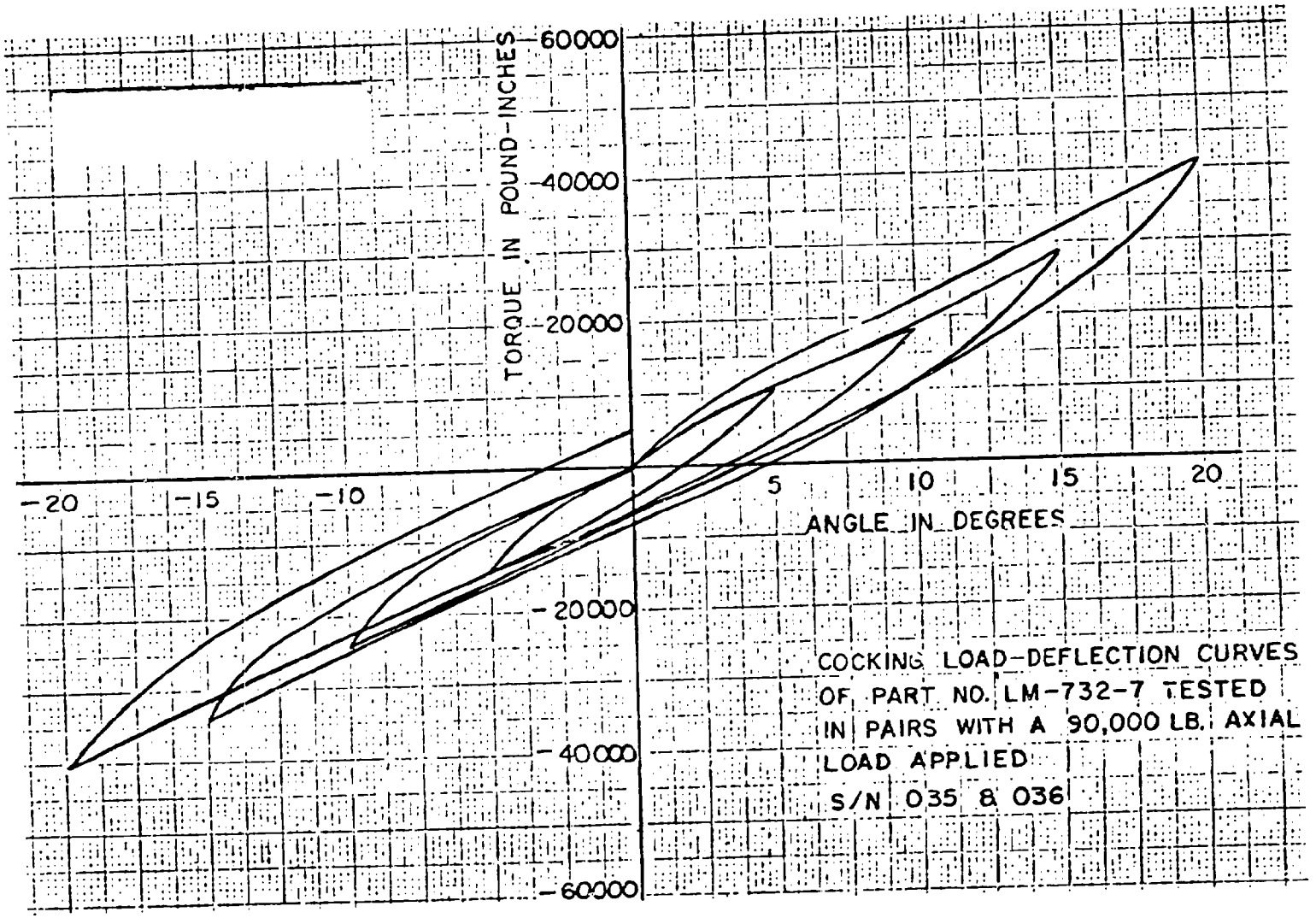

FIGURE 41. TORSIONAL LOAD-DEFLECTION CURVES

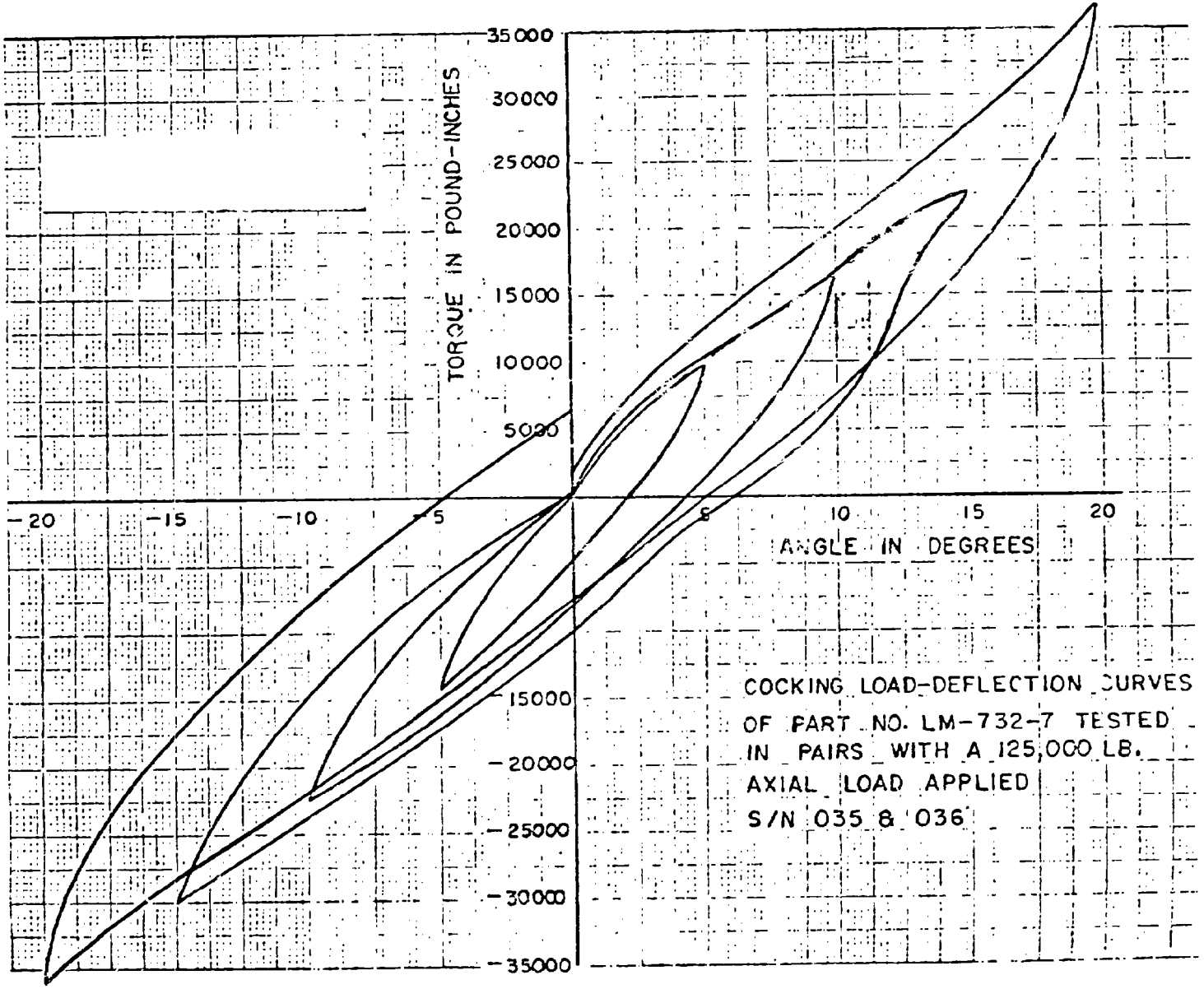

FIGURE 42. COCKING LOAD-DEFLECTION CURVES

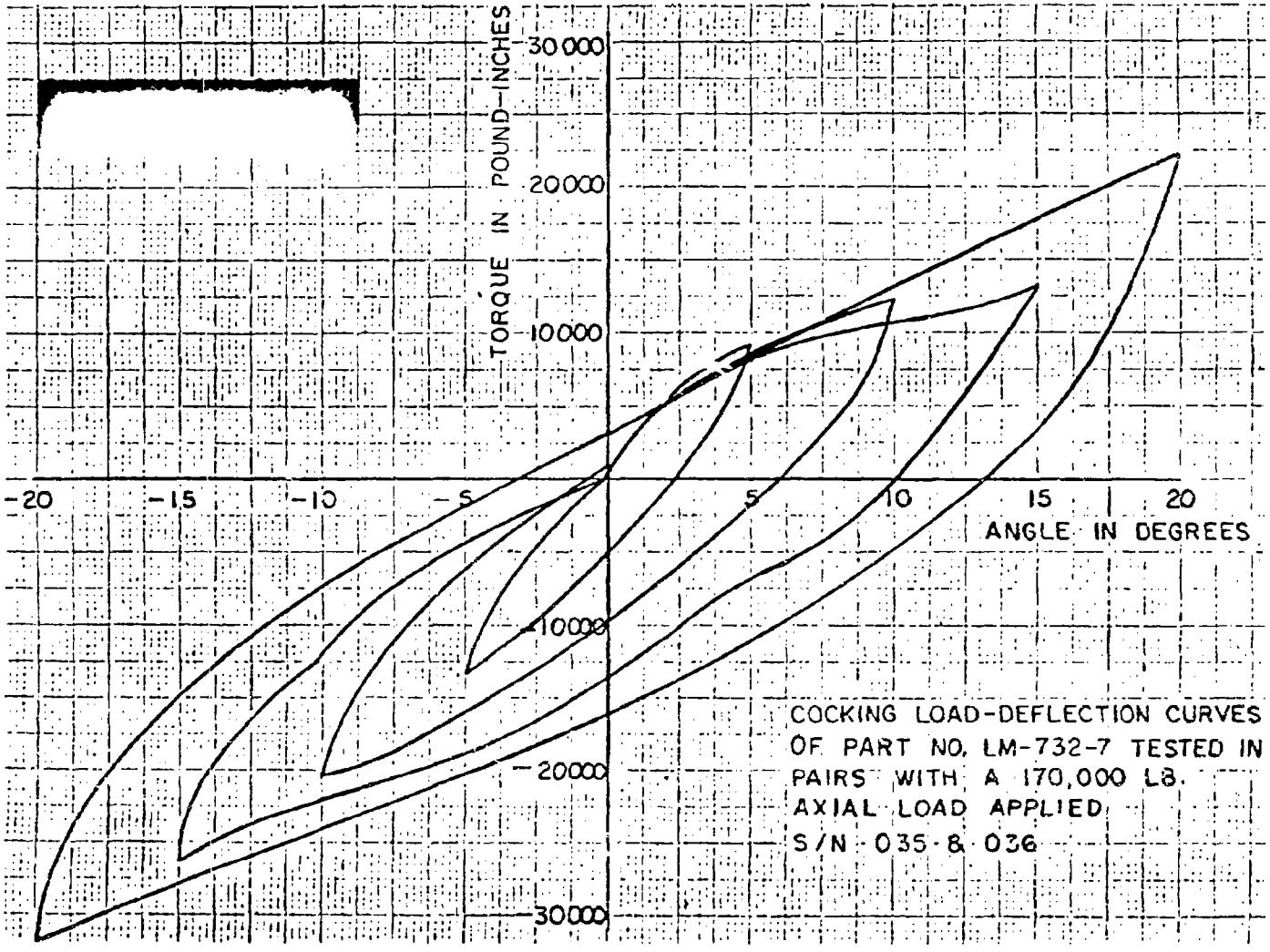

FIGURE 43. COCKING LOAD-DEFLECTION CURVES

torsional deflections, the spring rate is independent of axial load, but for alternating motions, hysteresis must be considered.

- The relationship among axial load, cocking moment, and cocking angle is evident in that the cocking spring rate decreases with increased axial load and would be unstable with axial load high enough. Also, the critical column load decreases with increased cocking angle.

- The stress levels measured during the experimental stress analysis indicate that the LM-732-7 bearing is satisfactory for its intended use.

- The energy absorbed by a bearing because of hysteresis is considerable. For example, for five degrees flapping alone, a high-speed level flight condition, each bearing converts approximately 1.3 horsepower to heat. This is a consideration in endurance testing.

- To make evident the extent of hysteresis, a term efficiency (η) is defined as the work absorbed by the bearing during one complete stroke between symmetrical limits about a zero force reference divided by the work in a stroke of constant loads of the peak values over the same displacement. The efficiencies for the conditions in Figures 42 and 43 were calculated and shown in Figure 44.

Static tests on the 10-inch bearings were conducted using a titanium loop as shown in Figure 45. The first bearing tested successfully sustained 399,000 pounds ultimate load at zero degrees cocking angle. Another similar bearing failed to meet the requirement of 266,000 pounds at 11 degrees. Lord Kinematics molded additional bearings with stiffer elastomer. The original bearings were designated "soft" and the later bearings "stiff". The stiffer bearings were expected to have greater column stability but with a penalty of reduced life. The stiff bearing exceeded the requirement at 11 degrees by a considerable margin and another bearing was molded with "intermediate" stiffness. The last bearing also showed considerable margin over the requirements, and it was considered desirable to continue the program with the extra margin recognizing a compromise of endurance life. Loading curves for these bearings are shown in Figure 46. All bearings for further usage were of this intermediate stiffness.

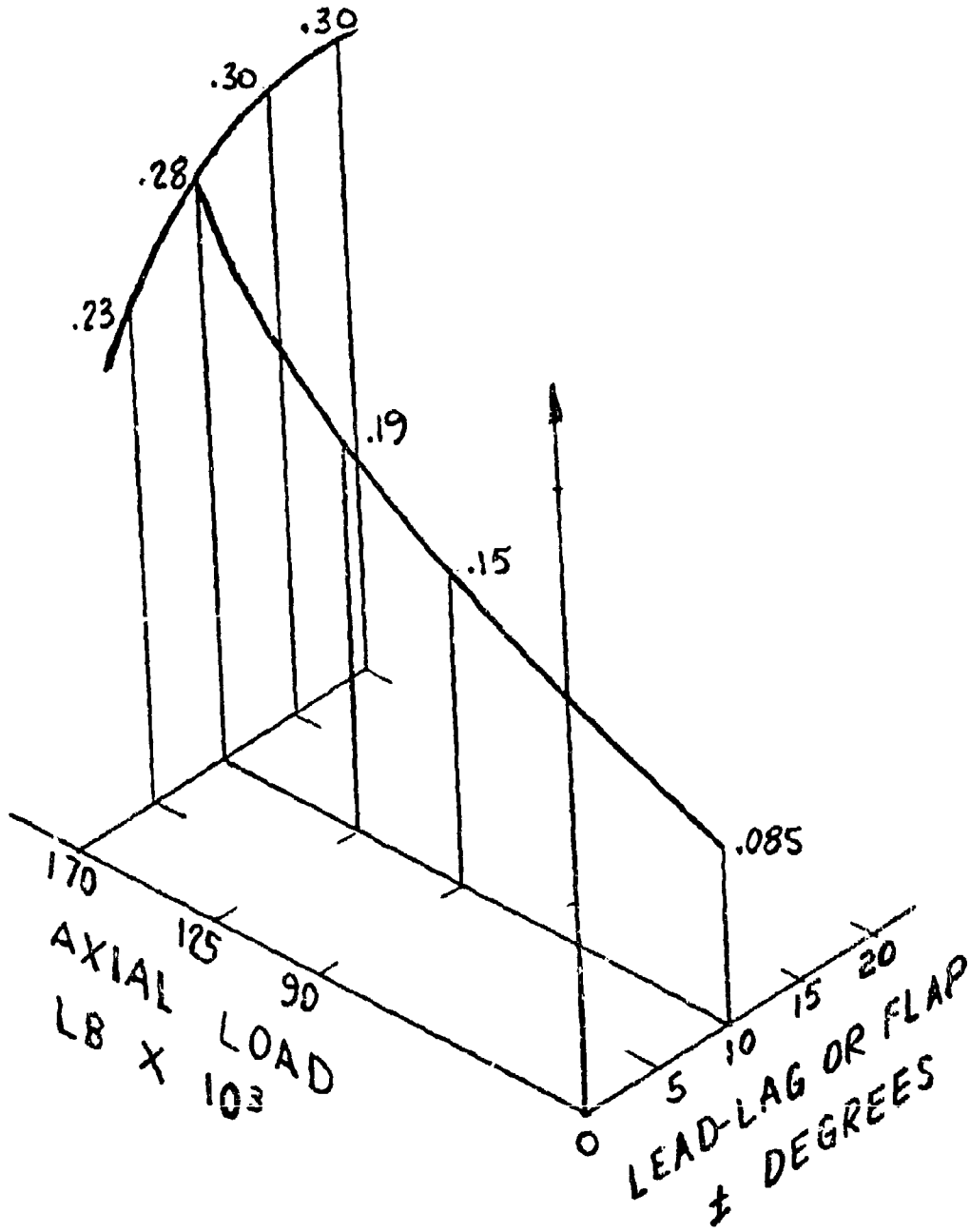

FIGURE 44. DAMPER EFFICIENCY

FIGURE 45. 10-INCH ELASTOMERIC BEARING AT BUCKLING LOAD

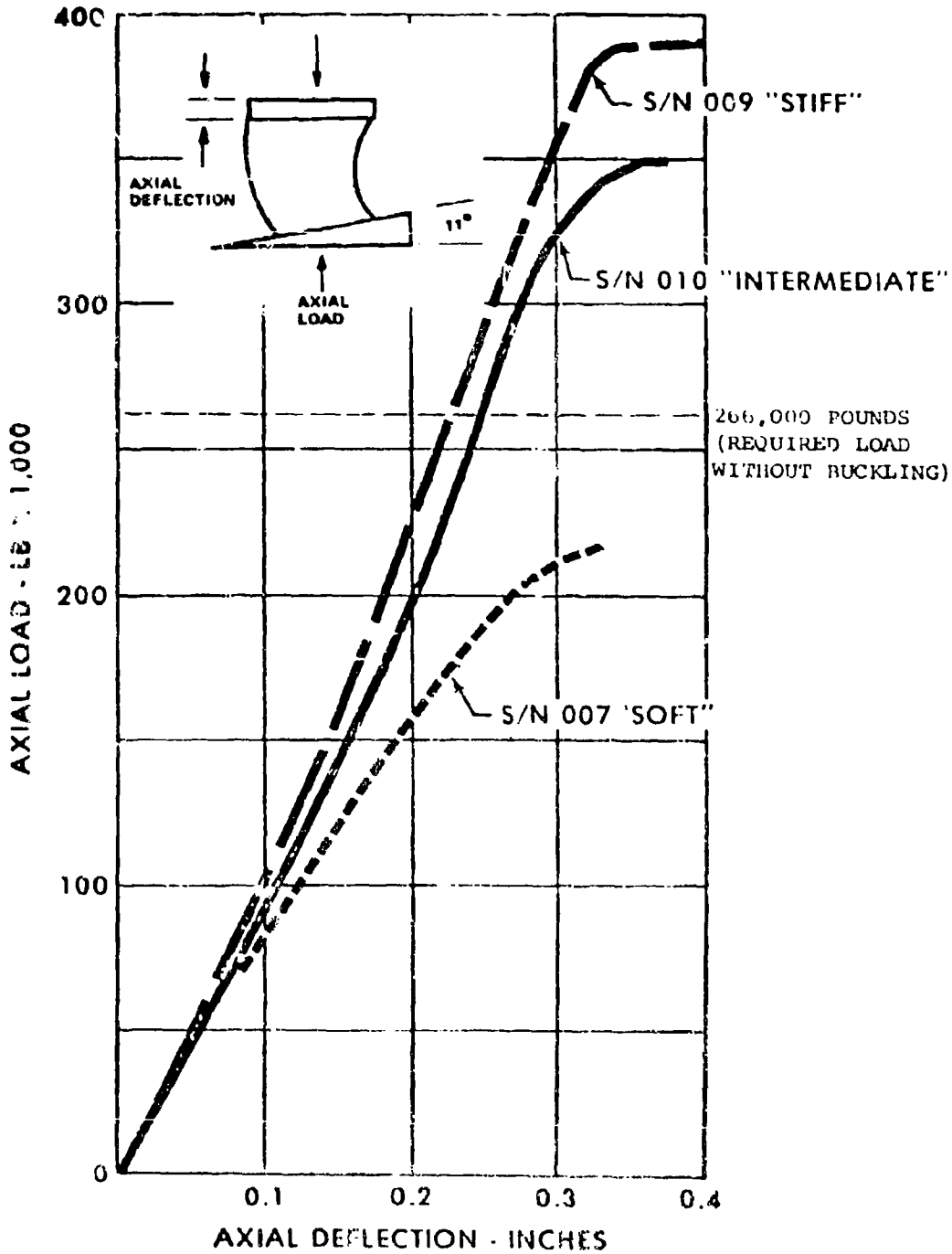

FIGURE 46. 10-INCH ELASTOMERIC BEARING AT 11° LAG ANGLE - TITANIUM SHIMS

The endurance test plan and test report are listed as References 21 and 22, respectively.

The objectives of the test program were:

- To determine the adequacy of the bearing configuration, including elastomeric element design, and evaluation of the strength of the metal components.
- To determine dynamic endurance capability of the LM-732-7 bearing under laboratory test stand simulation of typical aircraft loads and motions and selected environmental conditions.
- To determine the forces imposed on connecting rotor hub parts during start-up from low temperature.
- To establish inspection and replacement criteria for service bearings on the basis of endurance test results.

Significant events during the test are noted on the chronological chart on the following page.

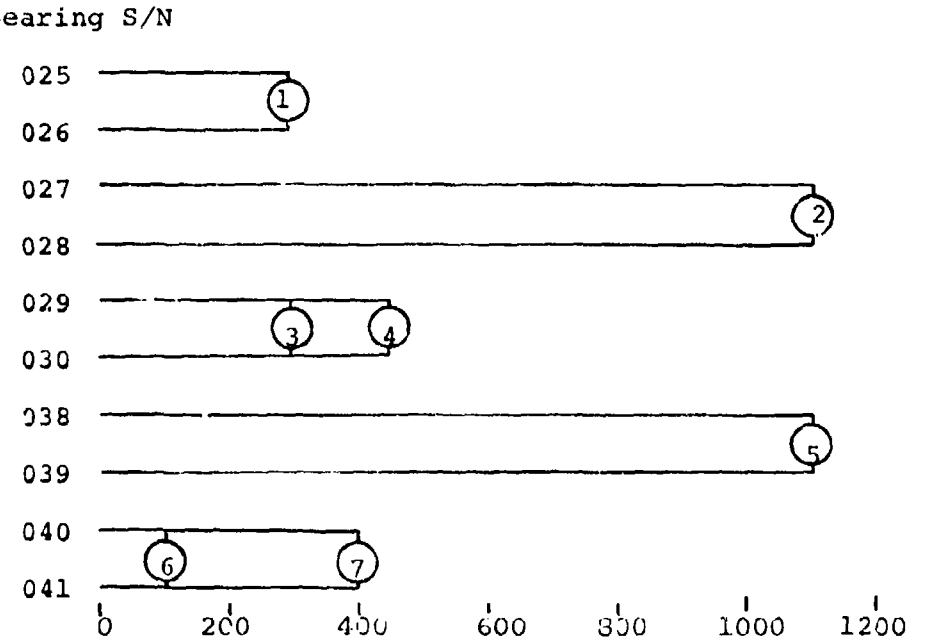

(1) Testing terminated at 300 hours because of poor condition. Testing conducted with one large floor pedestal fan blowing on bearings.

(2) Testing terminated at 1100 hours. Bearings declared worn out. Testing conducted with smaller blowers directed at several points on bearings.

(3) Completed 300 hours pre-endurance testing at ambient conditions same as bearings 027 and 028.

(4) Test terminated at 420 hours (120 hours of 120°F) by machine shutdown. One bearing was separated-bond failure accelerated by high temperature.

(5) Testing terminated at 1094 hours. Bearings declared worn out. Thermocouples installed on one bearing at beginning of test indicated temperatures for one and five hour blocks (see Figure 47). As a result, block time changed to one hour.

(6) Completed 100 hours pre-endurance. Pre-endurance time reduced from 300 hours because of success with previous bearings in pre-endurance.

(7) Testing terminated at 400 hours (300 hours planned at -65°F)

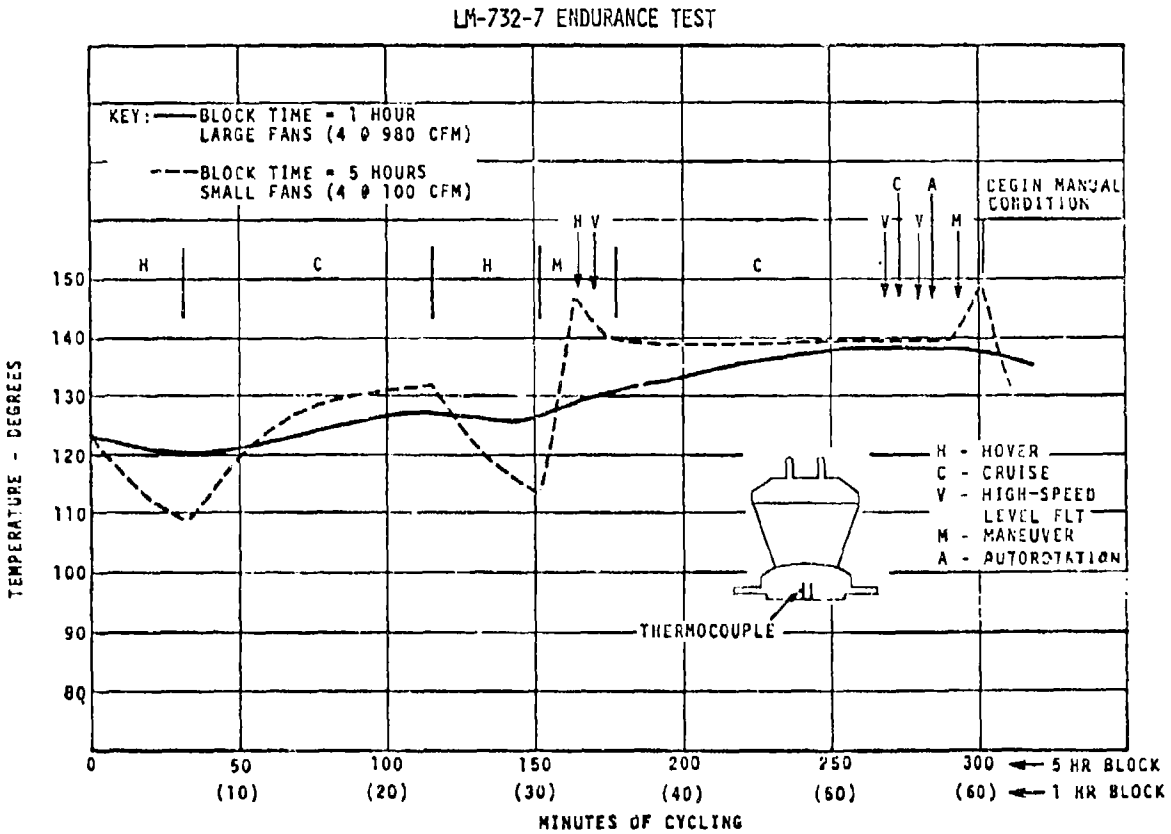

FIGURE 47. ELASTOMERIC BEARING BASEPLATE TEMPERATURES

All testing was terminated by direction with 6420 of the 12,000 planned hours accomplished. Testing was terminated to conserve resources. Further testing would not provide any new information but rather a better statistical base.

Data available from these tests include -

- (Torsional) pitch and axial load - deflection curves at several times during the endurance test
- Dimensions of the bearing assembly affected by changes in the elastomer/shim laminates at several times during the endurance test.
- External appearance of the bearings at several times during the endurance test (photographs)
- Time-temperature plot of a bearing during the test cycle of one and five hour blocks
- Load and deflection in loading versus time at -65°F (rotor start-up)

It is concluded that -

- The LM-732-7 bearing did not meet the design life goal of 1500 hours in laboratory testing. Two pairs of samples were tested for approximately 1100 hours each at room temperature.
- The primary cause of the failure to reach the design goal was believed to be accelerated fatigue due to the high internal bearing temperatures generated during the endurance test.
- The high temperature test resulted in an extremely short endurance life. The test was excessively severe in that there was no circulatory air in the chamber surrounding the bearings.
- The low temperature environmental test did not increase the rate of deterioration of the bearing. Although there is no quantitative measure of performance during low temperature operation, an improvement in fatigue performance probably occurs, because of increased heat dissipation.
- The free height and the axial spring rate decrease with usage. It does not appear that they can be used as indicators of expended or remaining useful life. The rotor hub design must make provisions for the change of radial position of the rotor blade as the bearing ages.

- The torsional spring rate and the other dimensional characteristics did not exhibit trends which would allow prediction of bearing life. In addition, these measurements would be difficult to perform in service.

- Visual appearance of the elastomer gives adequate indication of the status of deterioration of the bearing.

- The correlation of bench testing with service experience remains to be established, particularly in view of the large amount of heat generated and the sensitivity of bearing performance to bearing internal temperature.

4.5.4 Whirl Test

After 8.7 hours of operation of the demonstration rotor on the whirl tower, one of the bearings showed separation of the elastomer from the lower side of the spherical segment of the small end plate. When viewed from above, no separation was evident. All four bearings were removed and returned to Lord Kinematics. The failed bearing, serial no. 015, was completely separated when removed (Figure 48). Approximately 90% of the interface showed bare metal, indicating failure of the adhesive to bond. The remainder of the interface was separated by failure of the elastomer.

Failure analysis using scanning electron microscopy and other laboratory techniques reported in Reference 23 indicated that there was a contaminant on the surface of the small end base plate where the separation of the elastomer occurred. Where the elastomer had adhered, there was no contaminant. The contaminant was identified as the detergent that is used only in cleaning the metal parts before the adhesive is applied. Corrective action was taken to control the cleaning process.

The other three whirl test bearings, S/N 014, 016 and 017, were subjected to lead-lag static deflections through ±4°. No anomalous behavior was noted. The bearings were also subjected to pitch change cycling of ±12° at 156 cycles per minute for 30 minutes. Dynamic cycling was considered the best method for bringing out incipient bond failures. Two new bearings, S/N 033 and 034, that were being used by Lord Kinematics for their preliminary design evaluation work task were diverted and installed on the demonstration rotor. Two of the reinspected bearings were re-installed and a third held as a spare.

The careful inspection at this time revealed that the surface of the elastomer was covered with a network of shallow cracks. This checking was attributed to ozone attack, a well-known phenomenon with rubber. As was expected, there was no progression noticeable during the whole program, since elastomer bearings are extremely tolerant of this surface checking.

FIGURE 48. FAILED ELASTOMERIC BEARING

Immediately prior to the discovery of the separation of the elastomer, the rotor was probably operating with most of the base plate surface separated. There was no real indication from the rotor operation that there was separation. As an indication of what might happen with a complete bearing failure in this mode, a separated bearing was installed in the endurance test machine with a normal bearing. It was operated through a complete block of all the loads and motions. The machine and bearing operated with no unusual indications. Normal operation is not unexpected because the concentric spherical laminates of shims and elastomer nest more securely with axial load. The friction between the elastomer and the end plate was sufficient to prevent slippage during rotation about all axes. This laboratory demonstration gives confidence that the bearing will function for a limited time in a rotor even though there is a complete separation of the base plate.

4.5.5 DSTR

The difficulty in simulating operating environments for the bearing in the laboratory was emphasized when temperatures were measured on the 10-inch bearing during endurance testing. An attempt was made to measure temperatures on a bearing operating on a rotor for at least the hovering regime of flight. The DSTR would provide the loads and motions on the bearing and the thrust generated would provide the air flow. Four thermistors were bonded to the edge of the second shim from the small end plate in the 0.5-inch-diameter core hole of the bearing. The wires were directed to the small end plate and out through a hole drilled near the edge of the elastomer. The lower end of the core hole was potted with silicone rubber. The motions of shims caused the lead wires to break early so that no data were available. The low priority for these data and the rework to preload the bearings were the reasons that no further attempts were made to measure temperature.

It has been discovered on the DSTR that when the rotor is at rest for long periods, the bearings can develop local tearing in the rubber layer between the small end plate and the first shim on the lower lag side. One bearing was torn sufficiently to require replacement. The tearing is due to the tension on one side of the bearing resulting from being deflected in droop and lag as well as the axial tension reaction the lag damper driving the blade to the lag stop. It is the same condition that caused the bearing to separate on the whirl tower. That bearing failed early because of the poor bond. The solution was to provide a compressive preload of approximately 40,000 pounds on the bearing while the rotor is at rest. This was accomplished by the addition of the thrust button shown in Figure 49, and there was no further degradation of this type.

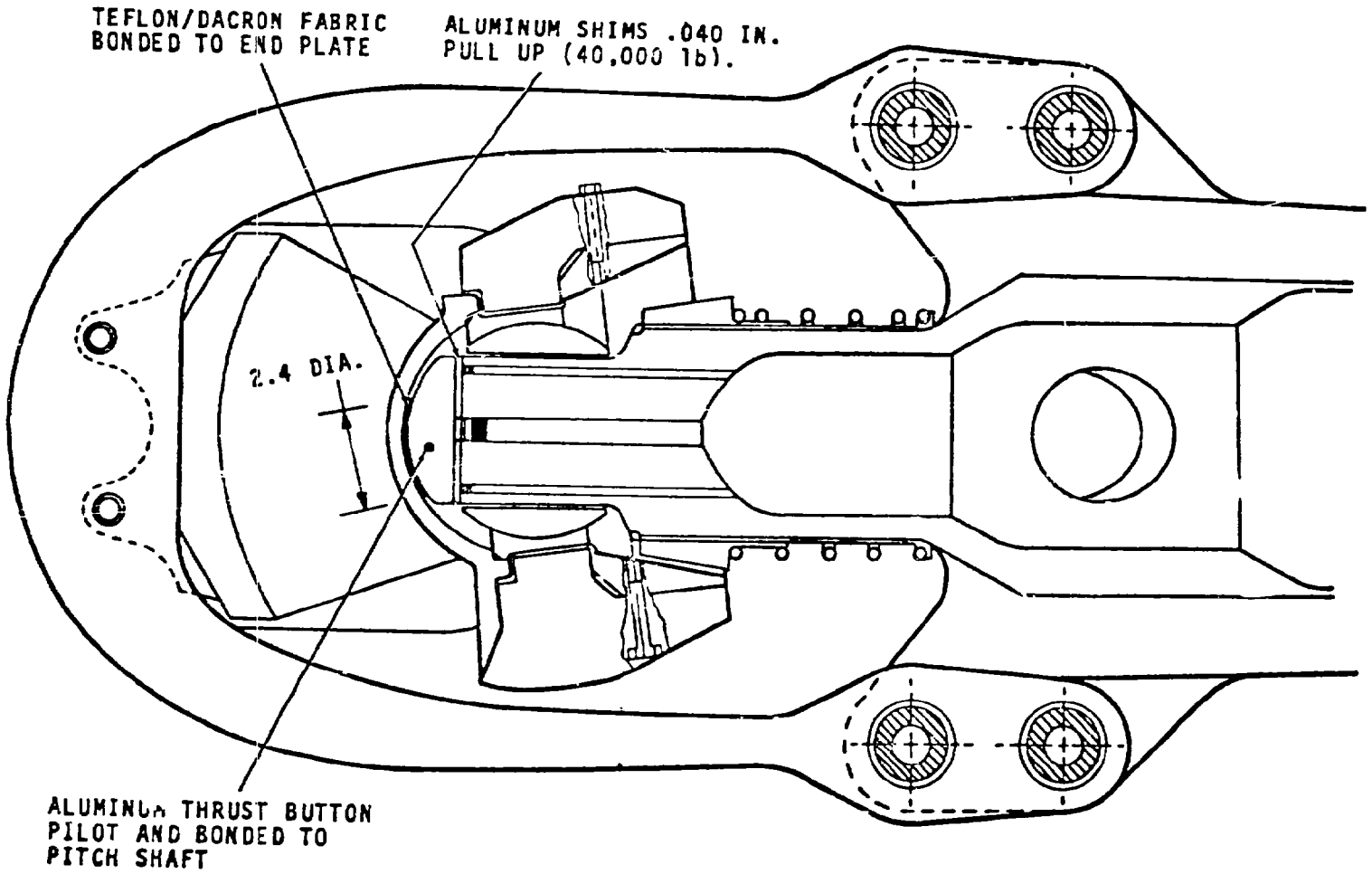

FIGURE 49. ELASTOMERIC BEARING PRELOAD

4.5.6 Conclusions

- The LM-732-7 bearing is adequate for the Prototype and also for an Engineering Development phase of an HLH program.
- The bearing is fail-safe in this application for separation failures.
- The bearing must be preloaded or otherwise protected from tensile loading to avoid damage.
- Visual examination is the best way to inspect for incipient failure or remaining life.
- Moderate checking (surface cracks) alone is not cause for rejection of a bearing in service.
- If there is to be design change of the Rotary Wing head, consideration should be given to the elastomeric bearing to reduce the compressive stress in the elastomer and to reduce elastomer stiffness. These changes would increase the life of the bearing. A secondary item for trade-off would be an open center to facilitate heat dissipation.

4.6 DROOP STOP

The droop stop function is to support the blade above the ground and the fuselage when the rotor is at rest, but not contact in flight.

The HLH configuration is such that the position of the blade at rest is higher than the flight clearance requirement. Therefore, a two-position droop stop was required.

The moment of the blade is reacted essentially vertically on the outboard lip of the crossbeam and the shear bearing. The crossbeam contains a titanium stop block replaceable if damaged. The droop stop part on the pitch housing is a conical ring lined with Teflon Dacron fabric that slides and rolls on the inboard shaft end. A spring holds the ring at rest in the inboard position. In this position, the ring between the pitch shaft and the crossbeam holds the blade in the higher position. As the rotor increases speed, the centrifugal force on the droop stop ring overcomes the force from the spring, and the ring moves outboard between 95 and 115 rpm.

With the full rotor assembled for the first time on the whirl tower, the centrifugal droop stops worked out of engagement with the rotor at rest, causing the blade to drop to the lower flight stop position, and the edge of the droop stop to be chipped. The droop stop had a cylindrical bore fitting over the pitch housing shaft, and a conical outer surface that contacts the pads in the cross beam. When at rest, the forces on the cylindrical and conical surfaces caused an outward component of force on the stop. When totally at rest, friction opposed that outward force. When winds caused the blade to move slightly in lead/lag, the rolling motion of the stop was sufficient to allow it to work itself outward against the centrifugal restraining spring.

A set of redesigned stop rings, SK301-11751-1, was installed. These rings had a cylindrical outside as well as inside. With no radial component of forces from the pitch shaft and stop blocks, the centrifugal spring is adequate to hold the stop block during all the rolling. The stop blocks now have two shorter surfaces rather than the single surface that would accommodate both droop angles. The stop ring or block will yield at a lower g load but deformation of droop stops is not expected to present a safety hazard. The DSTR parts showed no noticeable yielding.

The static position of the blade tips was measured on the DSTR. They were lower than expected; hence, the blade-fuselage clearance was decreased. The reason for the increased droop at the tip was the greater deflections in the hub components. This was concluded by measuring the angle from horizontal at a number of points on the hub and pitch housing with the blade off the droop stop, and with the droop stop supporting the blade weight. A set of droop stop blocks that provided -1° droop angle rather than the original -2° were fabricated and installed on the DSTR rotor head to preclude excessive droop during starting and stopping. The control system for the aircraft will require limitations on the applied cyclic control (nominally zero) during these operations to restrict the blade from negative flapping and to prevent the droop stop rings from engaging.

4.7 FREQUENCY SELECTIVE BLADE LAG DAMPER

The detail design, fabrication, fatigue and qualification testing of full-scale frequency selective lag dampers was subcontracted to the Bertea Corporation, Irvine, California. This damper incorporated an 8000-pound preload to pull the rotor blades back against the lag stop to prevent aircraft wallowing on rotor startup. A combination accumulation - reservoir mounted inside the hollow rotor shaft serviced all four dampers.

Five frequency selective lag dampers were delivered to Boeing Vertol and are retained at Bertea for qualification testing. Four of the five Boeing Vertol dampers were installed on the rotor (Figure 50), and the spare unit was bench tested in the laboratory.

Performance testing of the lag damper in a mixed frequency laboratory environment showed energy dissipation well in excess of specification requirements.

The whirl tower testing showed two basic and unforeseen problems, however. The first is a limit cycle phenomenon, or "hunting"; the second is a frequency-selective-damper control valve by passing due to low rate changes in blade lag position which accompany changes in power; i.e., maneuver transients.

Limit Cycling

A hunting or limit cycle phenomenon in which there is alternately a loss of tension and compression cycle damper force was experienced during the whirl tower test program. This condition is illustrated in the time history of Figure 51. Prior to "Cycle 0", the damper is developing load in response to the 1/4Ω blade motion only in the extension (tension) direction. Just prior to "Cycle 0" the damper begins to develop load during the retraction (compression) cycle which is followed almost immediately by a forward shift in the blade mean lag position and a loss in extension cycle damper force. At "Cycle 39" the reverse process takes place. It is evident that this switching phenomenon will be repeated, giving rise to an unacceptable low-frequency hunting of the blade about its equilibrium position. Similar results, Figure 52, have been obtained with an effective C.F. spring and an existing analytical model of the damper. The analytical time history differs slightly from the test results in that the condition has been initiated by an impulse at time zero. Displacement of the FSD control valve has been shown for reference purposes and explains the mechanism of the low-frequency oscillation. In response to the initial disturbance, the FSD valve is displaced to one side of its null or center position which unloads the damper during the retraction cycle. In turn, the absence of a

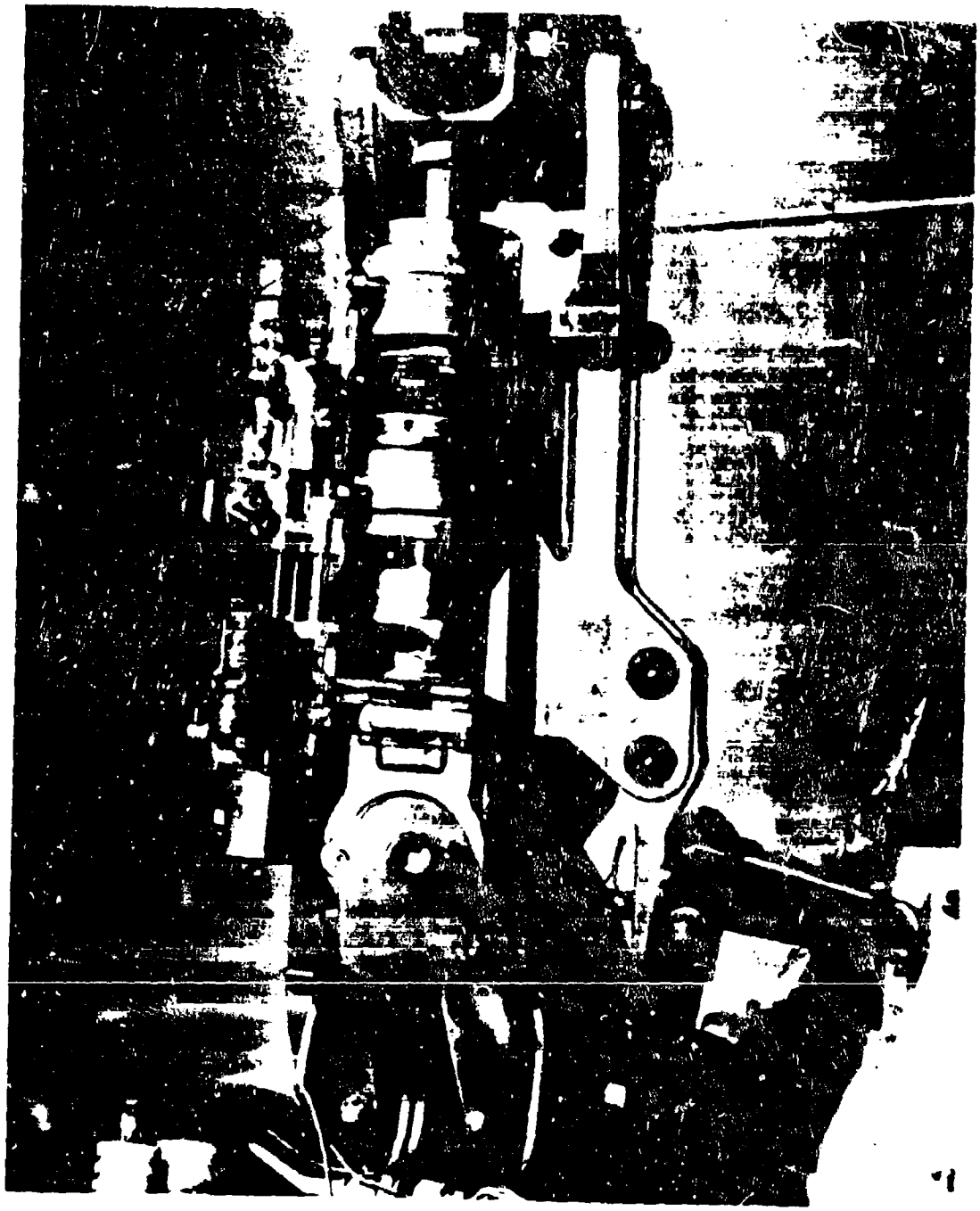

FIGURE 50. FREQUENCY-SELECTIVE DAMPER

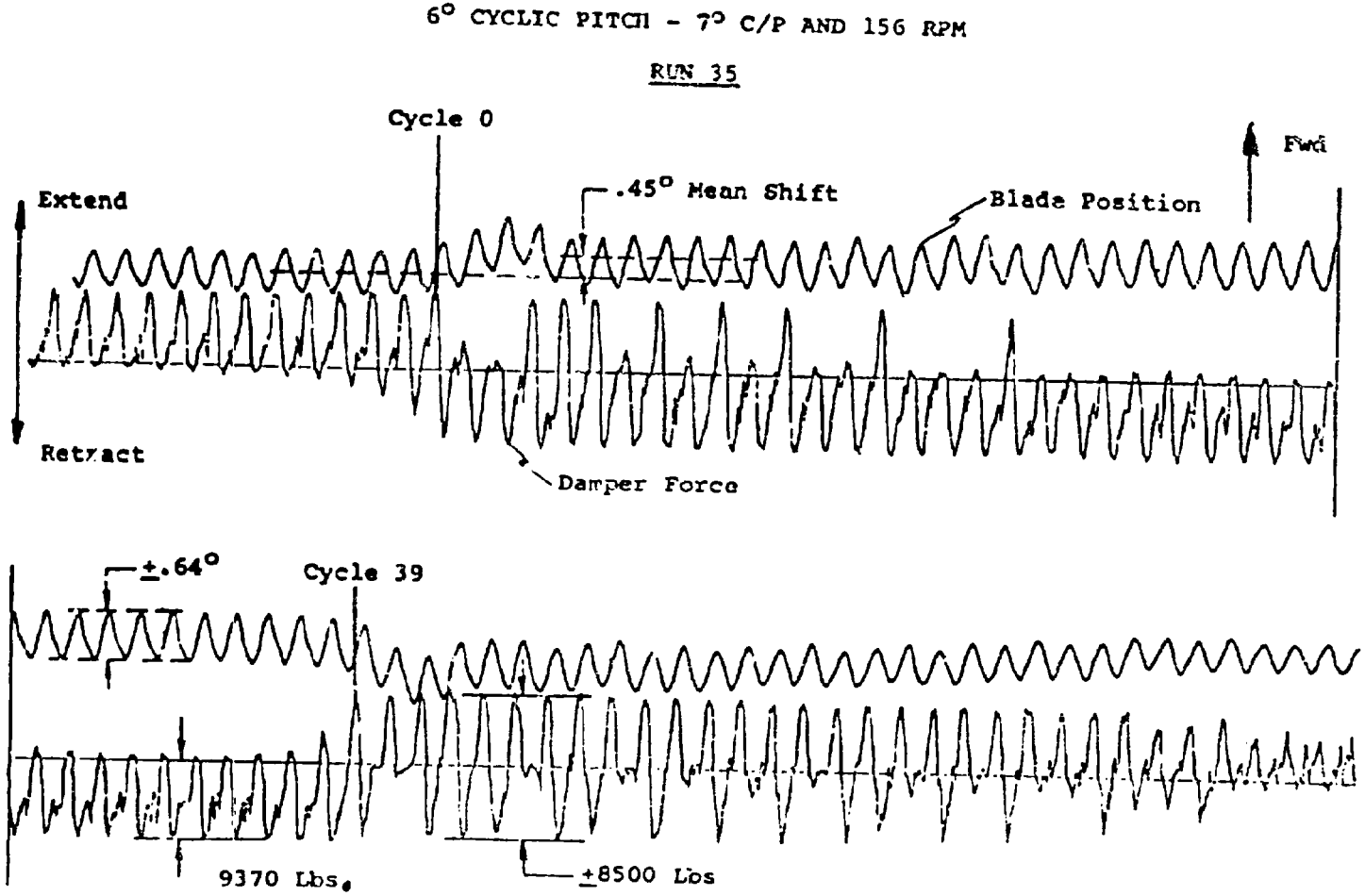

FIGURE 51. WHIRL TOWER DATA - FREQUENCY-SELECTIVE DAMPER

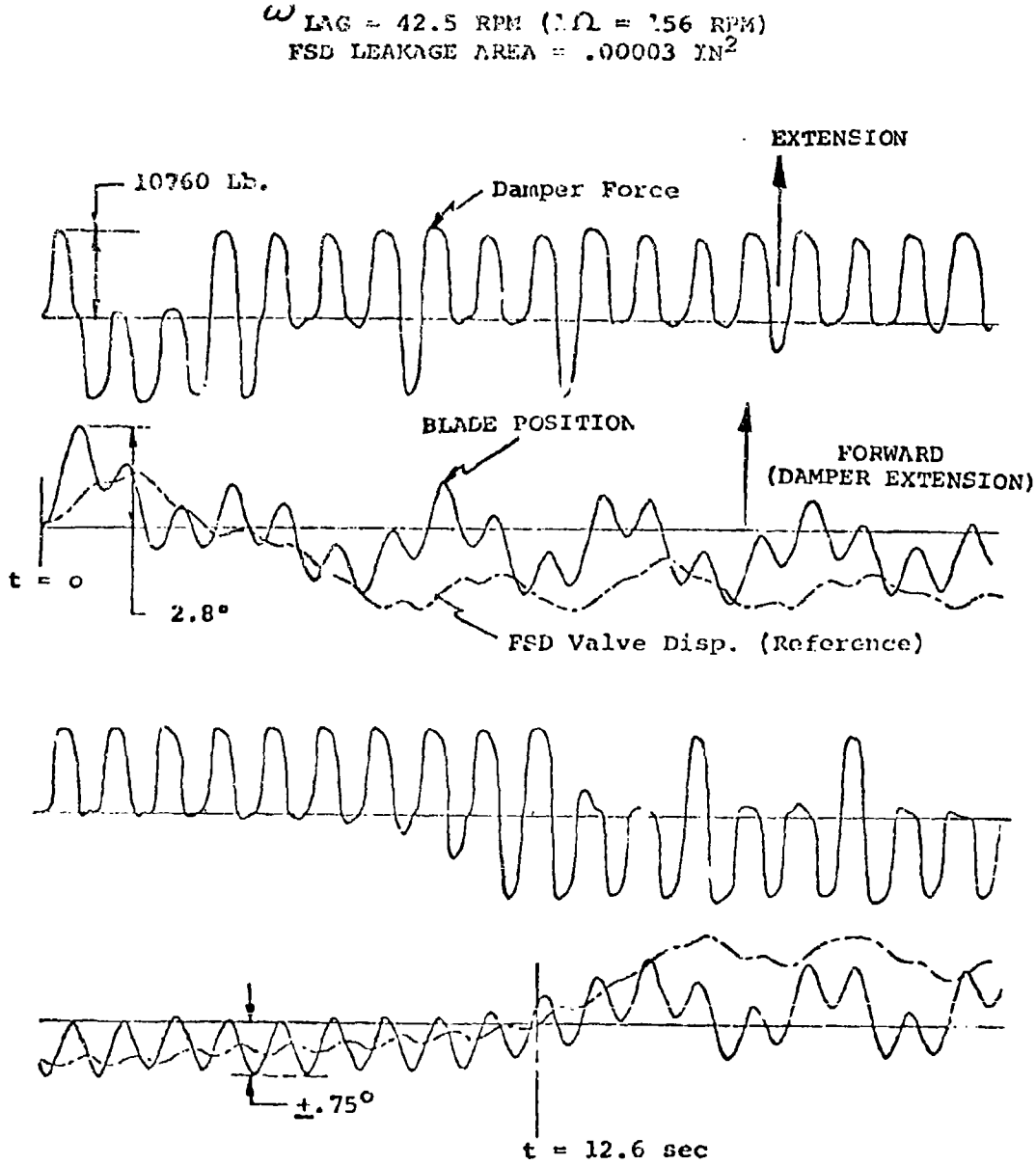

FIGURE 52. FSD ANALYSIS WITH SMALL DRIVE CYLINDER BLEED

retraction cycle force causes the blade to oscillate about a position aft of its equilibrium position. As the decaying valve displacement approaches its equilibrium position, the retraction cycle forces begin to build up and the blade starts to move forward. Due to the blade inertia, the blade main lag position overshoots the equilibrium position which drives the FSD control valve over center in the opposite direction, causing a loss of extension cycle damper force. At this point, it is apparent that the cycle is repetitive and essentially undamped.

Degradation During Maneuver Transient

During entry or recovery from a maneuver, therotor horsepower increases or decreases at a rate which is determined by the pilot's rate of collective input. The change in rotor horsepower produces a change in the mean blade lag angle, which, in turn,affects the damper performance. If the maneuver entry and recovery are represented by ramp changes in mean blade angle, the analytical plot of Figure 53 shows the conditions which affect the damper. For damper ramp velocities less than .02/ in/sec, the FSD control valve remains within the center deadband (overlap region) and FSD operation is essentially unchanged. At higher ramp velocities, the FSD control valve is driven off center, resulting in a loss of damping force in one direction (1/2 cycle damping). The loss in damping will persist until the blade is stabilized at the new mean lag position and the FSD valve has recentered. Valve recentering time based on laboratory testing is typically on the order of 3.5 seconds. When the ramp duration is such that the FSD valve is driven to the hardover position, the valve is closed and the damper operates as a non-FSD damper. Lines of constant maneuvering horsepower indicate that delta horsepower up to approximately 1000 horsepower lie within the 1/2 cycle damping region for the typical maneuver time of 2 to 4 seconds. Since a delta of 1000 horsepower represents roughly 11% of full power, a large number of maneuvers will be performed in the 1/2 cycle damping region. Thus, a typical ramp duration of 2 to 4 seconds together with a 3.5 second valve recovery results in up to 7.5 seconds of 1/2 cycle damping. While this may or may not be unacceptable, it is clearly undesirable since it degrades the damping action at all frequencies.

Extent and Impact of Necessary Modifications

Analytical investigations revealed that the low frequency limit cycle is a function of the leakage area across the FSD drive cylinder. While a complete analysis was performed, there is evidence to indicate that additional overlap in the FSD control valve is also beneficial. Figure 54 shows a comparison between a non-FSD damper and an FSD damper incorporating a larger leakage area. Examination of the damper displacement waveforms

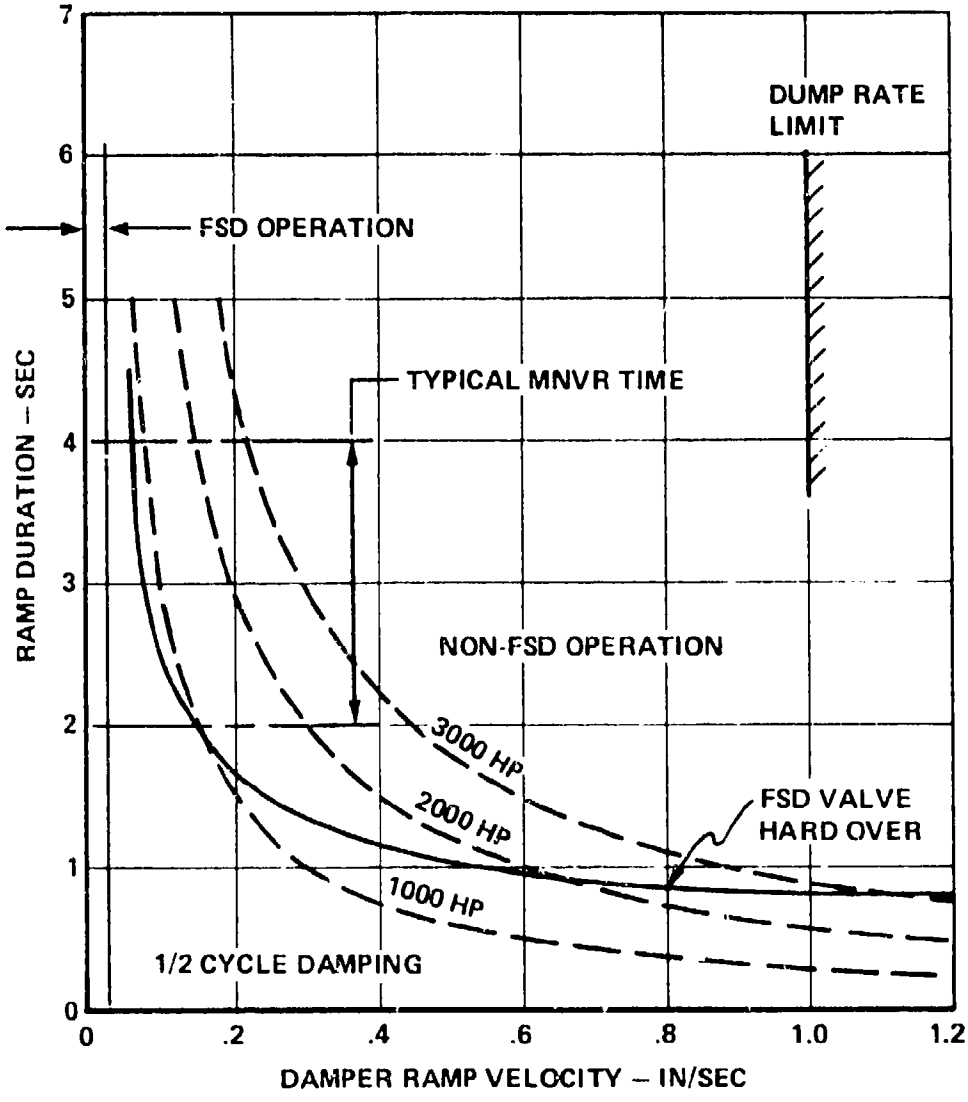

FIGURE 53. DAMPING CHARACTERISTICS WITH RAMP CHANGE IN BLADE POSITION

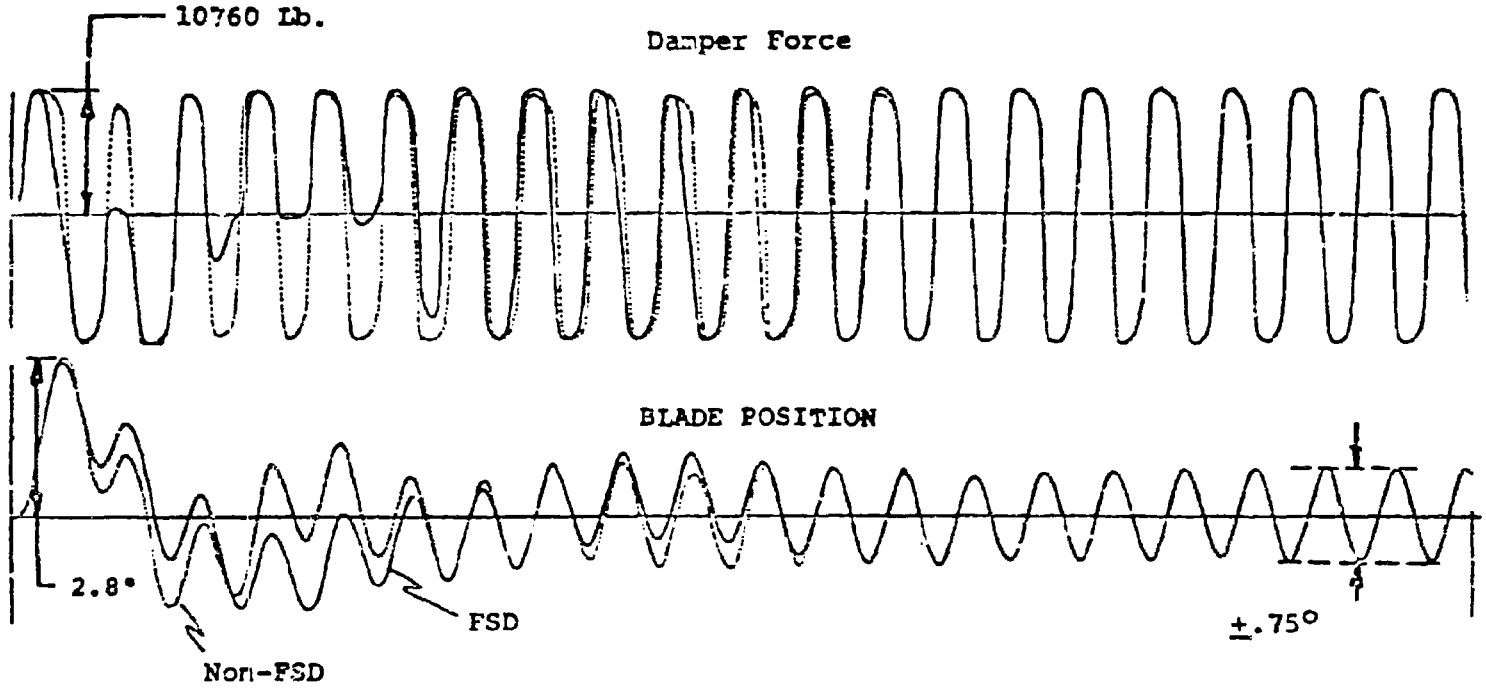

FIGURE 54. TRANSIENT RESPONSE COMPARISON

indicates the modified FSD configuration stabilizes almost as rapidly as the non-FSD configuration.

A brief laboratory test was conducted to evaluate the effects of increased drive cylinder leakage. Response to transient inputs showed a significant improvement in FSD control valve recovery time, as illustrated in Figure 55. Several single frequency steady-state conditions were investigated and the results are summarized below. The results indicate a significant reduction in energy dissipation for small amplitude low frequency inputs (low velocities) due to the increased drive cylinder leakage. Based on current analyses, this reduction in small amplitude damping is believed marginal for ground stability and unacceptable for engine/drive system torsional stability. There is a strong possibility, however, that this situation can be alleviated by means of additional overlap in the FSD control valve.

STEADY STATE PERFORMANCE TEST - MODIFIED FSD

LEAKAGE AREA = .00025 IN^2

		ENERGY DISSIPATION		
Stroke	Frequency	Unmodified % Non-FSD	Modified % Non-FSD	Spec. % Non-FSD
±.025"	42.5 RPM	61	38	--
±.05"	42.5 RPM	88	55	85
±.1"	42.5 RPM	79	69	85
±.05"	156 RPM	93	84	85

While increased drive cylinder leakage cures the limit cycle problem and provides a significant improvement in valve recovery time, this feature alone is not an adequate solution to the ramp displacement transient problem. On the contrary, the increased leakage compounds this problem to the extent that the region of 1/2 cycle damping is enlarged. The ideal solution consists of a mechanism which permits the FSD control to sense only alternating lag motions. Since the damper will also respond to very low frequencies (less than approximately .5 cps) in the same manner as a ramp it is also necessary to exclude these frequencies from the damper.

Resolution of these basic problems with the FSD was impractical within the scope of the ATC program. Since all damper parts were fabricated, the dampers were reworked to lock out the frequency selective feature for the DSTR testing with no other change in the basic damper configuration.

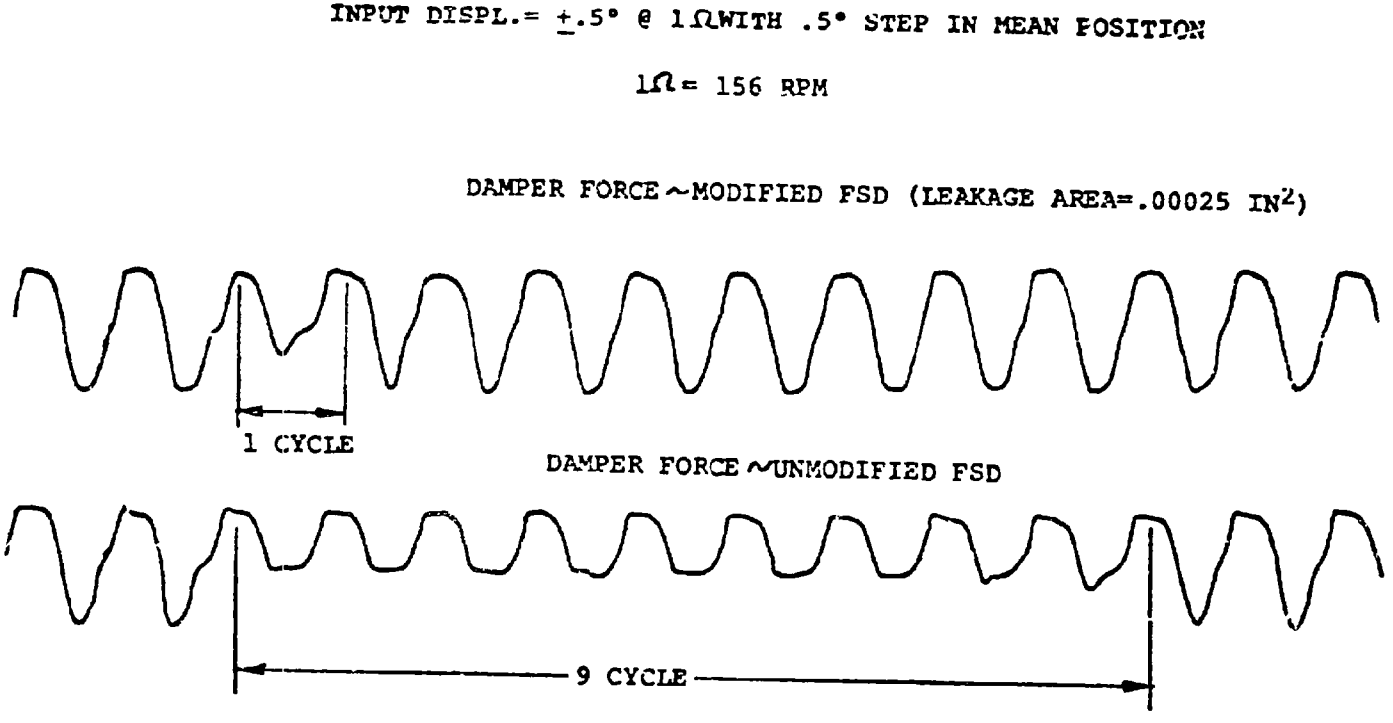

FIGURE 55. LABORATORY TRANSIENT RESPONSE TEST

Despite the present shortcomings, it is still believed that the FSD concept correctly implemented offers a potentially significant damping improvement for the mixed frequency air resonance condition. The following future program is recommended:

1) Define and investigate analytically a mechanism to eliminate the degradation due to ramp displacement transients.

2) Assuming a satisfactory solution of Item (1), optimize FSD cylinder leakage and valve overlap to eliminate limit cycling while retaining acceptable low velocity single frequency damping.

3) Modify an existing FSD damper and conduct sufficient bench testing to confirm analytical results.

4) Conduct a preliminary flight test evaluation with one operational FSD.

Modify additional units and conduct a thorough flight test evaluation to obtain comparative FSD and non-FSD performance.

4.8 SWASHPLATE

The swashplate rings were machined from 7075T7 aluminum alloy forging. Each ring is basically a U-shape with a closing cap. The section is closed hermetically by AF-30 adhesive and an O-ring. The structural joint is made by the same adhesive and two rows of studs. Boron-epoxy-wound rings were bonded into grooves on the rings with TAME 200 PB-2 acrylic adhesive (Reference 24). The boron rings were covered with a urethane strip bonded in place. The double-row ball bearing was 51.5 diameter at the ball path. Lip seals contained the grease lubrication with the upper seal lip directed to pass grease out during purging. The seal lips rubbed on thin corrosion resistant steel bands bonded to spacer rings. The other surfaces of clamping rings were originally specified to be coated with nylon as a fretting inhibitor, but considerable difficulty was encountered in this process. The coating was changed to MIL-L-8937 Solid Film Lubricant. This material served satisfactorily in the light fretting environment. The lugs for the control actuators on the stationary ring and those on the rotating ring for the pitch links are fail-safe in that one lug of the clevis will sustain flight for 100 hours. The bolts at these attachments are hollow and filled with a dye so that a crack will be evident upon visual inspection. The ends of these bolts are retained so that neither end will fall out should the bolt separate. The stationary ring has six grease fittings so that purging may be accomplished around the complete periphery of the bearing without turning the rotor. The stationary ring also has a threaded hole for the shock pulse meter transducer for bearing failure detection.

The swashplate endurance test was performed on two sets of ATC swashplate assemblies and one set of prototype assemblies.

The primary objectives of this test were:

a. The evaluation of swashplate performance under a duty cycle providing the extremes of anticipated flight operation.

b. Demonstration that the upper controls are capable of satisfactory operation over a substantial portion of their design lives.

Secondary objectives include evaluation of the swashplate bearing failure detection system, and the wear characteristics of pitch link rod end bearings under simulated flight loading.

The testing was performed in a back-to-back configuration as shown in Figure 56, requiring two sets of test components as noted. Dummy or simulated components were utilized where their substitution will not compromise test results. The specimens

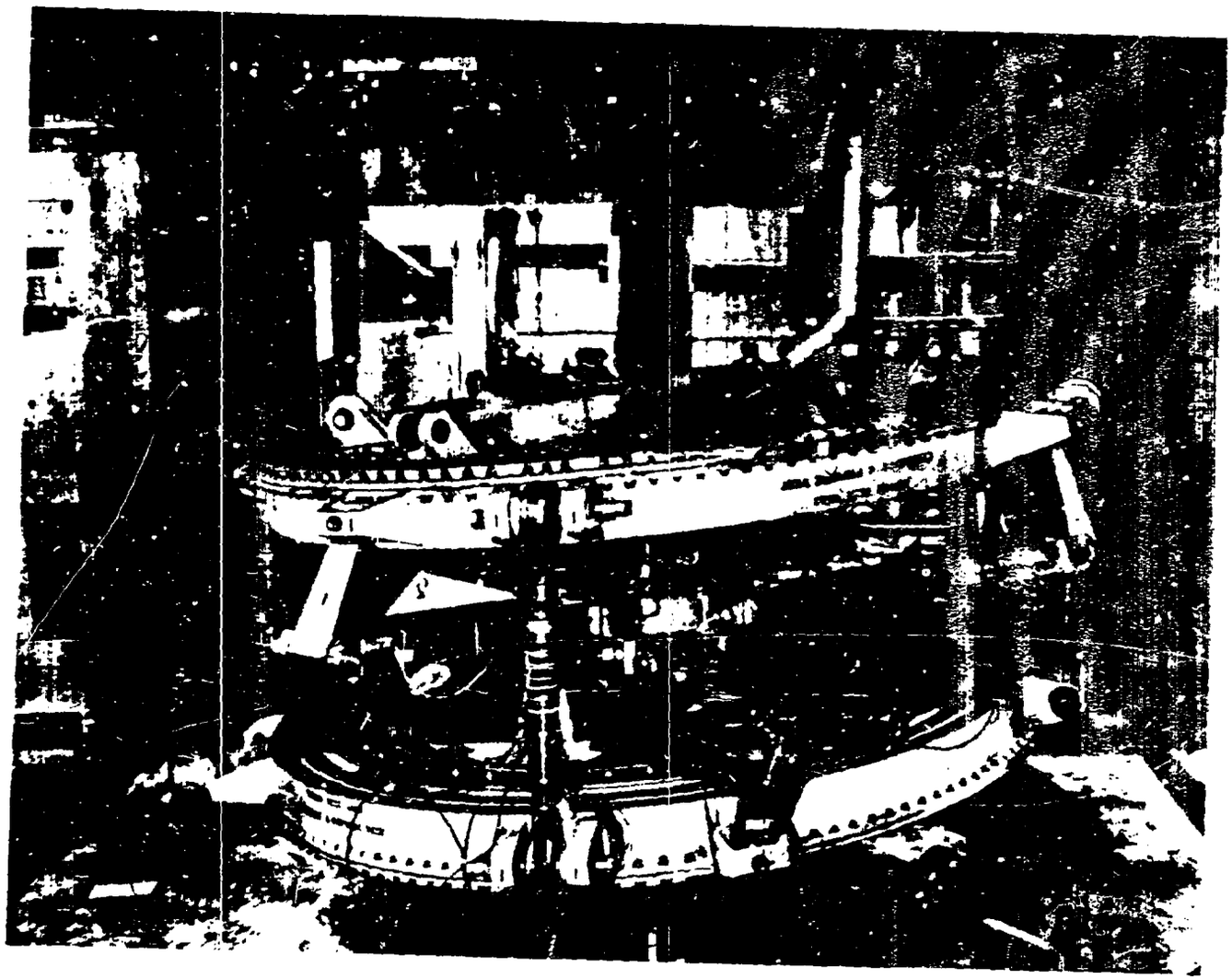

FIGURE 56. HLH SWASHPLATE ENDURANCE TEST FIXTURE

under test consisted of: 2 complete swashplate assemblies; 4 pitch link assemblies (without the inner non-load carrying link); 4 drive scissors link assemblies, and 2 stationary scissors assemblies.

It should be noted that the same set of drive scissors, stationary scissors, and pitch links were used on each of the tests. The loading schedules for each of the tests are shown in Table 16. The maximum load test 2 was the projected capability of the bearing used. Test 3 loads encompass all flight loads. For the first test the load was applied in increments until a steady compressive load of 150 pounds with an alternating load of 2790 pounds (-150 ± 2790) was obtained in the pitch links. This load condition was run for a total endurance time of 211.0 hours. Upon completion of 211.0 hours at this load level, the loads conforming to condition (1) as shown on Table 16 were applied and the testing continued for an additional 28.8 hours.

At 239.8 hours endurance time and still on load condition (1), the vibration sensor on the fixture automatically shut the test down. The indicator on the upper swashplate rotating ring assembly showed loss of vacuum at some time between 230.7 and 239.8 endurance hours when the automatic shutdown occurred. Inspection of the upper swashplate assembly showed several cracks in the rotating ring, and spalling of the balls and a failed cage in the swashplate bearing assembly (S/N 4). For a complete description of damage to the swashplate see Appendix 1 of Reference 25.

Following this unsuccessful test, strain surveys were conducted on the lower swashplate assembly, a portion of the failed swashplate assembly, and the Dynamic System Test Rig (DSTR) swashplate assembly. The results of these surveys confirmed that the rings needed stiffening in order to adequately support the swashplate bearings, or that a considerably deeper race was required to contain the ball path.

A third completed swashplate was modified for the second ATC test. Modification consisted of bonding 12 bulkheads within the rotating ring as defined by SK301-11742. Swashplate S/N A-101 (from ATC Test 1) was also modified the same way. In addition, the two boron stiffening rings, and the ridges on the cover retaining the boron rings, were machined off. Steel rings, with the same EA value as the boron rings, were bonded and pinned to the cover. Bearings with a maximum depth of 27% were used for this test.

The rotating ring was checked and found to be leaking air into the swashplate rotating ring in the area of the steel rings on the cover. These leaks were plugged, the ring evacuated, and testing continued at load condition 1. Once in operation, the leakage reoccurred in this ring.

TABLE 16. HLH/ATC SWASHPLATE ENDURANCE TEST LOADING SCHEDULE

TEST 1

CONDITION	HOURS	PITCH LINK LOAD-LB		THRUST LB	MOMENT IN-LB
		STEADY	ALT.		
(1) HIGH SPEED LEVEL FLIGHT AND MANEUVER	249.25 (99.7%)	-4260	±4365	-17,040	298,455
(2) MAXIMUM MANEUVER	0.75 (0.3%)	-7420	±7350	-29,680	502,735
(3) INCIPIENT BEARING FAILURE		-2360	±3185	- 9,430	217,770
TEST 2					
(1) 95%V_H	238.7	-1250	±4275	- 5,000	292,410
(2) TURNS & CONTROL REVERSALS	1.6 (0.64%)	-5730	±6532	-22,920	446,790
(3) AUTOROTATION & CONTROL REVERSALS	9.7 (3.88%)	-6120	±6976	-24,480	447,160
TEST 3					
(1) 95%V_H	237.0	-1200	±4105	- 4,400	257,180
(2) TURNS & CONTROLS REVERSALS	1.6 (0.64%)	-5730	±6530	-22,920	446,660
(3) AUTOROTATION & CONTROL REVERSALS	9.7 (3.88%)	-6120	±6980	-24,480	477,430
(4) PULL UPS	1.7 (0.68%)	-8200	±9350	-32,800	639,530

Testing was continued for an additional 27.8 hours while monitoring the leak rate. During this period of operation, the leak rate continued to increase. After 126.8 hours of endurance operation, the rig was shut down to permit a leak check, ultrasonic and X-ray examinations of the lower portion of the rotating ring.

Visual inspection of the raceways of each of the swashplate bearings after tests 1, 2 and 3 provided important information concerning the performance of the bearing under various test loads. The swashplate bearing was initially analyzed using Boeing Vertol bearing Computer Program S33 both for an ideal rigid support structure and for a modified flexible support structure. Examination of the raceways after test 1 showed that the ball path analysis provided a reasonable prediction except in the areas of maximum loading which resulted in significant bearing and support structure deflections. These deflections resulted in the balls riding over the race shoulder of the P/N 301-11426-1 bearing (22% depth) causing premature failure.

The results of test 1 indicated that the bearing did not have adequate race depth to insure that the ball path would remain below the race shoulder under maximum loads with the particular back-up structure. Bearings in the process of being manufactured were redirected to have the maximum depth available from the rings, which was 27%, for the second test.

This test was terminated for other than bearing failure at 126.8 hours. Examination of the bearing showed no distress but did reveal that the balls were riding close to the race shoulder under loads lower than predicted, even with the stiffening provided by the ring modification.

The prototype 35% race depth bearings in thicker wall swashplate rings completed the 250 hour test under all load conditions without any signs of distress. Visual inspection of the raceways indicated that the ball path was below the shoulder, even under the maximum forward rotor pitch link load of -8200 +9350. The results of the visual inspections are shown in Table 17.

The ball path measurements of the prototype bearings in the third test were taken following the endurance test. The maximum load ball path was not distinctly visible in the bearing raceway since it was operating in this condition for only 1.7 hours. The depth noted in Table 17 is not extremely precise. It had been planned to etch the races and run for a short time at the maximum load during the damaged bearing segment of the test. This would have provided a clear ball path as had been obtained with the other bearings. The measurement does indicate, however, that the margin of available ball path (race

TABLE 17. HLH SWASHPLATE BEARING BALL PATH INSPECTION AFTER TEST

TEST NUMBER	BEARING P/N	RACE DEPTH (% BALL DIA.)	MAX. PITCH LINK TEST LOAD (LBS)	MEASURED RACE DEPTH (% BALL DIA.)	COMMENTS
1	301-11426-1	22	-4260 ± 4365	22+	Bearing damaged due to balls riding over race shoulder. Insufficient race depth.
2	301-11426-1-902	27	-1250 ± 4275	26-27	Bearing race depth higher than predicted by computer program. Bearing not damaged. Bearing not capable of reacting maximum pitch link loads.
3	301-11426-2	35	-8200 ± 9350	28-30	Swashplate structure stiffness increased for this test. All components completed test with no distress. Bearing design adequate for maximum fwd rotor pitch link loads.

depth) is more than adequate. Cracks were located in the area of one rotating drive scissors attachment and at the outboard flange radius of the inner boron ring. At this time further endurance testing was terminated.

Examination of Failure. An evaluation of strain levels on the ring in the areas of failure as well as a physical examination of the ring indicated evidence of debonding of some of the bulkheads and marginal fatigue strength based on wall thickness.

Based on the first two tests, the HLH prototype swashplate rings were designed to have heavier walls and integral ribs in the rotating ring. The ridges for containing the boron rings were eliminated, and the boron rings were increased in thickness. The bearing race depth was maximized (35%). Two swashplates of this configuration were fabricated for testing. These swashplates completed the 250-hour test without incident.

The swashplate endurance tests and DSTR experience conclude that:

- The prototype swashplate configuration with 35% race depth bearing is more than adequate to meet endurance requirements. It should be possible to reduce the wall thicknesses of the rings to reduce weight.

- The pitch links, drive scissors and stationary scissors are satisfactory for use on the prototype aircraft. The bearings in these components have a reasonable chance of meeting 1000 hours life.

- The 300-hour interval for greasing the swashplate can be expected based on the quantity and quality of the grease remaining after the third test, during which none was added.

- The urethane covering for the boron rings is inadequate because the swashplate is used as a work platform. Thin aluminum covers were planned for the prototype, but drawings do not exist.

- Fatigue tests of the stationary and rotating rings remain to be performed on the prototype configuration. The bearing failure indicator portion of the endurance test should also be performed.

4.9 DRIVE SCISSORS

The four drive scissors cause the swashplate to rotate with the rotor hub, and maintain the swashplate concentric with the rotor shaft. Each scissors kinematically is a four bar linkage in a radial plane with the links consisting of the upper arm, lower arm, swashplate, and rotor shaft/drive collar. The lower drive arm-to-swashplate connection is a spherical bearing, and the swashplate-to-rotor shaft connection is determined by the position of the three swashplate actuators. The drive scissors offer no restraint to vertical or tilting motions of the swashplate. The three control actuators determine the position and limits of vertical and tilting motion. The kinematic arrangement cannot be accomplished with rigid linkage; the lower scissors arm connection to the swashplate moves out of the radial plane when tilted in other than through one of the connections. The HLH accommodates this kinematic error through torsional deflection of the upper scissors arm. This part is made of two titanium pieces hollowed to channel sections which are plasma arc welded together. The inner end is hinged on Teflon-Dacron-flanged sleeve bearings in a titanium drive collar. The upper and lower scissors are also joined with similar bearings. The attachment to the swashplate is through a Teflon-Dacron-lined spherical bearing.

Two valid fatigue tests were performed on specimens consisting of a simulated drive collar with the lug configuration, upper and lower scissors, including bearings and attaching hardware. The test setup is shown in Figure 57, and the test is reported in Reference 26.

The first failure in Specimen No. 1 was a crack that occurred at the upper (drive collar) end of the upper drive arm. This crack originated at an area of fretting between the flange of the brass-fit bushing and the face of the lug. As a consequence of this and because of other adverse experience, it was decided to replace the original anti-fretting coating (Sermetel 72, with aluminum-bronze containing 10% Ekonol. There was also a fatigue failure of the flange of a lower arm bushing. The redesign included thickening of the bushing flanges.

A second test with the scissors arms fitted with the new bushings was discontinued on the discovery of a crack in the upper arm originating in an area in which the wall had a sharp run out due to mismachining. This result is considered invalid and is disregarded in the analysis of results.

The third test was stopped at $.152 \times 10^6$ cycles on the failure of the bolt connecting the upper and lower arms. When the assembly was taken apart it was found that the shrunk-in

FIGURE 57. DOUBLE SCISSORS FATIGUE TEST SETUP

bushings did not fit properly due to irregular aluminum coating. To facilitate manufacture to the required tolerances, further redesign was necessary before continuation of the test. The test was completed with the final bushing design which has a modified flange-cylinder radius and is finished by grinding after coating for dimensional control.

Two further bolts were tested to failure before the upper arm failed, having accumulated 1.468×10^6 cycles. Based on analysis the predictions of part life are as shown in Table 18.

It should be noted that the titanium parts at the upper arm/drive collar joint, with a demonstrated safe life of 2,700 hours due to the limitations of the test, may be expected to exhibit lives exceeding 3,600 hours if more specimens are tested.

Although there were several instances of cracked bushings, the structural parts were never affected; there was never an indication that the crack in the bushing caused damage to structural parts. Therefore, the cracked bushings are not considered critical to the fatigue strength or mode of failure.

The inner stationary ring of the swashplate was initially restrained from rotating by a single scissors attached to the transmission upper cover. The parts were similar in construction to the drive scissors. The swashplate endurance test, the whirl test, and the DSTR all operated for a time with the single scissors. To further steady the swashplate, and to provide fail safety, a second scissors was added. The second was identical to the first, and future parts could be lighter since, under normal conditions, each carries approximately one half the load. This reduced load scissors would also be required to carry the load alone for 100 hours for the fail-safe condition.

TABLE 18. HLH/ATC DRIVE SCISSORS - RESULTS OF FATIGUE TEST AND CALCULATED PART LIVES

COMPONENT	PART NO.	(M-3σ) END.LIMIT LB	SAFE LIFE HOURS	M-σ END.LIMIT LB	[illegible] LIFE HOURS
UPPER ARM	301-11408-5	± 1,051	3,700	± 1,357	111
LOWER ARM	301-11409-1	± 1,123	5,200	± 1,460	16
*DRIVE COLLAR (LUGS ONLY)	301-11448-1	± 1,051	2,700	± 1,357	11
BOLT - UPPER ARM TO COLLAR	301-11395-1	± 1,414	5,500	± 1,826	12
BOLT - LOWER TO UPPER ARM	301-11395-6	± 1,387	4,700	± 1,791	111

*No Failures

4.10 PITCH LINK

The pitch link connects the swashplate to the blade pitch arm. The link consists of two concentric load path assemblies, each consisting of a pair of rod ends connected by a turnbuckle. The turnbuckles are timed so that adjustment of both links is simultaneous. Spherical Teflon-Dacron-lined bearings are pressed into the outer path rod ends. The bores of these rod ends contained wrought aluminum bronze bushings. The bushings were originally corrosion resistant steel coated with Sermetel 72 which were replaced at the time the hub fatigue test showed Sermetel to be inadequate as a fretting inhibitor. The rod ends of the inner load path link had bores larger than the bearing so that no load was carried as long as the outer load path link remained in tact. Care must be exercised in assembling the link to assure this function. During load calibration of one fatigue test link, the load was shared between the two links beginning at a low load because the bearing and the inner load path rod end were not concentric initially. With load, the outer link changed length until the clearance in the inner rod end was taken up. Portions of the inner rod ends are covered with Teflon-Dacron fabric. These areas support the inner link within the outer link avoiding the possible fretting of a metal-to-metal contact.

Two pitch link assemblies were fatigue tested as reported in Reference 27. Each specimen was assembled to requirements stated on its assembly drawing except for the following:

- The rod ends were placed in the same plane rather than displaced by 43°. This was done to permit the development of the same loading on both the upper and lower rod ends.

- Offset fitting assemblies were installed in place of the rod end bearings as shown in Figure 58. The purpose of the offset assembly was to permit the development of end moments, simulating those produced by bearing friction. The test setup is shown in Figure 59.

The first fatigue failures in both specimens occurred in the outer rod end lugs and were nearly identical in appearance and location. See Figure 60 for the location of failures. Testing was continued after cutting away a portion of the failed lug so that the load was on the remaining lug of the outer load path clevis. The second failure in Specimen No.1 occurred in the shank region of the remaining outer pitch link lug. Light fretting was evident in the lug failure origin areas of both specimens.

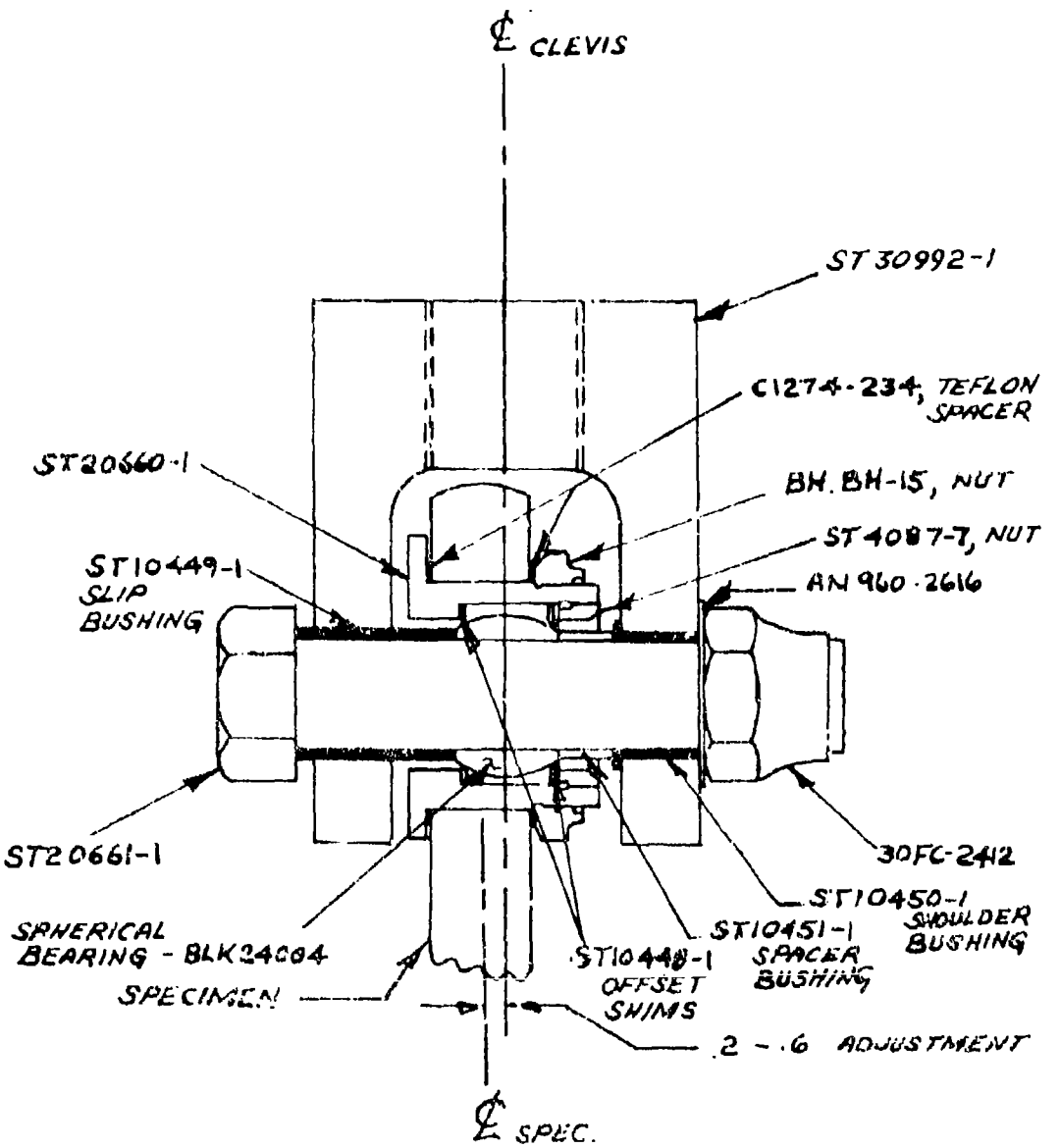

FIGURE 58. PITCH LINK OFFSET END FITTING

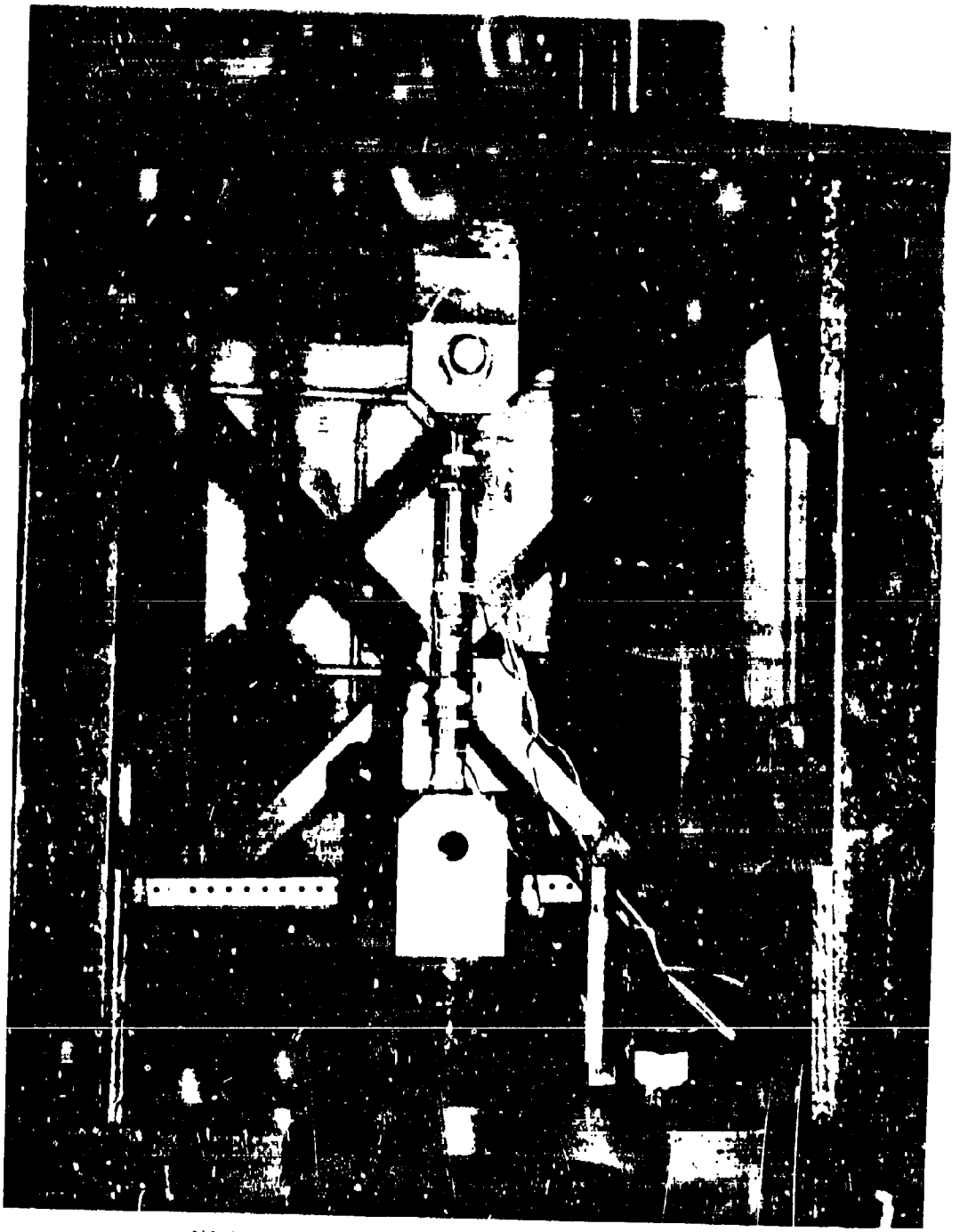

FIGURE 56. PITCH LINK TEST FIXTURE

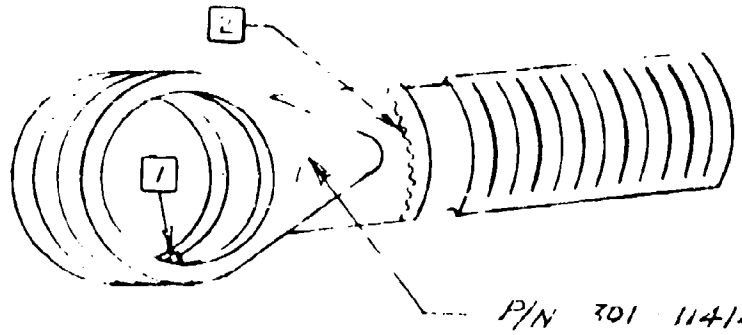

SPECIMEN NO. 1

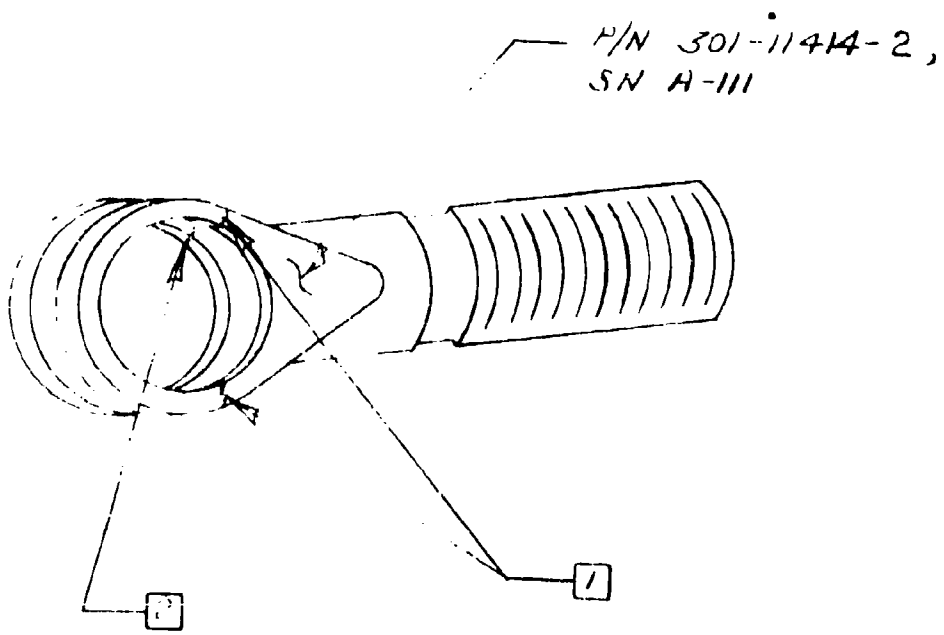

SPECIMEN NO. 2

FIGURE 60. LOCATION OF FAILURES - PITCH LINK FATIGUE TEST

Cracking followed a small undercut between the shank bore wall and the intersecting spherical inner surface. The second failure in Specimen No. 2 occurred in the remaining outer pitch link lug in approximately the same location as that of the first failure.

The secondary load path of both specimens successfully withstood one million cycles at 5000 ±5000 pounds and a subsequent proof load to 20,500 pounds without failure. In addition, Specimen No. 2 was run for another one million cycles at 6500 ±6500 pounds followed by proof loading to 20,000 pounds without failure.

All threads, both internal and external, looked very good in both specimens after completion of fatigue testing. There was no binding of these threads when the specimens were disassembled. The fabric lining material on the secondary links in both specimens showed no apparent deterioration at completion of fatigue testing.

From analysis of the test data, a safe life of 560 hours, and a fail-safe life of 105 hours were determined. These lives, however, derive from the test failure points and, therefore, from the test loading in which a tensile steady load = 1.1 x alternating load was used. Actual flight loads will be less severe according to the results of the wind tunnel and whirl tower tests reported in References 28 and 29. These show steady pitch link loads to be compressive, just as they are now in the CH-47 helicopter. Since any reduction in steady tensile loads will reduce lug cyclic stresses, a significant increase in predicted life would result. With the tensile load equal to one-half the alternating, the calculated safe life is 7800 hours.

The prototype pitch links were changed only in that the bushings in the rod ends were changed to be corrosion-resistant steel with aluminum bronze with Rkonol, the best fretting inhibitor tested during the program.

4.11 DEMONSTRATION ROTOR

A complete rotor hub and upper controls assembly was fabricated and installed with four blades on the whirl tower (Figure 61). A brief whirl test was performed and is reported in Reference 29. Items of the test significant to the rotor hub and upper controls were:

- Clearance check of moving parts for clearance.
- Proof loading of the controls through application of blade pitching moment.
- Stress and motion surveys indicating stresses as predicted.
- Operation of rotor at the overspeed condition (125% normal) for one hour.
- Evaluation of the frequency selective damper.

This test revealed deficiencies in the elastomeric bearing, droop stops, and the frequency selective damper. Each of these conditions is described in the detail discussion of that component. The titanium hub retention nut deflected excessively when installed in accordance with drawing specifications. The nut screws onto the rotor shaft loosely, and thrust preload is applied by 28 screws applying force between the nut and the hub. The offset between the shaft threads and the center of the screws produce a moment tending to roll the nut inside out. For the required preload, the deflection of the nut allows the lower diameter to expand and the lower threads to separate substantially. A nut of more substantial cross-section was designed for the DSTR.

Upon completion of the whirl test, the demonstration rotor was installed on the DSTR (Figure 62) with engines and transmissions to operate as a rotor-drive system. The tests are reported in Reference 30. The DSTR provided more operating experience to increase confidence in the hub and upper controls while revealing other deficiencies.

Significant problem solving was accomplished on the DSTR for the hub and upper controls.

- Evaluated preload button for elastomeric pitch bearing as a solution to the tearing of the bearing.
- Evaluated fretting inhibitors that were identified for use on flight hardware and which demonstrated satisfactory results.

FIGURE 61. HLH/ATC ROTOR ON BOEING VERTOL WHIRL TOWER

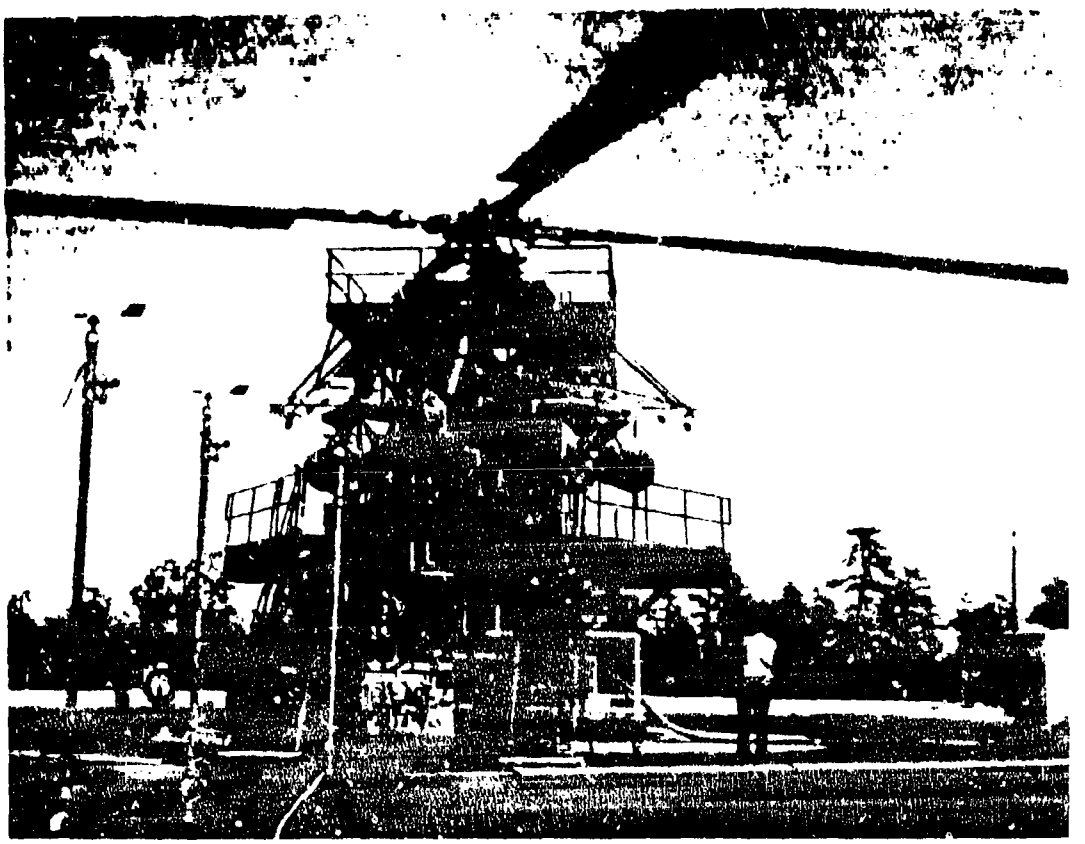

FIGURE 62. DYNAMIC SYSTEM TEST RIG

- Performed static hub blade deflection and strain measurements which revealed higher than predicted static blade loads.

- Photographed blade motions using hub cine camera under start up, shutdown, and high cyclic conditions.

The DSTR provided exposure to routine operation and maintenance of HLH hardware which would have been beneficial to initial HLH prototype operations.

- Random and sporadic periods of horizontal swashplate motion were visually observed and later measured. It was not possible to determine the causes of these motions, nor the significance, within the time of the tests.

- Gained significant insight into the initial operating temperature of the swashplate after replenishment of swashplate grease.

- Demonstrated field replacement of dynamic system components including hub, pitch housing, crossbeam, and elastomeric bearing.

Operating problems included tearing of the elastomeric bearing, corrected with the thrust button, and the disengagement of the droop stops, corrected with the cylindrical stop ring. On two occasions, failure of the DSTR (non-aircraft) control system caused substantial damage to the droop stop parts when the control system caused large flapping motion of the blades while the stop ring was in intermediate positions (between 95 and 115 RPM).

A new problem arose during the DSTR tests that did not occur during the short whirl test. The rotor blade lag damper has spherical bearings at each end and is free to rotate about its axis through these bearings. The fitting to which the inboard end is attached has buttons on either side of the clevis which contact the damper lug to limit this rotation. Because of the frequency selective mechanism, the center of gravity of the damper is above the axis and a component of centrifugal force causes a moment about this axis. The limiter button reacts the torque while rubbing due to flapping of the blade and damper. The original Nylon buttons wore severely and were replaced with bronze oilite. These also wore rapidly, but it was more expedient to replace the limiters a few times during the test rather than effect a design change. Future rotor heads would not try to correct the rapid wear with other materials, but rather do something to reduce the moment of the lag damper which loaded the buttons.

Upon teardown of the hub and upper controls at the completion of the test, the following unsatisfactory conditions were found.

- Joints in the titanium structure which still had Sermetel 72 as the fretting inhibitor showed incipient fretting. All joints in the prototype had been changed to use aluminum bronze with Ekonol.

- Fretting on the ends of bushings in the drive scissors was seen similar to that in the scissors fatigue test. Prototype parts were committed at the time the problem was initially recognized in bench test. No change for the prototype was decided based on successful fatigue testing of the scissors, and the limited degree of the fretting.

- Light rust was found on the fracture surfaces of the 440C corrosion-resistant steel outer race of the shear bearing. The bearings in the DSTR rotor were not passivated and the rust stains are most likely free iron on the surface. Prototype bearings specify passivation to prevent recurrence.

- White powdery products of corrosion were found on the outside bearing diameter of the aluminum stationary ring, and the swashplate bearing showed rust spots on the inside diameter. Rain water had seeped under the bearing retaining ring. The solution offered was to provide a preformed packing (O ring). This had not been implemented in the prototype swashplates.